UNIVERSITÉ DE STRASBOURG

ÉCOLE DOCTORALE DES SCIENCES DE LA VIE ET DE LA SANTE

UPR9022 – Modèles Insectes d'Immunité Innée (M3i)

THÈSE présentée par :

Claire ROUSSEAU

Soutenue le : **30 Septembre 2022**

pour obtenir le grade de : **Docteur de l'Université de Strasbourg**

Discipline/ Spécialité : Aspects moléculaires et cellulaires de la biologie

Caractérisation de l'interactome du récepteur d'ARNdb cytosolique Dicer-2 *in vivo* au cours de l'infection virale chez *Drosophila melanogaster*

THÈSE dirigée par :

Pr. Carine MEIGNIN	Professeur des Universités, Institut de Biologie Moléculaire et Cellulaire, CNRS UPR9022, Université de Strasbourg, France

RAPPORTEURS :

Pr. Alfredo CASTELLO	Professeur des Universités, Institute of Infection, Immunity and Inflammation, Université de Glasgow, Royaume-Uni
Dr Nolwenn JOUVENET	Directrice de Recherches (DR2), Institut Pasteur, Université Sorbonne Paris Cité, France

---

AUTRES MEMBRES DU JURY :

Dr. Sébastien PFEFFER	Directeur de Recherches (DR1), Institut de Biologie Moléculaire et Cellulaire, CNRS UPR9002, Université de Strasbourg, France

Acknowledgments

First and foremost, I would like to thank my PhD Advisor, Carine Meignin. Thank you for welcoming me into your team during my Master's degree and accompanying me until now. Thank you for you guidance, I have learned so many things during all those years, and for that I am very grateful. I would also like to thank Jean-Luc Imler for all the advice and critical reading of my review and future paper, and Joao Marques for the interesting discussions and insights.

I am deeply thankful to my PhD committee members, Sébastien Pfeffer, Alfredo Castello and Nolwenn Jouvenet for accepting to evaluate my work. It has been a pleasure having two of you in my PhD Advisors Committee as your comments have been a great help. I really enjoyed discussing my project with you and I have no doubt that the discussion will be even more interesting on the day of the defense with the addition of Nolwenn Jouvenet.

I have had the privilege of working alongside talented scientists who helped me with their expertise throughout this PhD thesis. I cannot thank Emilie enough, who has helped me so much during my PhD, I will almost miss the long hours on Friday nights sorting flies. Inês and Lena, thank you for helping me repeatedly with the mostly frustrating but sometime very rewarding world of statistics and R, and thank you also to everyone at the proteomics platform for their involvement in my project. I am also grateful for everything that I have learned by talking with Loïc, Ludmila, Inês and Gabrielle, thank you for all your advices and insights through the years. I have also been very lucky to have as my first intern Sophie, to whom I wish the best of luck for the future.

I would like to thank everyone in the UPR9022, and in particular the girls from my office Assel, Evelyne, Emilie, Melody, Ludmila, Yasmine and Juliette, as well as Matthieu who spends so much time there that he should be an honorary member of the office. Thank you for making this lab feel like a second home to me, mixing work with laughter has made me want to work harder. In particular, I cannot imagine my thesis without you Juliette, who has become my friend more than my colleague, and made all the deadlines and paperwork a little easier, knowing that you went through it with me. Thank you to Myriam, Audrey, Nathalie, Thomas, Gaetan, Lucie, Charlotte, and all the people who have made my stay at IBMC so memorable, both inside the unit and outside. Thank you to Natacha and Baptiste for helping me take a break sometimes, and to Mathilde, Miguel and Alina for the long-distance emotional support.

I would also like to thank my family as well as the Gilmer/Stoffel family for their continuous support, including my grand-parents, my brother and in particular my parents, who not only have been great role models, showing me what it is possible to achieve by working hard, but have also been there every step of the way to help me and support me. Finally, I am deeply grateful for Orian, who has helped me in every way he could although he was also finishing his own thesis. This PhD thesis has been a roller-coaster ride full of ups and downs, so thank you for being there for both, I hope I will be able to help you as much as you helped me.

Abbreviations

adjP: Adjusted p-value

Ago: Argonaute

AMP: Antimicrobial peptide

ANOVA: Analysis of variance

AP-MS: Affinity purification followed by mass spectrometry

BSA: Bovine serum albumin

Cas9: CRISPR associated protein 9

cDNA: Complementary DNA

cGAS: Cyclic GMP-AMP Synthase

CRISPR: Clustered regularly interspaced short palindromic repeats

CrPV: Cricket paralysis virus

CS flies: CantonS

Cter: C-terminal

DAPI: 4',6-diamindino-2-phenylindole

DCV: Drosophila C virus

DIAP1: Death-associated inhibitor of apoptosis 1

DLR: Dual luciferase reporter

DMSO: Dimethyl sulfoxide

dsRBP: Double-stranded RNA binding protein

dsRNA: Double stranded RNA

DTE: Dithioerythritol

DXV: Drosophila X virus

endo/exo-siRNA: Endogenous/exogenous siRNA

Fand: Fandango

FHV: Flock house virus

Fluc: Firefly luciferase

GO: Gene ontology

GST: Glutathione S transferase

HA: Hemagglutin

HEK293: Human embryonic kidney 293

hpi: Hour post infection

HRP: Horseradish peroxidase

IF: Immunofluorescence

IGR: Intergenic region

IMD: Immune deficiency

IP-MS: Immunoprecipitation followed by mass spectrometry

IRES: Internal ribosome entry site

JAK-STAT: Janus kinase-signal transducer and activator of transcription

KD: Knock-down

KO: Knock-out

Larp4B: La-related protein 4B

LC-MS/MS: Liquid chromatography with tandem mass spectrometry

lncRNA: Long non-coding RNA

Loqs: Loquacious

LSm-protein: Like Sm-protein

MDA5: Melanoma differentiation-associated protein 5

miRNA: MicroRNA

MOI: Multiplicity of infection

mRNA: Messenger RNA

MTS: 3-(4,5-dimethylthiazol-2-yl)-5-(3-carboxymethoxyphenyl)-2-(4-sulfophenyl)-2H-tetrazolium

NMD: Non-sense mediated decay

NTC: NineTeen complex

Nter: N-terminal

O.N.: Overnight

OE: Overexpression

ORF: Open reading frame

Pabp2: PolyA binding protein 2

PAMP: Pathogen-associated molecular pattern

PBS: Phosphate buffered saline

PCR: Polymerase chain reaction

PFA: Perfluoralkoxy alkane

PRR: Pattern recognition receptor

qPCR: Quantitative PCR

RACK1: Receptor for activated C kinase 1

RBP: RNA-binding protein

RdRp: RNA dependant RNA polymerase

RIG-I: Retinoic acid-inducible gene I

RISC: RNA-induced silencing complex

RLC: RISC-loading complex

RLR: RIG-I-like receptor

Rluc: Renilla luciferase

RNA: Ribonucleic acid

RNAi: RNA interference

RNase: Ribonuclease

RT: Reverse Transcription

RT: Room Temperature

RT-qPCR: Quantitative reverse transcription PCR

RVFV: Rift valley fever virus

S2: Schneider 2

siRNA: Small interfering RNA

Sm-protein: “Smith” protein

snRNA: Small nuclear RNA

snRNP: Small nuclear ribonucleoproteins

ssRNA: Single stranded RNA

STING: Stimulator of interferon genes

Tao: Thousand and one

TLR: Toll-like receptor

Tub84B: Tubulin 84B

UTR: Untranslated region

VPg: Viral protein genome-linked

vsiRNA: Viral silencing RNA

VSR: Viral suppressor of RNAi

VSV: Vesicular stomatitis virus

WB: Western blot

WT: Wild-type

Table of contents

General introduction

I. *Drosophila melanogaster* and antiviral immunity

A. *Drosophila melanogaster*, a century-old animal model

The fruit fly, *Drosophila melanogaster*, has been used as a model organism for over a century. It was first bred in large quantity by Charles W. Woodworth in 1900, who suggested it should be used to study genetics, and became a model of choice thanks to the work of Thomas Hunt Morgan (Ganetzky and Hawley, 2016). Morgan and his collaborators were looking for inexpensive biological material that could be bred in a limited space and the fruit fly matched those criteria perfectly. Indeed, not only are fruit flies inexpensive, they are also easy to maintain, produce a numerous progeny and have a short generation time. Moreover, as most scientists were also teachers, the ease of use of the fruit fly in practical courses was also appreciated. By observing the progeny of a large number of crosses, Morgan and colleagues were able to understand that genes are organized in a linear manner inside chromosomes and that traits that are related to each other correspond to genes that are close to each other on the chromosomes. Later, Thomas Hunt Morgan was rewarded by a Nobel Prize in Physiology or Medicine in 1933 for his studies on the role of chromosomes in heredity.

One of his former students, Hermann Muller, went on to be awarded the Nobel Prize in Physiology or Medicine as well, for “the discovery of the production of mutations by means of x-ray irradiation” in 1946. The use of mutations as an experimental strategy was then later used in developmental biology, as the combined work of Christiane Nüsslein-Volhard, Eric Wieschaus and Ed Lewis led to a third Nobel Prize with this model organism in 1995, for “their discoveries concerning the genetic control of early embryonic development”. By performing a systematic genome-wide mutagenic screen *in vivo*, they identified 15 genes which, if mutated, impaired segmentation of the embryo (Nüsslein-Volhard and Wieschaus, 1980; Wieschaus and Nüsslein-Volhard, 2016). Their research illustrates the power of *D. melanogaster* as a model in two ways. First, the magnitude of their experiment, an exploit that had never been done before except in microorganisms, exemplifies the scale at which experiments can be performed in this model organism. Second, most of the genes identified

by the three scientists were then found to have important functions in the development of the human embryo as well, highlighting the evolutionary conservation of umpteen pathways and mechanisms. In fact, many signal transduction pathways, developmental and cellular processes are conserved between *Drosophila* and vertebrates (Beckingham et al., 2005; Buchon et al., 2014).

In the 1990s, this evolutionary conservation was highlighted once more, this time in the field on innate immunology. In 1996, Jules Hoffmann and co-workers discovered a role of the gene Toll, previously found to be involved in development by Christiane Nüsslein-Volhard and Eric Wieschaus, in the antimicrobial response against bacteria and fungi in the fruit fly (Lemaitre et al., 1996). Two years later, Bruce Beutler and colleagues found that Toll homologues in mammals, called Toll-like receptors (TLRs), had the same effect in mammals (Poltorak et al., 1998). These findings illustrated the similarity between the molecules that activate innate immunity in flies and mammals, thus paving the way to the study of innate immunity in the model organism *Drosophila melanogaster* (Ferrandon et al., 2007). Moreover, as the fruit fly lacks adaptive immunity, it offers the opportunity to study innate immunity without the added complication of a more complex immune system.

Although studies on the topic of innate immunity in *D. melanogaster* initially focused on bacterial and fungal infections, there has been a growing interest in viral infections in this organism over time. Since the identification of the first *D. melanogaster* viruses like the *Sigma virus* (L'heritier, 1958) and the *Drosophila C virus* (Jousset et al., 1972), the study of antiviral immunity in *Drosophila melanogaster* has led to important discoveries in the field. Indeed, many insect viruses have enabled the characterization of the roles of the RNA interference (RNAi), Immune deficiency (IMD), Toll and autophagy pathways in innate antiviral immunity (Talide et al., 2020). Given that many arboviruses can infect *Drosophila*, some labs have started studying them in this model in the hope of discovering new therapeutic targets and arbovirus-vector interactions (Chotkowski et al., 2008; Filone et al., 2010; Paingankar et al., 2020; Palmer et al., 2020). For both natural Drosophila viruses and human viruses, the study of host-virus interactions or host factors involved in viral infections has been facilitated by a number of advances in this model. For example, the completion of the *D. melanogaster* genome sequence in 2000 (Adams et al., 2000; Myers et al., 2000) has been a considerable

breakthrough and has made the study of genes in this organism easier, along with the existence of a wide array of genetic tools allowing the control of gene expression both spatially and temporally (Mohr et al., 2014; Venken and Bellen, 2014), and the development of high-throughput technologies like RNA interference screens, transcriptional profiling and proteomics (Carmena, 2009; Mohr et al., 2010). Here an important advantage of the fruit fly model is the possibility to perform large-scale experiments *in vivo,* which allows the study of the viral infection while retaining the complexity of the whole organism. Indeed, although *ex vivo* studies of viral infections have greatly advanced our understanding of viruses and antiviral immunity, those studies usually rely on the use of immortalized tissue culture cell lines, which often do not reflect the behavior of cells in the tissues *in vivo*. Moreover, certain immune pathways are not expressed in all tissues as illustrated by the tissue-specific expression of the antiviral RNAi protein Loqs2 in the *Aedes* mosquito (Olmo et al., 2018), or express unique gene patterns not found in any cell type *in vivo* (Carter and Shieh, 2010). By opposition the fruit fly, which can be bred in large quantities in a short time and which causes less ethical concerns as mammals, offers a very interesting opportunity to perform large-scale "omics" experiments *in vivo* in order to further our understanding of the viral infection, an opportunity that was taken advantage of in this thesis.

B. The complex and fast-evolving *Drosophila* antiviral immunity

The *Drosophila* genre, which includes *Drosophila melanogaster,* can be infected by a wide variety of viruses, including natural pathogens of *Drosophila*, other insect viruses and arboviruses that can infect humans. In fact, different studies aiming to understand the diversity of viruses infecting the *Drosophila* genre hitherto discovered more than 100 viruses associated with *Drosophila*, of which at least 30 can infect *D. melanogaster* (Wu et al., 2010; Longdon et al., 2015; Webster et al., 2015; Medd et al., 2018; Webster et al., 2016; Wallace et al., 2021). These viruses include a broad range of genome types, including positive sense RNA (ssRNA(+)) genomes like the *Drosophila C Virus* (DCV), negative sense RNA (ssRNA(-)) genomes like the *Vesicular Stomatitis Virus* (VSV), double-stranded RNA (dsRNA) genomes like the *Drosophila X Virus* and dsDNA genomes like the *Kallithea Virus*. Amongst this wide diversity of viruses, the vast majority possess an RNA genome, with only a few DNA viruses identified. As the RNA-dependent RNA-polymerase (RdRp) of RNA viruses does not have a

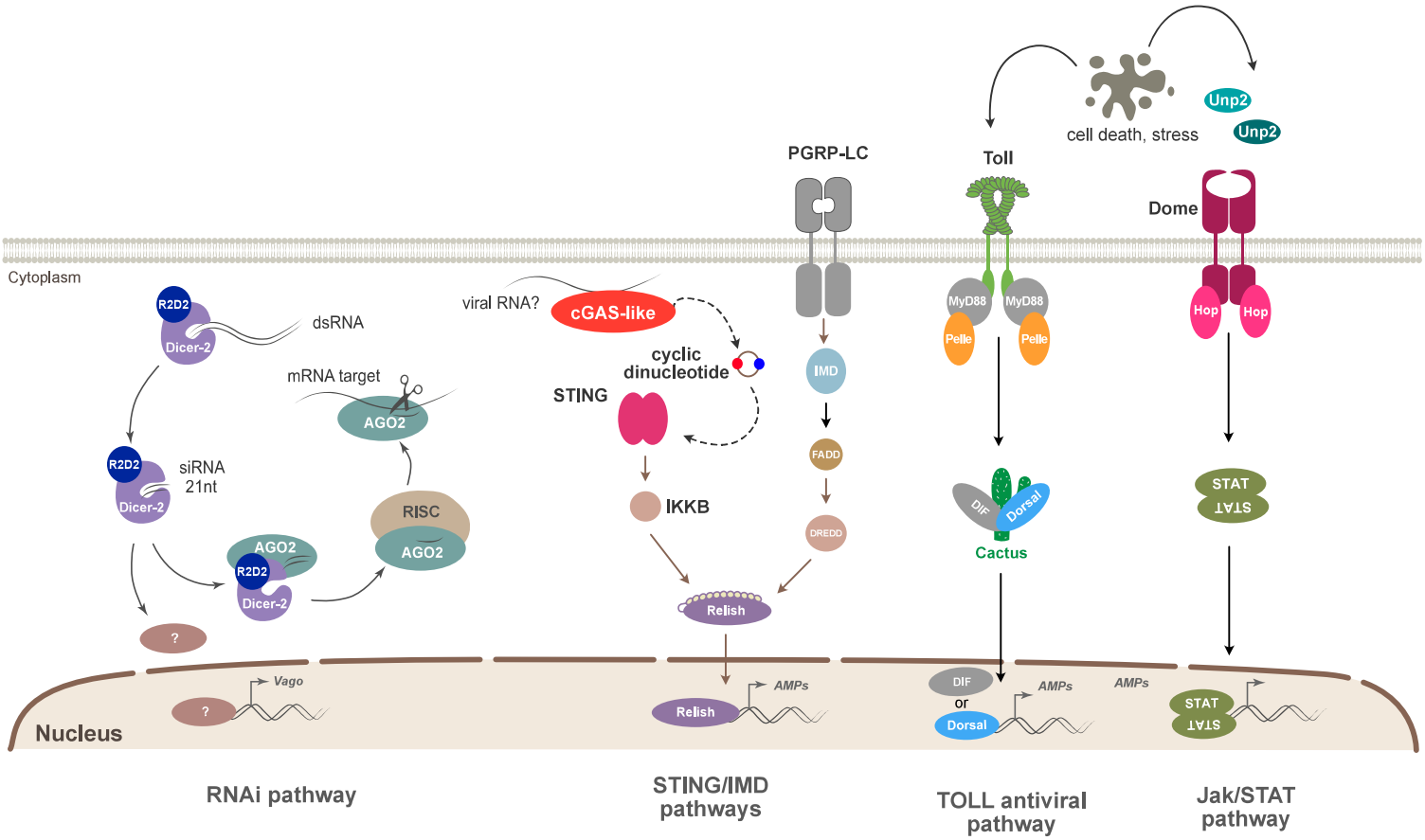

Figure 1. Antiviral immunity pathways in *Drosophila melanogaster (adapted from Mussabekova et al., 2017)*. In *D. melanogaster*, the viral infection is restricted by different antiviral innate immune responses, including the siRNA pathway and several inducible responses. Although the siRNA pathway depends on the recognition of dsRNA by Dicer-2, the triggers leading to the induction of the different inducile responses are less clear. After induction of the inducible responses, a signalling cascade is activated leading to the expression of antimicrobial peptides. Interestingly, Dicer-2 can also induce the expression of an antiviral protein, Vago, in an RNAi-independent manner.

proofreading activity (even though some RNA viruses do possess an RdRp-independent proofreading activity), RNA viruses have a higher mutation rate than DNA viruses (Peck and Lauring, 2018) and, especially ssRNA viruses, globally have very high rates of evolution.

In order to fight against this plethora of ever-changing viruses, *D. melanogaster* has developed a complex immune response. As mentioned above, this immune response relies solely on innate immunity, as insect do not have an adaptive immunity. Once an infection occurs, the innate immune system uses Pattern Recognition Receptors (PRRs) like the Toll-like receptors mentioned previously to detect Pathogen-Associated Molecular Patterns (PAMPs). In the case of viruses, these PAMPs can be viral nucleic acids or viral glycoproteins for example (Mogensen, 2009; Takeuchi and Akira, 2010). Upon recognition of the viral pathogen, the fruit fly employs an arsenal of antiviral mechanisms to neutralize viral infection (**Figure 1**), the main one being the antiviral RNA interference pathway (RNAi), which will be described in detail later on. Briefly, this pathway relies on the detection of a form of nucleic acid expressed by most viruses during their replication cycle, double-stranded RNA (dsRNA), by the DExD-box RNA helicase Dicer-2 and leads to the degradation of the viral RNA. As dsRNA can arise not only from RNA virus replication using a RNA-dependent RNA-polymerase (RdRp) but also from a number of processes including convergent transcription, this pathway was shown to provide immunity against a broad range of viruses, including DNA viruses (Mueller et al., 2010; Bronkhorst et al., 2012; Kemp et al., 2013; de Faria et al., 2022).

In addition to the RNAi pathway, the involvement of several inducible responses has been highlighted in *D. melanogaster*. Two pathways originally described to be involved in antibacterial and antifungal responses, the Toll and Immune Deficiency (IMD) pathways, have been shown to have an antiviral impact against several viruses, including the *Drosophila C virus* (DCV), *Cricket paralysis virus* (CrPV), *Drosophila X virus* (DXV), *Nora virus* and *Flock house virus* (FHV) (Costa et al., 2009; Ferreira et al., 2014, 2018; Zambon et al., 2005). The Janus kinase signal transducers and activators of transcription (JAK-STAT) pathway, has also been shown to be activated upon DCV and CrPV infections (Dostert et al., 2005; Kemp et al., 2013; Merkling et al., 2015). However, the role of these pathways in antiviral immunity is poorly understood, as it remains unclear exactly how they are activated and act on specific viruses in a general manner. Moreover, although these pathways could be directly activated by viruses,

this could be an indirect effect of their impact on cells (e.g. stress, cell damage) (Ming et al., 2014; Schneider and Imler, 2020). More recently the drosophila homologue of the mammalian STimulator of INterferon Genes (STING), an established key factor against DNA viruses in mammals (Ishikawa and Barber, 2008), has been shown to play an important role in *D. melanogaster* antiviral immunity (Goto et al., 2018; Liu et al., 2018). Two mechanisms have been suggested to explain the role of STING in *D. melanogaster*. On one hand, Liu and colleagues propose that the antiviral effect of STING is due to a stimulation of autophagy, as mammalian STING is known to stimulate this mechanism. (Liu et al., 2018). On the other hand, another hypothesis has been proposed by Goto *et al.*, involving the kinase IKKβ and the NF-κB transcription factor Relish (Goto et al., 2018), suggesting that this pathways shares some similarities with the IMD pathway and induce a transcriptional response. Finally, other pathways such as autophagy, apoptosis and the involvement of the proteasome have also been shown to play a minor role in the antiviral immune response in *D. melanogaster* (Lamiable et al., 2016). These pathways act together to restrict the viral infection, and form an intricate system that can prove difficult to entangle. For example, the IMD and STING pathways share several components (Goto et al., 2018). Moreover, the main actor of the RNAi pathway, Dicer-2, has been shown to be able to activate an inducible immune response relying on the antiviral protein Vago in an RNAi-independent manner (Deddouche et al., 2008). Therefore, in addition to the necessity to distinguish simple stress responses from *bona fide* immune mechanisms, it is also necessary to consider the fact that the lines between pathways are often blurry, even if distinct and separated mechanisms would be easier for us to comprehend.

In response to this large panel of antiviral immune responses, viruses have evolved counter-defence strategies to block the fruit fly immune pathways. These strategies can either prevent the recognition of the virus by the cell, or impair the subsequent immune response. Some viruses hide from the immune pathways by performing their genome replication cycle inside virus-induced vesicles called viral factories or replication organelles, as for example FHV, which induces the formation of compartments inside the mitochondrial membrane and performs its replication there (Kopek et al., 2007). Others express protein inhibitors of the fruit fly immune pathways, as illustrated by the expression of viral inhibitors of apoptosis by

viruses from the *Baculoviridae* and *Entomopoxviridae* families (Clem, 2015; Crook et al., 1993). In the case of RNA interference, these strategies often involve expressing proteins called Viral Suppressors of RNA silencing (VSRs) that will inhibit one or more steps of the antiviral RNAi pathway. The DCV 1A protein belongs to this category, as it was shown to bind dsRNA and prevent processing of the viral dsRNA by Dicer-2, one of the main actors of RNAi (van Rij et al., 2006). However, in an unexpected twist, it appears that the host cell possesses a counter-counter-defence against the DCV 1A VSR in the form of a long non-coding RNA (lncRNA) called VSR-interacting RNA (VINR). VINR binds to DCV 1A and this binding will ultimately lead to the expression of antimicrobial peptides (AMPs) by the cell (Zhang et al., 2020). The expression of immune suppressors is a very common strategy employed by most viruses, and by studying the evasion strategies of a specific virus, we can have a general idea of the immune mechanisms activated by the cell to defend itself against this virus.

This illustrates how, to keep up with an evolutionary arms race between the host and the virus, both sides have to continuously adapt defence, counter-defence and counter-counter-defence mechanisms. In light of this, it is not surprising that the evolutionary rates of key genes of antiviral immunity in the fruit fly, submitted to a constant evolutionary pressure by viruses, are higher than that of other genes. Indeed, a study by Obbard and colleagues found that adaptive substitutions in immunity genes are nearly twice the genome average (Obbard et al., 2009). According to the same study, the genes with the highest evolutionary rates belong to the RNAi and IMD pathways. In fact, RNAi genes display greater adaptive protein substitution rates than other genes not only in *D. melanogaster* but across several invertebrate species (Palmer et al., 2018), highlighting their importance in antiviral immunity.

C. The Drosophila C Virus

One of the most studied and best characterized viruses in *Drosophila melanogaster*, and the virus that I have used for most of my thesis, is the *Drosophila C Virus* (DCV). It was first identified in 1972 in France by Françoise-Xaviere Jousset (Jousset et al., 1972), and then found in several laboratory stocks and wild fruit fly populations worldwide (Plus et al., 1975; Gomariz-Zilber et al., 1995). The natural route of transmission of DCV is thought to be oral transmission. Although oral infection with DCV causes only a low lethality rate (Ferreira et al.,

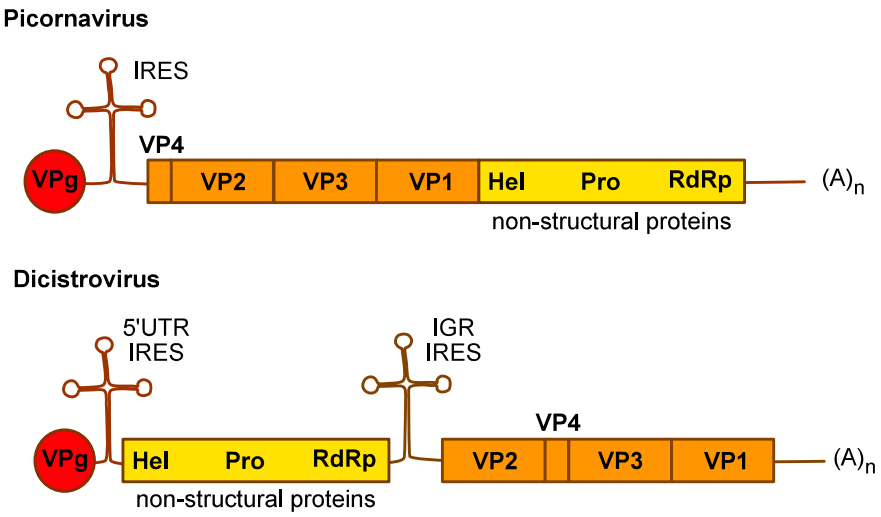

Figure 2. The genome of dicistroviruses is very similar to the genome of picornaviruses.
Because of similarities like the presence of a VPg protein covalently bound to the 5'end of the genome, the *Drosophila C Virus* was first thought to be a Picornavirus. However, the dicistronic organisation of the genome and the presence of non-structural proteins at the 5'end of the genome instead of the 3'end, among other characteristics, lead to the creation of a new family of viruses, the Dicistroviruses. Helicase (Hel), Protease (Pro) and RNA-dependent RNA-polymerase (RdRp) are non-structural proteins and VP1, VP2, VP3 and VP4 are structural proteins encoded by DCV. The virus possesses two Internal Ribosome Entry Sites (IRESs), one at the 5' end of the genome and one in the intergenic region (IGR), between the two ORFs.

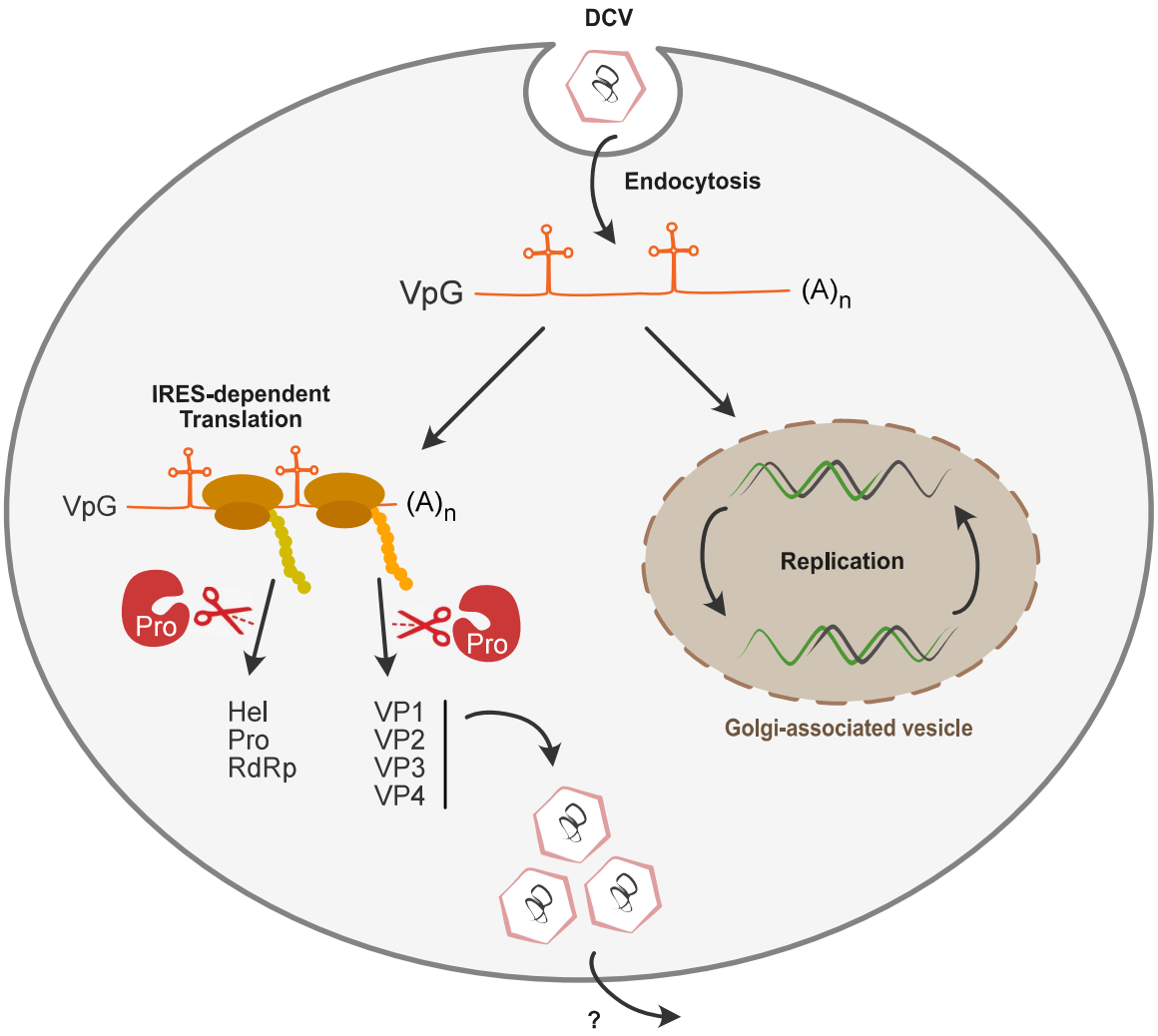

Figure 3. The viral cycle of the Drosophila C Virus.
After DCV enters the cell by clathrin-mediated endocytosis, its genome is replicated inside cellular vesicles derived from the Golgi apparatus, and its two open reading frames are translated into two polyproteins that are then processed and cleaved into structural and non-structural proteins. New viral particles are then assembled and exit the cell by an unclear mechanism.

2014; Gupta et al., 2017), this virus is highly pathogenic when injected into the body cavity of adult flies, replicates at high titers and causes high mortality (Cherry and Perrimon, 2004). The tropism of this virus includes smooth muscles surrounding the crop (a contracting organ allowing food to move into the midgut for digestion) of adult flies. During DCV infection, several midgut genes are repressed and the crop loses its function, causing a starvation-like phenotype and becoming visibly enlarged (Chtarbanova et al., 2014). Although flies reared together can infect each other, there does not seem to be evidence of vertical transmission or germline infections (Plus et al., 1975; Gomariz-Zilber et al., 1995). Of note, this virus is targeted by several immune pathways (Galiana-Arnoux et al., 2006; Goto et al., 2018), including the antiviral RNAi pathway.

The genomic organization of this non-enveloped RNA virus bears a strong resemblance to picornaviruses (**Figure 2**), which is why it was first thought to belong to this family of viruses (Jousset et al., 1977; Thomas-Orillard, 1988). Like picornaviruses, DCV viral particles are icosahedral and the capsid is composed of three major proteins: VP1 (33 kDa), VP2 (29 kDa) and VP3 (28 kDa). However some key differences, like the presence of two Open Reading Frames (ORFs) instead of just one, and the localization of the structural proteins on the 3'end of the genome instead of the 5'end, led to the formation of a new family of picorna-like viruses, called *Dicistroviridae*, by the International Committee on Taxonomy of Viruses (ICTV) (Johnson and Christian, 1998; Bonning and Miller, 2010). This name derives from the dicistronic nature of their genome, which is composed of two non-overlapping ORFs, or cistrons. The ssRNA(+) genome of DCV is relatively small (approx. 9.2 kb) and is covalently linked to a viral VPg protein at its 5'end and polyadenylated at its 3'end. In addition to the proteins mentioned before, DCV encodes a protease (called 2A) and a VSR, the protein 1A. Another characteristic of its genome is the presence of two Internal Ribosome Entry Sites (IRESs), one preceding each ORF. An IRES is an RNA structure that allows the recruitment of the ribosome to the viral mRNA without the requirement of the otherwise mandatory 5'cap, which DCV lacks. There are four classes of IRES structures, from class I IRESs that required all eukaryotic Initiation Factors (eIFs) for translation of the associated ORFs to class IV IRESs, which require no eIFs at all and are very rare. The 5'IRES of DCV is a class III IRES and as such requires a subset of eIFs, but the IRES located in the intergenic region (IGR) of the DCV genome

is a little more unusual, as IGR IRESs from Dicistroviruses are the only know class IV IRESs (Hertz and Thompson, 2011; Mailliot and Martin, 2018).

The work of Cherry and Perrimon has allowed an extensive characterization of the viral replication cycle of DCV (**Figure 3**). The virus enters the cell by internalization *via* clathrin-mediated endocytosis in a low pH compartment (Cherry and Perrimon, 2004; Cherry et al., 2005). Once inside the cytoplasm, the two ORFs are translated into polyproteins *via* IRES-dependent translation. In addition, Cap-dependent translation of cellular mRNAs is inhibited by DCV, leading to preferential translation of the viral mRNAs (Cherry et al., 2005). The polyproteins are then processed and cleaved into structural and non-structural proteins by a DCV-encoded protease (Reavy and Moore, 1983). Once non-structural proteins are synthesized, they induce the remodeling of cellular membranes to form cellular vesicles derived from the Golgi apparatus (Cherry et al., 2006). The viral genome is replicated inside those vesicles by the RdRp, probably by using the VPg protein to prime RNA synthesis in a manner similar to picornaviruses. Finally, mature virions are assembled and exit the cell, although the precise mechanism for their exit remains unclear.

II. Viral dsRNA sensing by RNA helicases

As described in the previous section of this introduction, *D. melanogaster*, similarly to organisms from all domains of life, can be infected by a variety of viruses. In order to fight those viruses, which are by definition obligate intracellular pathogens, the host organisms first need to be able to discriminate between “self” (i.e. cellular components) and “non-self” (i.e. viral components), before any effort to restrict the infection can be made. A common strategy to perform this distinction is the recognition of viral nucleic acids, and in particular viral dsRNA. This recognition can be performed by a family of proteins called DExD-box RNA helicases, which play an important role in antiviral immunity and are present in both mammals and insects.

During my thesis, I had the opportunity to write a review on this subject, which introduces many concepts necessary to the comprehension of my thesis projects, e.g. the conserved role of DExD-box helicases such as the RIG-I-like receptors (RLRs) in antiviral immunity, or the mechanism of Dicer-mediated sensing. For this reason, I have decided to attach this review, written in 2020 and published in the French scientific journal “Virologie”, to this introduction (Rousseau and Meignin, 2020).

Review

Virologie

Virologie 2020, 24 (6) : e36-e52

Viral sensing by RNA helicases

La détection virale par des hélicases agissant sur l'ARN

Claire Rousseau
Carine Meignin

Université de Strasbourg, CNRS UPR9022, Institut de biologie moléculaire et cellulaire, Strasbourg, France

Abstract. A key aspect of antiviral immunity is the distinction between "self" and "non-self" components. This distinction can be established through the detection of double-stranded RNA (dsRNA), a common sign of viral infection, by cytosolic RNA helicases. Depending on the organism, two major antiviral pathways can be induced by dsRNA helicases: RNA interference (RNAi) and interferon (IFN) signaling. In the RNAi pathway, dsRNAs are recognized by a Dicer protein, and are then used for the sequence-dependent recognition and subsequent degradation of the complementary viral RNAs. In the IFN signaling pathway, dsRNAs are recognized by a RIG-like receptor (RLR), which induces a signaling cascade in order to induce the expression of IFNs, cytokines and chemokines. In this review, we discuss the RNA features that can be used by the cell to detect a viral infection, the two aforementioned types of helicase-mediated sensing, as well as some viral escape mechanisms developed to avoid recognition.

Key words : dsRNA, nucleic acid sensing, cytosolic receptors, antiviral immunity, helicases

Résumé. Un élément clé de l'immunité antivirale est la distinction entre les éléments du « soi » et du « non-soi ». Cette distinction peut être effectuée à travers la détection d'ARN double-brin (ARNdb), un signe courant d'infection virale, notamment par des hélicases ARN cytosoliques. Selon l'organisme, deux voies antivirales majeures peuvent être induites par des hélicases ARN: la voie de l'ARN interférence et celle des interférons (IFN). Dans la voie de l'ARN interférence, les ARNdb sont détectés par une protéine Dicer, puis guident la reconnaissance séquence-dépendante et la dégradation subséquente de l'ARN viral complémentaire. Dans la voie de signalisation IFN, les ARNdb sont reconnus par un récepteur RIG-*like* (RLR), conduisant à l'expression d'IFNs, de cytokines et de chimiokines. Dans cette revue, nous abordons les caractéristiques des ARN qui peuvent être utilisées par la cellule afin de détecter une infection virale, les deux types de reconnaissance par des hélicases mentionnées plus haut, ainsi que certains mécanismes d'échappement qui permettent aux virus d'éviter la détection.

Mots clés : ARNdb, reconnaissance des acides nucléiques, récepteurs cytosoliques, immunité antivirale, hélicases

Introduction

Viruses are obligate intracellular pathogens hijacking the cell machinery and using it for their viral cycle. As both viral and host components are present together in the same cell, it is crucial for the host to be able to discriminate them. To this aim, organisms make use of cellular surveillance mechanisms to allow the distinction between "self" and "non-self". Consequently, host organisms have developed strategies to recognize viral components and target them. Furthermore, despite the great diversity of genome types and replication strategies present in the realm of viruses, all of them most of them expose some form of nucleic acids (NAs) to the host immune system at one point during their replication cycle. Indeed, even though most viruses "hide" their RNAs, by using different strategies to prevent their

Correspondence : C. Meignin
<c.meignin@unistra.fr>

doi:10.1684/vir.2020.0872

To cite this article: Rousseau C, Meignin C. Viral sensing by RNA helicases. *Virologie* 2020; 24(6):36-52 doi:10.1684/vir.2020.0872

recognition, all viruses need to transport their mRNAs to the ribosomes in order for them to be translated. It is thus not surprising that nucleic-acid-sensing has become a major part of virus recognition across species [1].

The sensing of one type of nucleic acid in particular, double-stranded RNA (dsRNA), allows the detection of a broad range of viruses. Indeed, in contrast to the others, this type of nucleic acid is, at least temporarily, present in the vast majority of viruses during their replication. In addition to the obvious example of dsRNA viruses, for which the genome itself is composed of dsRNA, there are multiple mechanisms involving the production of dsRNA by viruses. The presence of viral dsRNA can arise, for example, during the genome and antigenome replication by the RNA-dependent RNA-polymerase (RdRp) as in the case of positive-strand ssRNA (ssRNA(+)) viruses (*figure 1*) or as a product of converging bidirectional transcription (DNA viruses). Furthermore, dsRNA structures can also result from the formation of hairpin structures in ssRNAs. The presence of dsRNA was first detected in viruses characterized by a ssRNA(+), dsRNA or DNA genome [2], but also later in negative-strand RNA (ssRNA(-)) viruses [3, 4]. The broad range of viruses expressing dsRNA is further illustrated by the fact that antiviral RNA interference (RNAi), which relies on the detection of dsRNA, has been shown to provide immunity against a wide diversity of viruses, including negative-strand RNA viruses and DNA viruses [3, 5, 6]. No matter how they arise, the detection of the dsRNA molecules relies on host receptors to identify them as foreign NAs. Therefore, cells have developed a vast range of dsRNA sensors. These range from signaling cascade-inducing proteins like endosomal Toll-like receptor (TLR3) in mammals, cytoplasmic receptors like DExD-box RNA helicases family or restriction factors like Protein Kinase R (PKR). PKR, which is induced by interferons, inhibits both cellular and viral protein translation.

Helicases from the superfamilies 1 and 2 are enzymes that use ATP or other nucleotides to bind, move or unfold DNA or RNA molecules. These enzymes are involved at all levels of nucleic acid biogenesis [7]. The Dicer proteins, which are RNA helicases of the DExD-box helicases family, can act directly on the viral dsRNA. Those helicases are characterized by the presence of an Asp-Glu-x-Asp (DExD) motif, and a number of them play roles in the recognition of foreign NAs. Dicer is a key component of the RNAi pathway. In insects, this pathway is one of the main antiviral innate immunity mechanisms. In several organisms, proteins of the Dicer family are able to sense the presence of viral dsRNA, and process it into 20-25 nucleotides (nt) small interfering RNAs (siRNAs), which will serve as a guide to lead a protein of the Argonaute family to the complementary viral RNA (*figure 1*). After complementary intermolecular base pairing, the Argonaute protein will cleave the viral RNA, thus inhibiting viral replication [8]. In vertebrates, which have developed adaptive immunity, based on the recognition of specific antigens, innate immunity still remains active. In mammals, antiviral innate immunity relies on nucleic acid-sensing using receptors rather similar to Dicer, the Retinoid acid-inducible gene I (RIG-I)-like receptors (RLRs) (*figure 1*). RLRs are also members of the DExD-box helicases family, and are phylogenetically linked to the Dicer proteins. The three known members of the RLR family, namely RIG-I, Melanoma Differentiation-Associated protein 5 (MDA-5) and Laboratory of Genetics and Physiology 2 (LGP2), form one of the most important groups of antiviral pattern recognition receptors (PRRs). However, contrary to Dicer, they do not catalytically act on foreign dsRNA. In addition to their helicase domain, RIG-I and MDA-5 contain two amino-terminal caspase recruitment domains (CARDs) that allow them to interact with the mitochondrial adapter molecule MAVS [9]. This will lead to the induction of type I interferons (IFNs) (mainly IFNα and IFNβ) and type III IFNs (IFNλ) which are a hallmark of the NAs sensing by the innate immune system (*figure 1*). More recently, other helicases have been discovered to play a role in innate immunity (*e.g.* DHX9, DHX36 and DDX41) [10-13].

However, in the same way that hosts have evolved defense strategies against viruses, viruses have developed counter-strategies in order to evade the host's immune system. This is particularly well illustrated by arboviruses, as they infect both mammals and insects to complete their replication cycle. In both cases, arboviruses can be detected by host RNA helicases, they thus have developed escape mechanisms against both helicase-mediated viral sensing. As arboviruses generally possess small genomes, it would be interesting to see if they have similar means of escaping the two different antiviral immune systems. Moreover, arboviruses are especially important, as we are fully aware of the potential gravity of zoonotic emerging diseases and the utmost relevance of studying them both in mammals and in their vectors.

Viral RNAs *versus* cellular RNAs

With this pressure for being able to differentiate "non-self" from "self" NAs, host proteins, acting as foreign RNA-sensing receptors, have evolved to form what has been qualified as *nucleic acid immunity*. During the evolution of organisms, from bacteria to mammals, specific receptors as well as an arsenal of nucleases have been selected, allowing the activation of immune pathways and the cleavage of foreign NAs, respectively. This recognition is dependent on several criteria like the structure, the localization and the availability of the nucleic acid ligands.

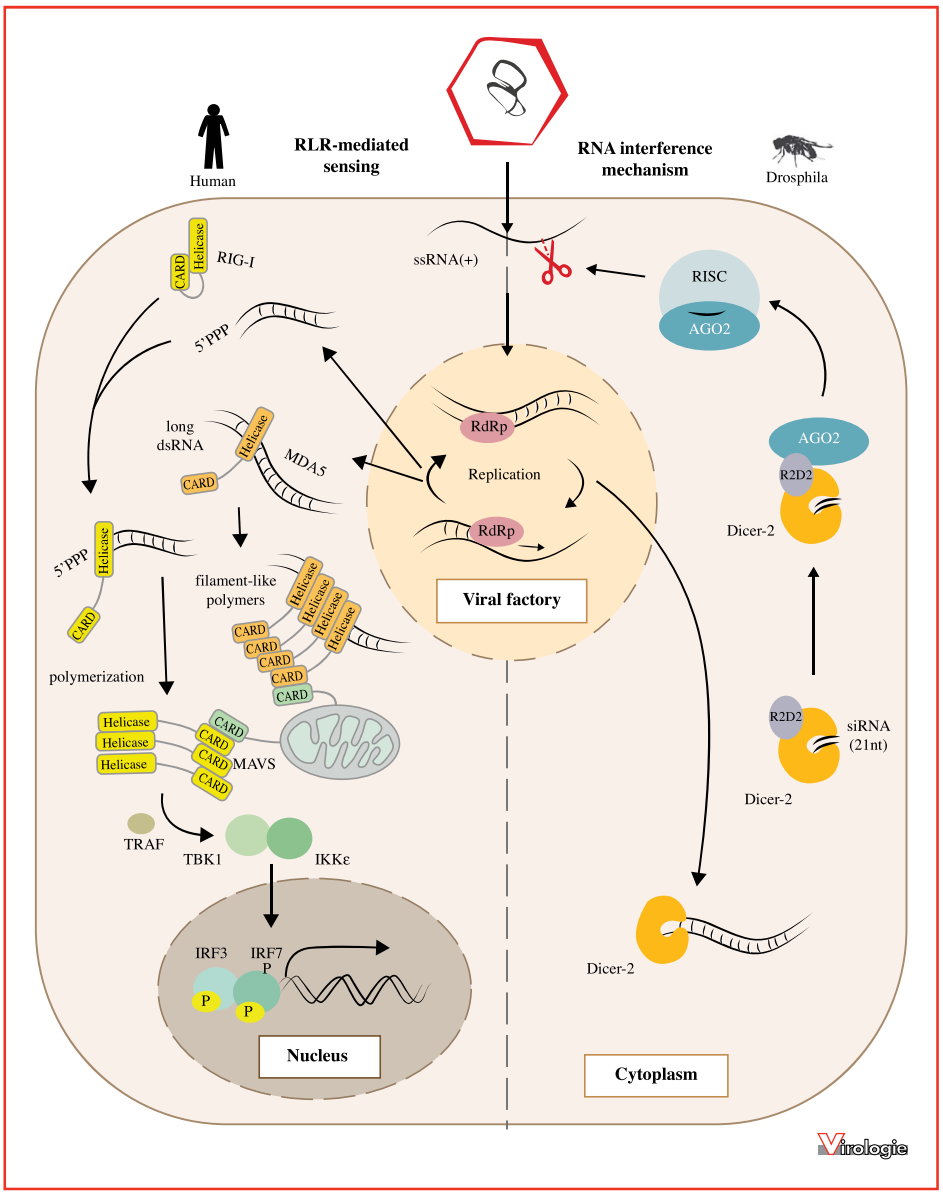

Figure 1. Example of two antiviral pathways against a ssRNA(+) virus: human RLR signalling versus Drosophila RNA interference. Once a ssRNA(+) virus enters the cell, its genome and anti-genome are synthesised by the RNA-dependent RNA polymerase (RdRp), which gives rise to the presence of a dsRNA intermediate, the RNA ligand required for both the RLR pathway and the RNAi pathway. RLR-mediated sensing (left): Once Retinoid acid-inducible gene I (RIG-I) and Melanoma Differentiation-Associated protein 5 (MDA-5) bind to their RNA ligands, RIG-I undergoes a conformational change which frees its CARD domains for interactions, while MDA-5 forms ATP-sensitive filament-like oligomers. They are t'en recruited to the mitochondria, where they interact with Mitochondrial Antiviral Signalling Protein (MAVS). This results in the formation of aggregates, which serve as a signalling platform for the recruitment, and activation of TRAF proteins. The TRAF proteins allow the activation of TANK-binding kinase 1 (TBK1) and IκB kinase-ε (IKKε), which in turn activate IRF3 and IRF7. These transcription factors, together with nuclear factor κB, then translocate to the nucleus, where they induce the expression of the interferons α and β. RNA interference mechanism (right): Once the ligand is recognised by the Dicer-2 endonuclease, it is processed by the endonuclease in order to produce small interfering RNAs (siRNAs) duplexes. These are then loaded onto the Argonaute 2 protein (AGO2) by Dicer-2 and its cofactor R2D2, in order to form the RNA-Induced Silencing Complex (RISC). Upon formation of the RISC complex, one of the two strands composing the siRNA will be discarded while the other one will serve as a guide to lead RISC to the complementary viral RNA. Once RISC reaches its target, it will be cleaved by an Argonaute protein and then degraded, thus inhibiting viral replication.

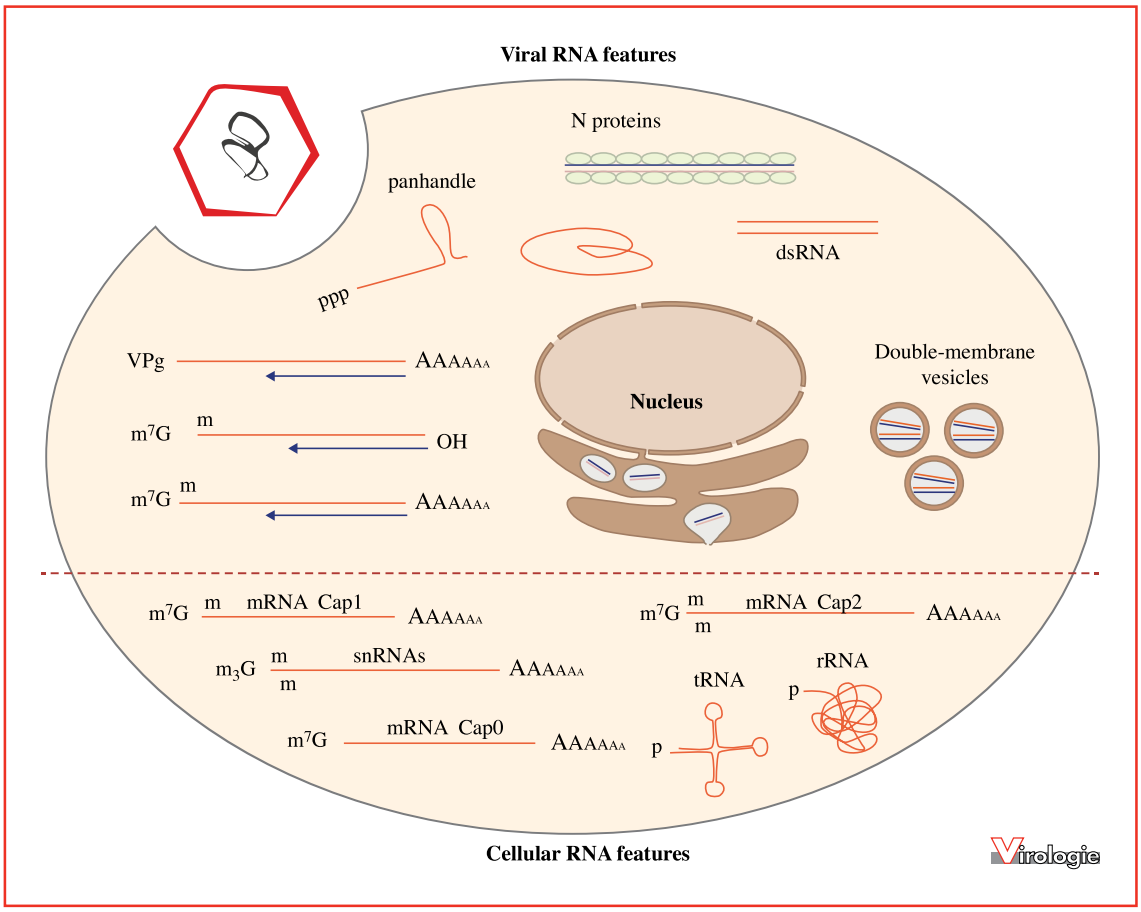

Figure 2. Viral versus cellular RNA features. As the nascent RNAs molecules are synthesized using nucleotide triphosphates (NTPs), the 5' extremity of the RNA molecule contains a free triphosphate. However, endogenous mRNAs are synthesized in the nucleus and then undergo further processing in order to remove this free 5' triphosphate end like base modifications, co-transcriptional 5'capping before their export into the cytosol. The capping pathway, which is found in all eukaryotic species, can contain different levels of methylation (Cap0, Cap1, and Cap2) and can even be hypermethylated as the 2,2,7-trimethylguanosine (m3G) cap. Certain species of cellular RNAs contain different 5' extremities, like tRNAs and rRNAs, which possess a monophosphate. On the contrary, RNA synthesis in the cytosol using an RNA-dependent RNA-polymerase (RdRp), as it is often executed by most RNA viruses, gives rise to the presence of a 5'PPP extremity. To disguise this extremity, some viruses produce their own cap using cellular or viral proteins, or alternatively use a cap-snatching mechanism to steal the cap from cellular mRNAs. Others have a covalently-bound protein like VPg on their 5'end. Moreover, some viruses shield their dsRNA inside viral factories (double-membrane vesicles or through membrane rearrangement of the cellular organelles), or by coating the dsRNA with dsRNA-binding proteins like the N proteins of VSV.

In order to recognize viral RNAs, RLRs and Dicer proteins can detect several structural features of viral RNAs that are different from cellular RNAs. One of those features is the double-stranded nature of the RNA (*figure 2*). In the cytoplasm, long dsRNA molecules generated during viral infection are a major molecular pattern detected by various NAs sensors. Intracellular cytosolic RNA helicases, like RLRs in mammals and Dicer-2 in insects, are essential to detect viral RNA and especially the double-stranded nature of the RNA [14]. Moreover, RIG-I was shown to recognize the 5' ends of the dsRNA [15-17]. Indeed, as the nascent RNAs molecules are synthesized using nucleotide triphosphates (NTPs), the 5' extremity of the RNA molecule contains a free triphosphate (5'PPP). However, eukaryotic endogenous RNAs are synthesized in the nucleus and then undergo further processing in order to remove this free 5'PPP end, for example base modifications like the 5'cap, which is co-transcriptionally added before the export into the cytosol in an RNA polymerase II-dependent manner (*figure 2*). Furthermore, the presence of a 5' monophosphate on RNAs (5'P RNA), common for host RNAs, actively antagonizes RIG-I signaling by inhibiting RIG-I activation [18]. On the contrary, the presence of a 5'PPP (5'PPP RNA) extremity highlights a polymerase activity in the cytosol and is recognized as "non-self" (*figure 2*). The presence of 5' diphosphate (5'PP RNA) blunt-ended RNA, as

found in reovirus genomic RNA, is also recognized by RIG-I and induces type I IFN [19]. For its part, MDA-5, another member of the RLR family, senses long dsRNAs. Indeed, it was shown that MDA-5 recognizes poly(I:C), which mimics dsRNA [20, 21]. In insects, long dsRNAs are sensed by the endonuclease Dicer-2 which is hitherto the only known antiviral cytosolic receptor. Drosophila Dicer-2 (dmDicer-2) has been shown to recognize two types of free 5' extremity structures of dsRNAs which are 3' 2-nt overhangs and blunt extremities. Indeed, the recognition of its substrate by dmDicer-2 relies on two domains: the platform-PAZ domain, which contains a phosphate-binding pocket and a 3' 2-nt overhang pocket [22] and the helicase domain, which uses ATP to process dsRNA [23-25]. Of note, Dicer-2 enzymes share a common phylogenetic origin for the helicase domain, which is required to sense NAs, with RLRs [14]. Structural, biochemical and genetic studies could give a better understanding on how this conserved helicase domain recognizes its RNA substrates.

RNA modifications, commonly referred to as the epitranscriptome, are observed on specific residues of cellular RNAs and play a key role in their processing and functionality, as these labels help discriminate between "self" and "non-self". Amongst more than 150 chemical modifications described, nucleotide methylation in different positions is the most abundant [26]. Several publications have highlighted the importance of these modifications for the recognition of viral RNA in mammals. RNAs with post-transcriptional modifications synthesized *in vitro* do not activate the mammalian immune system, suggesting that these modifications mask recognition by cytoplasmic receptors [27, 28]. For example, RNA editing by the adenosine deaminase ADAR1 prevents the sensing of endogenous dsRNA as "non-self" by MDA-5 [29]. Recent studies have also demonstrated the impact of 2'-O-methylation and N6-methyladenosine (m^6A) to escape viral sensing by RIG-I or MDA-5 [30, 31].

The presence of double-stranded structures, the biochemical nature of the 5' end of RNAs and the presence of epitranscriptomic marks thus constitute the determinants of nucleic acid recognition by the above-mentioned first aspect. A good example of the second aspect, localization, is the family of Toll-like receptors (TLRs). In mammals, TLRs are transmembrane glycoproteins localized in endosomal compartments or at the cell surface, which respond to extracellular or endocytosed NAs in the case of viruses. In 2001, TLR3 was the first RNA receptor described to induce type I IFNs in the presence of a dsRNA ligand [32]. In order to recognize all the aforementioned differences, however, the viral RNA molecule needs to be available to interact with the different sensors of the host. This is where the third aspect, availability, comes into play. The availability of the viral RNA is one of the factors which will determine if it will be detected by the host or not. The viral RNA sensing will also depend on its concentration in the cell, its degradation rate, and most importantly its shielding. Indeed, viruses have evolved a number of strategies to protect their components from the cell. An example of this is the formation of viral factories by some viruses, or the addition of proteins like the viral protein VPg from picornaviruses and dicistroviruses which is covalently linked to the 5' extremity of dsRNA and prevents degradation by the XRN1 exonuclease (*figure 2*). Finally, the shielding of RNA by viral proteins is also a masking mechanism used by some viruses.

Dicer-mediated sensing

In plants, fungi and invertebrates, RNAi provides RNA-based protection against viruses. The RNAi antiviral immune pathway is a defense mechanism used by many organisms to fight viruses, and relies on the detection of dsRNA. The antiviral activity of RNAi was first observed in plants [33] and then highlighted in animals with the finding that the Flock House Virus (FHV) both initiates and is a target of RNAi in drosophila S2 cells [34]. RNAi can be subdivided into three main pathways: the microRNA (miRNA) pathway, which allows for gene regulation; the piwiRNA (piRNA) pathway, which regulates transposons and the siRNA pathway, which is responsible for the inhibition of exogenous and endogenous RNAs and is the one responsible for the restriction of viral RNAs. As aforementioned, many viruses produce dsRNA at one point during their replication cycle. This dsRNA is recognized by a Dicer endonuclease, which will cleave it in order to produce small interfering RNAs (siRNAs) (*figure 1*, right). These will then be loaded onto an Argonaute protein in order to form the RNA-Induced Silencing Complex (RISC). Upon formation of the RISC complex, one of the two strands composing the siRNA will be discarded while the other one will serve as a guide to lead RISC to the complementary viral RNA. Once RISC reaches its target, it will be cleaved by the Argonaute protein and then degraded, thus inhibiting viral replication. A hallmark of the RNAi pathway is the production of small RNAs with specific sizes (generally 21 to 30-nt). A metagenomic analysis using small RNA sequencing has highlighted the presence of a diversity of virus-derived small RNAs, and highly divergent RNAi responses across multicellular eukaryotes. [35].

In the RNAi pathways, the proteins responsible for the recognition of dsRNAs are the Dicer proteins. Some organisms, like *Caenorhabditis elegans* or *Homo sapiens*, encode only one Dicer protein, which produces both miRNAs and siRNAs, and others, like *Drosophila melanogaster*, encode

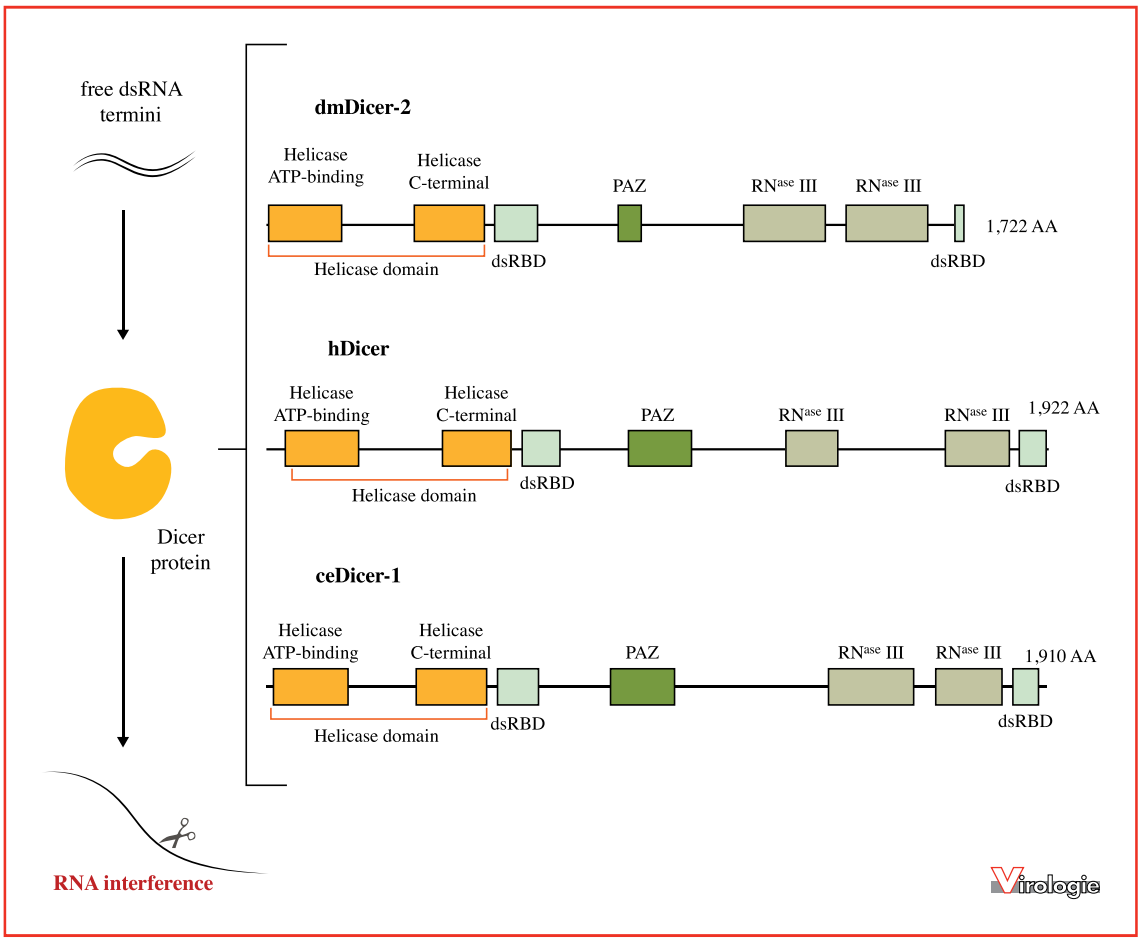

Figure 3. Dicer protein structures across species. Dicer proteins are dsRNA-specific endonucleases from the RN^{ase}III family and the DExD-box helicases family. Those helicases are characterized by the presence of an Asp-Glu-x-Asp (DExD) motif, and a number of them play roles in the recognition of foreign nucleic acids. Dicer proteins possess a central, atypical dsRNA-binding domain (dsRBD), a C-terminal dsRBD, two RN^{ase}III domains, a helicase domain and a PAZ domain. The helicase domain of Dicer, located at the Nter extremity of the protein, does not hydrolyse ATP in all Dicer proteins. Production of siRNAs from dsRNAs requires ATP in C. elegans and D. melanogaster (only for dmDicer-2 but not dmDicer-1). On the contrary, although the helicase domain is conserved in human Dicer, it does not hydrolyse ATP *in vitro*. The platform-PAZ domain contains a phosphate-binding pocket, which recognizes the 5'monophosphate of both long and short dsRNA substrates and anchors the 5'end of the RNA substrate.

two Dicer proteins, specific to one of the two pathways (*figure 3*). Dicer proteins are part of the RN^{ase}III family, which means that they are dsRNA-specific endonucleases. Indeed, they possess a central, atypical dsRNA-binding domain (dsRBD) previously known as DUF283, a C-terminal dsRBD and two RN^{ase}III domains (*figure 3*). The RN^{ase}III activity of Dicer requires Mg^{2+} [36, 37]. In addition, two other domains, the helicase domain and the platform-PAZ domain, have been shown to play a role in dsRNA sensing. The helicase domain of Dicer, located at the N-terminal extremity of the protein, does not hydrolyse ATP in all Dicer proteins described. Production of siRNAs from dsRNAs requires ATP in *C. elegans* and *D. melanogaster*. Of note, only drosophila Dicer-2 (dmDicer-2), associated with the siRNA pathway, possesses a functional helicase domain and is able to bind ATP [38]. On the contrary, drosophila Dicer-1 (dmDicer-1), associated with the miRNA pathway, has a degenerate helicase domain. Furthermore, although the helicase domain is conserved in human Dicer, ATP hydrolysis is not required for dsRNA cleavage *in vitro* [37]. For its part, the platform-PAZ domain contains a phosphate-binding pocket, which allows it to recognize the 5'-monophosphate of both long and short dsRNA substrates. It is thus able to anchor the 5'end of the RNA substrate. This ensures the high-fidelity production of 21-nt siRNAs, as the distance between the phosphate-binding pocket and the RN^{ase}III domains corresponds to a molecular ruler for the measurement of 21 nt [22].

In *Drosophila melanogaster*, two modes of action have been described for dmDicer-2, depending on the termini of the dsRNA substrate [39]. Using gel shift assays, Sinha *et al.*, demonstrated that dmDicer-2 requires a functional helicase domain in order to bind blunt dsRNA but not dsRNA with 3' 2-nt overhangs. Two types of substrate are recognized and cleaved. The first one, 3' 2-nt overhangs dsRNA, is dependent on the platform-PAZ domain and the second one, blunt dsRNA, is dependent on the helicase domain. The 3' 2-nt overhangs termini promotes an ATP-independent mechanism called distributive dicing, while blunt termini promotes an ATP-dependent mechanism called processive dicing. In the former, which is independent from the helicase domain, dmDicer-2 dissociates from the dsRNA molecule after each cleavage to produce a siRNA duplex of exactly 21-nt, whereas in the latter, which requires a functional helicase domain, dmDicer-2 produces a heterogeneous population of multiple siRNAs with less length-fidelity before dissociating. The platform-PAZ domain has been shown to be crucial for high siRNA length-fidelity, essential for distributive processing by dmDicer-2 [22]. Another hypothesis is that only the first cleavage of blunt dsRNA produces siRNAs of approximately 21 nt and that after the first cleavage, the 5'monophosphate-anchoring mechanism is possible, allowing dmDicer-2 to produce high-fidelity 21-nt siRNA even during processive dicing [22]. In contrast to dmDicer-2, human Dicer (hDicer) does not distinguish termini of the dsRNA substrate *in vitro* and the helicase domain does not have a threading activity [39]. Moreover, deletion of the helicase domain of hDicer increases its processivity, suggesting that the helicase domain disrupts its functionality but is not required for dsRNA sensing [40].

Purified dmDicer-2 and hDicer are catalytically active *in vitro* in the absence of binding partners [23, 24, 40]. Most of those partners are dsRNA-binding proteins (dsRBPs), and interact with the helicase domain of Dicer proteins. As dmDicer-2, which produces only siRNAs, and hDicer, which produces both siRNAs and miRNAs, share a similar domain architecture (*figure 3*), structural differences between dmDicer-1 and dmDicer-2 are unlikely to explain their substrates specificities [23]. However, it has been shown that the cofactors of the different Dicer proteins can modulate or restrict this substrate specificity. For example, two small dsRBPs, R2D2 and Loqs-PD, interact with dmDicer-2 and define the endo- and exo-siRNA pathways depending of the endogenous or exogenous origin of the dsRNAs [41, 42]. Indeed, R2D2 and inorganic phosphate can prevent dmDicer-2 from processing pre-miRNAs into miRNAs and restrict it to the production of siRNAs [23]. R2D2 forms a stable complex with dmDicer-2 and is necessary for the loading of siRNAs onto AGO2 [43, 44]. Moreover, also in *D. melanogaster*, different isoforms of the Loquacious (Loqs) protein are involved in different RNAi pathways: Loqs-PB and Loqs-PD are involved in miRNA and endo-siRNA dicing, respectively [41, 45]. Loqs-PD is required for and facilitates cleavage of its suboptimal substrate, endo-siRNA, but it is not required for antiviral RNAi [42, 46]. It is unclear if R2D2 and Loqs-PD can bind Dicer-2 simultaneously. In *Aedes aegypti*, a hematophagous insect vector, DENV fails to be controlled by the siRNA pathway in the midgut even though the canonical RNAi pathway is functional. The Loqs2 protein, a cofactor of R2D2, appears to be the missing component in the midgut and indispensable to activate the antiviral RNAi pathway in *Aedes aegypti* [47]. Taken together, these studies suggest that Dicer-2 could be a versatile protein whose mode of action is regulated by its cofactors *in vivo*. In humans, hDicer can form stable complexes with transactivation response RNA-binding protein (TRBP) or protein activator of PKR (PACT). The two RBPs both bind to the same subdomain of hDicer, which suggests that they interact in a mutually exclusive manner [48]. TRBP and PACT have been shown to have distinct effects on Dicer-mediated dsRNA processing [49]. Indeed, complexes containing PACT or TRBP do not result in the same isomiRNAs (miRNA sequences that have variations compared to the sequence of the pre-miRNA) being produced from the same pre-miRNA and PACT seems to inhibit the processing of pre-siRNA [49]. Interestingly, both PACT and TRBP bind to the interferon-induced protein kinase PKR, involved in RLR-mediated signaling. The two pathways thus share some interactants, suggesting that there may be some crosstalk. Of note, the RLR LGP2 binds hDicer and inhibits processing of dsRNAs to siRNAs [50]. The study of those interactants will allow the elucidation of the crosstalks between those two pathways.

Up to date, it is unclear if Dicer plays a role in antiviral defense in mammals. In insects, the role of Dicer-2 in antiviral RNAi has been clearly established [6, 34, 51]. However, on the contrary to plants and invertebrates, evolution has allowed mammals to select another defense system against viruses, the IFN system. The existence, as well as the relevance of an antiviral function of RNAi in mammals have therefore been questioned. First, the presence of poly(I:C), which mimics dsRNA, induces a strong RLR-dependent IFN response [20, 21]. Second, in somatic cells in which the IFN pathway had been inactivated, the introduction of dsRNA leads to the production of Dicer-dependent siRNAs and AGO2-dependent silencing [52]. Some studies go even further, as they suggest that mammalian RNAi is readily detectable in IFN-competent somatic cells [53, 54]. Moreover dmDicer-2 expression in human HEK293 cells impairs IFN response upon treatment with poly(I:C) and seems to compete with dsRNA-sensing factors like PKR [55]. This highlights a functional incompatibility between the Dicer

machinery and the IFN response. The presence of viral suppressors of RNAi (VSRs) in mammalian viruses could suggest the implication of the siRNA pathway as an antiviral response, as several of these viral proteins have been reported to interact directly with Dicer or encode dsRNA binding proteins [56, 57]. Some studies have highlighted an inherent conflict between the IFN pathway and the RNAi machinery [50, 55, 58]. This could, in part, explain the inefficiency of RNAi as an antiviral defense mechanism in mammalian somatic cells.

RLR-mediated sensing

In contrast to Dicer enzymes, RLRs induce a signaling cascade instead of directly acting on the dsRNA, in order to induce a global antiviral response (*figure 1*, left). Once they bind to their RNA ligands, RIG-I proteins undergo a conformational change that frees their CARD domains, rendering oligomerization possible. In order to complete its activation, RIG-I t'en undergoes the non-degradative polyubiquitination of several of its lysine residues, in the form of K63 polyubiquitin chains. Several proteins have been proposed as responsible for this activation by polyubiquitination. First of all, Gack *et al.,* suggested that the tripartite motif protein 25 (TRIM25), could be responsible for this activation, through the polyubiquitination of the RIG-I CARD domains, in particular on the K172 residue [59]. Two other proteins, MEX3C and TRIM4, were t'en suggested to be responsible for the polyubiquitination of CARD domains [60, 61]. Finally, Oshiumi *et al.*, proposed that the ubiquitin ligase Riplet is responsible for this activation, this time by polyubiquitination of the CTD of RIG-I [62]. The potential redundancy or complementarity of these different proteins remains to be elucidated, but in any case, this ubiquitination is crucial for the subsequent CARD-CARD interaction between RIG-I and the MAVS protein on the mitochondria [63]. By opposition, the activation mechanism of MDA-5 does not occur after polyubiquitination, but binding to its RNA ligands results in the formation of ATP-sensitive MDA-5 polymers that also interact with MAVS [64]. This results in the formation of aggregates which serve as a signaling platform for the recruitment and activation of TRAF proteins. The TRAF proteins allow the activation of TANK-binding kinase 1 (TBK1) and IκB kinase-ε (IKKε), which in turn activate IRF3 and IRF7. These transcription factors, together with nuclear factor κB (NFκB), en translocate to the nucleus, where they induce the expression of the interferons α and β (IFNα/β). The strength of this antiviral pathway is amplified by the presence of a positive-feedback loop, as RIG-I, MDA-5 and LGP2 are strongly induced by IFNs [65].

Upon binding to their RNA ligands, RIG-I and MDA-5 become activated and induce the type I IFN signaling pathway. Many studies have focused on the mechanism of auto-repression and activation of RIG-I [66, 67], before the study of crystal structures of RIG-I in both ligand-free and ligand-bound states showed the sequestration of the two CARD domains by a helical domain inside the helicase domain, maintaining RIG-I in a repressed state [68] (*figure 1*, left). The binding of both ATP and the RNA ligand to the helicase domain of RIG-I induces a conformational change that liberates the CARDs, and allows oligomerization and downstream signaling. In contrast to RIG-I, unbound MDA-5 CARD domains are flexible and do not interact with other MDA-5 domains [69]. Instead, MDA-5 autoregulates itself in a dsRNA length-dependent manner [64]. When MDA-5 binds its RNA ligand, it assembles into helical filament-like polymers through interaction of the CARD domains (*figure 1*, left). Those filaments are sensitive to ATP hydrolysis, which is stimulated by the binding of MDA-5 to the dsRNA, and induces length-dependent filament disassembly [64]. ATP hydrolysis enhances the binding specificity for long dsRNAs and promotes the formation of more continuous and stable filaments while promoting dissociation from shorter dsRNAs [70]. Moreover, ATP hydrolysis upon binding of MDA-5 to the dsRNA was shown to induce significant distortions in the dsRNA backbone, and was proposed to serve as a proofreading mechanism, that tests the physical properties of the RNA, therefore ensuring that MDA-5 only remains associated with a cognate ligand [71].

RIG-I and MDA-5 have mostly complementary roles, and they recognize distinct features of RNA ligands. Both RIG-I and MDA-5 can bind dsRNA ligand *in vitro* but RIG-I preferentially senses the extremities of short dsRNA between 30 to 300bp [66, 72-74] while MDA-5 senses dsRNA up to 2kb [21, 75]. These differences allow the recognition of a large range of viruses and the activation of the IFN response. The 5'PPP RNA, as well as 5'PP RNA, can be recognized by RIG-I if it is fully base-paired at its 5' end, as is the case for many negative-strand RNA viruses [15-17, 19, 72]. RIG-I can therefore recognize infections caused by many negative-strand RNA viruses like Influenza A virus (IAV) or Vesicular stomatitis virus (VSV), but also some positive-strand viruses (*e.g.* HCV) [21, 76]. By opposition, MDA-5 is activated during infections by picornaviruses like encephalomyocarditis virus (EMCV), as the 5' extremity of their RNA is protected by the covalently-bound viral protein VPg [21, 77]. Recently, a comparative genomic analysis has revealed that pangolins are MDA-5 deficient in opposition to the Carnivora order (cat-like and dog-like carnivorans) [78]. This data suggests that pangolins have different antiviral responses in comparison to other mammals and could therefore be more tolerant to some viral

infections. Finally, RIG-I and MDA-5 can have redundant roles during infection, as they both sense infections by reoviruses and flaviviruses (*e.g.* DENV and West Nile virus (WNV)), suggesting that these viruses could produce different RNA species in the course of infection [76, 79]. Interestingly, a recent study has identified a nuclear-resident RIG-I involved in nuclear viral RNA sensing and able to induce an IFN response against IAV, an RNA virus replicating in the nucleus [80]. This antiviral response was coordinated between nuclear RIG-I and the cytoplasmic components of the IFN system.

LGP2, the third member of the RLRs family, lacks the two CARD domains and therefore cannot induce any signaling cascade via MAVS (*figure 4*). Consequently, its role in antiviral immunity is unclear. Like MDA-5, LGP2 binds dsRNA independently of the 5'PPP RNA extremity [81]. There is some evidence pointing to a dual function of LGP2 as both a negative regulator of RIG-I and positive regulator of MDA-5 [82, 83]. It has been suggested that negative regulation of RIG-I signaling was performed *via* competition for dsRNA, and that positive regulation of MDA-5 signaling required ATP hydrolysis by LGP2 [81, 84]. Supporting the hypothesis of a positive regulation of MDA-5 by LGP2, Paramyxovirus V proteins target the helicase domain of both LGP2 and MDA5 (but not RIG-I as its helicase domain is divergent from LGP2 and MDA-5). By disrupting ATP hydrolysis, V proteins prevent positive regulation but not negative regulation of RLR signaling, as only positive regulation of MDA-5 has been shown to require ATP [85, 86]. Interestingly, the hDicer partner PACT was shown to also interact with LGP2, and this interaction was necessary for both positive regulation of MDA-5 signaling and negative regulation of RIG-I signaling [87]. This protein, being an interactant of both hDicer and a RLR, could be worth studying, as it indicates a connection between the RNAi machinery and the RLR signaling pathway [50].

Finally, the immunostimulatory activity of 5'PPP RNA is suppressed by common eukaryotic post-transcriptional modifications like 2'-O-methylation [15]. For example, the RIG-I tolerance to 2'O-methylated RNAs is mediated by a conserved amino acid in the RNA binding pocket of RIG-I, which prevents their recognition [88]. This tolerance mechanism is very important, as abnormal activity of RLRs (*e.g.* constitutive activation of RLRs due to mutations in the associated genes) can lead to aberrant sensing of cellular RNAs by RLRs. Accumulating evidence suggests that the hyperactivation of RLR pathways is associated with a number of diseases like some types of autoimmune diseases and autoinflammatory diseases. For example, mutations in the genes coding for MDA-5 and RIG-I were linked to the development of Singleton-Merten syndrome [89, 90], Aicardi-Goutières syndrome [91, 92] and systemic lupus erythematosus [93, 94]. Moreover, recent studies have highlighted the positive and negative impacts of RIG-I in different types of cancer, as ectopic activation of RIG-I in cancer cells can either promote their apoptosis or promote resistance to radiation and chemotherapy due to high levels of ISG expression [95-98]. Further research is needed in order to determine the exact impact of RLRs on cancer cells, and whether or not it could be used as a potential therapeutic target or as an element to consider before prescribing certain cancer treatments.

Other helicases involved in viral sensing

Interestingly, RLR-like proteins are also present in non-vertebrate organisms as in the worm *C. elegans,* where three genes encode RLR-like receptor homologs called dicer-related helicases 1, 2 and 3 (DRH1, DRH-2 and DRH-3) [99, 100]. It has been shown that DRH-1 is dispensable for exogenous long dsRNAs processing but is essential for antiviral RNAi, where it acts downstream of Dicer to enhance siRNA production [101, 102]. Beyond the canonical antiviral response through RIG-I and MDA5, several DExD/H box helicases have been implicated in viral RNA sensing [103]. RNA helicases DDX1, DDX21 and DHX36 were found to form a complex and sense dsRNA, resulting in the activation of type I IFN responses in myeloid dendritic cells [12]. Again in myeloid dendritic cells, DHX9 was shown to sense poly(I:C), reovirus and IAV and to induce an antiviral response [13]. This response was dependent on the interaction of DHX9 and MAVS, through the CARD domain of MAVS, and suggests a role of DHX9 in antiviral immunity. Moreover, DHX9 was recently found to enhance the expression of a subset of interferon-stimulated genes (ISGs) in response to Epstein-Barr virus (EBV), even though it did not have any impact on IFN production [10]. Interestingly, in apparent contradiction to this, DHX9 was found to be a proviral factor in several previous studies [104-106], and in contrast to the results of Zhang *et al.*, to enhance IAV RNA replication and transcription [107]. More research therefore seems to be needed in order to shed light onto the contradictory effects of DHX9 on different viruses. Other RNA helicases like DDX60 are themselves ISGs, allowing a reinforcement of the antiviral response [108, 109]. Finally, DHX36 was found to have an important role in RIG-I signaling, by facilitating dsRNA binding and phosphorylation of PKR [11]. As a great number of RNA helicases are often associated with viral RNAs, it would be interesting to study the exact role of each one, in order to understand how these proteins could play a role in antiviral immunity and/or in viral replication.

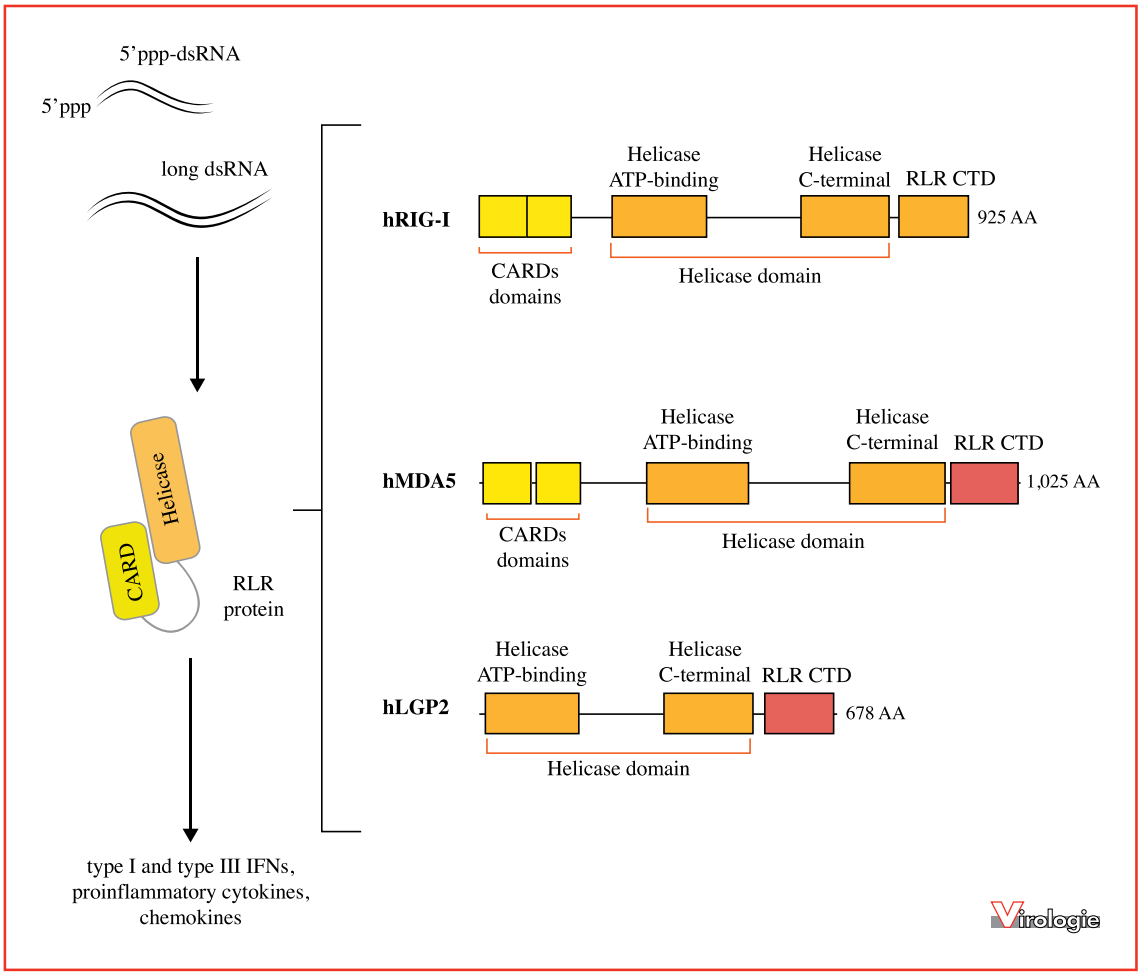

Figure 4. Structures of the different RLRs. Like Dicer proteins, RIG-I-like receptors are also part of the DExD-box helicases family, and also contain an Asp-Glu-x-Asp (DExD) motif. RIG-I, MDA-5 and LGP2 recognize different ligands. RIG-I recognizes 5'triphosphate, as well as 5'diphosphate, if it contains a portion of fully base-paired RNA at its 5'end, as is the case for many negative-strand RNA viruses. By opposition, MDA-5 recognizes long stretches of dsRNA (up to 2kb). Like MDA-5, LGP2 binds dsRNA independent of 5'PPP RNA. However, LGP2 lacks a CARD domain and therefore cannot induce any signaling cascade. Apart from that, the rest of the structure of the three proteins are similar, as they all contain a helicase domain and a C-terminal Regulatory Domain (CTD).

Arboviruses are targeted by both RLRs and Dicer

In order to escape recognition from helicase-mediated sensing, viruses have developed a number of different strategies, depending on the immune system against which they need to defend themselves. Arthropod-borne viruses, or arboviruses, have the particularity of having to defend themselves against both RNAi and RLR-mediated immunity, as they need to replicate both in the insect and the mammalian systems. They are transmitted to vertebrate hosts by hematophagous (blood-feeding) arthropod vectors like mosquitoes. Arboviruses from the *Flaviviridae* family include viruses that are particularly relevant for Public Health, such as Dengue virus (DENV), Yellow fever virus (YFV), West Nile virus (WNV), Kunjin virus (KUNV) and Zika virus (ZIKV), which can cause severe symptoms in humans [110].

In mammals, a variety of arbovirus proteins have functions linked to viral escape. To cite only one example, DENV is known to express a number of proteins, involved in the inhibition of RLR signaling, like NS2A, NS3, NS4A, NS4B and NS5 (*figure 5*). NS3 binds to the 14-3-3ε protein, responsible for the translocation of RIG-I to the mitochondria, thus inhibiting the interaction between MAVS and RIG-I [111], which is further inhibited by the interaction of NS4A with MAVS [112]. Moreover, NS4B and NS2A prevent the TBK1 phosphorylation and subsequent IRF3

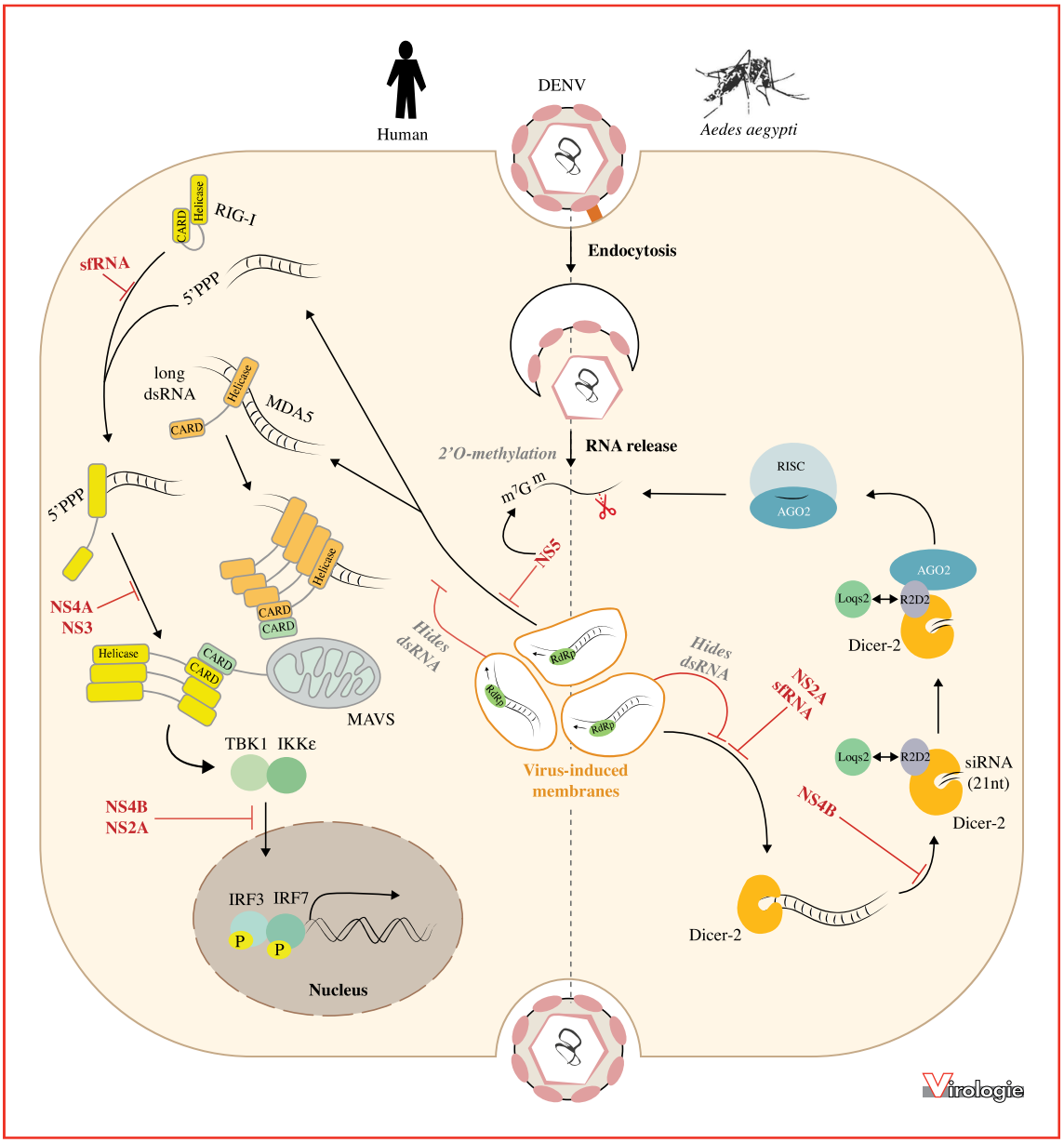

Figure 5. Dengue virus antiviral response and viral suppressors. Example of DENV, an arbovirus with escape mechanisms for both its human and mosquito hosts. DENV replicates inside virus-induced membranes [126], thus shielding its dsRNA from the recognition of both RLRs in humans and Dicer-2 in *aedes aegypti*. In mammals, several DENV proteins act at different levels of the IFN immune response. sfRNA inhibits activation of RIG-I by binding to the TRIM25 protein, which normally ubiquitinates RIG-I in order to activate it [116]. NS3 prevents the translocation of RIG-I to the mitochondria by binding to the protein responsible for this translocation, 14-3-3ε [145], and NS4A further inhibits binding between RIG-I and MAVS by interacting with MAVS [112]. Moreover, NS4B and NS2A prevent the TBK1 phosphorylation and subsequent IRF3 phosphorylation [113]. Finally, NS5 allows the mimicking of cellular mRNA by inducing a 2'O-methylation on viral RNA [114], which is a modification that inhibits recognition by RIG-I. In insects, three of those viral factors, sfRNA, NS2A and NS4B, have been shown to be VSRs, although they act by mechanisms distinct from those described for mammals just above. A model where highly expressed sfRNA acts as a decoy to prevent the RNAi machinery from processing the less abundant viral gRNA has been described [119]. In addition, NS2A and NS4B have been shown to sequester dsRNA and prevent its binding and processing by Dicer-2 [146, 147].

phosphorylation [113] and NS5 induces a 2'O-methylation on viral RNA, thus mimicking cellular mRNAs [114]. Finally, another factor from DENV has an impact on the RLR pathway: a small subgenomic flavivirus RNA (sfRNA) produced by all viruses of the *Flavivirus* genus. It was identified as the product of incomplete degradation by the 5′–3′ exoribonuclease XRN1, due to the presence of highly conserved structures that prevent this nuclease from digesting the 3'UTR [115]. sfRNA inhibits activation of RIG-I by binding to the TRIM25 protein, which normally ubiquitinates RIG-I in order to activate it [116].

However, the need to develop VSRs *per se* to fight RNAi in the mosquito has been subject to some debate. Indeed, arboviruses appear to be continually targeted by RNAi [117], but infections are usually asymptomatic in mosquito vectors when the RNAi pathway is functional. However, RNAi inhibition is detrimental to Aedes mosquitoes in the context of alphavirus infection, as the use of a recombinant Sindbis virus (SINV) expressing the B2 VSR from FHV increases mosquito mortality compared to wild-type SINV [118]. RNAi inhibition in mosquito vectors could therefore have an impact on the fitness of the vectors and thus hinder virus transmission. Therefore, do arboviruses really need VSRs, or can they simply let the vector's immune system control the virus titer in order to propagate for a longer period of time? Although the absence of VSRs in arboviruses has long been presumed, some VSRs have been identified in flaviviruses (DENV, WNV, KUNV and YFV), and later in other arboviruses such as the chikungunya virus (CHIKV, *Togaviridae* family, *Alphavirus* genus) [119-121].

The sfRNA from DENV and WNV was shown to suppress siRNA- and miRNA-induced RNAi pathways in mammalian and insect cells [119]. This was supported by results showing that sfRNA of DENV and KUNV significantly represses siRNA-mediated RNAi in infected human cells and during infection of the *Culex* mosquito vector and associates with Dicer-2 and AGO2 [120]. However, another study did not manage to see any significant difference in the abundance of viral siRNAs after infection with wild-type or sfRNA1-deficient WNV in *Culex* mosquitoes [122]. The authors did however show that sfRNA is processed by the mosquito RNAi machinery and that sfRNA1-defective WNV mutants have a differential virus-derived siRNA profile in the 3'UTR. The different studies seem to agree on the hypothesis that the abundantly produced sfRNA could act as a decoy to prevent the RNAi machinery from processing the less abundant genomic viral RNA.

Also in viruses from the *Flavivirus* genus, two proteins from DENV, NS4B [123] and then NS2A [124] were claimed to be VSRs. NS4B suppresses RNAi by interfering with hDicer activity in mammalian cells, however the underlying mechanism remains unknown. NS2A suppresses Dicer-dependent siRNA production in both mammals and mosquitoes. The authors found that NS2A, which is able to bind dsRNA *in vitro*, inhibits RNAi by sequestering dsRNAs from hDicer. However, a study using mosquitoes infected by SINV expressing the WNV sfRNA or the DENV NS2B protein failed to see any significant difference compared to the survival of mosquitoes infected with control viruses [121]. Those results were corroborated by viral load measurement, suggesting that those VSRs offer a negligible protection against RNAi in *Aedes aegypti*. This could suggest that the expression of these potential VSRs alone is not sufficient to inhibit RNAi, and that they might need the presence of another factor. Using the same system, the capsid of YFV was identified as another dsRNA-binding VSR. The authors suggest that YFV acts by shielding the dsRNA and preventing processing by Dicer-2. Finally, using a GFP reversion assay to assess for RNAi sensor suppressor activity in cells, Mathur *et al*., identified CHIKV nsP2 and nsP3 as VSRs [125]. They demonstrated that this RNAi suppressor activity relies on the RNA-binding motifs of the two proteins, conserved across all alphaviruses. This suggests a potential shielding or inhibition of dicing by the two VSRs.

To date, the potential role of most VSRs in arboviruses therefore remains unclear. As mentioned above, arboviruses go from an antiviral RNAi system in insects to an IFN system in mammals. The interactions between these two systems are not yet fully elucidated, but a competition between them has been highlighted. Therefore, could inhibiting RNAi in mammals potentially enhance the IFN system? The study of arboviruses could be useful to understand the differences and similarities between the RLR and RNAi pathways, as well as the potential viral evasion strategies that could apply to both mechanisms. Indeed, the existence of a selection pressure for evasion mechanisms effective against both systems is possible. This would potentially favor shielding mechanisms, such as the use of viral factories, compared to mechanisms targeting the actors of one of the two systems, like VSRs. As an example, arboviruses like DENV and other flaviviruses replicate in convoluted membranes [126], and those viral factories could prevent recognition from both RLRs and Dicer proteins. This strategy, and potentially others, could have evolved as a way to prevent recognition from both RNAi and the RLRs.

Viral escape from dsRNA sensing

The example of arboviruses illustrates some of the strategies used by viruses to escape the innate immune system. In general, those strategies will either prevent recognition of the dsRNA by the host immune system, or impair the subsequent immune response. In this review we will only detail strategies preventing the recognition of dsR-

NAs by helicases. One strategy to prevent recognition of the viral genome by cytoplasmic receptors is to disguise it, by mimicking cellular RNAs. This is achieved by many viruses, which induce epitranscriptomic modifications on their genetic material in order to tame the immune system. A number of viruses replicating in the cytoplasm have evolved a 2'O-methyltransferase to induce a ribose 2'O-methylation, similar to the one present on the 5'capped mRNAs. Using mouse and human coronavirus models, Züst *et al.,* have shown that this modification prevents recognition of the viral mRNA by MDA-5 [127]. Similarly, a recent study has shown that HIV RNA is modified by the 2'-O-methyltransferase FTSJ3 and helps the virus avoid triggering the interferon response [30]. Another modification, N6-methyladenosine (m^6A), was found on the mRNAs of viruses such as HCV (Hepatitis C), ZIKV, DENV, YFV and affects the replication as well as the localization of viral RNAs [27, 128, 129], which could be a regulation mechanism shared by many viruses [130]. Some viruses are transmitted to humans by insect vectors, and therefore it might be useful to study the role of these modifications in insect vectors such as mosquitoes, in order to find out if epitranscriptomic marks can prevent recognition by Dicer-2. However, very few studies have been devoted to the role of viral RNA modifications, despite the identification of some modifications present on the mRNAs of viruses [30]. Moreover, a recent study has shown that m^6A-deficient RNAs enhance sensing by RIG-I [31]. This modification could therefore be used by viruses in order to avoid detection by the innate immune system.

The acquisition of capped genomes is another type of viral mimicry of cellular mRNAs. This can be achieved through the use of cellular cap-synthesizing enzymes, like it is the case for most DNA viruses which, after replicating in the nucleus, are then capped, like cellular RNAs. Alternatively, some viruses encode their own capping machinery, like the vaccinia virus and the orthoreovirus [131, 132]. The cap can also be synthesized through an unconventional capping mechanism, like Rhabdoviruses or Alphaviruses [133, 134]. The caps synthesized in this manner are similar to caps synthesized through conventional capping, although the mechanism by which they are produced differs. Finally, some viruses use a mechanism called cap snatching in order to steal the caps of cellular mRNAs, like in the case of some ssRNA(-) viruses. For example, IAV is able to steal short, 5′ capped transcripts produced by the cellular DNA dependent RNA polymerase II and use them as a 5'cap and primer to initiate viral RNA transcription [135-137].

Another strategy is to completely hide the dsRNA from the sensors, for example using viral proteins to coat the dsRNA or by performing RNA replication inside virus-induced vesicles called viral factories, replication factories or replication organelles. RNA(+) viruses are well-known for replicating their genomes inside membrane structures (*e.g. Picornaviridae*, *Flaviviridae*, *Togaviridae*, *Coronaviridae* and *Arteriviridae*). Other than RNA(+) viruses, members of the Poxviridae family like the vaccinia virus are large DNA viruses known to form viral factories [138]. Unlike most DNA viruses, poxviruses replicate their genome in the cytoplasm, and therefore they need to shield their replication site from cellular factors. One of the most well known viruses that induces membrane alterations is the poliovirus, which induces a remodeling of ER membranes inside which it will replicate [139]. The same strategy is used to defeat RNAi, for example by DENV, which replicates in convoluted membranes of the endoplasmic reticulum [126]. Sequestration of flavivirus replication complexes in those vesicles limits the access of Dicer-2 to dsRNA replicative intermediates. Moreover, some ssRNA(-) viruses induce the formation of another type of viral factories, as in the case of the Negri bodies of the rabies virus, which are cytoplasmic inclusions similar to liquid phase separation organelles [140]. Finally, instead of shielding the dsRNA inside viral factories, some viral proteins can shield it by binding to it, thus preventing binding of the dsRNA sensors. This is the case of the EBOV and Marburg virus protein VP35 [141, 142], IAVs protein NS1 [143] and VSV N proteins [144].

In conclusion, the crucial role of cytoplasmic RNA helicases for viral dsRNA sensing has been extensively demonstrated. This role will be further detailed by the elucidation of the role of accessory proteins in the modulation and restriction of this sensing, as well as the precise molecular mechanism for their recognition and activation. This distinction between "self" and "non-self" is particularly relevant as its dysregulation has been shown to have an impact on human diseases, in the context of autoimmune diseases for example. As aforementioned, these two pathways might not be as separate as it seems and several studies have highlighted the potential cross-talk between the IFN and RNAi pathways. The interaction dynamics and potential incompatibility is still a matter for debate and studying the genetic and biochemical interactions between the two pathways could be interesting.

Acknowledgements. Claire Rousseau wrote the manuscript and made the figures. Carine Meignin corrected and edited the review. The authors thank Jean-Luc Imler for his critical reading of the manuscript and helpful remarks. Claire Rousseau is funded by a PhD fellowship from the Ministry of Education and Research.

Conflict of interest : none.

References

1. Schlee M, Hartmann G. Discriminating self from non-self in nucleic acid sensing. *Nat Rev Immunol* 2016 ; 16 : 566-80.

2. Weber F, Wagner V, Rasmussen SB, *et al*. Double-stranded RNA is produced by positive-strand RNA viruses and DNA viruses but not in detectable amounts by negative-strand RNA viruses. *J Virol* 2006 ; 80 : 5059-64.

3. Mueller S, Gausson V, Vodovar N, *et al*. RNAi-mediated immunity provides strong protection against the negative-strand RNA vesicular stomatitis virus in Drosophila. *Proceedings of the National Academy of Sciences of the United States of America* 2010 ; 107 : 19390-5.

4. Son K-N, Liang Z, Lipton HL. Double-Stranded RNA Is Detected by Immunofluorescence Analysis in RNA and DNA Virus Infections, Including Those by Negative-Stranded RNA Viruses. *J Virol* 2015 ; 89 : 9383-92.

5. Bronkhorst AW, van Cleef KWR, Vodovar N, *et al*. The DNA virus Invertebrate iridescent virus 6 is a target of the Drosophila RNAi machinery. *PNAS* 2012 ; 109 : E3604-13.

6. Kemp C, Mueller S, Goto A, *et al*. Broad RNA interference-mediated antiviral immunity and virus-specific inducible responses in Drosophila. *J Immunol* 2013 ; 190 : 650-8.

7. Mallam AL, Sidote DJ, Lambowitz AM. Molecular insights into RNA and DNA helicase evolution from the determinants of specificity for a DEAD-box RNA helicase. *eLife* 2014 ; 3 : e04630.

8. Talide L, Imler J -L, Meignin C. Sensing Viral Infections in Insects: A Dearth of Pathway Receptors. *Curr Issues Mol Biol* 2020 ; 34 : 31-60.

9. Kawai T, Akira S. Toll-like Receptors and Their Crosstalk with Other Innate Receptors in Infection and Immunity. *Immunity* 2011 ; 34 : 637-50.

10. Fu W, Verma D, Burton A, *et al*. Cellular RNA Helicase DHX9 Interacts with the Essential Epstein-Barr Virus (EBV) Protein SM and Restricts EBV Lytic Replication. *J Virol* ; 93. Epub ahead of print 15 2019. DOI : 10.1128/JVI.01244-18.

11. Yoo JS, Takahasi K, Ng CS, *et al*. DHX36 Enhances RIG-I Signaling by Facilitating PKR-Mediated Antiviral Stress Granule Formation. *PLOS Pathogens* 2014 ; 10 : e1004012.

12. Zhang Z, Kim T, Bao M, *et al*. DDX1. *DDX21, and DHX36 Helicases Form a Complex with the Adaptor Molecule TRIF to Sense dsRNA in Dendritic Cells. Immunity* 2011 ; 34 : 866-78.

13. Zhang Z, Yuan B, Lu N, *et al*. DHX9 Pairs with IPS-1 To Sense Double-Stranded RNA in Myeloid Dendritic Cells. *J Immunol* 2011 ; 187 : 4501-8.

14. Paro S, Imler J-L, Meignin C. Sensing viral RNAs by Dicer/RIG-I like ATPases across species. *Current Opinion in Immunology* 2015 ; 32 : 106-13.

15. Hornung V, Ellegast J, Kim S, *et al*. 5'-Triphosphate RNA Is the Ligand for RIG-I. *Science* 2006 ; 314 : 994-7.

16. Pichlmair A, Schulz O, Tan CP, *et al*. RIG-I-Mediated Antiviral Responses to Single-Stranded RNA Bearing 5'-Phosphates. *Science* 2006 ; 314 : 997-1001.

17. Schlee M, Roth A, Hornung V, *et al*. Recognition of 5′ Triphosphate by RIG-I Helicase Requires Short Blunt Double-Stranded RNA as Contained in Panhandle of Negative-Strand Virus. *Immunity* 2009 ; 31 : 25-34.

18. Ren X, Linehan MM, Iwasaki A, *et al*. RIG-I Selectively Discriminates against 5′-Monophosphate RNA. *Cell Reports* 2019 ; 26 : 2019-27.e4.

19. Goubau D, Schlee M, Deddouche S, *et al*. Antiviral immunity via RIG-I-mediated recognition of RNA bearing 5′-diphosphates. *Nature* 2014 ; 514 : 372-5.

20. Yoneyama M, Kikuchi M, Matsumoto K, *et al*. Shared and Unique Functions of the DExD/H-Box Helicases RIG-I, MDA5, and LGP2 in Antiviral Innate Immunity. *The Journal of Immunology* 2005 ; 175 : 2851-8.

21. Kato H, Takeuchi O, Sato S, *et al*. Differential roles of MDA5 and RIG-I helicases in the recognition of RNA viruses. *Nature* 2006 ; 441 : 101-5.

22. Kandasamy SK, Fukunaga R. Phosphate-binding pocket in Dicer-2 PAZ domain for high-fidelity siRNA production. *Proceedings of the National Academy of Sciences of the United States of America* 2016 ; 113 : 14031-6.

23. Cenik ES, Fukunaga R, Lu G, *et al*. Phosphate and R2D2 Restrict the Substrate Specificity of Dicer-2, an ATP-Driven Ribonuclease. *Molecular Cell* 2011 ; 42 : 172-84.

24. Welker NC, Maity TS, Ye X, *et al*. Dicer's Helicase Domain Discriminates dsRNA Termini to Promote an Altered Reaction Mode. *Molecular Cell* 2011 ; 41 : 589-99.

25. Donelick HM, Talide L, Bellet M, *et al*. In vitro studies provide insight into effects of Dicer-2 helicase mutations in Drosophila melanogaster. *RNA*. Epub ahead of print 25 August 2020. DOI : 10.1261/rna.077289.120.

26. Motorin Y, Helm M. RNA nucleotide methylation. *Wiley Interdiscip Rev RNA* 2011 ; 2 : 611-31.

27. Karikó K, Buckstein M, Ni H, *et al*. Suppression of RNA Recognition by Toll-like Receptors : The Impact of Nucleoside Modification and the Evolutionary Origin of RNA. *Immunity* 2005 ; 23 : 165-75.

28. Durbin AF, Wang C, Marcotrigiano J, *et al*. RNAs Containing Modified Nucleotides Fail To Trigger RIG-I Conformational Changes for Innate Immune Signaling. *mBio* 2016 ; 7 : e00833-16, /mbio/7/5/e00833-16.atom.

29. Liddicoat BJ, Piskol R, Chalk AM, *et al*. RNA editing by ADAR1 prevents MDA5 sensing of endogenous dsRNA as nonself. *Science* 2015 ; 349 : 1115-20.

30. Ringeard M, Marchand V, Decroly E, *et al*. FTSJ3 is an RNA 2′-O-methyltransferase recruited by HIV to avoid innate immune sensing. *Nature* 2019 ; 565 : 500-4.

31. Lu M, Zhang Z, Xue M, *et al*. N6-methyladenosine modification enables viral RNA to escape recognition by RNA sensor RIG-I. *Nat Microbiol* 2020 ; 5 : 584-98.

32. Alexopoulou L, Holt AC, Medzhitov R, *et al*. Recognition of double-stranded RNA and activation of NF-kappaB by Toll-like receptor 3. *Nature* 2001 ; 413 : 732-8.

33. Lindbo JA, Silva-Rosales L, Proebsting WM, *et al*. Induction of a Highly Specific Antiviral State in Transgenic Plants : Implications for Regulation of Gene Expression and Virus Resistance. *The Plant Cell* 1993 ; 5 : 1749-59.

34. Li H, Li WX, Ding SW. Induction and suppression of RNA silencing by an animal virus. *Science* 2002 ; 296 : 1319-21.

35. Waldron FM, Stone GN, Obbard DJ. Metagenomic sequencing suggests a diversity of RNA interference-like responses to viruses across multicellular eukaryotes. *PLOS Genetics* 2018 ; 14 : e1007533.

36. Provost P, Dishart D, Doucet J, *et al*. Ribonuclease activity and RNA binding of recombinant human Dicer. *The EMBO Journal* 2002 ; 21 : 5864-74.

37. Zhang H. Human Dicer preferentially cleaves dsRNAs at their termini without a requirement for ATP. *The EMBO Journal* 2002 ; 21 : 5875-85.

38. Lee YS, Nakahara K, Pham JW, *et al*. Distinct Roles for Drosophila Dicer-1 and Dicer-2 in the siRNA/miRNA Silencing Pathways. *Cell* 2004 ; 117 : 69-81.

39. Sinha NK, Iwasa J, Shen PS, *et al*. Dicer uses distinct modules for recognizing dsRNA termini. *Science (New York, NY)* 2018 ; 359 : 329-34.

40. Ma E, MacRae IJ, Kirsch JF, *et al*. Autoinhibition of human dicer by its internal helicase domain. *J Mol Biol* 2008 ; 380 : 237-43.

41. Hartig JV, Förstemann K. Loqs-PD and R2D2 define independent pathways for RISC generation in Drosophila. *Nucleic Acids Res* 2011 ; 39 : 3836-51.

42. Marques JT, Wang J-P, Wang X, *et al*. Functional Specialization of the Small Interfering RNA Pathway in Response to Virus Infection. *PLoS Pathogens* 2013 ; 9 : e1003579.

43. Liu Q, Rand TA, Kalidas S, *et al*. R2D2, a bridge between the initiation and effector steps of the Drosophila RNAi pathway. *Science* 2003 ; 301 : 1921-5.

44. Liu X, Jiang F, Kalidas S, *et al*. Dicer-2 and R2D2 coordinately bind siRNA to promote assembly of the siRISC complexes. *RNA* 2006 ; 12 : 1514-20.

45. Fukunaga R, Han BW, Hung J-H, *et al*. Dicer Partner Proteins Tune the Length of Mature miRNAs in Flies and Mammals. *Cell* 2012 ; 151 : 533-46.

46. Trettin KD, Sinha NK, Eckert DM, *et al*. Loquacious-PD facilitates Drosophila Dicer-2 cleavage through interactions with the helicase domain and dsRNA. *Proc Natl Acad Sci USA* 2017 ; 114 : E7939-48.

47. Olmo RP, Ferreira AGA, Izidoro-Toledo TC, *et al*. Control of dengue virus in the midgut of Aedes aegypti by ectopic expression of the dsRNA-binding protein Loqs2. *Nat Microbiol* 2018 ; 3 : 1385-93.

48. Hansen SR, Aderounmu AM, Donelick HM, *et al*. Dicer's Helicase Domain : A Meeting Place for Regulatory Proteins. *Cold Spring Harb Symp Quant Biol* 2020 ; 039750.

49. Lee HY, Zhou K, Smith AM, *et al*. Differential roles of human Dicer-binding proteins TRBP and PACT in small RNA processing. *Nucleic Acids Research* 2013 ; 41 : 6568-76.

50. Veen AG, Maillard PV, Schmidt JM, *et al*. The RIG-I-like receptor LGP2 inhibits Dicer-dependent processing of long double-stranded RNA and blocks RNA interference in mammalian cells. *EMBO J* 2018 ; 37. Epub ahead of print 15 February 2018. DOI:10.15252/embj.201797479.

51. Gammon DB, Mello CC. RNA interference-mediated antiviral defense in insects. *Curr Opin Insect Sci* 2015 ; 8 : 111-20.

52. Maillard PV, Van der Veen AG, Deddouche-Grass S, *et al*. Inactivation of the type I interferon pathway reveals long double-stranded RNA-mediated RNA interference in mammalian cells. *EMBO J* 2016 ; 35 : 2505-18.

53. Li Y, Basavappa M, Lu J, *et al*. Induction and suppression of antiviral RNA interference by influenza A virus in mammalian cells. *Nat Microbiol* 2017 ; 2 : 16250.

54. Qiu Y, Xu Y, Zhang Y, *et al*. Human Virus-Derived Small RNAs Can Confer Antiviral Immunity in Mammals. *Immunity* 2017 ; 46 : 992-1004.e5.

55. Girardi E, Lefèvre M, Chane-Woon-Ming B, *et al*. Cross-species comparative analysis of Dicer proteins during Sindbis virus infection. *Scientific Reports* 2015 ; 5 : 10693.

56. Maillard PV, Veen AG, Poirier EZ, *et al*. Slicing and dicing viruses : antiviral RNA interference in mammals. *EMBO J* 2019 ; 38. Epub ahead of print 15 April 2019. DOI:10.15252/embj.2018100941.

57. Bellott L, Gilmer D, Michel F. Hit two birds with one stone : the multiple properties of (viral) RNA silencing suppressors. *Virologie (Montrouge)* 2019 ; 23 : 335-8.

58. Seo GJ, Kincaid RP, Phanaksri T, *et al*. Reciprocal inhibition between intracellular antiviral signaling and the RNAi machinery in mammalian cells. *Cell Host Microbe* ; 14. Epub ahead of print 16 October 2013. DOI : 10.1016/j.chom.2013.09.002.

59. Gack MU, Shin YC, Joo C-H, *et al*. TRIM25 RING-finger E3 ubiquitin ligase is essential for RIG-I-mediated antiviral activity. *Nature* 2007 ; 446 : 916-20.

60. Kuniyoshi K, Takeuchi O, Pandey S, *et al*. Pivotal role of RNA-binding E3 ubiquitin ligase MEX3C in RIG-I-mediated antiviral innate immunity. *Proceedings of the National Academy of Sciences* 2014 ; 111 : 5646-51.

61. Yan J, Li Q, Mao A-P, *et al*. TRIM4 modulates type I interferon induction and cellular antiviral response by targeting RIG-I for K63-linked ubiquitination. *Journal of Molecular Cell Biology* 2014 ; 6 : 154-63.

62. Oshiumi H, Miyashita M, Inoue N, *et al*. The Ubiquitin Ligase Riplet Is Essential for RIG-I-Dependent Innate Immune Responses to RNA Virus Infection. *Cell Host & Microbe* 2010 ; 8 : 496-509.

63. Gack MU, Kirchhofer A, Shin YC, *et al*. Roles of RIG-I N-terminal tandem CARD and splice variant in TRIM25-mediated antiviral signal transduction. *PNAS* 2008 ; 105 : 16743-8.

64. Peisley A, Lin C, Wu B, *et al*. Cooperative assembly and dynamic disassembly of MDA5 filaments for viral dsRNA recognition. *Proceedings of the National Academy of Sciences* 2011 ; 108 : 21010-5.

65. Takeuchi O, Akira S. Pattern Recognition Receptors and Inflammation. *Cell* 2010 ; 140 : 805-20.

66. Takahasi K, Yoneyama M, Nishihori T, *et al*. Nonself RNA-Sensing Mechanism of RIG-I Helicase and Activation of Antiviral Immune Responses. *Molecular Cell* 2008 ; 29 : 428-40.

67. Yoneyama M, Kikuchi M, Natsukawa T, *et al*. The RNA helicase RIG-I has an essential function in double-stranded RNA-induced innate antiviral responses. *Nature Immunology* 2004 ; 5 : 730-7.

68. Kowalinski E, Lunardi T, McCarthy AA, *et al*. Structural basis for the activation of innate immune pattern-recognition receptor RIG-I by viral RNA. *Cell* 2011 ; 147 : 423-35.

69. Berke IC, Modis Y. MDA5 cooperatively forms dimers and ATP-sensitive filaments upon binding double-stranded RNA. *The EMBO Journal* 2012 ; 31 : 1714-26.

70. Peisley A, Jo MH, Lin C, *et al*. Kinetic mechanism for viral dsRNA length discrimination by MDA5 filaments. *Proc Natl Acad Sci USA* 2012 ; 109 : E3340-9.

71. Yu Q, Qu K, Modis Y. Cryo-EM Structures of MDA5-dsRNA Filaments at Different Stages of ATP Hydrolysis. *Molecular Cell* 2018 ; 72 : 999-1012.e6.

72. Kato H, Takeuchi O, Mikamo-Satoh E, *et al*. Length-dependent recognition of double-stranded ribonucleic acids by retinoic acid-inducible gene-I and melanoma differentiation-associated gene 5. *The Journal of experimental medicine* 2008 ; 205 : 1601-10.

73. Ranjith-Kumar CT, Murali A, Dong W, *et al*. Agonist and antagonist recognition by RIG-I, a cytoplasmic innate immunity receptor. *J Biol Chem* 2009 ; 284 : 1155-65.

74. Binder M, Eberle F, Seitz S, *et al*. Molecular mechanism of signal perception and integration by the innate immune sensor retinoic acid-inducible gene-I (RIG-I). *J Biol Chem* 2011 ; 286 : 27278-87.

75. Pichlmair A, Schulz O, Tan C-P, *et al*. Activation of MDA5 Requires Higher-Order RNA Structures Generated during Virus Infection. *Journal of Virology* 2009 ; 83 : 10761-9.

76. Loo Y-M, Fornek J, Crochet N, *et al*. Distinct RIG-I and MDA5 signaling by RNA viruses in innate immunity. *J Virol* 2008 ; 82 : 335-45.

77. Gitlin L, Barchet W, Gilfillan S, *et al*. Essential role of mda-5 in type I IFN responses to polyriboinosinic :polyribocytidylic acid and encephalomyocarditis picornavirus. *Proc Natl Acad Sci USA* 2006 ; 103 : 8459-64.

78. Fischer H, Tschachler E, Eckhart L. Pangolins Lack IFIH1/MDA5, a Cytoplasmic RNA Sensor That Initiates Innate Immune Defense Upon Coronavirus Infection. *Front Immunol* 2020 ; 11 : 939.

79. Fredericksen BL, Keller BC, Fornek J, *et al*. Establishment and Maintenance of the Innate Antiviral Response to West Nile Virus Involves both RIG-I and MDA5 Signaling through IPS-1. *Journal of Virology* 2008 ; 82 : 609-16.

80. Liu G, Lu Y, Thulasi Raman SN, *et al*. Nuclear-resident RIG-I senses viral replication inducing antiviral immunity. *Nature Communications* 2018 ; 9 : 3199.

81. Pippig DA, Hellmuth JC, Cui S, *et al*. The regulatory domain of the RIG-I family ATPase LGP2 senses double-stranded RNA. *Nucleic Acids Res* 2009 ; 37 : 2014-25.

82. Rothenfusser S, Goutagny N, DiPerna G, *et al*. The RNA Helicase Lgp2 Inhibits TLR-Independent Sensing of Viral Replication by Retinoic Acid-Inducible Gene-I. *The Journal of Immunology* 2005 ; 175 : 5260-8.

83. Venkataraman T, Valdes M, Elsby R, *et al*. Loss of DExD/H Box RNA Helicase LGP2 Manifests Disparate Antiviral Responses. *The Journal of Immunology* 2007 ; 178 : 6444-55.

84. Bruns AM, Pollpeter D, Hadizadeh N, *et al*. ATP Hydrolysis Enhances RNA Recognition and Antiviral Signal Transduction by the Innate Immune Sensor, Laboratory of Genetics and Physiology 2 (LGP2). *J Biol Chem* 2013 ; 288 : 938-46.

85. Parisien J-P, Bamming D, Komuro A, *et al*. A Shared Interface Mediates Paramyxovirus Interference with Antiviral RNA Helicases MDA5 and LGP2. *Journal of Virology* 2009 ; 83 : 7252-60.

86. Rodriguez KR, Horvath CM. Paramyxovirus V protein interaction with the antiviral sensor LGP2 disrupts MDA5 signaling enhancement but is not relevant to LGP2-mediated RLR signaling inhibition. *J Virol* 2014 ; 88 : 8180-8.

87. Sanchez David RY, Combredet C, Najburg V, *et al*. LGP2 binds to PACT to regulate RIG-I- and MDA5-mediated antiviral responses. *Sci Signal* 2019 ; 12 : eaar3993.

88. Schuberth-Wagner C, Ludwig J, Bruder AK, *et al*. A Conserved Histidine in the RNA Sensor RIG-I Controls Immune Tolerance to N1-2'O-Methylated Self RNA. *Immunity* 2015 ; 43 : 41-51.

89. Jang M-A, Kim EK, Now H, *et al*. Mutations in DDX58, which encodes RIG-I, cause atypical Singleton-Merten syndrome. *Am J Hum Genet* 2015 ; 96 : 266-74.

90. Rutsch F, MacDougall M, Lu C, *et al*. A specific IFIH1 gain-of-function mutation causes Singleton-Merten syndrome. *Am J Hum Genet* 2015 ; 96 : 275-82.

91. Oda H, Nakagawa K, Abe J, *et al*. Aicardi-Goutières syndrome is caused by IFIH1 mutations. *Am J Hum Genet* 2014 ; 95 : 121-5.

92. Rice GI, Del Toro Duany Y, Jenkinson EM, *et al*. Gain-of-function mutations in IFIH1 cause a spectrum of human disease phenotypes associated with upregulated type I interferon signaling. *Nat Genet* 2014 ; 46 : 503-9.

93. Munroe ME, Pezant N, Brown MA, *et al*. Association of IFIH1 and pro-inflammatory mediators: Potential new clues in SLE-associated pathogenesis. *PLoS ONE* 2017 ; 12 : e0171193.

94. Wang C, Ahlford A, Laxman N, *et al*. Contribution of IKBKE and IFIH1 gene variants to SLE susceptibility. *Genes Immun* 2013 ; 14 : 217-22.

95. Elion DL, Jacobson ME, Hicks DJ, *et al*. Therapeutically Active RIG-I Agonist Induces Immunogenic Tumor Cell Killing in Breast Cancers. *Cancer Res* 2018 ; 78 : 6183-95.

96. Heidegger S, Wintges A, Stritzke F, *et al*. RIG-I activation is critical for responsiveness to checkpoint blockade. *Science Immunology* ; 4. Epub ahead of print 13 September 2019. DOI:10.1126/sciimmunol.aau8943.

97. Nabet BY, Qiu Y, Shabason JE, *et al*. Exosome RNA Unshielding Couples Stromal Activation to Pattern Recognition Receptor Signaling in Cancer. *Cell* 2017 ; 170 : 352-366.e13.

98. Wolf D, Fiegl H, Zeimet AG, *et al*. High RIG-I expression in ovarian cancer associates with an immune-escape signature and poor clinical outcome. *International Journal of Cancer* 2020 ; 146 : 2007-18.

99. Tabara H, Yigit E, Siomi H, *et al*. The dsRNA binding protein RDE-4 interacts with RDE-1, DCR-1, and a DExH-box helicase to direct RNAi in C. elegans. *Cell* 2002 ; 109 : 861-71.

100. Duchaine TF, Wohlschlegel JA, Kennedy S, *et al*. Functional proteomics reveals the biochemical niche of C. elegans DCR-1 in multiple small-RNA-mediated pathways. *Cell* 2006 ; 124 : 343-54.

101. Guo X, Zhang R, Wang J, *et al*. Homologous RIG-I-like helicase proteins direct RNAi-mediated antiviral immunity in C. elegans by distinct mechanisms. *PNAS* 2013 ; 110 : 16085-90.

102. Coffman SR, Lu J, Guo X, *et al*. *Caenorhabditis elegans* RIG-I Homolog Mediates Antiviral RNA Interference Downstream of Dicer-Dependent Biogenesis of Viral Small Interfering RNAs. *mBio* 2017 ; 8 : e00264-17, /mbio/8/2/e00264-17.atom.

103. Taschuk F, Cherry S. DEAD-Box Helicases : Sensors, Regulators, and Effectors for Antiviral Defense. *Viruses* 2020 ; 12 : 181.

104. Fujii R, Okamoto M, Aratani S, *et al*. A Role of RNA Helicase A in cis-Acting Transactivation Response Element-mediated Transcriptional Regulation of Human Immunodeficiency Virus Type 1. *J Biol Chem* 2001 ; 276 : 5445-51.

105. Sadler AJ, Latchoumanin O, Hawkes D, *et al*. An Antiviral Response Directed by PKR Phosphorylation of the RNA Helicase A. *PLOS Pathogens* 2009 ; 5 : e1000311.

106. Xing L, Niu M, Kleiman L. In Vitro and In Vivo Analysis of the Interaction between RNA Helicase A and HIV-1 RNA. *Journal of Virology* 2012 ; 86 : 13272-80.

107. Lin L, Li Y, Pyo H-M, *et al*. Identification of RNA helicase A as a cellular factor that interacts with influenza A virus NS1 protein and its role in the virus life cycle. *J Virol* 2012 ; 86 : 1942-54.

108. Grünvogel O, Esser-Nobis K, Reustle A, *et al*. DDX60L Is an Interferon-Stimulated Gene Product Restricting Hepatitis C Virus Replication in Cell Culture. *J Virol* 2015 ; 89 : 10548-68.

109. Miyashita M, Oshiumi H, Matsumoto M, *et al*. DDX60, a DEXD/H box helicase, is a novel antiviral factor promoting RIG-I-like receptor-mediated signaling. *Mol Cell Biol* 2011 ; 31 : 3802-19.

110. Pierson TC, Diamond MS. The continued threat of emerging flaviviruses. *Nature Microbiology* 2020 ; 5 : 796-812.

111. Chan YK, Gack MU. Viral evasion of intracellular DNA and RNA sensing. *Nat Rev Microbiol* 2016 ; 14 : 360-73.

112. He Z, Zhu X, Wen W, *et al*. Dengue Virus Subverts Host Innate Immunity by Targeting Adaptor Protein MAVS. *J Virol* 2016 ; 90 : 7219-30.

113. Dalrymple NA, Cimica V, Mackow ER. Dengue Virus NS Proteins Inhibit RIG-I/MAVS Signaling by Blocking TBK1/IRF3 Phosphorylation : Dengue Virus Serotype 1 NS4A Is a Unique Interferon-Regulating Virulence Determinant. *mBio* ; 6. Epub ahead of print 1 July 2015. DOI : 10.1128/mBio.00553-15.

114. Chang DC, Hoang LT, Mohamed Naim AN, *et al*. Evasion of early innate immune response by 2'-O-methylation of dengue genomic RNA. *Virology* 2016 ; 499 : 259-66.

115. Pijlman GP, Funk A, Kondratieva N, *et al*. A Highly Structured, Nuclease-Resistant, Noncoding RNA Produced by Flaviviruses Is Required for Pathogenicity. *Cell Host & Microbe* 2008 ; 4 : 579-91.

116. Manokaran G, Finol E, Wang C, *et al*. Dengue subgenomic RNA binds TRIM25 to inhibit interferon expression for epidemiological fitness. *Science* 2015 ; 350 : 217-21.

117. Sánchez-Vargas I, Scott JC, Poole-Smith BK, *et al*. Dengue Virus Type 2 Infections of Aedes aegypti Are Modulated by the Mosquito's RNA Interference Pathway. *PLoS Pathog* 2009 ; 5 : e1000299.

118. Cirimotich CM, Scott JC, Phillips AT, *et al*. Suppression of RNA interference increases alphavirus replication and virus-associated mortality in Aedes aegypti mosquitoes. *BMC Microbiol* 2009 ; 9 : 49.

119. Schnettler E, Sterken MG, Leung JY, *et al*. Noncoding Flavivirus RNA Displays RNA Interference Suppressor Activity in Insect and Mammalian Cells. *Journal of Virology* 2012 ; 86 : 13486-500.

120. Moon SL, Dodd BJT, Brackney DE, *et al*. Flavivirus sfRNA suppresses antiviral RNA interference in cultured cells and mosquitoes and directly interacts with the RNAi machinery. *Virology* 2015 ; 485 : 322-9.

121. Samuel GH, Wiley MR, Badawi A, *et al*. Yellow fever virus capsid protein is a potent suppressor of RNA silencing that binds double-stranded RNA. *Proc Natl Acad Sci USA* 2016 ; 113 : 13863-8.

122. Göertz GP, Fros JJ, Miesen P, *et al*. Noncoding Subgenomic Flavivirus RNA Is Processed by the Mosquito RNA Interference Machinery and Determines West Nile Virus Transmission by Culex pipiens Mosquitoes. *J Virol* 2016 ; 90 : 10145-59.

123. Kakumani PK, Ponia SS, S RK, *et al*. Role of RNA Interference (RNAi) in Dengue Virus Replication and Identification of NS4B as an RNAi Suppressor. *Journal of Virology* 2013 ; 87 : 8870-83.

124. Qiu Y, Xu Y-P, Wang M, *et al*. Flavivirus induces and antagonizes antiviral RNA interference in both mammals and mosquitoes. *Sci Adv* 2020 ; 6 : eaax7989.

125. Mathur K, Anand A, Dubey SK, *et al*. Analysis of chikungunya virus proteins reveals that non-structural proteins nsP2 and nsP3 exhibit RNA interference (RNAi) suppressor activity. *Sci Rep* 2016 ; 6 : 38065.

126. Chatel-Chaix L, Cortese M, Romero-Brey I, *et al*. Dengue Virus Perturbs Mitochondrial Morphodynamics to Dampen Innate Immune Responses. *Cell Host Microbe* 2016 ; 20 : 342-56.

127. Züst R, Cervantes-Barragan L, Habjan M, *et al*. Ribose 2′-O-methylation provides a molecular signature for the distinction of self and non-self mRNA dependent on the RNA sensor Mda5. *Nat Immunol* 2011 ; 12 : 137-43.

128. Gokhale NS, Horner SM. RNA modifications go viral. *PLoS Pathog* 2017 ; 13 : e1006188.

129. Gonzales-van Horn SR, Sarnow P. Making the Mark : The Role of Adenosine Modifications in the Life Cycle of RNA Viruses. *Cell Host Microbe* 2017 ; 21 : 661-9.

130. Lichinchi G, Zhao BS, Wu Y, *et al*. Dynamics of Human and Viral RNA Methylation during Zika Virus Infection. *Cell Host Microbe* 2016 ; 20 : 666-73.

131. Cong P, Shuman S. Mutational analysis of mRNA capping enzyme identifies amino acids involved in GTP binding, enzyme-guanylate formation, and GMP transfer to RNA. *Mol Cell Biol* 1995 ; 15 : 6222-31.

132. Furuichi Y, Muthukrishnan S, Shatkin AJ. 5'-Terminal m-7G(5')ppp(5')G-m-p in vivo : identification in reovirus genome RNA. *Proc Natl Acad Sci USA* 1975 ; 72 : 742-5.

133. Ahola T, Kääriäinen L. Reaction in alphavirus mRNA capping : formation of a covalent complex of nonstructural protein nsP1 with 7-methyl-GMP. *PNAS* 1995 ; 92 : 507-11.

134. Ogino T, Banerjee AK. Unconventional Mechanism of mRNA Capping by the RNA-Dependent RNA Polymerase of Vesicular Stomatitis Virus. *Molecular Cell* 2007 ; 25 : 85-97.

135. Dias A, Bouvier D, Crépin T, *et al*. The cap-snatching endonuclease of influenza virus polymerase resides in the PA subunit. *Nature* 2009 ; 458 : 914-8.

136. Reich S, Guilligay D, Pflug A, *et al*. Structural insight into cap-snatching and RNA synthesis by influenza polymerase. *Nature* 2014 ; 516 : 361-6.

137. Yuan P, Bartlam M, Lou Z, *et al*. Crystal structure of an avian influenza polymerase PA(N) reveals an endonuclease active site. *Nature* 2009 ; 458 : 909-13.

138. Tolonen N, Doglio L, Schleich S, *et al*. Vaccinia virus DNA replication occurs in endoplasmic reticulum-enclosed cytoplasmic mini-nuclei. *Mol Biol Cell* 2001 ; 12 : 2031-46.

139. Suhy DA, Giddings TH, Kirkegaard K. Remodeling the Endoplasmic Reticulum by Poliovirus Infection and by Individual Viral Proteins : an Autophagy-Like Origin for Virus-Induced Vesicles. *J Virol* 2000 ; 74 : 8953-65.

140. Nikolic J, Le Bars R, Lama Z, *et al*. Negri bodies are viral factories with properties of liquid organelles. *Nat Commun* ; 8. Epub ahead of print 5 July 2017. DOI:10.1038/s41467-017r-r00102-9.

141. Bale S, Julien J-P, Bornholdt ZA, *et al*. Marburg Virus VP35 Can Both Fully Coat the Backbone and Cap the Ends of dsRNA for Interferon Antagonism. *PLoS Pathog* 2012 ; 8 : e1002916.

142. Cárdenas WB, Loo Y-M, Gale M, *et al*. Ebola Virus VP35 Protein Binds Double-Stranded RNA and Inhibits Alpha/Beta Interferon Production Induced by RIG-I Signaling. *JVI* 2006 ; 80 : 5168-78.

143. Turkington HL, Juozapaitis M, Kerry PS, *et al*. Novel Bat Influenza Virus NS1 Proteins Bind Double-Stranded RNA and Antagonize Host Innate Immunity. *J Virol* 2015 ; 89 : 10696-701.

144. Green TJ. Structure of the Vesicular Stomatitis Virus Nucleoprotein-RNA Complex. *Science* 2006 ; 313 : 357-60.

145. Chan YK, Gack MU. A phosphomimetic-based mechanism of dengue virus to antagonize innate immunity. *Nat Immunol* 2016 ; 17 : 523-30.

146. Kakumani PK, Ponia SS, S RK, *et al*. Role of RNA Interference (RNAi) in Dengue Virus Replication and Identification of NS4B as an RNAi Suppressor. *Journal of Virology* 2013 ; 87 : 8870-83.

147. Qiu Y, Xu Y-P, Wang M, *et al*. Flavivirus induces and antagonizes antiviral RNA interference in both mammals and mosquitoes. *Sci Adv* 2020 ; 6 : eaax7989.

III. RNA interference in Drosophila melanogaster

A. The discovery of RNA interference

The central dogma of molecular biology, stated by Francis Crick in 1958, considers that information contained in DNA is transcribed into messenger RNA (mRNA) that are subsequently translated into proteins, which are the important molecular players in cell function (Crick, 1958; Dogini et al., 2014). However, the more we discover about the genome and gene expression, the more we realize that it is tremendously complex. For example, what we first thought to be "junk DNA" because it was not translated into proteins, is far from being functionless, as exemplified by transposable elements, non-coding RNAs, and the mechanism of RNA interference. Of note, transposable elements have long been regarded as "junk" but they can play essential roles such as telomere formation in Drosophila, where chromosomes ends are structured by specific retrotransposons (Mason et al., 2008). The mechanism of RNA interference (RNAi), observed by several scientists in the 1990s without being fully understood, was truly discovered in 1998 by 2006 Nobel Prize winners Andrew Z. Fire and Craig C. Mello. At the time, the two scientists were investigating how gene expression is regulated in the nematode worm *Caenorhabditis elegans* by using a sequence of mRNA encoding an important muscle protein (Fire et al., 1998). They injected either sense or antisense RNA, and then both sense and antisense RNA (which would combine in the test tube to produce dsRNA) in *C. elegans*. In doing so, they realized that although neither sense nor antisense RNA alone had a significant impact on the worm, the injection of both RNAs together caused the worms to display twitching movements, similar to worms completely lacking a functional gene for the muscle protein. This prompted them to deduce that double-stranded RNA can silence genes, a completely new concept at the time (Fire et al., 1998).

After this breakthrough in *C. elegans,* several labs started to investigate the details of the RNAi mechanism. Early *in vitro* studies in several organisms discovered that dsRNA is cleaved into small RNAs with a size of approx. 25-nt, homologous to the target RNA (Hamilton and Baulcombe, 1999; Zamore et al., 2000; Elbashir et al., 2001). The following years the main components of the RNAi machinery, including the proteins Dicer and Argonaute, were discovered (Hammond et al., 2000; Bernstein et al., 2001; Hammond et al., 2001; Hutvágner

et al., 2001; Liu et al., 2003). Through this highly conserved pathway, both endogenous and exogenous dsRNA templates are processed into small RNAs that induce the inhibition of their expression. This allows the regulation of gene expression and functions as a defence mechanism against mobile genetic elements and, in some organisms, exogenous nucleic acids like viruses. This discovery led to the development of a widely used method to study genes, and it is now very common to assess the function of a gene by inducing its knock-down (KD) using RNAi. RNAi is particularly useful for high throughput screening, to highlight genes involved in a pathway or mechanism. A parallel can be made with the prokaryotic antiviral mechanism, called Clustered Regularly Interspaced Short Palindromic Repeat (CRISPR)/CRISPR-Associated Endonuclease Cas9, which has also become a popular way to silence gene expression. Instead of silencing the target gene by inducing its KD, CRISPR-Cas9 leads to a complete knock-out phenotype (KO). Both methods are commonly used both *ex vivo* and *in vivo*, as it is sometimes preferable to induce KO, e.g. to establish animal models for specific diseases, while sometime a KD is required, as complete KO of some genes can be too detrimental for the organism. The medical applications of RNAi are also very promising as it could be used to downregulate mutant genes in diseased cells. Some RNAi drugs have already been approved for sale due to their efficacy and safety (Weng et al., 2019).

B. The RNA interference pathways in *D. melanogaster*

In *D. melanogaster*, there are three major RNAi pathways, relying on three types of small RNAs: micro-RNAs (miRNAs), small interfering RNAs (siRNAs) and piwi-interacting RNAs (piRNAs). Those three types of small RNA perform different functions in the cell, possess specific characteristic and associate with distinct subsets of effector proteins to form three different RNAi pathways (**Figure 4**).

The miRNA pathway

The miRNA pathway (**Figure 4A**) allows the regulation of gene expression. It is crucial for normal animal development and a plethora of biological processes (Gebert and MacRae, 2019; DeVeale et al., 2021). The miRNA genes are encoded in the genome, and their transcription (usually by RNA polymerase II and in some cases RNA polymerase III) gives rise to the presence

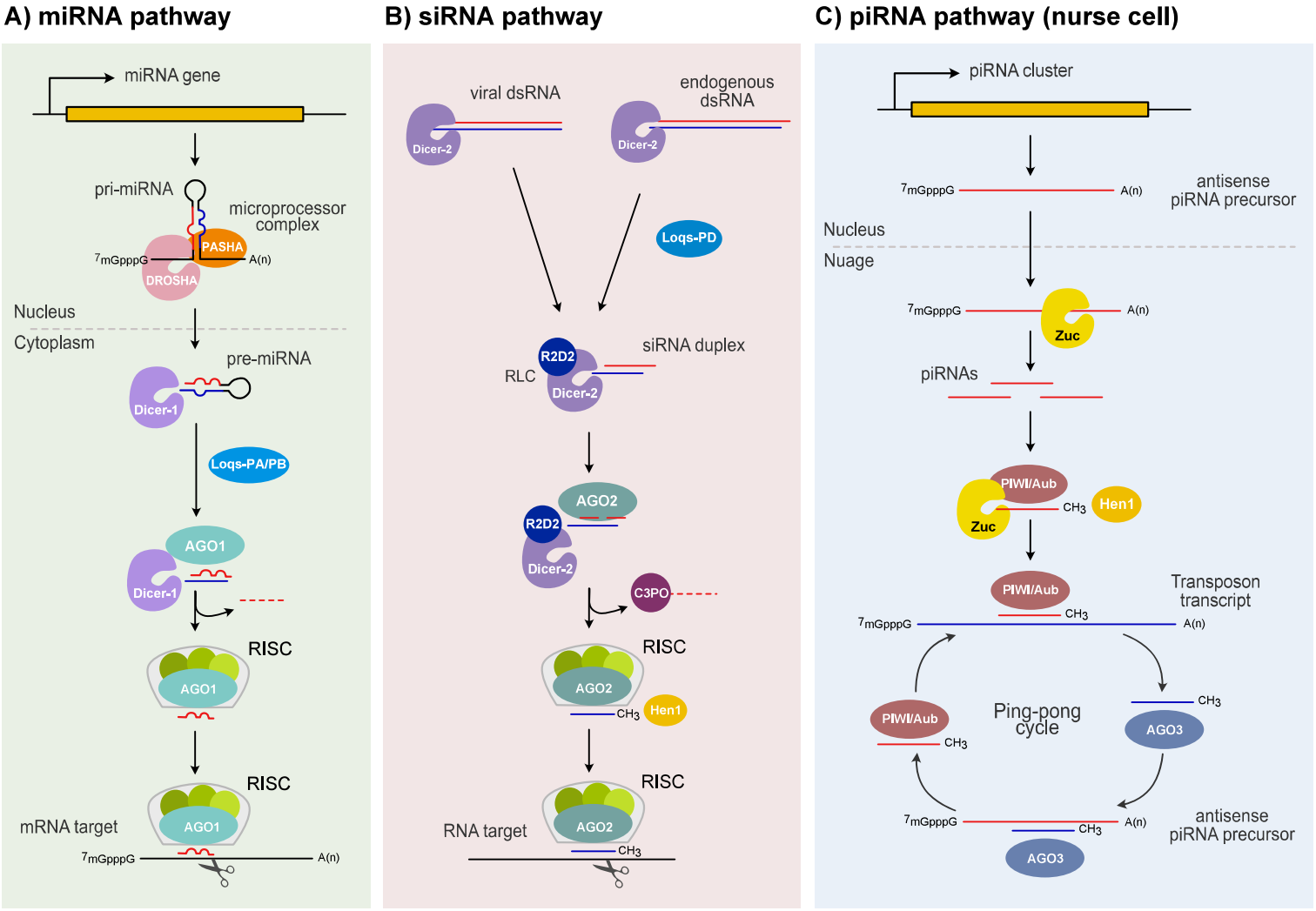

Figure 4. The RNA interference pathways in *Drosophila melanogaster*.
A) In the microRNA (miRNA) pathway, miRNA genes are transcribed into primary-miRNAs (pri-miRNAs) and processed in the nucleus by the microprocessor complex, composed of the endonuclease DROSHA and its RNA-binding protein (RBP) partner PASHA. The resulting precursor miRNA (pre-miRNA) is then exported to the cytoplasm, where it is further processed into a miRNA duplex by Dicer-1, interacting with Loquacious-PA/PB (Loqs-PA/PB). The miRNA duplex is then loaded onto the Argonaute-1 protein, where one strand will be discarded and auxiliary proteins are added, leading to the formation of the RISC complex. This complex will be lead to the complementary mRNA target by the miRNA, leading to its cleavage or translation inhibition. **B)** In the small interfering RNA (siRNA) pathway, endogenous or exogenous dsRNA are detected by Dicer-2 and processed into siRNA duplexes. The RBP Loquacious-PD is necessary for endo-siRNA processing but dispensable for virus-derived siRNA (vsiRNA) processing. The newly synthesized siRNAs are then loaded onto Argonaute-2, with the help of R2D2, and one of the strand of the duplex is discarded thanks to the C3PO protein. After formation of the RISC complex, the siRNA is methylated by Hen1 and leads the complex to the complementary RNA target, which is then cleaved by Ago2. **C)** The piwi-associated RNA (piRNA) pathway is restricted to germline cells and follicular somatic cells. In the germline nurse cells, piRNA genes are transcribed into antisense piRNA precursors and exported from the nucleus into a perinuclear area called Nuage. Zucchini-mediated processing then allows the synthesis of antisense piRNAs, which will be loaded onto PIWI or Aubergine(Aub) and methylated by Hen1. The piRNA will then lead the complex to the complementary transposon transcript, leading to its cleavage. In the process, this cleavage will lead to the formation of a new, sense piRNA, which is then loaded Argonaute 3 (Ago3) and lead to the cleavage of the complementary antisense piRNA precursor, leading to the synthesis of a new antisense piRNA. This loop process is called the ping-pong cycle.

of primary miRNAs (pri-miRNAs), which are long RNAs with one or more stem-loop structures in which the mature miRNA sequences are embedded. In some cases, they can form clusters of miRNA genes, which are often functionally related and are transcribed as one transcript that can be several kilobases long (Wang et al., 2016).

These transcripts are recognized by the microprocessor complex formed by the RNase III Drosha and its double-stranded RNA-binding protein (dsRBP) partner Pasha (Denli et al., 2004; Gregory et al., 2004), and processed into a 60-70 nt pre-miRNA with a hairpin structure and, as a result of processing by an RNase III, a 2-nt 3'overhang and 5'phosphate group. The pre-miRNAs are then exported from the nucleus to the cytoplasm by the Exportin 5/RanGTP complex (Yi et al., 2003). There, they are processed into a miRNA duplex of approx. 22 nt by another RNase III, Dicer-1. This processing is facilitated by the binding of Dicer-1 to either the PA- or PB-isoform of another dsRBP, Loquacious (Loqs) (Förstemann et al., 2005; Jiang et al., 2005; Saito et al., 2005), which allows the production of miRNAs with the right size and seed sequence (Fukunaga et al., 2012). The miRNA duplex is then loaded onto the Argonaute1 (Ago1) protein, in order to form the RNA-induced Silencing Complex (RISC). One of the strands of the miRNA duplex (called the passenger strand) is then discarded, while the other (called the guide strand) will lead the complex to the complementary RNA. As *D. melanogaster* expresses several Argonaute proteins, correct loading onto Ago1 instead of the very similar Ago2 is directed by the presence of central mismatches in the guide strand, at positions 9-10 (Czech et al., 2009; Kawamata et al., 2009; Ghildiyal et al., 2010). Once the target RNA is reached, its expression is prevented by one of two mechanisms, depending on the complementarity of the miRNA to its target. For most miRNAs in flies and mammals, pairing with the target occurs with only a region of their sequence, called the seed region, in which case the miRNA induces the translation inhibition of the target RNA (Lewis et al., 2003; Huntzinger and Izaurralde, 2011). However, a few miRNAs are nearly fully complementary to their target RNA, in which case they induce its cleavage by the Argonaute protein.

The siRNA pathway

The siRNA pathway (**Figure 4B**) is subdivided into the endo-siRNA and the exo-siRNA pathways, and depending on the type of siRNA it either regulates the expression of transcripts and transposons or acts as an antiviral immune system, respectively. In both cases, the second

Dicer protein expressed by *D. melanogaster*, called Dicer-2, recognizes a long dsRNA molecule. These dsRNA molecules can for example arise from long endogenous transcripts with extensive double-stranded structures, convergently transcribed mRNAs, or transcription of transposons in inverted orientation, and will be processed into endo-siRNAs. The dsRNA can also come from an exogenous source, like experimentally introduced dsRNA, or viral RNA. In the case of viral RNA, the siRNAs subsequently produced are called virus-derived siRNAs (vsiRNAs) and the dsRNA substrate can come from various sources, such a dsRNA genome or a dsRNA intermediate induced by the viral replication by the RdRp (Weber et al., 2006). These vsiRNAs can be detected by small-RNA sequencing and are a hallmark of the antiviral RNAi response. Moreover, they can be used as a molecular footprint for the discovery and characterization of novel viruses (Aguiar et al., 2016).

Whatever the source, once the dsRNA is recognized by Dicer-2, it is processed into siRNA duplexes of approx. 21 nt, by a mechanism that depends on the nature of their extremities and which will be explained in detail in the next section. The help of a third isoform of the Loquacious protein, Loqs-PD is necessary for the processing of endo-siRNAs, while the interaction of Dicer-2 with inorganic phosphate and another dsRBP, R2D2, is necessary to prevent it from processing pre-miRNA substrates (Cenik et al., 2011). Once produced, the siRNA duplexes are then loaded onto Ago2 by the RISC-loading complex (RLC), of which the main components are Dicer-2 and R2D2. A study by Liang et al. suggests that a transcription factor, TAF11, associates with Dicer-2 and R2D2 in the D2 bodies and enhances the efficiency of the RLC at this step (Liang et al., 2015). The Hsc70/Hsp90 chaperone machinery is required for proper RISC loading as well (Iwasaki et al., 2010). Similarly to miRNAs, the passenger strand of the siRNA duplex is then discarded. For this step, R2D2 is again necessary, as it sense the thermodynamic asymmetry of the siRNA and facilitates the loading of the duplex in a fixed orientation, thus determining which strand will become the passenger strand (Tomari et al., 2004; Yamaguchi et al., 2022). The passenger strand is then cleaved by Ago2 and subsequently removed by the endonuclease C3PO (Liu et al., 2009), and the termini of the guide strand is methylated by the S-adenosyl methionine-dependent methyltransferase Hen1 (Horwich et al., 2007). Once RISC is completely formed, the guide strand leads the complex to the

complementary target RNA. Contrary to miRNAs, siRNAs are always fully complementary to their target, which is therefore cleaved by Ago2.

The piRNA pathway

In *D. melanogaster*, the piRNA pathway (**Figure 4C**) is restricted to the ovarian germline cells and their surrounding follicular somatic cells, where their function is to protect the integrity of germ cell genomes by silencing transposable elements. This process is Dicer-independent, and relies on a specific family of Argonaute proteins, PIWI proteins, which contain the three other Argonaute proteins expressed in *D. melanogaster*: Ago3, Aubergine (Aub) and Zucchini (Zuc).

The mechanisms involved in piRNA biogenesis are very complex and far from fully understood. There are at least two identified pathways that allow the synthesis of piRNAs, called Zuc-dependent synthesis and the ping-pong cycle, respectively. Although Zuc-dependent synthesis can occur in both nurse and follicular cells, the ping-pong cycle seems to be restricted to nurse cells in *D. melanogaster*. For Zuc-dependent synthesis, the process starts with the transcription of piRNA precursors in the nucleus. In contrast with the miRNA and siRNA pathways, piRNA precursors are single-stranded. Antisense piRNA precursors are transcribed from genomic hotspots called piRNA clusters, which harbour transposon fragments and thus provide a genetic memory of past transposition invasion (Brennecke et al., 2007). In *D. melanogaster*, the most famous piRNA cluster is the *flam* piRNA cluster, which controls the expression of retrotransposons from the *gypsy* family (Prud'homme et al., 1995; Desset et al., 2003).

Once exported from the nucleus to the cytoplasm, the antisense piRNA precursors are then processed by Zuc in perinuclear structures (Ipsaro et al., 2012; Nishimasu et al., 2012). The resulting antisense piRNA is then loaded onto Piwi or Aub and 2'O-methylated by Hen1, leading to the cleavage of the complementary transposon transcript and, in the process, the creation of a whole new piRNA (Brennecke et al., 2007; Gunawardane et al., 2007; Horwich et al., 2007). The newly created sense piRNA is then loaded onto Ago3, leading to the cleavage of the complementary antisense transposon transcript and the generation of more antisense piRNAs in the loop known as the ping-pong cycle. Historically, the Zuc-dependent pathway

was called primary synthesis and the ping-pong pathway was considered as a secondary synthesis, but different studies showed that the interdependence between the pathways might be more complicated than that as the ping-pong pathway in follicular cells might be necessary for Zuc-dependent synthesis (Czech et al., 2018).

How strict are the limits between those small RNA pathways?

Interestingly, although the two Dicer proteins of *D. melanogaster* have evolved to be specialized in different functions (i.e. regulation of gene expression or defence against endogenous or exogenous dsRNA), there are still some instances where an interdependence between the two pathways can be observed. For example, Shcherbata and colleagues identified a role of dmDicer-1 in germline stem cell maintenance, and showed that this role was Dicer-2-dependent (Shcherbata et al., 2007). In addition, it is not clear to what extend the endo- and exo-siRNA pathways are distinct from each other. Indeed, although Hartig and colleagues proposed that Loqs-PD and R2D2 define two distinct pathways (i.e. the endo-siRNA pathway and the exo-siRNA pathway), another hypothesis is that the two dsRBP act sequentially and that while Loqs-PD is necessary for siRNA processing, R2D2 is required for loading onto Ago2 (Hartig and Förstemann, 2011; Marques et al., 2010). It is possible that the truth lies in the middle and that, although Loqs-PD is required for endo-siRNA processing but completely dispensable for processing of viral dsRNA (Marques et al., 2013), the rest of the pathway might be common to both substrates. Another interesting question is what happens to endo-siRNA production upon infection. Is the RNAi machinery refocused completely on fighting the viral infection and if so, how is the switch between the two mechanisms activated?

IV. RNA interference and Dicer-2 in antiviral immunity

A. Antiviral RNAi mechanisms

In plants, nematodes and arthropods, the RNAi pathway is not only used for gene regulation and transposon control, but it is also the main antiviral defence mechanism. In particular, the siRNA pathway allows the restriction of viral replication by directly targeting viral RNA. Although the basic mechanism of this restriction by the siRNA pathway has been well characterized over the years, important aspects of this mechanism remain unclear. One of those aspects concerns the very first step of antiviral RNAi, i.e. the recognition of the viral RNA by Dicer-2. Indeed, although processing of the dsRNA by Dicer-2 has been linked *in vitro* to the binding of the free termini of the dsRNA (Sinha et al., 2015, 2018), most viruses possess protected termini *in vivo*. For example, the genome extremities of DCV are protected at the 5'end by the covalent binding of a viral protein, VPg, and by a polyA tail at the 3'end. This suggest that it should be immune to degradation by exonucleases and that its extremities should therefore be hidden to Dicer-2. Moreover, the viral dsRNA is often produced inside viral factories, inside which it would be very difficult for a large protein such as Dicer-2 to enter. The question of where and how Dicer-2 can sense the viral dsRNA remains therefore unsolved. Another key aspect of the antiviral RNAi mechanism that is still not completely understood is if, and how, a systemic antiviral RNAi response can be induced in *D. melanogaster*. In *C. elegans*, not only can siRNAs be transferred to other cells in order to induce a systemic response, they can also be transferred to the progeny (Fire et al., 1998). This response relies on the amplification of the RNAi response by an RdRp that allows the production of secondary siRNAs, and the uptake of dsRNAs by the surrounding cells thanks to the Sid1 protein. However, *D. melanogaster* does not encode an RdRp or a Sid-1-like protein. Despite this, a model for systemic RNAi immunity has been proposed, wherein the amplification depends on the action of a reverse transcriptase from an unknown retrotransposon (Saleh et al., 2009). In order to transfer the dsRNA between insects cells, strategies such as nanotube-like structures or exosome-like vesicles have been proposed (Karlikow et al., 2016; Yoon et al., 2020). However, the expression of inverted repeat transgenes in flies clearly does not trigger a systemic response, as gene knock-down using this

technique can be induced at the resolution of a single-cell type (Roignant et al., 2003). Until this contradiction is elucidated, the question of dsRNA systemic transfer remains open.

The siRNA pathway was long thought to be the only small RNA pathway involved in the viral infection, but an implication of the three main types of small RNAs has since then been discovered. The piRNA pathway does not seem to be involved in antiviral RNAi in *D. melanogaster* (Petit et al., 2016). However, the identification of virus-derived piRNAs (vpiRNAs) in the soma of the mosquito opened the question of the involvement of this pathway in antiviral immunity in this organism (Morazzani et al., 2012). Other studies reported the same observation after infection with different families of viruses, both *in vivo* and *ex vivo* (Dietrich et al., 2017; Miesen et al., 2015; Vodovar et al., 2012). Not only did the small RNAs detected exhibit the characteristic size of piRNAs (around 24-30 nt, longer than both miRNAs and siRNAs), they also showed a nucleotide bias in the sequence (U1 and A10) that is specific to piRNAs. However, it is important to nuance this, as the detection of piRNAs after viral infection does not mean that those piRNAs have an antiviral effect on the virus. Still, these observations came as a surprise, as most studies on antiviral RNAi had been performed in the *D. melanogaster* model organism, which produces piRNAs only in specific cell types (Petit et al., 2016). However, a pan-arthropod metagenomics study revealed that *D. melanogaster* might be the exception rather than the rule in this situation, as piRNAs have been identified in the soma of several other arthropods (Lewis et al., 2018). Although the extent of the involvement of the piRNA pathway in the mosquito antiviral immunity remains to be determined, the apparent difference between the piRNA pathways in the mosquito compared to the fruit fly highlights the fact that we have to be careful when extrapolating a general mechanism from an animal model.

In addition to the piRNA pathway in the mosquito, there seems to be strong interactions between the miRNA pathway and the virus as well, especially in mammals. Indeed, viral infection seems to drastically impact the cellular miRNA expression profile in mammalian cells (Ingle et al., 2015; Li et al., 2017; Rosenberger et al., 2017). Several miRNAs have been shown to impact viral infection either in a proviral or antiviral manner, by binding either directly to the viral genome or by affecting the expression of host factors, therefore indirectly impacting the viral infection. For example, the cellular miRNA miR-122 that normally regulates hepatic

function and cholesterol/fatty acid metabolism in the liver has been shown to be hijacked by the Hepatitis C Virus (HCV) and to have a proviral impact on HCV infection (Jopling et al., 2005). Indeed, the virus seems to have evolved to select a binding site for this cellular miRNA, which directly interacts with the HCV 3' and 5' UTRs, thus promoting IRES-dependent translation of viral proteins and preventing the decay of the viral RNA. Direct interactions between cellular miRNAs and viral RNA with an antiviral impact have also been reported, although this is more surprising, as contrary to siRNAs that arise because of the dsRNA nature of viral RNAs, cellular miRNAs are encoded in the genome and the virus could easily adapt by mutating (Skalsky and Cullen, 2010). Finally, indirect impact on the infection has also been shown, as several cellular miRNAs can modulate viral infection by regulating the expression of proviral or antiviral genes. In *D. melanogaster*, the miRNAs miR-8-5p and miR-956-3p have been shown to regulate the proviral gene *dJun* and the antiviral gene *Ect4*, respectively, during DCV infection (Monsanto-Hearne et al., 2017a, 2017b).

The cellular miRNA machinery has also been domesticated by viruses, as several of them, mostly in mammals, have been shown to express virus-encoded miRNAs against both viral and cellular targets (Pfeffer et al., 2004; Sullivan et al., 2005; Umbach et al., 2008). These miRNAs can serve as a switch between latent and lytic infection, promote cell survival or proliferation to allow viral replication, or modulate immune responses (Bellare and Ganem, 2009; Kincaid et al., 2014; Sullivan et al., 2005). This is the case for the SARS-CoV-2 virus, for which a virus-encoded miRNA has recently been discovered to bind the 3'UTR of interferon stimulated genes (ISGs) and repress their expression in human cells (Singh et al., 2022). In insects, only a few virus-encoded miRNAs have been identified, for the majority in dsDNA viruses (Singh et al., 2012; Zhu et al., 2013), but also miRNA-like small RNAs in the West Nile Virus (WNV) and Dengue Virus (DENV) (Hussain and Asgari, 2014; Hussain et al., 2012). Although virus-encoded miRNAs are poorly characterized in fruit fly viruses, the identification of an abundant miRNA in the Kallithea Virus (KV) showed that this type of regulation also exists for this organism (Webster et al., 2015). The scarcity of virus-encoded miRNAs observed in insect viruses might be due to the relatively small size of the viruses studied and the discovery of new viruses by metagenomics studies might uncover more.

B. The evolution of Dicer proteins in animals

The antiviral siRNA pathway relies on Dicer proteins, both for viral nucleic acid sensing and to produce virus-derived siRNAs (vsiRNAs). To understand more about this antiviral mechanism, we decided to study this protein, which belongs to both the RNase III family and the DExD-box helicase family.

Although the RNase III family exists in both prokaryotes and eukaryotes, the combination of a RNase III and helicase domain is an eukaryotic signature (Ciechanowska et al., 2021). Indeed, Dicer proteins are absent from bacteria and archaea, but they are present throughout eukaryotes, which suggest an early eukaryote origin. The evolutionary switch from prokaryotic to eukaryotic biology, or eukaryogenesis, led to an expansion and over-representation of RNA viruses (Koonin et al., 2015). This is illustrated by the fact that there is an important difference between the viromes of eukaryotes and prokaryotes, as the former contains mainly RNA viruses and the latter DNA viruses. As a result, hosts had to adapt their defenses and RNase III proteins, already present in prokaryotes, could therefore have been repurposed in order to serve as an antiviral defense mechanism against viral RNA, leading to the apparition of Dicer proteins and the RNA interference system (Aguado and tenOever, 2018).

Drosophila melanogaster, like other arthropods, encodes two Dicer proteins: dmDicer-1, which is dedicated to miRNA processing and dmDicer-2, which is required for siRNA biogenesis (Jia et al., 2017). This duplication, contrary to what was believed previously, did not happen in insects but much earlier, before cnidarians diverged from the main animal branch (Mukherjee et al., 2013). This means that the second Dicer would then have been lost in both nematodes and deuterostomes (including vertebrates). For vertebrates, this could have been due to the presence of RIG-I-like receptors (RLRs) and the IFN system, as it has been proposed to be mutually exclusive with RNAi activity (Maillard et al., 2016). The two systems still possess many similarities, as described in the review in Section II of this introduction. However, although the duplication itself happened early in animal evolution, the specialization of the two Dicers seemed to have occurred later in multiple lineages, including in arthropods. Indeed, this specialization has been linked with the loss of a functional DExD-box helicase (Welker et al., 2011) and *C. elegans*, expresses an antiviral Dicer-1 with a functional helicase

domain that is able to produce both vsiRNAs and miRNAs (Mukherjee et al., 2013). In this organism, the differentiation between the two mechanisms could be mediated by RDE4, a dsRBP that is necessary for vsiRNA production and exogenous substrates but not endogenous substrates and miRNAs (Ashe et al., 2013; Lu et al., 2009; Tabara et al., 2002). These differences between organisms should be taken into account when comparing different antiviral RNAi systems across species, and inferring general antiviral RNAi mechanisms from the study of a single model organism should be done with caution.

C. Structure and function of dmDicer-2

Structural insight into Dicer-2 processing

The endonuclease Dicer was first identified in *D. melanogaster* and named by Emilie Bernstein, then a PhD student in the lab of Prof. Hannon (Bernstein et al., 2001). As they were investigating the RNAi mechanism, Bernstein *et al*. discovered that Dicer was the protein responsible for the processing of dsRNAs into siRNAs and identified three important domains of this protein: the RNase III, PAZ and helicase domains (**Figure 5A & 5B**). To understand its role, several biochemical and structural studies have focuses on Dicer in different species, providing us with a better understanding of its mode of action, called “dicing”.

In the early 2000s, an idea of the general organization of the protein was formed. Successive electron microscopy (EM) structures of hsDicer reported an L-shaped molecule (Lau et al., 2009; Wang et al., 2009), and allowed the observation that hsDicer can adopt either a closed or open conformation (Taylor et al., 2013). This was induced by a modification of the position of the helicase relative to the rigid core of hsDicer, in response to the interaction between Dicer and its pre-miRNA substrate.

As the RNAi mechanism had been correlated with the cleavage of dsRNA into smaller RNA molecules (Zamore et al., 2000), the role of the RNase III domain of Dicer was easy to predict. Like all proteins from the RNase III family, Dicer-2 leaves 2-nt 3’-overhangs and 5’phosphate groups as a signature after cleavage of the dsRNA (Elbashir et al., 2001). However, compared to some prokaryotic RNase III proteins, intramolecular dimerization of the RNase III domains allows the cleavage of the dsRNA molecule without the need for intermolecular dimerization

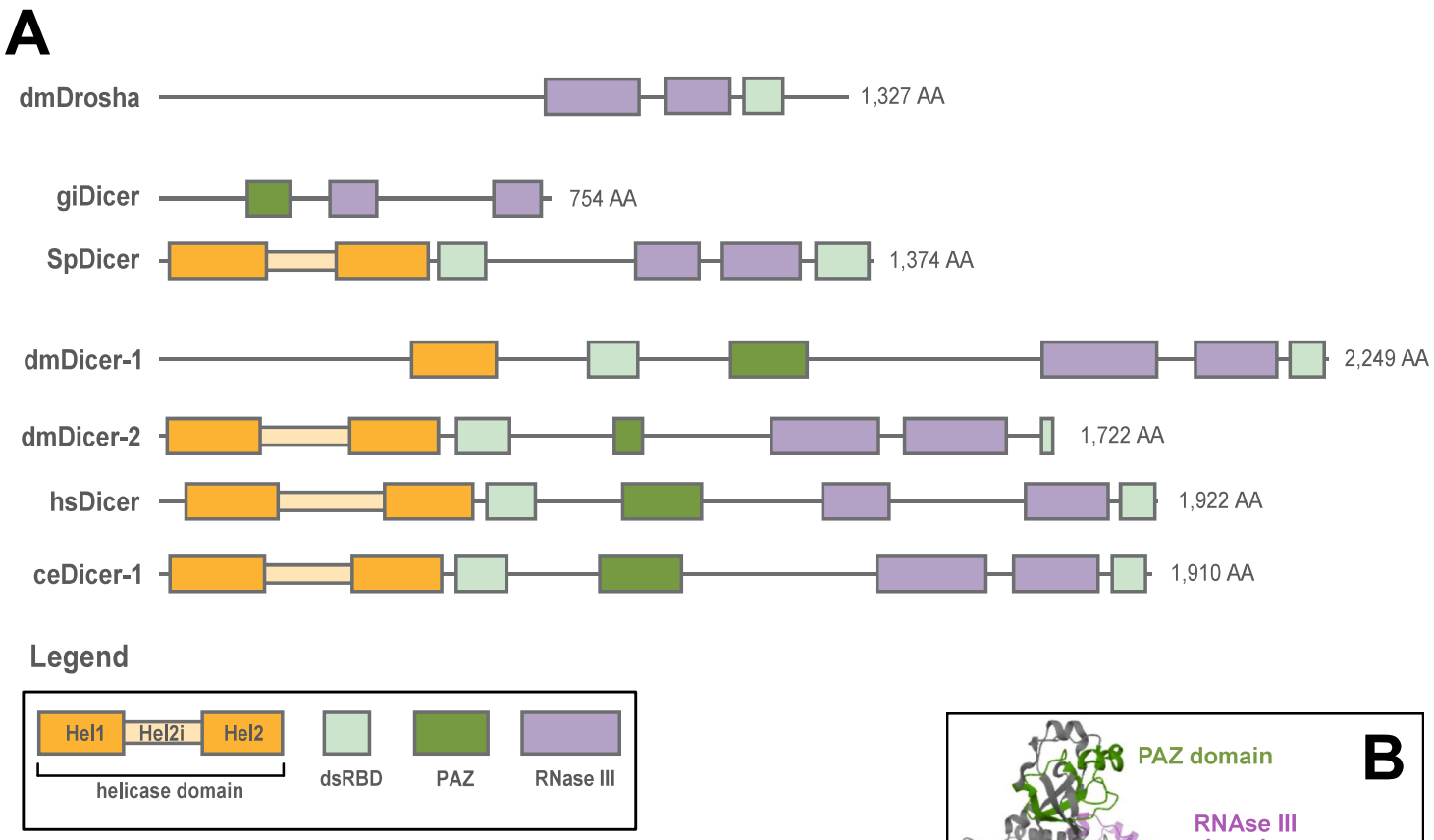

Figure 5. Domain organisation of Dicer proteins in different species
Drosophila melanogaster Drosha (dmDrosha) and Dicer proteins belong to the RNase III family. Different species express Dicer proteins with an overall conservation of the structure, although some Dicer proteins lack some of the domains normally found: *Giardia intestinalis* Dicer (giDicer) lacks the helicase domain, while *S. pombes* Dicer (spDicer) lacks the PAZ domain. In contrast, dmDicer-1/2 and *homo sapiens* Dicer (hsDicer) are contain all those domains, although the helicase domains of dmDicer-1 and hsDicer are non-functional B) Predicted 3D structure of dmDicer-2 using AlphaFold2. The PAZ, RNase III, dsRBD and helicase domains are represented in the same color scheme as in A).

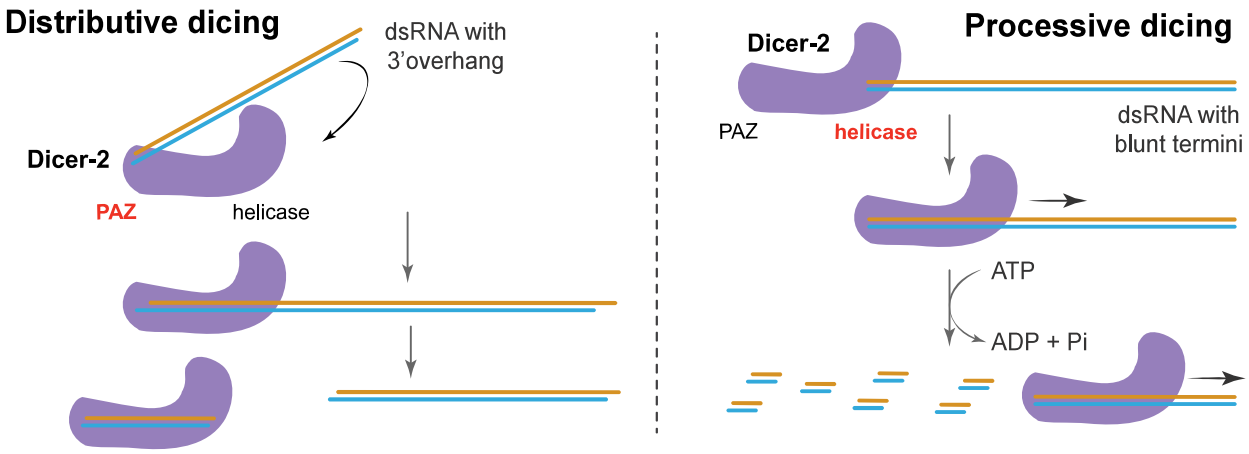

Figure 6. Termini-dependent dicing mechanism of Dicer-2
According to different *in vitro* studies from the Bass lab (Singh et al., 2021; Sinha et al., 2015; 2018), dmDicer-2 is able to cleave dsRNA either through a distributive mechanism relying on the PAZ domain if the substrate contains a 2nt 3'overhang, or though an ATP-dependent processive mechanism for substrates with a blunt termini.

(Zhang et al., 2004). This cleavage is performed through hydrolysis, as an acidic residue cluster of the RNase III domain associates with water molecules, in the presence of Mg^{2+} cations (Blaszczyk et al., 2001).

Insights into the role of the Piwi/Ago/Zwille (PAZ) domain were also obtained quite early. Because of the large size and the complexity of metazoan Dicer proteins such as human Dicer (hsDicer) or *D. melanogaster* Dicer (dmDicer-2), obtaining crystal structures proved difficult. The Dicer from *Giardia intestinalis* (giDicer) however, lacks some of the domains present in those species (**Figure 5A**), and it is thus easier to crystallize. The establishment of its structure demonstrated that Dicer uses a "molecular ruler" mechanism and that, as proposed by Zhang and colleagues earlier, the distance between the PAZ domain and RNase III domains is responsible for the constant length of the siRNAs produced (Macrae et al., 2006; Zhang et al., 2004). This mechanism for high-fidelity siRNA production depends on the anchoring of the dsRNA substrate by a phosphate-binding pocket in the PAZ domain of dmDicer-2, which seems to be highly conserved across species (Kandasamy and Fukunaga, 2016).

However, some Dicer proteins such as *Schizosaccharomyces pombe* Dicer-1 (spDicer-1) lack the PAZ domain, and are still able to produce siRNAs (**Figure 5A**). An alternative mechanism, depending on the helicase domain instead of the PAZ domain, was therefore suggested (Colmenares et al., 2007). Four years later, the work of Prof. Bass and her team led to the discovery that dmDicer-2 is able to process dsRNA molecules by using two distinct mechanisms, depending the termini of its substrate: a helicase-independent mechanism for dsRNA with 2nt 3'overhangs and an helicase-dependent mechanism for blunt dsRNA (Welker et al., 2011) (**Figure 6**). They called these mechanisms distributive and processive dicing, respectively, and showed that although the Platform•PAZ domain is required for ATP-independent binding of dsRNAs with 2nt 3'overhangs, it is the helicase domain that binds blunt dsRNA in an ATP-dependent manner (Singh et al., 2021; Sinha et al., 2015, 2018). During distributive dicing, dmDicer-2 has to detach from the substrate after each cleavage and reattach in order to cleave again. By opposition, once blunt dsRNA binds the helicase domain of dmDicer-2, this domain will bind and hydrolyse ATP to unwind the dsRNA and thread through it, thus allowing the production of multiple siRNAs before dmDicer-2 dissociates.

The presence of these two distinct dicing mechanisms in *D. melanogaster* is interesting because it explains how certain Dicer proteins lacking either the Platform•PAZ or the helicase domain are still able to process siRNAs, and how in some species Dicer cleavage is ATP-dependent (e.g *C. elegans* or *S. pombe*) while in others (e.g. *H. sapiens*) ATP is not required. Indeed, it was shown that not only is ATP not necessary for Dicer processing in *H. sapiens*, but hsDicer seems to be more efficient *in vitro* when depleted of from the helicase domain (Ma et al., 2008).

Modulation of Dicer-2 function by its protein partners

Although the different structural studies performed over the years have highlighted a similar global structure of Dicer proteins in different species, they have also showed that the different Dicers can also be very specific when it comes to selecting a substrate. The specificity of Dicer is modulated by small dsRNA-binding protein partners of Dicer. For example, although dmDicer-2 can cleave pre-miRNAs *in vitro*, it does not do so *in vivo*. This specificity comes from the involvement of R2D2, which prevents dmDicer-2 from processing pre-miRNAs (Cenik et al., 2011). Moreover, another dsRBP, Loqs-PD, allows Dicer to process sub-optimal substrates such as endo-siRNA precursors (Sinha et al., 2015). In contrast, this dsRBP is completely dispensable for the processing of viral dsRNAs (Marques et al., 2013). The interaction between these dsRBP and Dicer is mediated by the helicase domain of Dicer, which is a meeting place for Dicer protein partners. In light of this, the interaction between Dicer proteins and their protein partners has become a very important topic recently, as several studies have focused on the matter in the last few years. In particular, two CryoEM structures of Dicer-2 in a complex with either R2D2 or Loqs in *D. melanogaster* have been published this year (Su et al., 2022; Yamaguchi et al., 2022). Moreover, different proteomics studies have allowed the establishment of interactomes of Dicer proteins in different organisms recently (Montavon et al., 2021; Varjak et al., 2020), although an *in vivo* interactome in *D. melanogaster* is still lacking.

V. Aim and projects

In conclusion, although the RNAi pathway has been rather well characterized over the years, some key questions remain. For example, it is still unclear how dmDicer-2 is able to recognize viral RNAs, as the dicing mechanism relies heavily on the termini of the dsRNA. Indeed, in most viruses these termini are protected (e.g. the viral protein VPg that is covalently bound to the 5'end of the *Drosophila C Virus* genome), and the dsRNA of many viruses is hidden in viral factories. Could other partners of Dicer-2 be involved? Moreover, although structural studies and *in vitro* assays have been fundamental in understanding the dicing mechanism, it is clear that this mechanism is heavily modulated by partner proteins *in vivo*. Some screens or interactomes of Dicer-2 have already been conducted in the context of viral infection (Cherry et al., 2005; Majzoub et al., 2014), however these studies used drosophila S2 cells and as mentioned before, *in vitro* studies do not always reflect the responses at the level of the organism. In order to identify all the actors of the RNAi pathway, *in vivo* studies might be helpful, and *Drosophila melanogaster* is particularly adapted for large-scale *in vivo* studies such as proteomics experiments. The study of dmDicer-2 may even reveal new and unsuspected roles of Dicer-2, as this protein has been shown to not only important for the RNAi mechanism but also for other functions. Indeed, since the discovery that dmDicer-2 can induce the expression of the antiviral protein Vago in an RNAi-independent manner (Deddouche et al., 2008), other non-RNAi-related functions of Dicer proteins have been uncovered. For example, dmDicer-2 was shown to have a role in polyadenylation of some RNA transcripts (Coll et al., 2018) and hsDicer to control endogenous dsRNA accumulation in the nucleus (White et al., 2014).

To try to understand these questions, the main goal of my thesis has been to study how the interactome of dmDicer-2 is modulated by the DCV infection *in vivo* (**Chapter I**). This project forms part of my host lab's general interest in the sensors of antiviral immunity. As part of a broader effort to uncover new sensors of antiviral immunity, we also identified the protein Fandango as a poly(I:C) interactant during an affinity-purification (Pennemann et al., 2021), and as a side-project I also studied this protein and its role in antiviral immunity (**Chapter II**).

Chapter I – Characterization of the RNP network of Dicer-2 during viral infection in *Drosophila melanogaster*

I. Preamble

As explained in the Introduction, the main objective of my thesis was to establish an interactome of Dicer-2 in *Drosophila melanogaster* and understand how it is modulated by viral infection. To this aim, we chose to use the *Drosophila C Virus* (DCV), a virus from the *Dicistroviridae* family, which is highly protected and hidden from the immune system in viral factories, and we therefore still do not understand how Dicer-2 is able to detect it.

In order to investigate how the protein network surrounding dmDicer-2 is modulated by the infection, I injected different fly lines expressing a GFP::Dicer-2 fusion with TRIS (mock-infection) or DCV. These flies are *dicer-2* null mutants in which the endogenous *dicer-2* gene contains a mutation on the Leucine 811 codon (*dicer-2*^{L811fsX}) that causes a frameshift, resulting in a premature STOP codon (Lee et al., 2004). They were complemented with different versions of a GFP::Dicer-2 fusion : a wild-type version of Dicer-2 fused to a GFP tag GFP::Dicer-2^{WT} and two mutants (GFP::Dicer-2^{Hel1} and GFP::Dicer-2^{RNaseIII}), and the ability of GFP::Dicer-2^{WT} to rescue the *dicer-2* null mutation was demonstrated in previous studies (Donelick et al., 2020; Girardi et al., 2015). The GFP::Dicer-2^{Hel1} mutant is able to process a 3'overhang dsRNA substrate using distributive dicing, but unable to hydrolyze ATP and thus to process a blunt dsRNA substrate. The other mutant, GFP::Dicer-2^{RNaseIII}, contains two mutations in the RNase III domain that prevent cleavage, but not binding, of the dsRNA and might help us identify more transient interactions with Dicer-2. These three different transgenic lines all contain a white inverted repeat (*w*^{IR}) transgene on the X chromosome that, when transcribed and spliced, folds into a hairpin RNA structure sensed by Dicer-2. This will result in the production of siRNAs targeting the *white* gene, which is necessary for the red color of drosophila eyes (Ewart and Howells, 1998). As a result, if RNAi is active the flies will have white eyes because this gene will be silenced, and if RNAi is impaired, the inhibition will not work properly and the flies will have red eyes, thus allowing us to monitor RNAi efficiency (**Figure 7**). In addition to these flies, we used as controls *CantonS* wild-type (WT) flies and GFP-

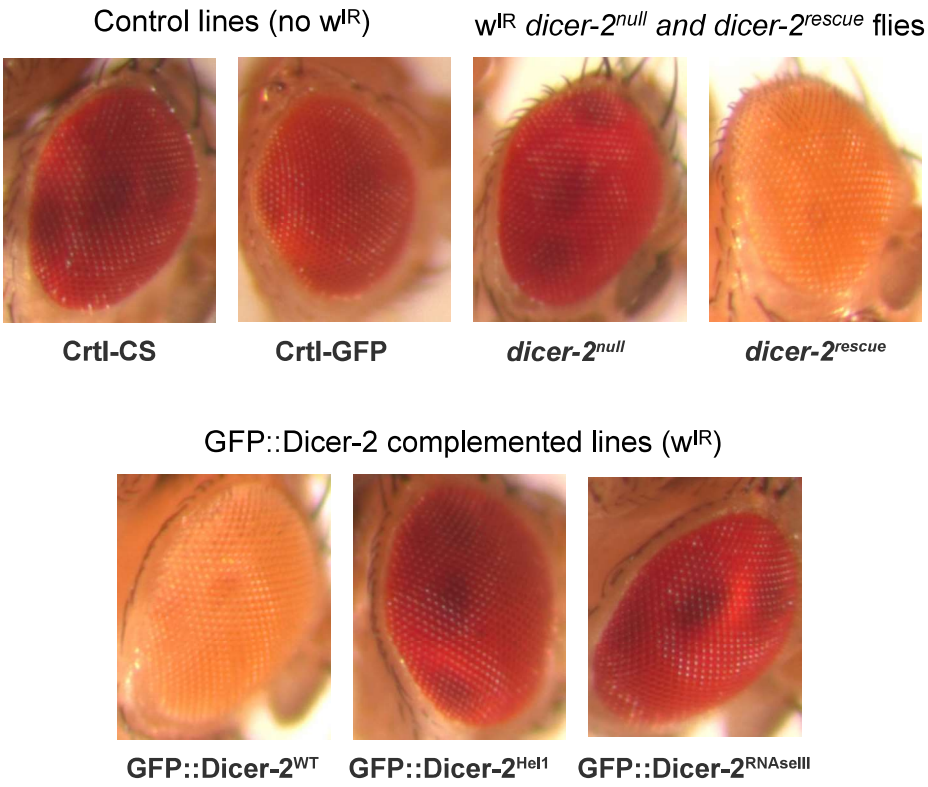

Figure 7 - Eye color of the indicated phenotypes. The color of the eyes of wIR flies allow the monitoring of RNAi efficiency. The *dicer-2*^{null} and *dicer-2*^{rescue} flies are described in Kemp et al., 2013. Flies without the transgene normally have red eyes (see Ctrl-CS and Ctrl-GFP). When the flies contain the transgene, if RNAi is efficient it induces KD of the *white* gene and results in a white eye phenotype (see *dicer-2*^{rescue}) and if RNAi is inefficient the KD is not effective and eyes are red like WT flies (see *dicer-2*^{null}). We can observe that RNAi works normally in GFP::Dicer-2^{WT}, but not GFP::Dicer-2^{Hel1} or GFP::Dicer-2^{RNaseIII} flies.

expressing flies (Ctrl-GFP). Both control lines express the endogenous *dicer-2* gene, and after immunoprecipitation, the WT flies will allow us to account for proteins that might bind to the beads aspecifically ("sticky" proteins), while GFP flies will help us identify candidates that bind specifically to the GFP protein.

After immunoprecipitation of Dicer-2, its protein partners were identified by LC-MS/MS to establish an interactome of Dicer-2 in different conditions. The goal of this project was to identify new protein partners of Dicer-2, which already has several known partners. Therefore, we did not want to limit ourselves to the identification of only direct and stable interactions, but we wanted to really get a grasp of all the protein complexes surrounding Dicer-2. This is why we decided to use an immunoprecipitation followed by mass spectrometry (IP-MS) approach. Mass spectrometry is a highly sensitive technique and, coupled to an immunoprecipitation done in low stringency conditions (here, wash buffer contained only 50 mM NaCl and 0.1% Nonidet P-40 detergent), it is a very powerful tool to establish a protein network.

I then conducted a functional screen of the highlighted candidate proteins *ex vivo* in drosophila S2 cells, wherein each candidate was tested for its impact on DCV infection. Finally, a functional validation screen was performed on selected Dicer-2 partners *in vivo* after depletion in adult followed by DCV infection. The survival rate and the viral load were monitored during DCV infection. In cells, knock-down of the candidate genes was performed by incubating long dsRNAs targeting the candidate genes. In flies however, we had to consider the possibility that some candidates may induce developmental defects that could either prevent us from testing their impact on viral infection, or influence the results. Therefore, we decided to use the Gal4-Gal80^{TS} system, which allows KD induction at the adult stage. Gal4, first identified in *S. cerevisiae*, is a transcription factor that can induce gene expression by binding to a specific sequence, called upstream activating sequence (UAS). However, when bound to Gal80, its repressor, Gal4 is inactivated. Using a thermos-sensitive version of the repressor, Gal80^{TS}, which is functional at 18°C but undergoes a structural change at 29°C that prevents it from binding to Gal4, allows us to efficiently control the driver activity with temperature (Brand and Perrimon, 1993). This system is often used in my host laboratory and has already proved its efficiency is previous studies (Pennemann et al., 2021).

The results of this work will be submitted for publication in the following weeks, and therefore I wrote this Chapter in the form of a draft paper. However, the immunoprecipitations of the different candidates in this draft still need to be improved, which we will do soon, and in the meantime I presented the preliminary IPs that have been obtained thus far.

Definition of the Dicer-2 interactome during viral infection in *Drosophila melanogaster*

Claire Rousseau[1], Émilie Lauret[1], Lauriane Kuhn[2], Julie Blagojevic[2], Johanna Chicher[2], Philippe Hammann[2] and Carine Meignin[1]*.

[1]Université de Strasbourg, M3i CNRS UPR9022, Strasbourg, France.

[2]Plateforme Protéomique Strasbourg-Esplanade, Université de Strasbourg, CNRS FRC1589, Strasbourg, France.

Shortened title: Dicer-2 interactome *in vivo*

Key words: Dicer-2, innate immunity, antiviral

*Corresponding author: c.meignin@ibmc-cnrs.unistra.fr (C.M.)

INTRODUCTION

In metazoans, virus-derived double-stranded RNAs (dsRNAs) allow the detection of a broad range of viruses by pattern recognition receptors (PRRs), allowing the activation of antiviral innate immunity (Rousseau and Meignin, 2020). Dicer proteins are dsRNA sensors with an endoribonuclease activity from the RNase III family, enabling the production of microRNAs (miRNAs) and small interfering RNAs (siRNAs) (Baldaccini and Pfeffer, 2021). *Drosophila melanogaster*, like other arthropods, encodes two Dicer proteins: Dicer-1 which is dedicated to miRNA processing, and Dicer-2 which is required for siRNA biogenesis (Lee et al., 2004). Invertebrates rely mainly on the siRNA pathway for antiviral defense through the detection of viral dsRNA by Dicer-2 (Galiana-Arnoux et al., 2006; van Rij et al., 2006; Kemp et al., 2013; Webster et al., 2015; de Faria et al., 2022; Wang et al., 2006). The virus-derived siRNAs (vsiRNAs) produced by Dicer-2 are then loaded onto Argonaute2 (Ago2) protein to form the RNA-induced silencing complex (RISC), which targets and degrades the complementary RNA (Hammond et al., 2001; van Rij et al., 2006; Wang et al., 2006).

Dicer-2 is able to recognize and discriminate between two types of dsRNA termini and subsequently initiate two distinct types of cleavage mechanisms, called processive and distributive dicing (Welker et al., 2011; Sinha et al., 2015, 2018). *In vitro*, blunt dsRNA promotes processive cleavage, whereby the helicase domain of Dicer-2 will bind the dsRNA termini and thread through the dsRNA molecule using ATP hydrolysis to produce multiple siRNA duplexes of heterogeneous size in one go. In contrast, dsRNA with a 3'overhang promotes distributive cleavage, whereby the 5′-monophosphate of the dsRNA substrate is anchored by the phosphate-binding pocket in the Dicer-2 Platform•PAZ domain (Kandasamy and Fukunaga, 2016; Kandasamy et al., 2017) and Dicer-2 dissociates after each high-fidelity cleavage in an ATP-independent manner.

The helicase domain of all Dicer proteins is phylogenetically linked to the retinoic acid-inducible gene-I (RIG-I)-like receptors RLRs (Baldaccini and Pfeffer, 2021). RLRs are cytosolic dsRNA sensors that induce an interferon response, suggesting that the helicase domain is a sensor of viral infection. Viral dsRNAs can be synthetized as an intermediate product of viral replication in RNA viruses, or can originate from the convergent transcription of DNA viruses. In drosophila, all viruses tested so far are detected by Dicer-2 and induce the production of vsiRNAs (Kemp et al., 2013; de Faria et al., 2022). However, as the dicing mechanism relies on the recognition of the termini of the substrate, and viral dsRNAs produced during viral replication *in vivo* do not usually contain free ends, this raises the question of how Dicer-2 and the RLRs are able to sense viral infection. For example, the genome of the *Drosophila C virus* (DCV) is protected at the 5'end by a covalently bound protein called VPg and at the 3'end by a polyA tail.

To perform its function, Dicer-2 associates with several dsRNA-binding proteins (dsRBPs). It has been shown that the two accessory dsRBPs Loqs and R2D2 both bind the helicase domain of Dicer-2, consisting of 3 subdomains, Hel1, Hel2i and Hel2 (**Figure 8A**) (Lim et al., 2008; Nishida et al., 2013; Yamaguchi et al., 2022). More specifically, Loqs binds the Hel2 domain (Trettin et al., 2017) and R2D2 binds the Hel2i domain (Yamaguchi et al., 2022). Other dsRBPs (e.g. TRBP, PACT, PKR and ADAR) have also been shown to interact with the helicase domain of human Dicer (Ota et al., 2013; Wilson et al., 2015; Liu et al., 2018b; Montavon et al., 2021). The helicase domain therefore appears to be of the utmost importance for the interaction of the different regulatory proteins with Dicer. Moreover, it has been shown that the helicase domains of human Dicer and drosophila Dicer-2 are important for an antiviral response (Deddouche et al., 2008; Marques et al., 2013; Montavon et al., 2021).

Dicer-2 forms a heterodimer with the dsRBP R2D2, and this association is essential for several steps in the siRNA biogenesis. Although Dicer-2 is able to cleave pre-miRNAs *in vitro*, R2D2 and inorganic phosphate restrict the specificity of Dicer-2, preventing pre-miRNA cleavage (Cenik et al., 2011; Hartig and Förstemann, 2011). R2D2 further amplifies this distinction between Dicer-1 and Dicer-2 by localizing Dicer-2 to cytoplasmic foci, called D2 bodies, where endo-siRNAs will be cleaved, away from the pre-miRNAs (Nishida et al., 2013). After siRNA processing by Dicer-2, R2D2 is then also required for exo-siRNA loading onto Ago2 (Liu et al., 2003, 2006; Marques et al., 2010), which is then stabilized by the Hsc70/Hsp90 chaperone machinery (Iwasaki et al., 2010; Miyoshi et al., 2010; Iwasaki et al., 2015). One strand of the siRNA duplex is then discarded, such that the remaining strand can guide the RISC complex to the complementary target RNA for silencing. For this step, R2D2 is needed again, as it functions as a protein sensor for thermodynamic differences in the base-pairing stabilities of the 5'end of the siRNAs. Thus, it allows the siRNA loading onto Ago2 in a specific orientation, thereby determining which strand will be discarded and which one will serve as the guide (Tomari et al., 2004; Yamaguchi et al., 2022).

Another dsRBP, the TRBP drosophila homologue Loquacious (Loqs), plays an important role in the determination of Dicer-2 specificity. Because of alternative splicing, there are four distinct Loqs isoforms, with specific activities in the Dicer-1-dependent miRNA biogenesis pathway or the Dicer-2-dependent endo-siRNA pathway. While the function of Loqs-PC remains unknown, Loqs-PA and Loqs-PB interact with Dicer-1 for miRNA biogenesis (Förstemann et al., 2005; Jiang et al., 2005; Saito et al., 2005). By contrast, and Loqs-PD interacts with Dicer-2 for the biogenesis of endo-siRNAs, but not for the targeting of viral dsRNA for the viruses tested (Hartig et al., 2009; Zhou et al., 2009; Marques et al., 2013, 2010). This last isoform is able to modulate the termini dependence of Dicer-2 by enabling the cleavage of sub-optimal substrates such as dsRNA with blocked, structured, or frayed ends (Sinha et al., 2015). This

modulation is not achieved by changing the cleavage mode between processive and distributive, but rather by affecting the probability for Dicer-2 to cleave the sub-optimal substrate (Naganuma et al., 2021).

In order to get a clearer picture of the protein network associated with Dicer-2 during viral infection and the impact of Dicer-2 partners in the antiviral immunity, we used an IP-MS approach, in a fly line expressing the wild-type version of Dicer-2 fused to a GFP tag, GFP::Dicer-2^{WT}. As we were mostly interested in the early steps of the RNAi pathway (i.e. the viral dsRNA sensing by Dicer-2), we also used two Dicer-2 mutants that were able to sense the dsRNA but unable to process it. One of those mutants expresses a GFP-tagged version of Dicer-2 with a mutation on the Hel1 domain, and we will call it GFP::Dicer-2^{Hel1}. This Dicer-2 mutant is able to process a 3'overhang dsRNA substrate using distributive dicing, but not a blunt dsRNA substrate, which requires ATP hydrolysis for processive dicing. It has been described in previously published work, as well as the impact of this mutation on endo- and exo-siRNA production (Donelick et al., 2020). We also used another Dicer-2 mutant fly line, GFP::Dicer-$2^{RNaseIII}$, with two mutations in the RNase III domains, in the hope of identifying more transient interactions, as this mutant is able to bind dsRNA but not cleave it. Amongst the proteins identified by IP-MS, we observed a group of proteins, including Rumpelstinskin (Rump) and Syncrip (Syp) that seem to interact with Dicer-2 in an RNA-dependent manner only in mock-infected conditions. On the contrary, we observed some proteins, such as Rasputin (Rin) and Lost, for which the interaction is not RNA-dependent. By performing two RNAi screens, both *in vivo* and *ex vivo*, we have highlighted several of those proteins as having an impact on viral DCV infection. In particular, the protein Rin has an antiviral impact on DCV RNA load both *in vivo* and *ex vivo*, as well as an impact on the survival after DCV infection *in vivo*. In addition to Rin, this work provides a resource composed of several candidates, available to the scientific community that can now be investigated further to gain a better understanding of the proteins involved in Dicer-2-mediated antiviral RNAi.

RESULTS

Definition of the Dicer-2 interactome *in vivo*

To study the dynamics of the protein network surrounding Dicer-2 *in vivo* in response to viral infection, we infected *Drosophila melanogaster* with the *Drosophila C virus* (DCV) and performed immunoprecipitation (IP) of Dicer-2. We established an IP followed by mass spectrometry (MS) approach that allowed the definition of the Dicer-2 interactome *in vivo* in mock-infected and virus-infected conditions. To this aim, *dicer-2* null mutant fly lines were

complemented with different GFP::Dicer-2 versions and injected with TRIS (mock-infection) or with DCV. After immunoprecipitation of the GFP::Dicer-2 versions, their protein partners were then identified by LC-MS/MS (**Figure 8A & B, Supplementary Figure S1A**). In addition to a wild-type version of Dicer-2 (GFP::Dicer-2^{WT}), two mutants were used for this study: a helicase mutant unable to hydrolyze ATP and hence to perform processive dicing (GFP::Dicer-2^{Hel1}), and a RNase III double mutant unable to cleave dsRNAs (GFP::Dicer-$2^{RNaseIII}$). Both mutant versions of Dicer-2 could bind dsRNA but could then either only proceed to distributive dicing (Dicer-2^{Hel1}) or no dicing at all (Dicer-$2^{RNaseIII}$) (Donelick et al., 2020). Therefore, the Hel1 and RNase III mutants should give us an overview of the interactome of Dicer-2 in its early steps of dsRNA recognition. All experiments were performed in adult flies, and the ability of the wild-type version of Dicer-2 (GFP::Dicer-2^{WT}) to rescue the *dicer-2* null mutation was demonstrated in previous studies (Kemp et al., 2013; Girardi et al., 2015; Donelick et al., 2020). Furthermore, two control fly lines were used to determine non-specific interactants, both expressing endogenous *dicer-2* normally: a wild-type CantonS line (Ctrl-WT) and a transgenic line expressing GFP ubiquitously (Ctrl-GFP). Of note, the level of expression of GFP::Dicer-2 complemented lines is comparable to the endogenous expression of Dicer-2 in control lines (**Supplementary Figure S1A**).

In total, 2511 peptides were identified by LC-MS/MS across all samples. As our approach uses several versions of Dicer-2, a first analysis was performed using the SAINTexpress tool to have a global overview of the Dicer-2 partners (Teo et al., 2014). This has allowed us to create a list of 288 proteins that were significantly enriched overall (**Supplementary Figure S1B and Supplementary Table 1**). Visualization of this analysis using Prohits-viz shows that the bait protein Dicer-2 is enriched in all GFP::Dicer-2 lines as expected (**Figure 8C**) (Knight et al., 2017). MS analysis allowed us to detect specific peptides of the different GFP::Dicer-2 fusions confirming the presence of Dicer-2^{WT}, Dicer-2^{Hel1} and Dicer-$2^{RNaseIII}$ in the complemented lines (data not shown). Moreover, we can observe amongst the main interactants several proteins known to be involved in RNAi, like R2D2, a known cofactor of Dicer-2, AGO2, Loqs and CRIF (**Supplementary Table 1**). These results, consistent with the literature, validate the reliability of the approach (Liu et al., 2003; Czech et al., 2008; Miyoshi et al., 2010; Cernilogar et al., 2011; Hartig and Förstemann, 2011; Lim et al., 2014).

Global analysis of the protein network surrounding Dicer-2 *in vivo*

Analysis of the biological processes associated with the GFP::Dicer-2^{WT} interactome revealed eight statistically enriched GO terms, of which five were non-generic (**Figure 8D**). As expected, Dicer-2 interactomes reveal an enrichment in proteins linked to small RNA pathways and antiviral defense. After ranking candidates obtained with SAINTexpress based on Bayesian

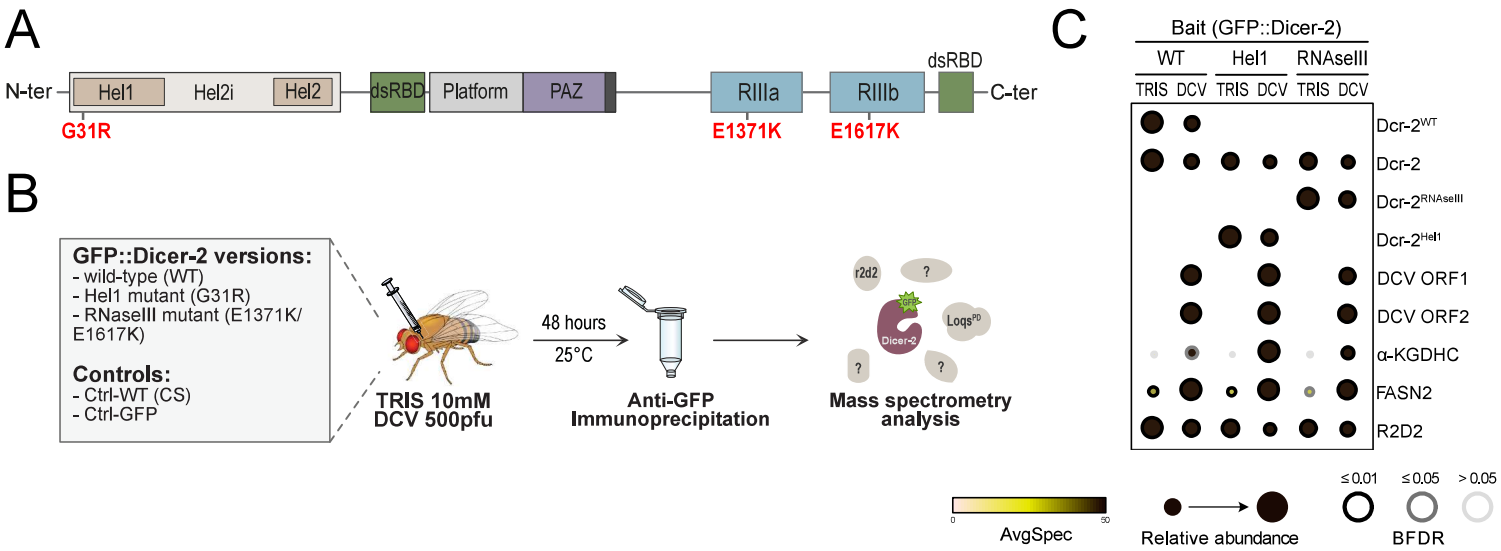

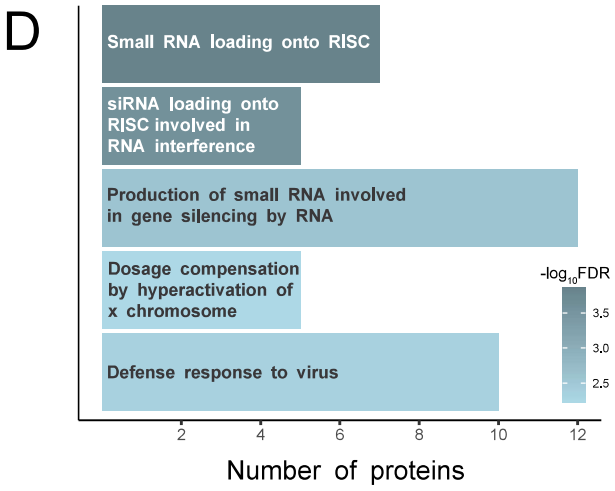

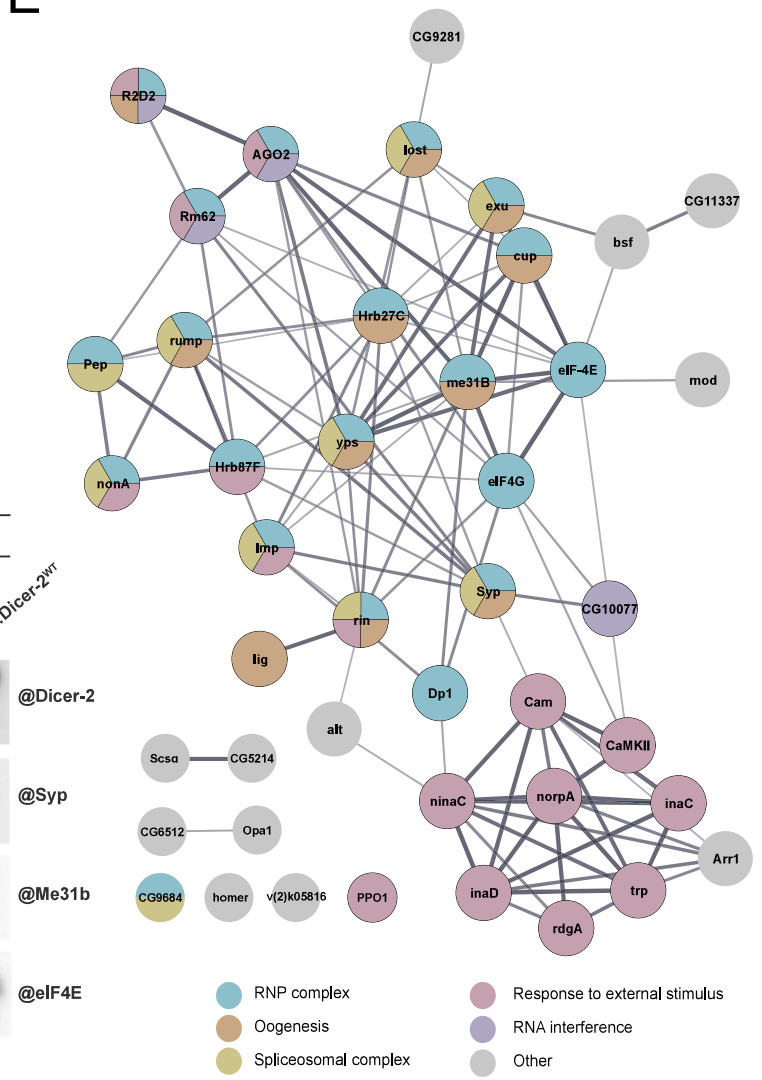

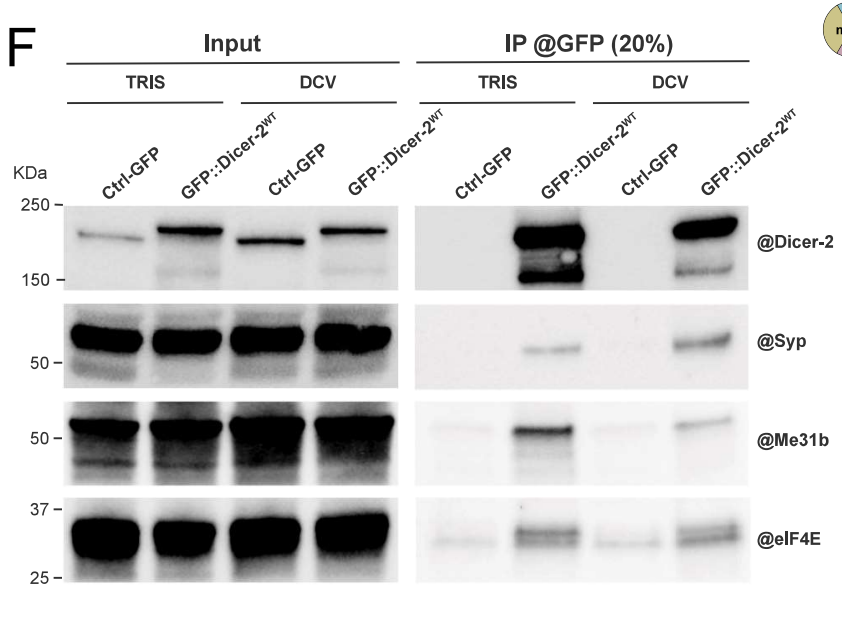

Figure 8: Global Dicer-2 interactome network during viral infection *in vivo*.
(A) Schematic representation of Dicer-2 domain architecture. The Dicer-2 protein (1722 amino acids) is composed of a helicase domain (which contains the Hel1, Hel2i and Hel2 sub-domains), two double-strand RNA binding domains (dsRBD), a PAZ domain, and two ribonuclease III domains (RIIIa and RIIIb). G31R and E1371K/E1671K represent the point mutations of *dicer-2* used in this study. **(B)** Scheme illustrating the experimental strategy for IP & LC-MS/MS used to identify Dicer-2 partners *in vivo* in mock-infected (TRIS) and DCV-infected conditions. All genotypes used are presented in the grey box. **(C)** Top candidates of the SAINTexpress analysis from 3 independent experiments for each condition. The average number of spectra (AvgSpec), the relative abundance and BFDR are represented. Among the top proteins, R2D2 is the second interactant of Dicer-2 for all three GFP::Dicer-2 lines and independent of the infection. **(D)** GO:biological processes enrichment analysis of GFP::Dicer-2^{WT} interactome proteins in mock-infected condition. **(E)** Global interaction network obtained with STRING/Cytoscape from the top 15% Dicer-2 partner proteins (i.e. top 44 proteins). **(F)** Immunoblot of Dicer-2 partners before and after IP using @GFP beads. GFP alone or GFP::Dicer2WT were immunoprecipitated with anti-GFP beads. In the input, endogenous Dicer-2 protein is detected in Crl-GFP lines whereas only the fusion GFP::Dicer2 is detected in the GFP::Dicer-2^{WT}. Syncrip, Me31b and eIF4E interact with GFP::Dicer-2^{WT} in mock- and DCV infected conditions.

false discovery rate (BDFR) values and fold-change between all the GFP::Dicer-2 lines, we selected the top 15% proteins (i.e. the 44 top candidates) to establish a global network into the STRING database (**Figure 8E**). Of note, four proteins involved in RNAi were found amongst the top 15% candidates. Moreover, we observed amongst the top candidates a node of proteins involved in the response to external stimulus that interact with each other. One of those proteins, NorpA, is a phospholipase C enzyme which genetically interacts with the NF-κB pathway regulating neuronal cell death in drosophila (Chinchore et al., 2012). Of note, several members of this node have been reported to interact physically (Ye et al., 2018; Chen and Montell, 2020; Chen et al., 2021). The GO term "Ribonucleoprotein complex" was also highlighted both in the enrichment analysis and in the top candidates' network. Finally, we found several proteins involved in the spliceosome complex. These results may point to as of yet uncharacterized roles of Dcr-2.

Among the main candidates interacting with Dicer-2, we then validated the interaction of some of them with Dicer-2 by IP and western blot. We confirmed that Me31b, Rump, eIF4E and Syp co-immunoprecipitated with GFP::Dicer-2^{WT}(**Figure 8F, Supplementary Figure S1C**). Some of the proteins are already known to form complexes associated with mRNAs (Nakamura et al., 2004; Igreja and Izaurralde, 2011; McDermott et al., 2012; Wang et al., 2017). The interaction between Dicer-2 and its partners does not appear to be dependent of the DCV infection suggesting that Dicer-2 associates with mRNP complexes linked to translation repression. However, some of these interactions weaken after infection of the flies with DCV, suggesting that they are displaced by other interactions or a change of localization.

Dicer-2 point mutations reveal specific interaction profiles in mock-infected and DCV-infected samples.

In addition to the global analysis, we performed separate statistical analyses of each GFP::Dicer-2 line, in order to compare them. To achieve this, we used a negative-binomial test to identify proteins enriched in each GFP::Dicer-2 line compared to the control lines (Ctrl-CS and Crtl-GFP), with a fold-change > 2 and an adjusted *p*-value < 0.01. Using the same approach, we then determined the impact of the infection by the DCV virus on the interactome of Dicer-2. This allowed us to group the different proteins interacting with Dicer-2 into categories depending on their enrichment in the different GFP::Dicer-2 lines and in DCV-infected samples (**Figure 9A-C, Supplementary Figure S2A-D**). We can observe that 146 proteins appear to be enriched in all GFP-Dicer-2 lines, including 25 proteins that were also enriched in the DCV-infected samples.

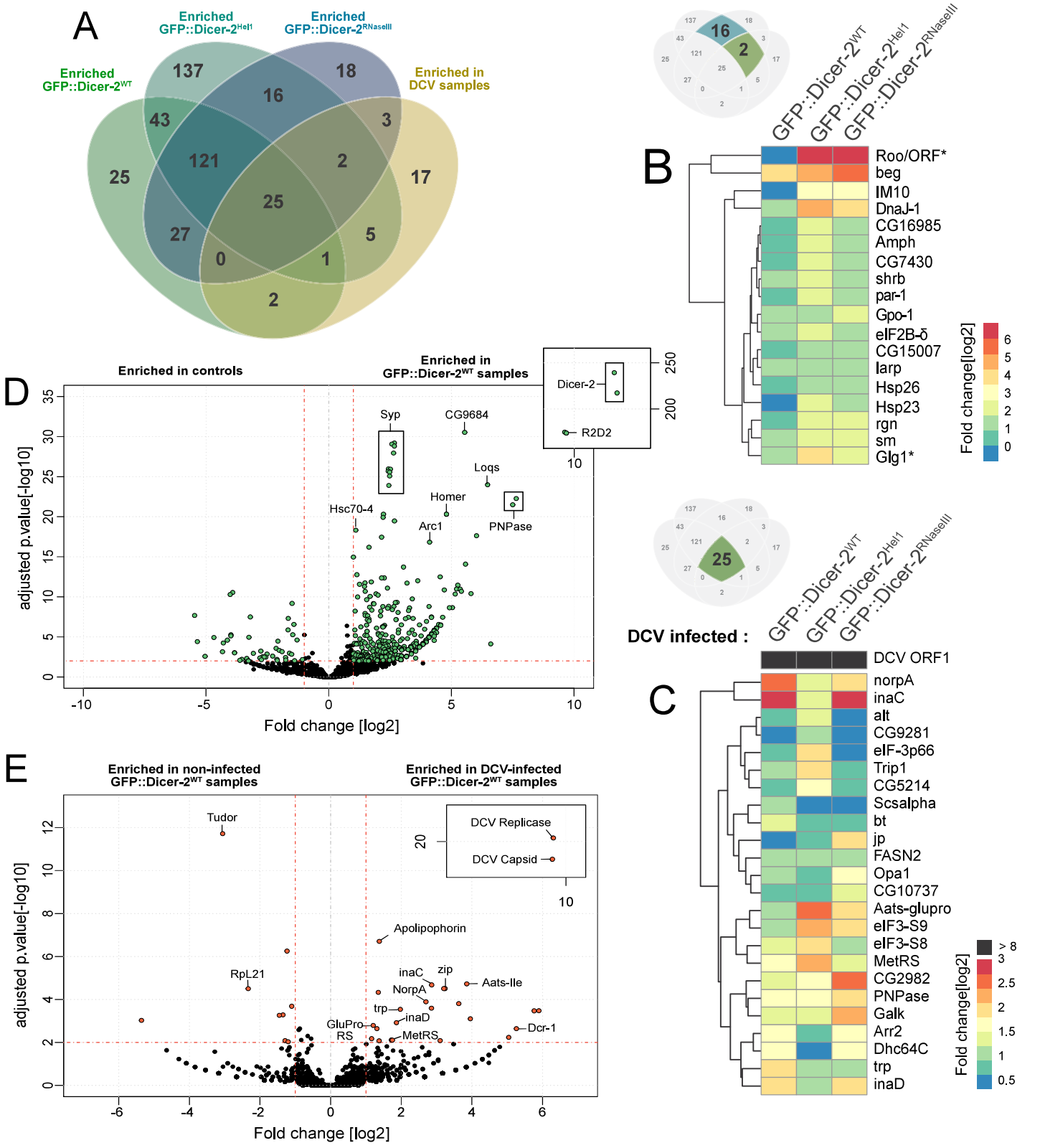

Figure 9: Impact of the Dicer-2 mutations on the RNP network during DCV infection. (A) Venn diagram showing the number of proteins identified in each GFP::Dicer-2 line in mock-infected and DCV-infected adult flies. Candidates are selected with a fold-change > 2 and an adjusted *p*-value < 0.01. **(B)** Heatmap representing the fold-change in comparison to the controls of the 18 proteins enriched only in the two GFP::Dicer-2 mutants (Hel1 and RNAseIII). 16 proteins are stable in mock-infected and DCV-infected samples. Two proteins, Roo/ORF and Glg1, are specifically enriched during DCV-infection and indicated with an asterisk. Log2 fold-change for each protein and each genotype is represented. **(C)** Heatmap representing the fold-change in comparison to the controls of the 25 proteins enriched with all GFP::Dicer-2 lines during DCV infection. The set of proteins is composed of 24 Drosophila proteins and DCV RdRp (ORF1). Log2 fold-change for each protein and each genotype during DCV infection is represented. **(D)** Volcano plot representing the fold changes and adjusted *p*-value of the Dicer-2 partners in GFP::Dicer-2^{WT} lines in mock- and DCV-infected conditions *versus* the control lines (Crtl-CS and Crtl-GFP). All the proteins with fold change > 2 and an adjusted *p*-value < 0.01 are represented in green. **(E)** Volcano plot representing the fold changes and adjusted *p*-value of the GFP::Dicer-2^{WT} partners in mock-infected *versus* DCV-infected adult flies. All the proteins with fold change > 2 and an adjusted *p*-value < 0.01 are represented in orange.

For every GFP::Dicer-2 line, R2D2 was always one of the top partners of Dicer-2, consistent with the presence of a stable heterodimer Dicer-2/R2D2 *in vivo* (Liu et al., 2003). This is illustrated in the volcano plots comparing each GFP::Dicer-2 line *versus* the controls (**Figure 9D, example of GFP::Dicer-2^{WT}**). Among the most enriched proteins in GFP::Dicer-2^{WT} samples, the Tudor protein (CG9864) and the chaperonin Hsc70-4 are involved in small RNA pathways (Iwasaki et al., 2010; Handler et al., 2011). We can also observe the presence of Syncrip (Syp), and another candidate from the global analysis, Polynucleotide phosphorylase (PNPase). PNPase is involved in RNA import into mitochondria and RNAs degradation during apoptosis in mammals (Portnoy et al., 2008; Liu et al., 2018a). Finally, Arc1 is a Gag-like retrotransposon able, in mammals, to self-assemble into capsids to encapsulate RNA and release it in extracellular vesicles (Pastuzyn et al., 2018). All these proteins represent the Dicer-2^{WT} network *in vivo*. Interestingly, GFP::Dicer-2^{Hel1} interacts specifically with 142 proteins, including 137 in mock-infected conditions whereas GFP::Dicer-2^{WT} and GFP::Dicer-2^{RNaseIII} have only 27 and 21 specific interactants respectively (**Figure 9A**). This result suggests that some proteins could interact transiently with Dicer-2 and be stabilized with Dicer-2^{Hel1}.

To better characterize the early steps of Dicer-2 sensing, we focused on the 18 proteins interacting specifically with the two mutant lines GFP::Dicer-2^{Hel1} and GFP::Dicer-2^{RNaseIII}, including two proteins, Roo/ORF and Glg1, that were also enriched in DCV infected conditions. These proteins are represented on a heatmap on **Figure 9B**, and studying them could help us understand the molecular mechanism of dicing and the ribonucleoprotein complexes involved (**Supplementary Figure S2B**). Taken together, these results illustrate how different the protein networks of the two Dicer-2 mutants used in this analysis are compared to GFP::Dicer-2^{WT}. Moreover, the legitimacy of the top 15% candidates chosen after the global analysis is further confirmed by the fact that out of those 44 proteins, 36 of them are also found in 146 proteins enriched in all GFP::Dicer-2 samples (**Supplementary Figure S2C**). Out of the 6 proteins remaining, 4 of them were enriched in two of the different GFP::Dicer-2 lines. Most candidates on this list have therefore been highlighted in four different analyses, using two different methods.

Next, we analyzed the impact of the DCV infection on Dicer-2 networks by studying the proteins enriched in the DCV-infected samples compared to the mock-infected samples (**Figure 9E**, example of DCV-infected GFP::Dicer-2^{WT} samples compared to mock-infected GFP::Dicer-2^{WT} samples). By adding this data to the one obtained during the previous analysis, we were able to categorize the different proteins depending on their enrichment in the different GFP::Dicer-2 lines and/or the DCV-infected samples (**Figure 9C, Supplementary Figure S2D**). Amongst those 25 proteins, 11 are present in the top 15% list of candidates from

the global analysis. The interactions between Dicer-2 and those proteins seem to increase after infection with DCV, which could indicate a connection of those proteins with the antiviral RNAi function of Dicer-2. Moreover, we can notice a protein called “ORF1”, an RNA-dependent RNA polymerase (RdRp), which belong to the DCV virus. GO term analysis for “Biological processes” terms shows that the GFP::Dicer-2 lines are enriched for proteins involved in small RNA pathways. However, these GO terms are highly enriched in the GFP::Dicer-2^{Hel1} suggesting a stabilization of the antiviral Dicer-2 interactome in this genetic background (**Supplementary Figure S2E**).

The RNA-dependent protein network of Dicer-2.

As we decided to perform the immunoprecipitations in low stringency conditions, the IP-MS analysis allowed us to identify a high number of interactions with Dicer-2. Those could be direct protein-protein interactions, but also indirect interactions through other proteins or RNAs, as we were interested in studying the complexes as a whole. However, knowing which interactions are mediated through RNA would allow us to define Dicer-2 interactomes further. To this aim, we performed a second IP-MS experiment on GFP::Dicer-2^{WT} with or without RNase A treatment. Adult flies expressing either GFP alone (Ctrl-GFP) or GFP::Dicer-2^{WT} were injected with TRIS (mock-infection) or DCV. Before immunoprecipitation, each sample was separated in two and one of the two halves was treated with RNase A to dissociate interactions mediated through RNA (**Supplementary Figure S3**). We then performed four independent statistical analyses using the same strategy as described above, in order to compare each condition (mock-infected or DCV-infected and/or treated with RNase A) to the corresponding control.

In total, this new set of data allowed us to highlight 448 proteins interacting with GFP::Dicer-2^{WT} in the different conditions compared to Crtl-GFP flies. Among them, we were able to distinguish 18 proteins enriched in all conditions, amongst which Dicer-2 and R2D2 (**Figure 10A**). Moreover, we were able to identify most of the candidates from the previous MS analysis in the non-RNase treated samples, which demonstrates the reproducibility of the two IP-MS experiments. We were therefore able to sort the top candidates obtained previously into different categories, depending on whether or not they were still enriched in GFP::Dicer-2^{WT} samples after RNAse A treatment (**Figure 10B**). According to these results, 17 proteins were enriched in at least one RNase A treated sample, including six proteins that were enriched in both, and are therefore likely to interact with Dicer-2 in an RNA-independent manner: R2D2, FASN2, Dp1, bsf, Cam, and Scs-α. It is important to point out however that the interaction could also be indirect, through an intermediary protein. Moreover, 12 of the top candidates seem to interact with Dicer-2 only in mock-infected and non-RNase-treated conditions. This

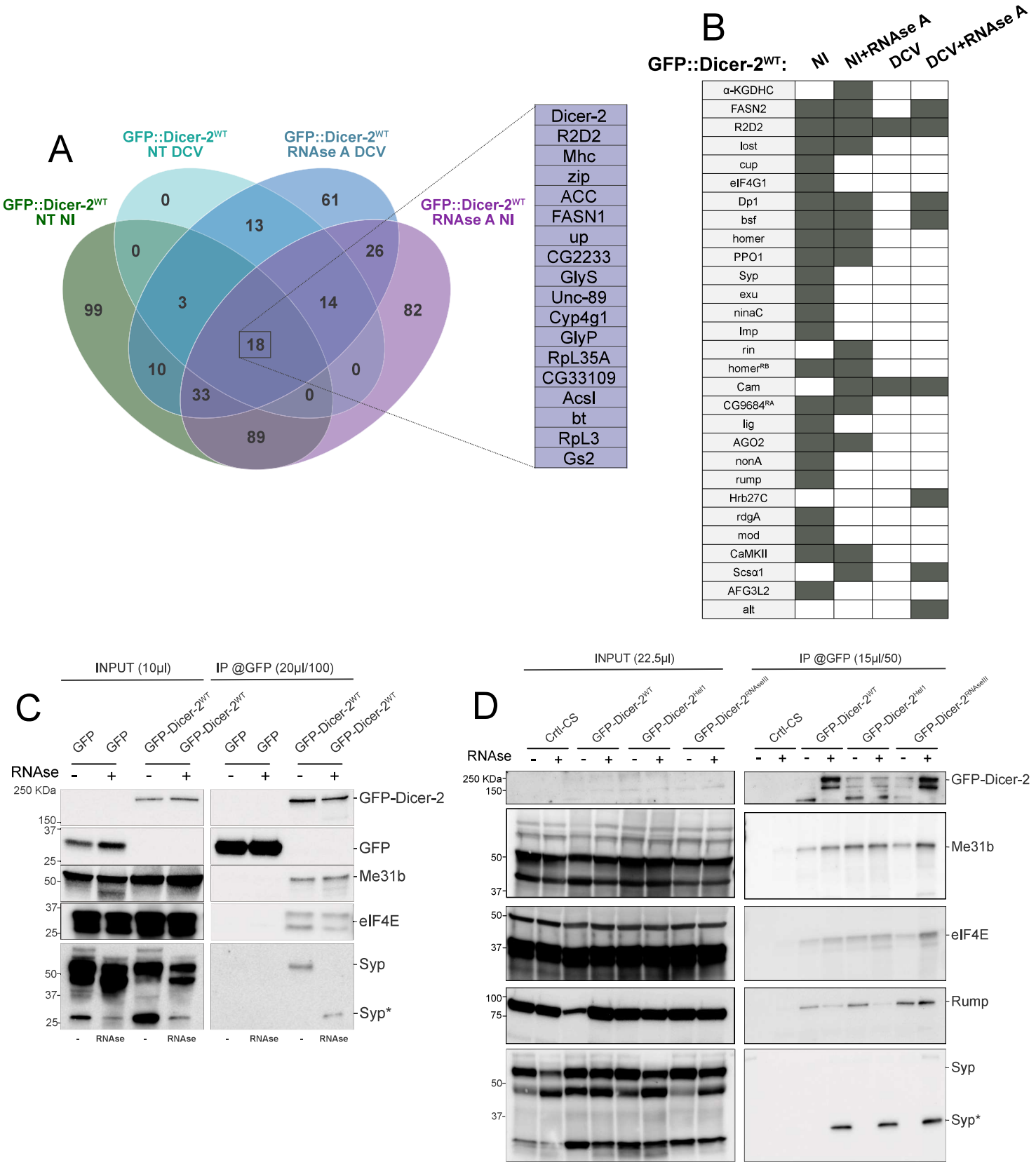

Figure 10: The RNA-dependent protein network of Dicer-2. (A) Venn diagram showing the number of proteins identified in the GFP::Dicer-2^{WT} line in mock-infected and DCV-infected adult flies with or without RNAse A treatment. Candidates are selected with a fold-change > 2 and an adjusted *p*-value < 0.01. The 18 proteins enriched in all conditions are highlighted. **(B)** Cross table representing the top 15% Dicer-2 partners depending on the RNA and DCV infection dependency. **(C)** Immunoprecipitation of GFP::Dicer-2^{WT} in comparison to the Ctrl-GFP line. Western blot analysis reveals the presence of GFP alone or GFP::Dicer-2^{WT} confirming the immunoprecipitation using anti-GFP beads. GFP::Dicer-2^{WT} interacts with Mei31b, eIF4E1 and Syncrip. The interaction with Syncrip is displaced during RNAse A treatment. **(D)** Immunoprecipitation of GFP::Dicer-2^{WT}, GFP::Dicer-2^{Hel1} and GFP::Dicer-2^{RNAseIII} in comparison to wilt-type CantonS flies (Ctrl-CS). Western blot analysis reveals the presence of GFP::Dicer-2 constructs confirming the immunoprecipitation using anti-GFP beads. All GFP::Dicer-2 lines interact with Mei31b, eIF4E1, Rump and Syncrip. The interaction with Rump is reduced with GFP::Dicer-2^{WT} and GFP::Dicer-2^{Hel1}. The interaction with Syncrip is displaced during RNAse A treatment.

could suggest that their interaction with Dicer-2 is mediated by RNA, and that it is displaced by the DCV infection.

According to the results of the different analyses, Rump and Syp seem to be interacting with Dicer-2 in an RNA-dependent manner, and this interaction could to be displaced by DCV infection (**Figure 10B**). To validate the RNA-dependency of Dicer-2 with its partners, we performed IP of GFP::Dicer-2 with or without RNase A treatment. We showed previously that Syp interacts with Dicer-2 (**Figure 8F**). After RNase A treatment an interaction is observed but at a lower molecular weight. Of note, the RNase A treatment shows a different molecular weight of Syp in the total protein extract (**Figure 10C & 10D**). Syncrip encoded several isoforms and the interaction between Syp and RNA could change its weight (McDermott et al., 2012, 2014). Therefore, this result could reflect the importance of RNA for the interaction between Dicer-2 and Syp (**Figure 10C & 10D**). Although Me31b and eIF4E1 were not significantly enriched in the IP-MS experiment with or without RNase A treatment, we also decided to test the RNA dependency of their interaction with Dicer-2, as were able to validate it previously (**Figure 8F**), and these two proteins seem to interact with Dicer-2 in a RNA-independent manner (**Figure 10C & 10D**). To go further, we performed IP with the three GFP::Dicer-2 lines, GFP::Dicer-2^{WT}, GFP::Dicer-2^{Hel1} and GFP::Dicer-$2^{RNaseIII}$, with or without RNase A treatment. While Me31b and eIF4E1 interact with Dicer-2 in an RNA-independent manner, Syp and Rump interact with all GFP::Dicer-2 lines and this interaction is displaced after RNase A treatment. Taken together, these results confirm the IP-MS experiments for some of the candidates and allow us to characterize the RNA-dependence or independence of the interactions between the top candidates and Dicer-2.

Impact of the candidates on viral infection *ex vivo* and *in vivo*

After establishing the different interactomes of Dicer-2, characterizing the different interactions and whether or not they are mediated through RNA, we further defined our interactome by studying which of the candidates had an impact on viral infection by DCV. The top 15% candidates of the global SAINT analysis were therefore subjected to an RNAi screen in S2 cells, to test their function during viral infection. To this end, the expression of the different candidate genes was inhibited in S2 cells using dsRNAs from DRSC Harvard, the cells were then infected by the DCV virus at a MOI of 0.01, and the viral RNA load was measured 20h later (**Figure 11A**). The data was normalized and analyzed using a linear mixed effect model and the candidates with a viral RNA load significantly different from the dsLacZ control are highlighted (**Figure 11B**). We found that eIF4G1 (2/2 dsRNAs) and Rin (1/2 dsRNA) exhibit an antiviral phenotype against DCV infection. Moreover, knock down of *lig* led to a significantly decreased DCV RNA load suggesting a proviral function of the Lig protein (1/2 dsRNA). A high

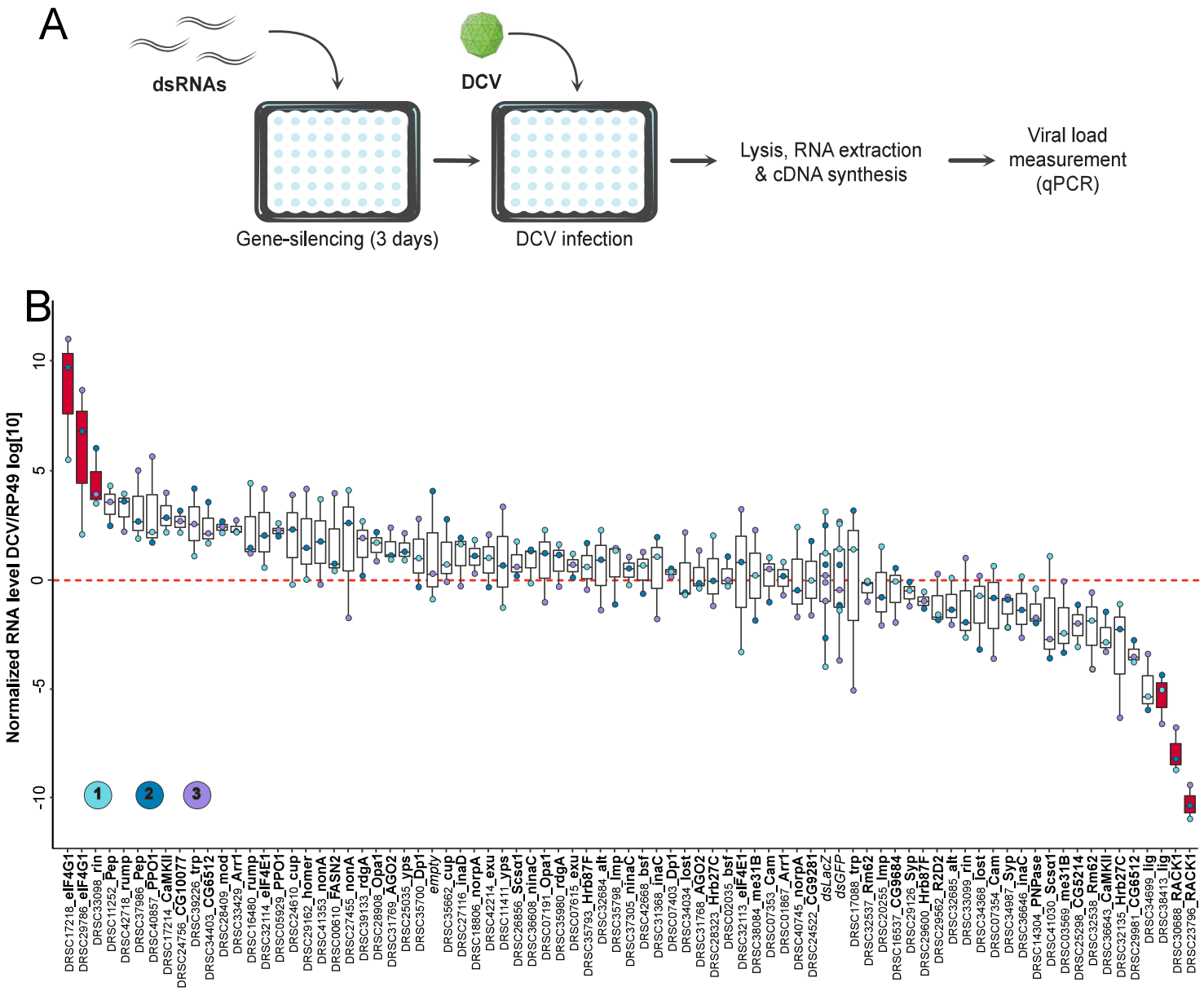

Figure 11: Role of the candidates in antiviral immunity in drosophila S2 cells. (A) Schematic representation of the experiment procedure. Knock-downs (KD) of gene expression were performed by soaking drosophila S2 cells with dsRNA targeting the candidate genes during 3 days. On day 3, cells were infected with DCV at 0.001 MOI for 20h. **(B)** Box plot representing the DCV viral RNA load of S2 cells after KD of the top 15% candidates followed by DCV infection. The dsRNAs targeting candidate genes are represented with the DRSC number and the gene name. Negative controls are infected S2 cells that were not treated with any dsRNA (empty), dsRNA against GFP, dsRNA against LacZ. In adition, dsRACK1 was used as a proviral control. The DCV RNA level is normalised to the housekeeping mRNA *RP49*. The three independent experiments are indicated by the color of the dots. The significant antiviral and proviral candidates are in red with a *p*-value < 0.05.

proportion of the candidate genes show an increase of DCV viral load after KD although not statistically significant, suggesting that they could still play a minor role in antiviral immunity.

The impact of the candidates was then studied *in vivo*, by using the same list of candidates to perform another screen in adult flies. A knock-down (KD) of the different candidate genes was induced through temperature shift in adult flies using the [actin-Gal4; tub-Gal80^{TS}] system, which were then injected with the DCV virus at 500PFU per fly (**Figure 12A**). Viral RNA load was then measured by RT-qPCR at 1 and 2 dpi (**Figure 12B**). Survival analysis was assessed by counting flies every day for 20 days after injection with TRIS or DCV 50PFU (**Figure 12C**).

These experiments highlighted different candidates, for which the inhibition of their expression seemed to have a significant impact on viral infection by DCV. The most striking impact on viral infection was observed for Rin. Indeed, this candidate had a consistent impact on DCV infection in all experiments: it showed an antiviral impact on viral RNA load both *ex vivo* (**Figure 11B**) and *in vivo* (**Figure 12B**), as well as an impact on survival after DCV infection *in vivo* (**Figure 12C**). This impact on survival was not observed in the mock-infected flies injected with TRIS only, this phenotype is not due to a general decrease of fitness in the KD flies. These data strongly suggest that Rin is involved in the antiviral response against DCV in *Drosophila melanogaster*. In the mosquito, this protein was shown to bind the Chikungunya virus (CHIKV) protein nsP3 and this interaction had a proviral impact on CHIKV infection rate and transmissibility (Fros et al., 2018). Other proteins have been shown to be both antiviral and proviral, depending on the virus, e.g. ADARs (Samuel et. al, 2011).

We were also able to observe an antiviral impact of Rump KD in flies, as it induced a higher viral RNA load at both timepoints (**Figure 12B**) and a concomitant decreased survival after DCV infection (**Figure 12C**). Again, this impact on survival is not due to a general decrease in fitness, as the flies injected with TRIS only show no significant decrease in survival. In cells, although the antiviral impact of Rump was not significant at the chosen timepoint and in this cell type, we can observe that after Rump KD the viral loads were amongst the highest of the candidates tested (**Figure 11B**). Rump is a hnRNP M homologue that binds to *nos* and *osk* mRNAs and has hitherto not been implicated in antiviral immunity.

Finally, we identified two candidates with proviral impacts on DCV infection: Lig and Rm62. With Lig, we observed a significant impact on DCV RNA load in cells (**Figure 11B**). Although it was not significantly different from shmCherry in flies, it was significantly different from the internal control KK line (**Figure 12B**). The flies knocked-down for Lig exhibited the lowest viral RNA load of all the flies from this batch. However, this did not translate into an increase in the survival rate in flies after DCV infection, meaning that its impact on viral infection may be mild.

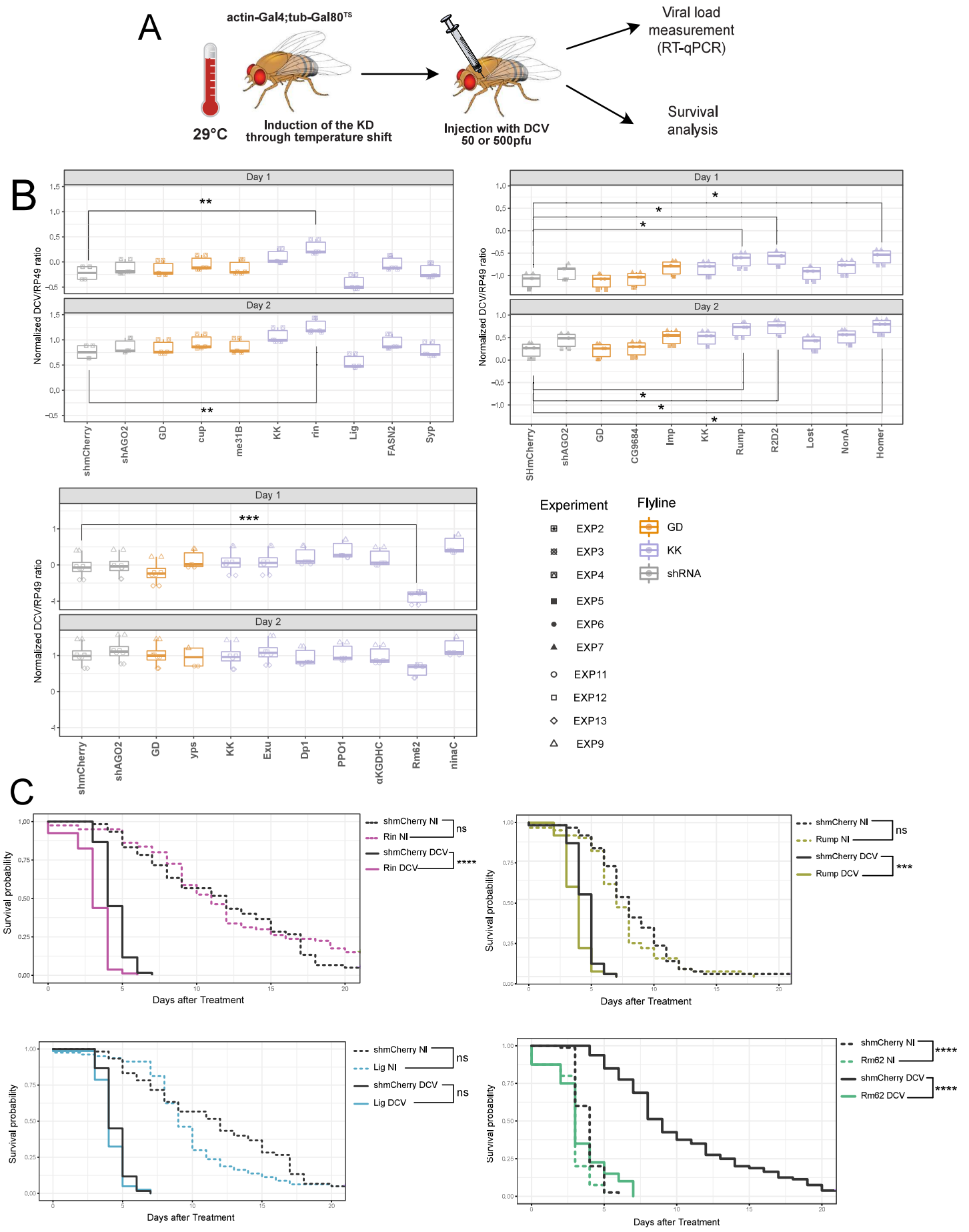

Figure 12: Role of the candidates in antiviral immunity in adult drosophila flies.
(A) Schematic representation of the experiment procedure. Knock-down (KD) of gene expression were established by crossing inducible UAS-dsRNA for each candidate gene with an ubiquitous Gal4 driver (actin5C-Gal4) under the control of thermosensitive ubiquitous Gal80 (tub-Gal80^{TS}) during five days at 29°C. Adult flies were injected with DCV 50pfu and analysed for survival or DCV 500pfu followed by RT-qPCR at days 1 and 2 post-infection. B) Box plot representing the DCV viral RNA load after infection of DCV 500 pfu at day 1 and day 2 post-infection. Triplicate experiments represented in three batches. Control lines: shmCherry, shAGO2, shGD and shKK lines. Significant viral load compared to shmCherry line are represented. C) Survival analysis of KD Rin, Rump, Lig and RM62 *in vivo* after infection DCV 50 pfu. Significant survival compared to shmCherry line are represented in non infected (**NI**) and DCV infected.

With Rm62, we observed a strong impact in flies, on both DCV RNA load and survival (**Figure 12B & 12C**). However, this was not the case in S2 cells at the chosen timepoint (**Figure 11B**). Moreover, the impact on survival after DCV infection in flies could be explained by a general impact on survival, as the flies injected with TRIS only also had a decreased survival rate in the Rm62 KD flies. Rm62 could be involved in the fitness of the flies as the TRIS-injection induces a decrease of the survival rate. Rm62 belongs to the DEAD-box family, which have a particularly important role in antiviral immunity.

In conclusion, these two KD screens *ex vivo* and *in vivo* have highlighted four different candidates: two proteins with antiviral phenotypes, Rin and Rump, and two proteins with proviral phenotypes, Lig and Rm62. In particular, Rin behaved in a consistently antiviral manner in all conditions tested with DCV infection.

DISCUSSION

The crucial role of the different protein partners of Dicer-2 in regulating or facilitating its activity has been extensively proven (papers). In order establish the protein network of Dicer-2 in different conditions, we have used different tagged GFP::Dicer-2 constructs and an IP-MS approach. We have confirmed the reliability of this approach by the identification of the usual key players of RNAi, also found in other interactomes of RNAi proteins (Frohn et al., 2012; Gerbasi et al., 2010; Joosten et al., 2021; Montavon et al., 2021; Varjak et al., 2020), e.g. R2D2, Ago1, Ago2 and Loqs. Moreover, we were also able to observe recurring interactions in our interactomes compared to other networks established in other studies. Indeed, we were able to confirm the interaction of Me31b, also known as DDX6, with Dicer-2 in drosophila *in vivo*, and this protein was also identified in mammalian cells as a potential interactant of Ago2 (Frohn et al., 2012). Another protein identified in this study was found in the list of 146 proteins interacting with all three GFP::Dicer-2 lines used, Larp4B. This protein was identified as a nucleic acid binding protein and shown to be antiviral against DCV, CrPV, SINV and VSV (Pennemann et al., 2021). Moreover, we have been able to identify proteins that were shown to interact with Dicer *ex vivo* in other species, e.g. DHX9/Mle and proteins from the Heat shock protein family 70 (Montavon et al., 2021; Varjak et al., 2020).

By opposition with the previous interactomes of Dicer-2 in other species this is, to our knowledge, the first interactome of Dicer-2 performed *in vivo* in adult flies. Moreover, in addition to a global analysis of the protein network of Dicer-2, we have also studied the impact of two point mutations on the interactome of Dicer-2 by using not only a WT version of Dicer-2 (GFP::Dicer-2^{WT}), but also the mutant fly lines GFP::Dicer-2^{Hel1} and GFP::Dicer-$2^{RNaseIII}$. This

has allowed us to highlight proteins interacting with only one, two, or all GFP::Dicer-2 samples. These categories can give us some information on the type of interaction that exists between the candidates and Dicer-2, as an interaction with only the WT version of Dicer-2 could mean that Dicer-2 must be functional and to produce siRNAs for the interaction to happen. On the contrary, an interaction with only the two mutants, which sequestrate the dsRNA in an unproductive complex (Donelick et al., 2020), could mean that the candidate interacts with Dicer-2 in a very transient manner, and by prolonging the interaction between Dicer-2 and the dsRNA, the interaction with the candidates is more easily observed. An interaction lost in only one of the two mutants could mean that this specific mutation could disturb the interaction between Dicer-2 and its partners. Finally, an interaction with all three GFP::Dicer-2 lines indicates a very stable interaction, not disturbed by those specific mutations and that is also reproducible as it was observed with three different GFP::Dicer-2 fly lines. Therefore, by choosing to study the list of 44 top candidates from the global analysis, we have biased our study towards very stable interactions with Dicer-2. However, it is important to mention that one of the candidates from the global analysis, Rin, was not significantly enriched (with a adjp-value < 0.01) in the GFP::Dicer-2^{RNaseIII} mutant in our fly line-specific analysis. This could mean that the RNase III domain in necessary for this interaction, although this needs to be confirmed biochemically. Moreover, we have noticed a very strong interaction of the two GFP::Dicer-2 mutants with a transposable element called Roo/ORF, which is not present for the WT version of Dicer-2. Keeping in mind that an unknown transposable element could be responsible for the reverse-transcription of viral RNA and play a role in systemic antiviral RNAi (Goic et al., 2013, 2016), the study of Roo/ORF could prove interesting.

During our study, we also looked at the impact of the DCV-infection on the protein network of Dicer-2. To this aim, we injected the different GFP::Dicer-2 lines with DCV in order to further categorize the protein network of Dicer-2. We subsequently studied the impact of the KD of the different candidates from the global analysis on DCV infection, both *in vivo* and *ex vivo*. These experiments have highlighted four candidates (Rump, Lig, Rin and Rm62).

Rm62 is a member of the DDX5/Dbp2 subfamily of DEAD-box helicases (Xing et al., 2019), and DEAD-box helicases have been shown to be important for antiviral immunity (Rousseau and Meignin, 2020). Moreover, it has been shown to play a role in RNAi and to bind dsRNA in an ATP-dependent manner (Huang and Liu, 2002; Ishizuka et al., 2002). Furthermore, stem loop recognition by Rm62 was also shown to facilitate miRNA processing and antiviral defense against the Rift Valley fever virus (RVFV) in drosophila both *in vivo* and *ex vivo* (Moy et al., 2014). Rm62 thus possesses a role in the recognition of stem loops for both pre-miRNAs and viral RNAs.

The protein Rin belongs to the GTPase activating protein (SH3 domain) binding protein family (also known as G3BPs) a family of RBPs that regulate gene expression in response to environmental stresses. In unstressed cells, Rin plays a role in the stabilization and upregulation of target mRNAs translation (Laver et al., 2020). This regulation can happen inside stress granules (SGs), of which they are core components, or outside of them (Alam and Kennedy, 2019). As SGs are induced in response to viral infections, some viruses sequestrate G3BPs (Lloyd, 2013) while others such as the poliovirus (*Picornaviridae* family) target and cleave them in order to disrupt the formation of stress granules (White et al., 2007). This is interesting as DCV is a picorna-like virus. In some cases, e.g. in alphaviruses, a conserved interaction with the viral proteins Nsp3 and SG proteins (Nowee et al., 2021) not only prevents SG formation but also act in favor of the virus, as in the case of the Rin-Nsp3 interaction for the chikungunya (CHIKV) virus (Fros et al., 2015). CHIKV is able to utilize Rin in order to increase infection rate and transmissibility. Interestingly, although we saw an antiviral effect of Rin and a proviral effect of Lig during DCV infection, the two proteins have been shown to act in concert to regulate cell proliferation during development (Baumgartner et al., 2013). Nevertheless, the human homologue of Lig, UBAP2L, was identified after pull-down of the human homologue of Rin, G3BP1, in HEK293T cells and was shown to localize in stress granules and modulate amyotrophic lateral sclerosis (ALS) in an *in vivo* Drosophila ALS model (Markmiller et al., 2018). A diversion of Lig by DCV in a similar manner to that of CHIKV and Rin could explain the proviral effect of Lig despite the antiviral effect of stress granules.

In the global analysis of the Dicer-2 network, a large number of proteins are well described for their functions during drosophila oogenesis, including three of the proteins for which the interaction with Dicer-2 was confirmed by WB: Me31b, eIF4E1 and Rump. By looking deeper into those candidates, we noticed that most of them (e.g. Dp1, Lost, Cup, eIF4E1, Me31b, Imp, Syp, Bsf, Rump, Exu & Yps) were associated with mRNA localization regulation mechanisms, like the regulation of *nanos* or *oskar* mRNA translation. Indeed, Me31b has been shown to form a complex with Tral, eIF4E1, Cup and PABP involved in RNP-mediated translational repression of maternal mRNAs during oogenesis and embryogenesis (Wang et al., 2017). It has also been shown to form a complex with Exu and Yps involved in the translational silencing of mRNAs (such as oskar) during their transport to the oocyte (Nakamura et al., 2001). The presence of eIF4E1, Cup, Exu and Yps in the top candidates of the global analysis could therefore suggest that Dicer-2 could interact with those two complexes formed by Me31b. An impact of Dicer-2 in oogenesis could explain the decreased fertility of *dicer-2 null* mutants. In addition, Rump and Lost, which interact together, have also been shown to be involved in mRNA regulation in the oocyte (Jain and Gavis, 2008; Sinsimer et al., 2011) and this is also the case for Syp (McDermott et al., 2012). This would not be the first time that an RNAi-

independent role in mRNA regulation of Dicer-2 is reported, as previous studies have already reported an RNAi-independent role of Dicer-2 in the regulation of mRNA expression, and more specifically in the activation of the expression of *Toll* and *R2D2* mRNAs through cytoplasmic polyadenylation (Coll et al., 2018; Wang et al., 2015). Interestingly, another small RNA factor, Aubergine (aub), has been implicated in both mRNA localization regulation and Wispy-related mRNA regulation mechanisms (Dufourt et al., 2017) and has been implicated as a *nanos* mRNA localization factor in a mechanism implicating Rump (Becalska et al., 2011). If Dicer-2 does have a link with the regulation of mRNA expression during oogenesis, it would underline the interconnection between small RNA factors and RNAi-independent mRNA regulation mechanisms.

Overall, this work has produced a resource and a large amount of data that is now available for the community. Our network hints at a potential involvement of Dicer-2 and several candidates in different mechanisms, in both mRNA regulation and antiviral immunity.

MATERIAL AND METHODS

Flies, drosophila S2 cells and virus

The GFP::Dicer-2 fusion drosophila fly lines were obtained by crossing [w^{IR}; *dicer-2*^{L811fsx}/*CyO*] virgins with: [w^{IR}; *dicer-2*^{L811fsx}/*CyO*; ubi>GFP::Dicer-2^{WT}] males (GFP::Dicer-2^{WT}), [GFP::Dicer-2^{Hel1} : w^{IR}; *dicer-2*^{L811fsx}/*CyO*; ubi>GFP::Dicer-2^{G31R}] males (GFP::Dicer-2^{Hel1}), or [w^{IR}; *dicer-2*^{L811fsx}/*CyO*; ubi>GFP::Dicer-2$^{E1371K/E1617K}$] males (GFP::Dicer-2^{RNaseIII}). The first two fly lines (GFP::Dicer-2^{WT} and GFP::Dicer-2^{Hel1}), were established as described previously (Donelick et al., 2020) and the third one, GFP::Dicer-2^{RNaseIII}, was established in the same manner with the following mutations in the Dicer-2 sequence: E1371K and E1617K, thus inactivating the activity of its RNase III domain. The control fly lines used were *CantonS* flies and GFP expressing flies, obtained by crossing *P{UAS-GFP.S65T}Myo31DF[T2]* line (BDSC #1521) under the control of the *actin5C* promoter (BDSC #25374).

S2 cells were grown in Schneider's medium (Biowest) supplemented with 10% fetal calf serum, Glutamax (Invitrogen) and Penicillin/Streptomycin (100x mix, 10 mg/mL/ 10000 U, Invitrogen).

DCV virus stock was produced as described (Kemp et al., 2013).

Viral infection and immunoprecipitations for MS analysis

Infections were performed on 3- to 5-day-old flies. Forty flies (20 females and 20 males) of each phenotype were injected with TRIS (10 mM, pH7.5) or DCV (500PFU) with 4.6 nL of TRIS (10 mM pH7.5) or DCV (500PFU) by intrathoracic injection (Nanoject II apparatus; Drummond

Scientific). Flies were kept at 25°C for either 2 or 3 days, and then collected in Precellys tubes with zirconium beads and frozen overnight at -80°C. The flies were first shredded at 10°C without any buffer and then a second time with 1 mL lysis buffer (30 mM HEPES KOH pH 7.5, 50 mM NaCl, 2 mM Mg(OAc)2, 1% NP40, 2X cOmplete Protease Inhibitor Cocktail [Roche]). If the impact of RNase A on the interactants was tested, samples were separated in two halves and one half was treated with 15 µg RNase A for 30 min at 4°C. Samples were then centrifuged and the rest of the protocol was performed in the same manner as for the other MS experiment. After centrifugation, 20 µL (0.05%) of the protein supernatant was kept to be loaded on a gel later on (**Supplementary Figure S1A**) and the rest was incubated with anti-GFP bead (Miltenyi) for 40 min at 4°C on a spinning wheel. The protein samples were then added onto a microcolumn placed on an uMACS separator (Miltenyi) after equilibration of the microcolumn with lysis buffer. Three washes were performed using wash buffer (30 mM HEPES KOH pH 7.5, 50 mM NaCl, 2 mM Mg(OAc)2, 0.1% NP40, 2X cOmplete Protease Inhibitor Cocktail [Roche]) and the elution was performed using elution buffer (Miltenyi) heated to 95°C. Five microliters (25%) of the elution was kept to confirm the IP on a WB and the rest was immediately used for mass spectrometry analysis.

Mass spectrometry analysis

Proteins were digested with sequencing-grade trypsin (Promega, Fitchburg, MA, USA). Each sample was further analyzed by nanoLC-MS/MS on a QExactive+ mass spectrometer coupled to an EASY-nanoLC-1000 (Thermo-Fisher Scientific, USA) as described previously (Chicher et al., 2015). Data were searched against the Drosophila melanogaster UniprotKB sub-database with a decoy strategy (UniprotKB release 2018_02 and 2022_01, taxon 7227, 42551 forward protein sequences). The correlation between spectrum matches for common baits of the two different MS queries was assessed, as the two MS experiments were performed using different UniprotKB releases, and was greater than 0.999. Peptides and proteins were identified with Mascot algorithm (version 2.5.1, Matrix Science, London, UK) and data were further imported into Proline v1.4 software (http://proline.profiproteomics.fr/). Proteins were validated on Mascot pretty rank equal to 1, and 1% FDR on both peptide spectrum matches (PSM score) and protein sets (Protein Set score). The total number of MS/MS fragmentation spectra was used to quantify each protein from at least three independent biological replicates. The mass spectrometric data will be deposited to the ProteomeXchange Consortium *via* the PRIDE partner repository before publication.

Statistical post-processing of the MS data and bioinformatics analysis

For each fly line, statistical post-processing of the data was performed through the R package (v3.2.5). After a column-wise normalization of the data matrix, the spectral count values were

submitted to a negative-binomial test using an edgeR GLM regression as well as the msmsTests R package (release 3.6, Gregori et al., 2013). For each identified protein, an adjusted *p*-value (adjp) corrected by Benjamini–Hochberg was calculated, as well as a protein fold-change (FC). The results are presented in a Volcano plot using protein log2 fold changes and their corresponding adjusted log10 *p*-values to highlight upregulated proteins. Duplicate genes were manually removed and the results of the lists of genes enriched in the different conditions were put in JVenn to produce Venn diagrams (Bardou et al., 2014), or in R using the Pheatmap function to produce heatmaps.

An overall analysis of the data was performed using the Significance Analysis of INTeractome (SAINT) tools for interaction scoring. The data was then represented using Prohits-viz. A protein network was represented using the STRING tool in Cytoscape (version v3.9.1), after inputting the top 15% of the SAINT analysis candidates. The GO term functional enrichment analysis was conducted with STRING (https://string-db.org), using the full protein list and log fold-change.

Confirmation of the interactions by immunoblot analysis

The input and elution samples obtained after immunoprecipitation using anti-GFP beads (Miltenyi or agarose beads from Chromotek). If necessary, injections followed by RNase A treatment or not were performed as described above. Protein extracts were separated on a Biorad gel and transferred to a nitrocellulose membrane. Membranes were then blocked in TBST containing 5% milk powder for 1h at RT and incubated overnight at 4°C with the different primary antibodies listed in **Supplementary Table 2**. After washing, the corresponding secondary antibodies fused to horseradish peroxidase (HRP) were added to the membrane for 2h at RT. Membranes were then washed and visualized with enhanced chemiluminescence reagent (GE Healthcare) in a ChemiDoc (Bio-Rad) apparatus.

RNAi screen in S2 cells

After clustering of the 288 candidates highlighted by SAINT analysis after LC-MS/MS, the top 15% were selected to be part of a RNAi mini-screen. The dsRNAs were ordered at Drosophila RNAi Screening Center (DRSC) at Harvard Medical School. 47 dsRNAs were ordered in total, amongst which *dsAGO2* and *dsRACK1*, which were used as antiviral and proviral controls, respectively. Moreover, two negative controls (*dsGFP* and *dsLacZ*) and on RNAi knockdown (KD) efficiency control (*dsThread*) were placed in triplicate for each plate and put at different positions on the plate. *dsGFP* and *dsLacZ* were used to detect and normalize column and/or line effect, and *dsThread* controls were used to check that RNAi was working properly for each plate. Cells were seeded in 96-well plates and incubated with 1µg of dsRNA in FBS-free Schneider medium for 4h. After this starving period, normal S2 medium containing FBS was

added, and the cells were incubated for 3 days before infection. Infections were performed at 25°C with MOI of 0.01 for 20h, after adsorption on ice for 1h. Cell lysis and reverse transcription were then performed using the Cells-to-CT kit (ThermoFisher Scientific) according to the manufacturer protocol, and used to perform quantitative real-time qPCR using the iTaq Universal SYBR Green Supermix (Biorad). The primers used are listed in the **Supplementary Table 3**. After calculating the $2^{\Delta Ct}$ for each sample, different mixed effect linear models were tested to search for bias in the data (lme2 R package (version 1.1-29)). As variations in plate, rows and columns had a significant impact after ANOVA, they were used as random factors in the final mixed effect model chosen. Corrected ratios (estimates) were extracted from the model and statistical significance was calculated by comparing estimates of each dsRNA to that of the dsLacZ control using the emmeans function.

Genetic UAS-RNAi screen in an actin-Gal4-tub-Gal80^{TS} system

The top 15% candidates highlighted by the SAINT analysis were selected for the genetic screen *in vivo*. KK and GD inverted repeat transgenic fly lines for each candidate gene were acquired from the VDRC stock center (**Supplementary Table 4**), and *shmCherry* (BDSC #35787) and *shAGO2* (BDSC #34799) were used as controls, in addition to the respective KK and GD control lines. Transgenic males containing the inverted repeat of the target gene under the control of Gal4 regulated upstream activating sequence (UAS) were crossed with virgin females [Actin5C-Gal4/*CyO*; Tubulin-Gal80^{TS}] at 18°C. The F1 generation was placed at 29°C for 5 days to induce the knockdown of candidate genes. All experiments were subsequently performed at 29°C. Infections were then performed as described above. The flies were then either counted every day in order to assess survival or collected at 1 or 2 dpi for RT-qPCR. In this case, three males and three females per condition were collected. Total RNA from the flies was then extracted using Trizol-chloroform, and 500 ng of total RNA was reverse transcribed using the iScript™ gDNA Clear cDNA Synthesis Kit (Biorad) according to the manufacturer's instructions, and used to perform quantitative real-time qPCR using the iTaq Universal SYBR Green Supermix (Biorad), on a CFX384 Touch Real-Time PCR platform (Bio-Rad). The qPCR primers used are listed in **Supplementary Table 2**.

Normalization and qPCR/survival analysis

All statistical analyses were performed in R (version 3.6.1). After calculating the $2^{\Delta Ct}$ for each sample, different mixed effect linear models were tested to search for bias in the data (lme2 R package (version 1.1-29)). Each batch was analyzed independently and the data was tested for normality and homoscedasticity. As variations in replicates had a significant impact after ANOVA, this parameter was used as a random factor in the final mixed effect model chosen. Moreover, dependence between the "Gene" and "dpi" fixed factors was tested and found to be

true for Batch 3; the models were adjusted accordingly. Corrected ratios (estimates) were extracted from the model and statistical significance was calculated by comparing estimates of each fly line to that of the shmCherry control using the emmeans function. P-values were adjusted using the Dunnett method.

Acknowledgments:

This work of the Interdisciplinary Thematic Institute IMCBio, as part of the ITI 2021-2028 program of the University of Strasbourg, CNRS and Inserm, was supported by IdEx Unistra (ANR-10-IDEX-0002), and by SFRI-STRAT'US project (ANR 20-SFRI-0012) and EUR IMCBio (ANR-17-EURE-0023) under the framework of the French Investments for the Future Program. The Rump monoclonal antibody developed by Gavis, E.R. was obtained from the Developmental Studies Hybridoma Bank, created by the NICHD of the NIH and maintained at The University of Iowa, Department of Biology, Iowa City, IA 52242.

BIBLIOGRAPHY

Alam, U., and Kennedy, D. (2019). Rasputin a decade on and more promiscuous than ever? A review of G3BPs. Biochim Biophys Acta Mol Cell Res *1866*, 360–370. https://doi.org/10.1016/j.bbamcr.2018.09.001.

Baldaccini, M., and Pfeffer, S. (2021). Untangling the roles of RNA helicases in antiviral innate immunity. PLoS Pathog *17*, e1010072. https://doi.org/10.1371/journal.ppat.1010072.

Bardou, P., Mariette, J., Escudié, F., Djemiel, C., and Klopp, C. (2014). jvenn: an interactive Venn diagram viewer. BMC Bioinformatics *15*, 293. https://doi.org/10.1186/1471-2105-15-293.

Baumgartner, R., Stocker, H., and Hafen, E. (2013). The RNA-binding proteins FMR1, rasputin and caprin act together with the UBA protein lingerer to restrict tissue growth in Drosophila melanogaster. PLoS Genet *9*, e1003598. https://doi.org/10.1371/journal.pgen.1003598.

Becalska, A.N., Kim, Y.R., Belletier, N.G., Lerit, D.A., Sinsimer, K.S., and Gavis, E.R. (2011). Aubergine is a component of a nanos mRNA localization complex. Developmental Biology *349*, 46–52. https://doi.org/10.1016/j.ydbio.2010.10.002.

Cenik, E.S., Fukunaga, R., Lu, G., Dutcher, R., Wang, Y., Tanaka Hall, T.M., and Zamore, P.D. (2011). Phosphate and R2D2 Restrict the Substrate Specificity of Dicer-2, an ATP-Driven Ribonuclease. Molecular Cell *42*, 172–184. https://doi.org/10.1016/j.molcel.2011.03.002.

Cernilogar, F.M., Onorati, M.C., Kothe, G.O., Burroughs, A.M., Parsi, K.M., Breiling, A., Sardo, F.L., Saxena, A., Miyoshi, K., Siomi, H., et al. (2011). Chromatin-associated RNA interference components contribute to transcriptional regulation in Drosophila. Nature *480*, 391–395. https://doi.org/10.1038/nature10492.

Chen, Z., and Montell, C. (2020). A Family of Auxiliary Subunits of the TRP Cation Channel Encoded by the Complex inaF Locus. Genetics *215*, 713–728. https://doi.org/10.1534/genetics.120.303268.

Chen, W., Shen, Z., Asteriti, S., Chen, Z., Ye, F., Sun, Z., Wan, J., Montell, C., Hardie, R.C., Liu, W., et al. (2021). Calmodulin binds to Drosophila TRP with an unexpected mode. Structure *29*, 330-344.e4. https://doi.org/10.1016/j.str.2020.11.016.

Chinchore, Y., Gerber, G.F., and Dolph, P.J. (2012). Alternative pathway of cell death in Drosophila mediated by NF-κB transcription factor Relish. Proceedings of the National Academy of Sciences *109*, E605–E612. https://doi.org/10.1073/pnas.1110666109.

Coll, O., Guitart, T., Villalba, A., Papin, C., Simonelig, M., and Gebauer, F. (2018). Dicer-2 promotes mRNA activation through cytoplasmic polyadenylation. RNA *24*, 529–539. https://doi.org/10.1261/rna.065417.117.

Czech, B., Malone, C.D., Zhou, R., Stark, A., Schlingeheyde, C., Dus, M., Perrimon, N., Kellis, M., Wohlschlegel, J.A., Sachidanandam, R., et al. (2008). An endogenous small interfering RNA pathway in Drosophila. Nature *453*, 798–802. https://doi.org/10.1038/nature07007.

Deddouche, S., Matt, N., Budd, A., Mueller, S., Kemp, C., Galiana-Arnoux, D., Dostert, C., Antoniewski, C., Hoffmann, J.A., and Imler, J.-L. (2008). The DExD/H-box helicase Dicer-2 mediates the induction of antiviral activity in drosophila. Nat. Immunol. *9*, 1425–1432. https://doi.org/10.1038/ni.1664.

Donelick, H.M., Talide, L., Bellet, M., Aruscavage, P.J., Lauret, E., Aguiar, E.R.G.R., Marques, J.T., Meignin, C., and Bass, B.L. (2020). In vitro studies provide insight into effects of Dicer-2 helicase mutations in Drosophila melanogaster. RNA *26*, 1847–1861. https://doi.org/10.1261/rna.077289.120.

Dufourt, J., Bontonou, G., Chartier, A., Jahan, C., Meunier, A.-C., Pierson, S., Harrison, P.F., Papin, C., Beilharz, T.H., and Simonelig, M. (2017). piRNAs and Aubergine cooperate with Wispy poly(A) polymerase to stabilize mRNAs in the germ plasm. Nat Commun *8*, 1305. https://doi.org/10.1038/s41467-017-01431-5.

de Faria, I.J.S., Aguiar, E.R.G.R., Olmo, R.P., Alves da Silva, J., Daeffler, L., Carthew, R.W., Imler, J.-L., and Marques, J.T. (2022). Invading viral DNA triggers dsRNA synthesis by RNA polymerase II to activate antiviral RNA interference in Drosophila. Cell Rep *39*, 110976. https://doi.org/10.1016/j.celrep.2022.110976.

Förstemann, K., Tomari, Y., Du, T., Vagin, V.V., Denli, A.M., Bratu, D.P., Klattenhoff, C., Theurkauf, W.E., and Zamore, P.D. (2005). Normal microRNA maturation and germ-line stem cell maintenance requires Loquacious, a double-stranded RNA-binding domain protein. PLoS Biol. *3*, e236. https://doi.org/10.1371/journal.pbio.0030236.

Frohn, A., Eberl, H.C., Stöhr, J., Glasmacher, E., Rüdel, S., Heissmeyer, V., Mann, M., and Meister, G. (2012). Dicer-dependent and -independent Argonaute2 protein interaction networks in mammalian cells. Mol Cell Proteomics *11*, 1442–1456. https://doi.org/10.1074/mcp.M112.017756.

644 Fros, J., Geertsema, C., Zouache, K., Baggen, J., Domeradzka, N., Leeuwen, D. van, Flipse, J.,
645 Vlak, J., Failloux, A.-B., and Pijlman, G. (2015). Mosquito Rasputin interacts with chikungunya
646 virus nsP3 and determines the infection rate in Aedes albopictus. Parasites and Vectors *8*,
647 464. https://doi.org/10.1186/s13071-015-1070-4.

648 Galiana-Arnoux, D., Dostert, C., Schneemann, A., Hoffmann, J.A., and Imler, J.-L. (2006).
649 Essential function in vivo for Dicer-2 in host defense against RNA viruses in drosophila. Nat
650 Immunol *7*, 590–597. https://doi.org/10.1038/ni1335.

651 Gerbasi, V.R., Golden, D.E., Hurtado, S.B., and Sontheimer, E.J. (2010). Proteomics
652 identification of Drosophila small interfering RNA-associated factors. Mol Cell Proteomics *9*,
653 1866–1872. https://doi.org/10.1074/mcp.M900614-MCP200.

654 Girardi, E., Lefèvre, M., Chane-Woon-Ming, B., Paro, S., Claydon, B., Imler, J.-L., Meignin, C.,
655 and Pfeffer, S. (2015). Cross-species comparative analysis of Dicer proteins during Sindbis
656 virus infection. Scientific Reports *5*, 10693. https://doi.org/10.1038/srep10693.

657 Goic, B., Vodovar, N., Mondotte, J.A., Monot, C., Frangeul, L., Blanc, H., Gausson, V., Vera-
658 Otarola, J., Cristofari, G., and Saleh, M.-C. (2013). RNA-mediated interference and reverse
659 transcription control the persistence of RNA viruses in the insect model Drosophila. Nat.
660 Immunol. *14*, 396–403. https://doi.org/10.1038/ni.2542.

661 Goic, B., Stapleford, K.A., Frangeul, L., Doucet, A.J., Gausson, V., Blanc, H., Schemmel-Jofre,
662 N., Cristofari, G., Lambrechts, L., Vignuzzi, M., et al. (2016). Virus-derived DNA drives
663 mosquito vector tolerance to arboviral infection. Nat Commun *7*, 12410.
664 https://doi.org/10.1038/ncomms12410.

665 Hammond, S.M., Boettcher, S., Caudy, A.A., Kobayashi, R., and Hannon, G.J. (2001).
666 Argonaute2, a Link Between Genetic and Biochemical Analyses of RNAi. Science *293*, 1146–
667 1150. https://doi.org/10.1126/science.1064023.

668 Handler, D., Olivieri, D., Novatchkova, M., Gruber, F.S., Meixner, K., Mechtler, K., Stark, A.,
669 Sachidanandam, R., and Brennecke, J. (2011). A systematic analysis of Drosophila TUDOR
670 domain-containing proteins identifies Vreteno and the Tdrd12 family as essential primary
671 piRNA pathway factors. EMBO J *30*, 3977–3993. https://doi.org/10.1038/emboj.2011.308.

672 Hartig, J.V., and Förstemann, K. (2011). Loqs-PD and R2D2 define independent pathways for
673 RISC generation in Drosophila. Nucleic Acids Research *39*, 3836–3851.
674 https://doi.org/10.1093/nar/gkq1324.

675 Hartig, J.V., Esslinger, S., Böttcher, R., Saito, K., and Förstemann, K. (2009). Endo-siRNAs
676 depend on a new isoform of loquacious and target artificially introduced, high-copy
677 sequences. EMBO J *28*, 2932–2944. https://doi.org/10.1038/emboj.2009.220.

678 Huang, Y., and Liu, Z.-R. (2002). The ATPase, RNA Unwinding, and RNA Binding Activities of
679 Recombinant p68 RNA Helicase ∗. Journal of Biological Chemistry *277*, 12810–12815.
680 https://doi.org/10.1074/jbc.M200182200.

Igreja, C., and Izaurralde, E. (2011). CUP promotes deadenylation and inhibits decapping of mRNA targets. Genes Dev. *25*, 1955–1967. https://doi.org/10.1101/gad.17136311.

Ishizuka, A., Siomi, M.C., and Siomi, H. (2002). A Drosophila fragile X protein interacts with components of RNAi and ribosomal proteins. Genes Dev. *16*, 2497–2508. https://doi.org/10.1101/gad.1022002.

Iwasaki, S., Kobayashi, M., Yoda, M., Sakaguchi, Y., Katsuma, S., Suzuki, T., and Tomari, Y. (2010). Hsc70/Hsp90 chaperone machinery mediates ATP-dependent RISC loading of small RNA duplexes. Mol. Cell *39*, 292–299. https://doi.org/10.1016/j.molcel.2010.05.015.

Iwasaki, S., Sasaki, H.M., Sakaguchi, Y., Suzuki, T., Tadakuma, H., and Tomari, Y. (2015). Defining fundamental steps in the assembly of the Drosophila RNAi enzyme complex. Nature *521*, 533–536. https://doi.org/10.1038/nature14254.

Jain, R.A., and Gavis, E.R. (2008). The Drosophila hnRNP M homolog Rumpelstiltskin regulates nanos mRNA localization. Development *135*, 973–982. https://doi.org/10.1242/dev.015438.

Jiang, F., Ye, X., Liu, X., Fincher, L., McKearin, D., and Liu, Q. (2005). Dicer-1 and R3D1-L catalyze microRNA maturation in Drosophila. Genes Dev. *19*, 1674–1679. https://doi.org/10.1101/gad.1334005.

Joosten, J., Taşköprü, E., Jansen, P.W.T.C., Pennings, B., Vermeulen, M., and Rij, R.P.V. (2021). PIWI proteomics identifies Atari and Pasilla as piRNA biogenesis factors in Aedes mosquitoes. Cell Reports *35*. https://doi.org/10.1016/j.celrep.2021.109073.

Kandasamy, S.K., and Fukunaga, R. (2016). Phosphate-binding pocket in Dicer-2 PAZ domain for high-fidelity siRNA production. Proceedings of the National Academy of Sciences 201612393. https://doi.org/10.1073/pnas.1612393113.

Kandasamy, S.K., Zhu, L., and Fukunaga, R. (2017). The C-terminal dsRNA-binding domain of Drosophila Dicer-2 is crucial for efficient and high-fidelity production of siRNA and loading of siRNA to Argonaute2. RNA rna.059915.116. https://doi.org/10.1261/rna.059915.116.

Kemp, C., Mueller, S., Goto, A., Barbier, V., Paro, S., Bonnay, F., Dostert, C., Troxler, L., Hetru, C., Meignin, C., et al. (2013). Broad RNA interference-mediated antiviral immunity and virus-specific inducible responses in Drosophila. J Immunol *190*, 650–658. https://doi.org/10.4049/jimmunol.1102486.

Knight, J.D.R., Choi, H., Gupta, G.D., Pelletier, L., Raught, B., Nesvizhskii, A.I., and Gingras, A.-C. (2017). ProHits-viz: a suite of web tools for visualizing interaction proteomics data. Nat Methods *14*, 645–646. https://doi.org/10.1038/nmeth.4330.

Laver, J.D., Ly, J., Winn, A.K., Karaiskakis, A., Lin, S., Nie, K., Benic, G., Jaberi-Lashkari, N., Cao, W.X., Khademi, A., et al. (2020). The RNA-Binding Protein Rasputin/G3BP Enhances the Stability and Translation of Its Target mRNAs. Cell Reports *30*, 3353-3367.e7. https://doi.org/10.1016/j.celrep.2020.02.066.

718 Lee, Y.S., Nakahara, K., Pham, J.W., Kim, K., He, Z., Sontheimer, E.J., and Carthew, R.W.
719 (2004). Distinct roles for Drosophila Dicer-1 and Dicer-2 in the siRNA/miRNA silencing
720 pathways. Cell *117*, 69–81. .

721 Lim, D.H., Kim, J., Kim, S., Carthew, R.W., and Lee, Y.S. (2008). Functional analysis of dicer-2
722 missense mutations in the siRNA pathway of Drosophila. Biochemical and Biophysical
723 Research Communications *371*, 525–530. https://doi.org/10.1016/j.bbrc.2008.04.118.

724 Lim, S.J., Scott, A., Xiong, X.-P., Vahidpour, S., Karijolich, J., Guo, D., Pei, S., Yu, Y.-T., Zhou, R.,
725 and Li, W.X. (2014). Requirement for CRIF1 in RNA interference and Dicer-2 stability. RNA
726 Biology *11*, 1171–1179. https://doi.org/10.4161/rna.34381.

727 Liu, Q., Rand, T.A., Kalidas, S., Du, F., Kim, H.-E., Smith, D.P., and Wang, X. (2003). R2D2, a
728 bridge between the initiation and effector steps of the Drosophila RNAi pathway. Science
729 *301*, 1921–1925. https://doi.org/10.1126/science.1088710.

730 Liu, X., Jiang, F., Kalidas, S., Smith, D., and Liu, Q. (2006). Dicer-2 and R2D2 coordinately bind
731 siRNA to promote assembly of the siRISC complexes. RNA *12*, 1514–1520.
732 https://doi.org/10.1261/rna.101606.

733 Liu, X., Fu, R., Pan, Y., Meza-Sosa, K.F., Zhang, Z., and Lieberman, J. (2018a). PNPT1 Release
734 from Mitochondria during Apoptosis Triggers Decay of Poly(A) RNAs. Cell *174*, 187-201.e12.
735 https://doi.org/10.1016/j.cell.2018.04.017.

736 Liu, Z., Wang, J., Cheng, H., Ke, X., Sun, L., Zhang, Q.C., and Wang, H.-W. (2018b). Cryo-EM
737 Structure of Human Dicer and Its Complexes with a Pre-miRNA Substrate. Cell *173*, 1191-
738 1203.e12. https://doi.org/10.1016/j.cell.2018.03.080.

739 Lloyd, R.E. (2013). Regulation of stress granules and P-bodies during RNA virus infection.
740 WIREs RNA *4*, 317–331. https://doi.org/10.1002/wrna.1162.

741 Markmiller, S., Soltanieh, S., Server, K.L., Mak, R., Jin, W., Fang, M.Y., Luo, E.-C., Krach, F.,
742 Yang, D., Sen, A., et al. (2018). Context-Dependent and Disease-Specific Diversity in Protein
743 Interactions within Stress Granules. Cell *172*, 590-604.e13.
744 https://doi.org/10.1016/j.cell.2017.12.032.

745 Marques, J.T., Kim, K., Wu, P.-H., Alleyne, T.M., Jafari, N., and Carthew, R.W. (2010). Loqs
746 and R2D2 act sequentially in the siRNA pathway in Drosophila. Nat. Struct. Mol. Biol. *17*, 24–
747 30. https://doi.org/10.1038/nsmb.1735.

748 Marques, J.T., Wang, J.-P., Wang, X., de Oliveira, K.P.V., Gao, C., Aguiar, E.R.G.R., Jafari, N.,
749 and Carthew, R.W. (2013). Functional specialization of the small interfering RNA pathway in
750 response to virus infection. PLoS Pathog. *9*, e1003579.
751 https://doi.org/10.1371/journal.ppat.1003579.

752 McDermott, S.M., Meignin, C., Rappsilber, J., and Davis, I. (2012). Drosophila Syncrip binds
753 the gurken mRNA localisation signal and regulates localised transcripts during axis
754 specification. Biology Open *1*, 488–497. https://doi.org/10.1242/bio.2012885.

McDermott, S.M., Yang, L., Halstead, J.M., Hamilton, R.S., Meignin, C., and Davis, I. (2014). Drosophila Syncrip modulates the expression of mRNAs encoding key synaptic proteins required for morphology at the neuromuscular junction. RNA *20*, 1593–1606. .

Miyoshi, T., Takeuchi, A., Siomi, H., and Siomi, M.C. (2010). A direct role for Hsp90 in pre-RISC formation in Drosophila. Nat. Struct. Mol. Biol. *17*, 1024–1026. https://doi.org/10.1038/nsmb.1875.

Montavon, T.C., Baldaccini, M., Lefèvre, M., Girardi, E., Chane-Woon-Ming, B., Messmer, M., Hammann, P., Chicher, J., and Pfeffer, S. (2021). Human DICER helicase domain recruits PKR and modulates its antiviral activity. PLoS Pathog *17*, e1009549. https://doi.org/10.1371/journal.ppat.1009549.

Moy, R.H., Cole, B.S., Yasunaga, A., Gold, B., Shankarling, G., Varble, A., Molleston, J.M., tenOever, B.R., Lynch, K.W., and Cherry, S. (2014). Stem-loop recognition by DDX17 facilitates miRNA processing and antiviral defense. Cell *158*, 764–777. https://doi.org/10.1016/j.cell.2014.06.023.

Naganuma, M., Tadakuma, H., and Tomari, Y. (2021). Single-molecule analysis of processive double-stranded RNA cleavage by Drosophila Dicer-2. Nat Commun *12*, 4268. https://doi.org/10.1038/s41467-021-24555-1.

Nakamura, A., Amikura, R., Hanyu, K., and Kobayashi, S. (2001). Me31B silences translation of oocyte-localizing RNAs through the formation of cytoplasmic RNP complex during Drosophila oogenesis. Development *128*, 3233–3242. https://doi.org/10.1242/dev.128.17.3233.

Nakamura, A., Sato, K., and Hanyu-Nakamura, K. (2004). Drosophila Cup Is an eIF4E Binding Protein that Associates with Bruno and Regulates oskar mRNA Translation in Oogenesis. Developmental Cell *6*, 69–78. https://doi.org/10.1016/S1534-5807(03)00400-3.

Nishida, K.M., Miyoshi, K., Ogino, A., Miyoshi, T., Siomi, H., and Siomi, M.C. (2013). Roles of R2D2, a cytoplasmic D2 body component, in the endogenous siRNA pathway in Drosophila. Mol. Cell *49*, 680–691. https://doi.org/10.1016/j.molcel.2012.12.024.

Nowee, G., Bakker, J.W., Geertsema, C., Ros, V.I.D., Göertz, G.P., Fros, J.J., and Pijlman, G.P. (2021). A Tale of 20 Alphaviruses; Inter-species Diversity and Conserved Interactions Between Viral Non-structural Protein 3 and Stress Granule Proteins. Front Cell Dev Biol *9*, 625711. https://doi.org/10.3389/fcell.2021.625711.

Ota, H., Sakurai, M., Gupta, R., Valente, L., Wulff, B.-E., Ariyoshi, K., Iizasa, H., Davuluri, R.V., and Nishikura, K. (2013). ADAR1 forms a complex with Dicer to promote microRNA processing and RNA-induced gene silencing. Cell *153*, 575–589. https://doi.org/10.1016/j.cell.2013.03.024.

Pastuzyn, E.D., Day, C.E., Kearns, R.B., Kyrke-Smith, M., Taibi, A.V., McCormick, J., Yoder, N., Belnap, D.M., Erlendsson, S., Morado, D.R., et al. (2018). The Neuronal Gene Arc Encodes a Repurposed Retrotransposon Gag Protein that Mediates Intercellular RNA Transfer. Cell *172*, 275-288.e18. https://doi.org/10.1016/j.cell.2017.12.024.

Pennemann, F.L., Mussabekova, A., Urban, C., Stukalov, A., Andersen, L.L., Grass, V., Lavacca, T.M., Holze, C., Oubraham, L., Benamrouche, Y., et al. (2021). Cross-species analysis of viral nucleic acid interacting proteins identifies TAOKs as innate immune regulators. Nat Commun *12*, 7009. https://doi.org/10.1038/s41467-021-27192-w.

Portnoy, V., Palnizky, G., Yehudai-Resheff, S., Glaser, F., and Schuster, G. (2008). Analysis of the human polynucleotide phosphorylase (PNPase) reveals differences in RNA binding and response to phosphate compared to its bacterial and chloroplast counterparts. RNA *14*, 297–309. https://doi.org/10.1261/rna.698108.

van Rij, R.P., Saleh, M.-C., Berry, B., Foo, C., Houk, A., Antoniewski, C., and Andino, R. (2006). The RNA silencing endonuclease Argonaute 2 mediates specific antiviral immunity in Drosophila melanogaster. Genes Dev *20*, 2985–2995. https://doi.org/10.1101/gad.1482006.

Rousseau, C., and Meignin, C. (2020). Viral sensing by RNA helicases. Virologie *24*, 36–52. https://doi.org/10.1684/vir.2020.0872.

Saito, K., Ishizuka, A., Siomi, H., and Siomi, M.C. (2005). Processing of pre-microRNAs by the Dicer-1-Loquacious complex in Drosophila cells. PLoS Biol. *3*, e235. https://doi.org/10.1371/journal.pbio.0030235.

Sinha, N.K., Trettin, K.D., Aruscavage, P.J., and Bass, B.L. (2015). Drosophila Dicer-2 Cleavage Is Mediated by Helicase- and dsRNA Termini-Dependent States that Are Modulated by Loquacious-PD. Molecular Cell *58*, 406–417. https://doi.org/10.1016/j.molcel.2015.03.012.

Sinha, N.K., Iwasa, J., Shen, P.S., and Bass, B.L. (2018). Dicer uses distinct modules for recognizing dsRNA termini. Science *359*, 329–334. https://doi.org/10.1126/science.aaq0921.

Sinsimer, K.S., Jain, R.A., Chatterjee, S., and Gavis, E.R. (2011). A late phase of germ plasm accumulation during Drosophila oogenesis requires Lost and Rumpelstiltskin. Development *138*, 3431–3440. https://doi.org/10.1242/dev.065029.

Teo, G., Liu, G., Zhang, J., Nesvizhskii, A.I., Gingras, A.-C., and Choi, H. (2014). SAINTexpress: improvements and additional features in Significance Analysis of INTeractome software. J Proteomics *100*, 37–43. https://doi.org/10.1016/j.jprot.2013.10.023.

Tomari, Y., Matranga, C., Haley, B., Martinez, N., and Zamore, P.D. (2004). A protein sensor for siRNA asymmetry. Science *306*, 1377–1380. https://doi.org/10.1126/science.1102755.

Trettin, K.D., Sinha, N.K., Eckert, D.M., Apple, S.E., and Bass, B.L. (2017). Loquacious-PD facilitates Drosophila Dicer-2 cleavage through interactions with the helicase domain and dsRNA. Proc. Natl. Acad. Sci. U.S.A. *114*, E7939–E7948. https://doi.org/10.1073/pnas.1707063114.

Varjak, M., Gestuveo, R.J., Burchmore, R., Schnettler, E., and Kohl, A. (2020). aBravo Is a Novel Aedes aegypti Antiviral Protein That Interacts with, but Acts Independently of, the Exogenous siRNA Pathway Effector Dicer 2. Viruses *12*, 748. https://doi.org/10.3390/v12070748.

Wang, M., Ly, M., Lugowski, A., Laver, J.D., Lipshitz, H.D., Smibert, C.A., and Rissland, O.S. (2017). ME31B globally represses maternal mRNAs by two distinct mechanisms during the Drosophila maternal-to-zygotic transition. ELife *6*, e27891. https://doi.org/10.7554/eLife.27891.

Wang, X.-H., Aliyari, R., Li, W.-X., Li, H.-W., Kim, K., Carthew, R., Atkinson, P., and Ding, S.-W. (2006). RNA interference directs innate immunity against viruses in adult Drosophila. Science *312*, 452–454. https://doi.org/10.1126/science.1125694.

Wang, Z., Wu, D., Liu, Y., Xia, X., Gong, W., Qiu, Y., Yang, J., Zheng, Y., Li, J., Wang, Y.-F., et al. (2015). Drosophila Dicer-2 has an RNA interference–independent function that modulates Toll immune signaling. Sci Adv *1*, e1500228. https://doi.org/10.1126/sciadv.1500228.

Webster, C.L., Waldron, F.M., Robertson, S., Crowson, D., Ferrari, G., Quintana, J.F., Brouqui, J.-M., Bayne, E.H., Longdon, B., Buck, A.H., et al. (2015). The Discovery, Distribution, and Evolution of Viruses Associated with Drosophila melanogaster. PLOS Biology *13*, e1002210. https://doi.org/10.1371/journal.pbio.1002210.

Welker, N.C., Maity, T.S., Ye, X., Aruscavage, P.J., Krauchuk, A.A., Liu, Q., and Bass, B.L. (2011). Dicer's Helicase Domain Discriminates dsRNA Termini to Promote an Altered Reaction Mode. Molecular Cell *41*, 589–599. https://doi.org/10.1016/j.molcel.2011.02.005.

White, J.P., Cardenas, A.M., Marissen, W.E., and Lloyd, R.E. (2007). Inhibition of cytoplasmic mRNA stress granule formation by a viral proteinase. Cell Host Microbe *2*, 295–305. https://doi.org/10.1016/j.chom.2007.08.006.

Wilson, R.C., Tambe, A., Kidwell, M.A., Noland, C.L., Schneider, C.P., and Doudna, J.A. (2015). Dicer-TRBP complex formation ensures accurate mammalian microRNA biogenesis. Mol Cell *57*, 397–407. https://doi.org/10.1016/j.molcel.2014.11.030.

Xing, Z., Ma, W.K., and Tran, E.J. (2019). The DDX5/Dbp2 subfamily of DEAD-box RNA helicases. Wiley Interdiscip Rev RNA *10*, e1519. https://doi.org/10.1002/wrna.1519.

Yamaguchi, S., Naganuma, M., Nishizawa, T., Kusakizako, T., Tomari, Y., Nishimasu, H., and Nureki, O. (2022). Structure of the Dicer-2-R2D2 heterodimer bound to a small RNA duplex. Nature *607*, 393–398. https://doi.org/10.1038/s41586-022-04790-2.

Ye, F., Huang, Y., Li, J., Ma, Y., Xie, C., Liu, Z., Deng, X., Wan, J., Xue, T., Liu, W., et al. (2018). An unexpected INAD PDZ tandem-mediated plcβ binding in Drosophila photo receptors. ELife *7*, e41848. https://doi.org/10.7554/eLife.41848.

Zhou, R., Czech, B., Brennecke, J., Sachidanandam, R., Wohlschlegel, J.A., Perrimon, N., and Hannon, G.J. (2009). Processing of Drosophila endo-siRNAs depends on a specific Loquacious isoform. RNA *15*, 1886–1895. https://doi.org/10.1261/rna.1611309.

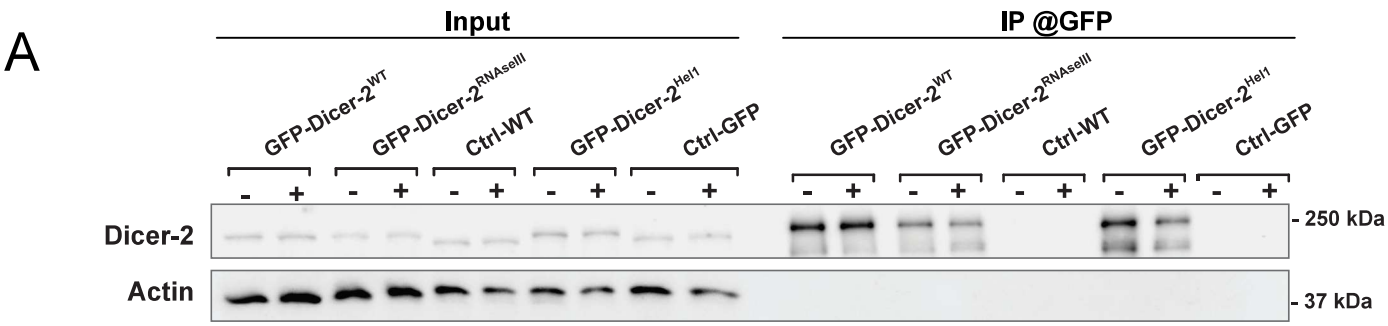

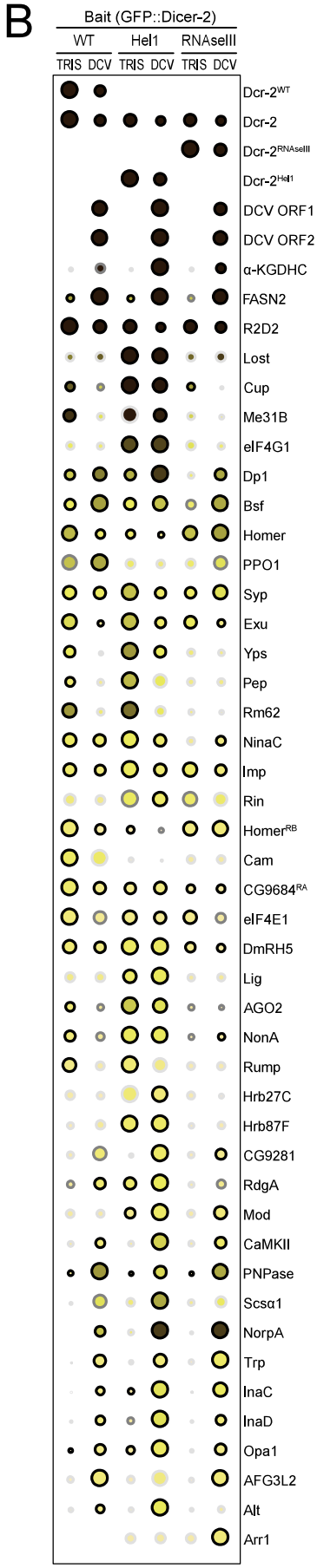

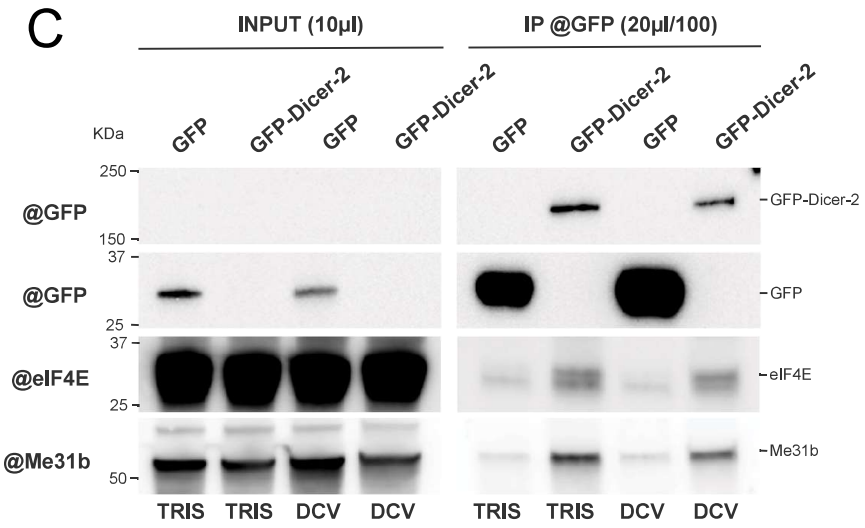

Supplementary figure S1: Global Dicer-2 interactome network during viral infection *in vivo*. (A) Immunoblot showing the presence of the Dicer-2 in all the samples before immunoprecipitation (IP) using anti-GFP beads, and in the GFP::Dicer-2 samples after IP. The band for the GFP::Dicer-2 fusion protein is slightly higher than Dicer-2 due to the added size molecular weight of the GFP, as expected. Actin, which does not interact with Dicer-2, can be seen in the input but not in the elution. **(B)** Top 15% of the candidates highlighted by the IP-MS experiment. The color represents the average number of spectra (AvgSpec) detected in the samples, the size of the dot represent the relative abundance of the protein in the condition compared to the controls, and the color of the outline of the dot represents the BFDR (Baysian False Discovery Rate). **(C)** Immunoblot of Dicer-2 partners before and after IP using @GFP beads. GFP alone or GFP::Dicer2WT were immunoprecipitated with anti-GFP beads. Syncrip, Me31b and eIF4E interact with GFP::Dicer-2^{WT} in mock- and DCV infected conditions.

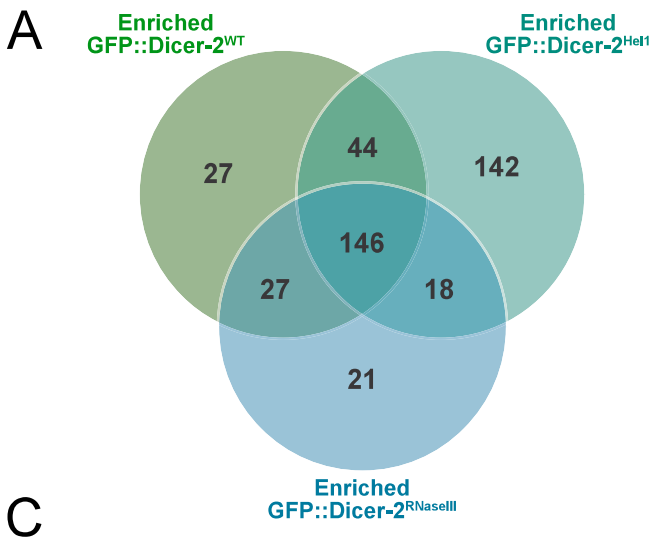

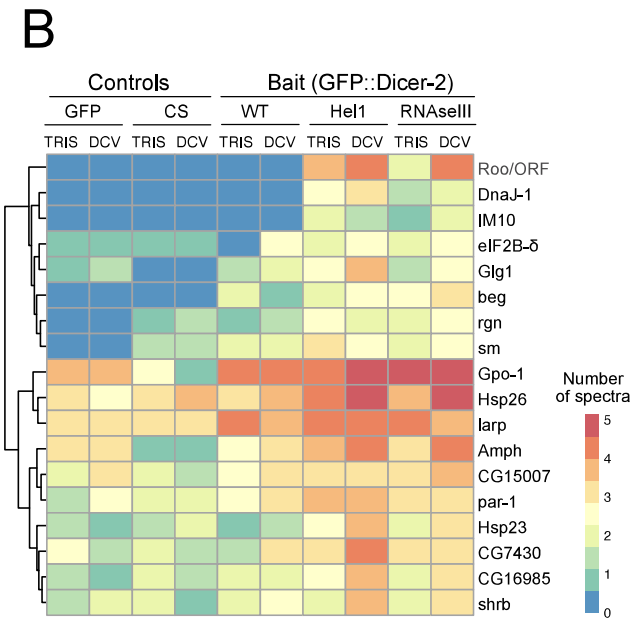

C

Rank	Candidate	Rank	Candidate	Rank	Candidate	Rank	Candidate
2	FASN2	64	Iva	124	CG13850	193	tyf
3	r2d2	66	Map205	125	Hexo2	195	stau
4	lost	67	Hsp27	126	TM4SF	197	mub
5	cup	68	AGO1	127	CG6255	198	CG5728
6	me31B	69	larp-RB	129	vari	200	mle
8	Dp1	70	Arc1	130	Lmpt	201	SCAR-RA
9	bsf	71	Zn72D	131	r	202	aub
10	homer	72	loqs	133	Klp10A	203	Pp1alpha-96A
12	Syp	75	clu	134	rept	204	CG7382
13	exu	77	Hsc70-5	136	wal	205	numb
14	yps	78	FK506-bp1	137	Sac1	206	Sec22
15	Pep	79	par-1	139	CG8768	208	Drp1
16	Rm62	81	piwi	141	gag	214	Myo31DF
18	Imp	82	128up	142	sm	222	woc
19	rin	83	Tailor	144	CG5787	224	ND-B17.2
20	homer-RB	84	Hem	146	beg	225	RnrL
21	Cam	85	Cdep	147	scu	226	NAT1
22	CG9684-RA	86	ps	148	Amph	228	Ns1
23	eIF-4E	87	Sra-1	149	pont	229	tud
25	lig	88	CG15784	150	shrb	230	Tor
26	AGO2	89	CG5641	151	Kank	235	Dcr-1
27	nonA	90	lark	152	Glg1	239	IM33
28	rump	92	gag-r	154	yl	241	HIP
29	Hrb27C	93	RnpS1	158	Top3beta	251	BEST:GH10831
30	Hrb87F	94	Cbp80	160	SRPK	253	nwk
31	CG9281	95	Ge-1	161	Smn	254	tacc
32	rdgA	96	rig	162	rtp	256	Syt7
33	mod	97	ND-B14.5B	163	qkr58E-1	258	msn
34	CaMKII	98	eIF4G2	164	Ddx1	259	Sgs7
37	norpA	99	Ostgamma	167	DCP1	260	ens
38	trp	102	GIP	170	Edc3	261	Chro
39	inaC	103	Adar	171	Psi	262	Prp31
40	inaD	105	CG5913	172	Upf1	263	fit
41	Opa1	106	Not1	173	CG2246	265	OstDelta
43	alt	108	Nsf2	174	DnaJ-1	266	msps
44	Arr1	109	Lon	175	rgn	267	ND-13B
46	Acp26Aa	110	CG10912	177	dhd	268	CG7300
47	Arr2	111	DIP1	178	nocte	269	sle
48	CG10737	112	gammaCOP	179	Atx2	271	CG33523-RD
49	jp	113	FASN3	180	FeCh	272	cg12493
50	Lsd-1	115	Acsl	182	Abi	275	HnRNP-K
53	alphaCOP	118	Galk	183	Iswi	276	BicC
54	Dhc64C	119	MetRS	187	mask	278	mago
60	Cyp4g1	120	CG16935	188	Cand1	280	Bx42
61	kdn	121	Tango5	190	Cpr49Ab	281	CG12128
62	ORF	122	CG8360	191	Tdrd3	282	Nnp-1
63	Hsp26	123	AP-1-2beta	192	l(1)G0020	284	Nopp140

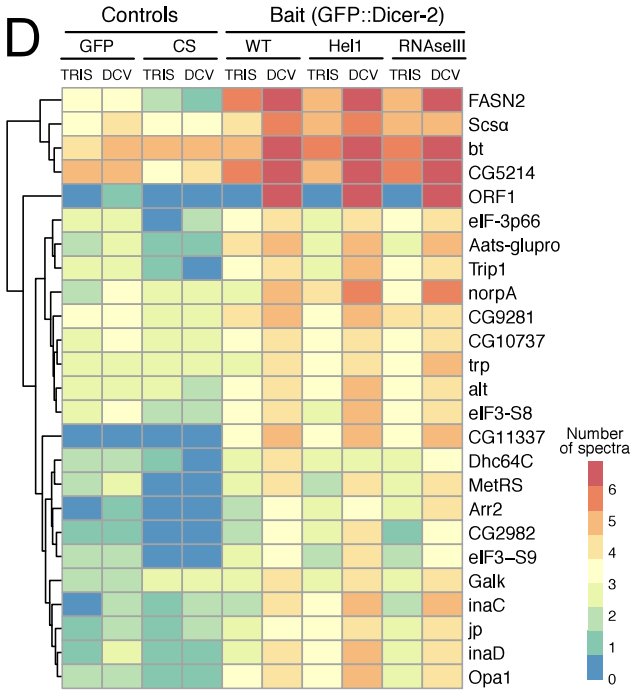

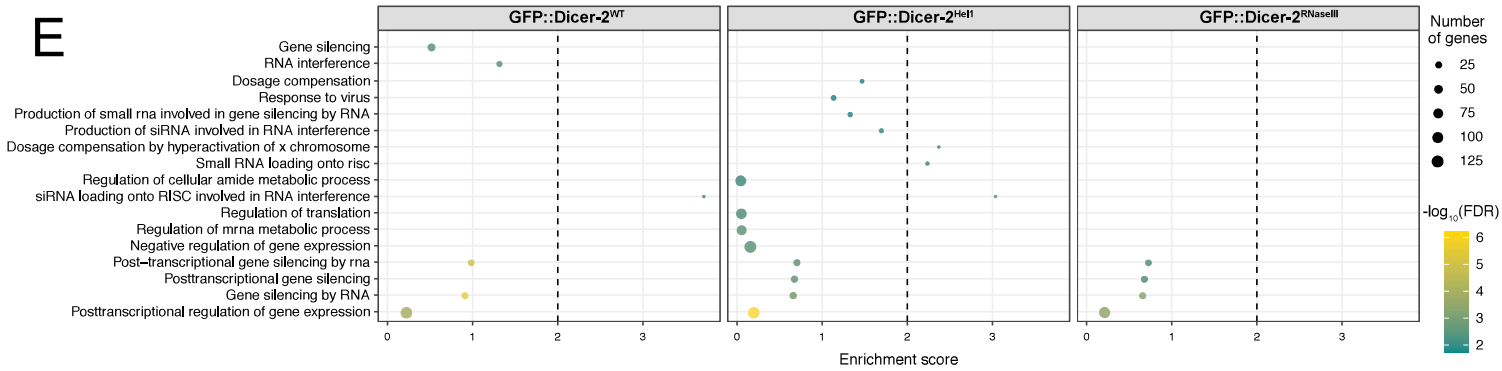

Supplementary Figure S2: Impact of the Dicer-2 mutations on the RNP network of Dicer-2. (A) Venn diagram showing the number of proteins identified in each GFP::Dicer-2 line. Candidates are selected with a fold-change > 2 and an adjusted *p*-value < 0.01. **(B)** Heatmap representing the number of spectra of the identified in each sample 18 proteins enriched only in the two GFP::Dicer-2 mutants (Hel1 and RNAseIII). **(C)** Table containing the candidates that were highlighted by both the global analysis and at least one of the line-specific analyses. **(D)** Heatmap representing the number of spectra of the 25 proteins enriched with all GFP::Dicer-2 lines during DCV infection. (E) GO term enrichment analysis "Biological Processes" for each GFP::Dicer-2 fly line compared to the controls.

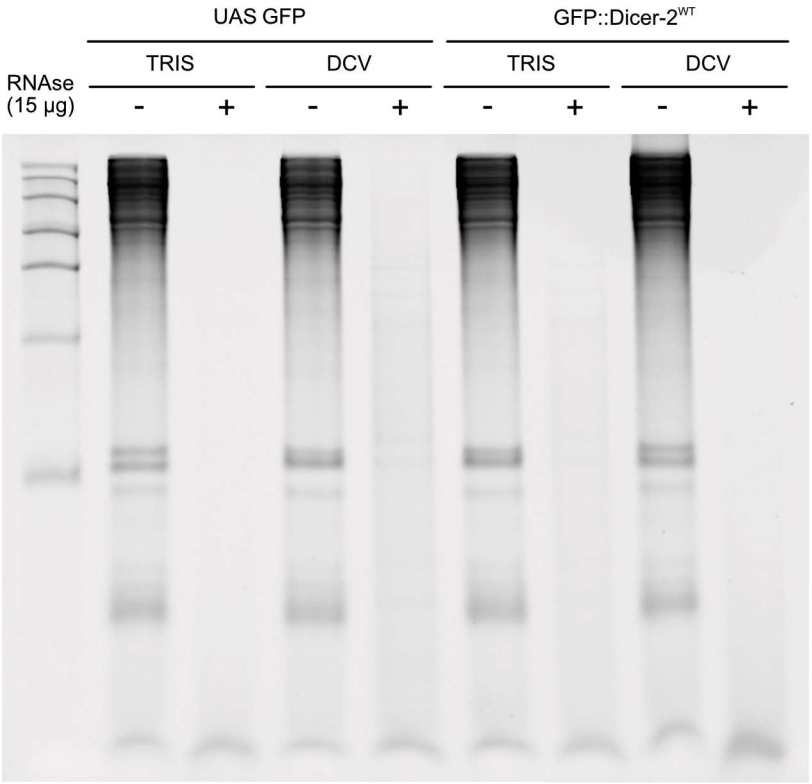

Supplementary Figure S3: The RNA-dependent protein network of Dicer-2. Urea/Acrylamide gel showing total RNA after no treatment or treatment with 15 µg of RNase A. Adult flies were injected or not with DCV and protein extraction was performed in the same manner as for the IPs. Instead of proceeding with the IP, total RNA was extracted after no treatment or treatment with RNase A to confirm the efficiency of the RNase treatment.

Target	Reference	Animal	Dilution WB
Mouse IgG	M365FK (Rockland)	Goat	1:10,000
Rabbit IgG	NA934 (Amersham)	Goat	1:10,000
Dicer-2	ab4732 (Abcam)	Rabbit	1:500
GFP	A11122 (Invitrogen)	Rabbit	1:2,000
R2D2	ab14750 (Abcam)	Rabbit	1:1,000
DCV VP2	3593 (IGBMC)	Rabbit	1:1,000
DCV RdRp#2	homemade	Guinea pig	1:2,000
eIF4E1	Kindly provided by Izzauralde lab	rabbit	1:1,000
Rump	AB_10571461 (DSHB)	mouse	1:300
Lost	AB_2618045 (DSHB)	mouse	1:500
Me31b	Kindly provided by Izzauralde lab	rabbit	1:1,000
Syp	homemade	guinea pig	1:2,000

Supplementary Table 2: Antibodies used

Gene	Sequence	Orientation
RP49	GCCGCTTCAAGGGACAGTATCT	Forward
RP49	AAACGCGGTTCTGCATGAG	Reverse
DCV	TCATCGGTATGCACATTGCT	Forward
DCV	CGCATAACCATGCTCTTCTG	Reverse

Supplementary Table 3: Primer used for qPCR

Gene	Reagent ID	dsRNA length (bp)
LacZ	Ctrl	593
GFP	Ctrl	609
Thread	Ctrl	809
AGO2	DRSC31768	265
AGO2	DRSC31769	239
Rack1	DRSC23796	512
Rack1	DRSC30688	255
CG5214	DRSC25298	363
FASN2	DRSC00610	511
r2d2	DRSC29562	319
lost	DRSC34368	368
lost	DRSC34034	266
Cup	DRSC24610	465
Cup	DRSC35662	206
me31B	DRSC03569	501
me31B	DRSC38084	301
eIF4G1	DRSC17218	503
eIF4G1	DRSC29786	379
Dp1	DRSC07403	511
Dp1	DRSC35700	290
bsf	DRSC42668	545
bsf	DRSC02035	505
homer	DRSC29162	348
PPO1	DRSC05929	511
PPO1	DRSC40857	404
Syp	DRSC34987	267
Syp	DRSC29126	525
exu	DRSC07615	515
exu	DRSC42214	215
yps	DRSC25035	234
yps	DRSC11411	473
Pep	DRSC37986	367
Pep	DRSC11252	297
Rm62	DRSC32537	203
Rm62	DRSC32538	159
ninaC	DRSC37305	346
ninaC	DRSC36608	317
Imp	DRSC20255	510
Imp	DRSC35798	347
rin	DRSC33098	220
rin	DRSC33099	178
Cam	DRSC07354	225
Cam	DRSC07353	205
CG9684	DRSC16537	500
eIF4E1	DRSC32114	203
eIF4E1	DRSC32113	195
CG10077	DRSC24756	348
lig	DRSC34699	205
lig	DRSC38413	537
nonA	DRSC27455	283
nonA	DRSC41353	140
rump	DRSC16480	520
rump	DRSC42718	366
Hrb27C	DRSC28323	325
Hrb27C	DRSC32135	265
Hrb87F	DRSC29600	417
Hrb87F	DRSC35793	320
CG9281	DRSC24522	435
rdgA	DRSC35980	405
rdgA	DRSC39133	307
mod	DRSC28409	310
CaMKII	DRSC17214	312
CaMKII	DRSC36643	310
PNPase	DRSC14304	506
Scsalpha1	DRSC26856	313
Scsalpha1	DRSC41030	212
norpA	DRSC40745	534
norpA	DRSC18806	163
trp	DRSC17088	575
trp	DRSC39226	492
inaC	DRSC36646	383
inaC	DRSC31368	292
inaD	DRSC27116	367
Opa1	DRSC28908	429
Opa1	DRSC07191	511
CG6512	DRSC34403	391
CG6512	DRSC29981	331
alt	DRSC32685	207
alt	DRSC32684	160
Arr1	DRSC01867	513
Arr1	DRSC33429	245

Supplementary Table 4: dsRNAs ordered from DRSC

Ranking	Gene name	Accession number
Bait	Dicer-2^{WT}	-
Bait	Dicer-2	A1ZAW0
Bait	Dicer-2^{RNaseIII}	-
Bait	Dicer-2^{Hel1}	-
Virus	ORF1	O36966
Virus	O36967	O36967
1	alpha-KGDHC	Q9VGQ1
2	FASN2	M9PB21
3	r2d2	Q2Q0K7
4	lost	Q9VN21
5	cup	Q9VMA3
6	me31B	P23128
7	eIF4G1	A8DZ29
8	Dp1	Q7KN75
9	bsf	Q95NR4
10	homer	O96607
11	PPO1	Q27598
12	Syp	A0A0B4KGF9
13	exu	P28750
14	yps	Q95RE4
15	Pep	M9NG39
16	Rm62	P19109
17	ninaC	P10676
18	Imp	M9NF14
19	rin	Q9NH72
20	homer-RB	E8NH56
21	Cam	P62152
22	CG9684-RA	N0A2N3
23	eIF4E1	P48598
24	DmRH5	Q8MZI3
25	lig	Q86S05
26	AGO2	Q9VUQ5
27	nonA	Q04047
28	rump	Q9VHC7
29	Hrb27C	P48809
30	Hrb87F	P48810
31	CG9281	Q9VXR5
32	rdgA	A0A023GPM5
33	mod	P13469
34	CaMKII	A4V134
35	PNPase	Q5U1D1
36	Scsalpha1	Q94522
37	norpA	P13217
38	trp	P19334
39	inaC	P13677
40	inaD	Q24008
41	Opa1	A0A0B4LGF5
42	AFG3L2	Q8T4G5
43	alt	Q960Y8
44	Arr1	P15372
45	CG1814	A1Z7V9
46	Acp26Aa	P10333
47	Arr2	P19107
48	CG10737	B7YZL1
49	jp	Q7JV09
50	Lsd-1	A0A0B4KHZ1
51	eIF3m	Q7JVI3
52	AspRS	Q7K0E6
53	alphaCOP	Q9W0B8
54	Dhc64C	P37276
55	eIF3i	O02195
56	eIF3d1	Q9VCK0
57	eEF1gamma	Q9NJH0
58	eIF3c	A1ZAX1
59	GluProRS	P28668
60	Cyp4g1	Q9V3S0
61	kdn	Q9W401
62	ORF	Q23992
63	Hsp26	P02517
64	Iva	Q8MSS1
65	E3	Q9VVL7
66	Map205	P23226
67	Hsp27	P02518
68	AGO1	Q32KD4
69	larp-RB	F9W325
70	Arc1	Q7K1U0
71	Zn72D	Q86BI3
72	loqs	Q9VJY9
73	eIF4A	Q02748
74	mEFTu2	Q7K3V6
75	clu	A1ZAB5
76	mahe	Q9W3M7
77	Hsc70-5	P29845
78	FK506-bp1	P54397
79	par-1	E1JGN0
80	EP(2)2054	A1Z9K0
81	piwi	Q9VKM1
82	128up	P32234
83	Tailor	A0A0B4KGN4
84	Hem	P55162
85	Cdep	A0A0C4DHA1
86	ps	Q0KI96
87	Sra-1	Q9VF87
88	CG15784	A9YIM2
89	CG5641	Q9VG73
90	lark	Q94901
91	RtcB	Q9VIW7
92	gag-r	P91787
93	RnpS1	Q9VHC0
94	Cbp80	Q7K4N3
95	Ge-1	Q9VKK1
96	rig	Q86BY9
97	ND-B14.5B	Q9VQM2
98	eIF4G2	Q9VCH1
99	Ostgamma	Q8SY53
100	fest	A0A0B4JCT9
101	TrpRS-m	Q8SZU2
102	GIP	P04146
103	Adar	M9NEQ7
104	CG17593	Q9VQR9
105	CG5913	Q960C1
106	Not1	A0A0B4LEZ3
107	BEST:CK01174	Q9VSH0
108	Nsf2	P54351
109	Lon	Q7KUT2
110	CG10912	E1UI89
111	DIP1	A4V4V2
112	gammaCOP	A0A0B4KHL2
113	FASN3	Q7PLB8
114	ctp	Q24117
115	Acsl	A0A0B4KFE4
116	NO66	Q7K4H4
117	eIF3b	Q0E940
118	Galk	Q95U34
119	MetRS	A1ZBE9
120	CG16935	Q9V6U9
121	Tango5	Q9W2S1
122	CG8360	Q9VLR3
123	AP-1-2beta	Q24253
124	CG13850	Q9VD14
125	Hexo2	Q9W3C4
126	TM4SF	A0A0B4KFZ4
127	CG6255	A0AMM0
128	Echs1	Q7JR58
129	vari	M9PDB2
130	Lmpt	M9MRX0
131	r	P05990
132	CCT4	Q9VK69
133	Klp10A	Q960Z0
134	rept	Q9V3K3
135	shv	Q9VPQ2
136	wal	Q7KLW5
137	Sac1	Q9W0I6
138	eIF2alpha	P41374
139	CG8768	E1UIK3
140	BcDNA:GH07921	Q9VT61
141	gag	P10405
142	sm	A0A0B4K7B0
143	Larp4B	Q9I7T7
144	CG5787	Q9VK59
145	Stip1	Q9VPN5
146	beg	Q8T3L6
147	scu	O18404
148	Amph	A0A0B4KEW6
149	pont	Q9VH07
150	shrb	Q8T0Q4
151	Kank	A0A0B4JCT6
152	Glg1	Q9VP27
153	BcDNA:RE30174	Q9VZZ6
154	yl	P98163
155	CG3967	Q9VSY4
156	Hsp22	P02515
157	Trap1	A1Z6L9
158	Top3beta	O96651
159	CCT7	Q9VHL2
160	SRPK	A0A0B4KF69
161	Smn	Q9VV74
162	rtp	Q9VN91
163	qkr58E-1	A0A0B4LG88
164	Ddx1	Q9VNV3
165	CG31879	Q7KTG0
166	Q6AWL1	Q6AWL1
167	DCP1	Q9W1H5
168	CG3071	O46069
169	san	Q9NHD5
170	Edc3	Q9VVI2
171	Psi	A1ZAK7
172	Upf1	Q9VYS3
173	CG2246	A0A0B4JD23
174	DnaJ-1	Q24133
175	rgn	Q9Y102
176	His3;	P02299
177	dhd	P47938
178	nocte	M9PE74
179	Atx2	Q8SWR8
180	FeCh	Q9V9S8
181	Pabp2	Q7KNF2
182	Abi	A0A0B4K774
183	Iswi	Q24368
184	Pss	M9PIC3
185	AspRS-m	Q9VJH2
186	Sf3b3	Q5BI86
187	mask	Q9VCA8
188	Cand1	Q9VKY2
189	Mccc1	Q9V9T5
190	Cpr49Ab	A1Z8Y3
191	Tdrd3	Q9VUH8
192	l(1)G0020	Q9W3C1
193	tyf	E1JJD6
194	hnRNP	A1ZBB4
195	stau	P25159
196	Q9VU21	Q9VU21
197	mub	A4IJ59
198	CG5728	Q9VC94
199	mtgo	B7YZW3
200	mle	P24785
201	SCAR-RA	C1C3C5
202	aub	O76922
203	Pp1alpha-96A	P48461
204	CG7382	Q9VMR0
205	numb	P16554
206	Sec22	O77434
207	Q494I6	Q494I6
208	Drp1	Q8IHG0
209	RanBPM	Q4Z8K6
210	Caf1-55	Q24572
211	MEP-1	Q0E8J0
212	stck	Q8IGP6
213	AIMP3	Q8MKK1
214	Myo31DF	Q23978
215	LeuRS	Q8MRF8
216	CCT6	Q9VXQ5
217	CG14445	A8JUZ6
218	CG44242	B7YZH7
219	Vha36-1	Q9V7D2
220	gish	A0A0B4K697
221	gammaTub37C	P42271
222	woc	A0A0B4KHZ0
223	epsilonCOP	Q9Y0Y5
224	ND-B17.2	Q8MSI7
225	RnrL	P48591
226	NAT1	A1Z968
227	Rpn13	Q7K2G1
228	Ns1	Q8MT06
229	tud	P25823
230	Tor	Q9VK45
231	Marf	Q7YU24
232	EG:115C2.2	O77426
233	Cklalpha	P54367
234	caz	Q27294
235	Dcr-1	Q9VCU9
236	AcCoAS	Q9VP61
237	Sarm	Q6IDD9
238	eRF1	Q9VPH7
239	IM33	Q9VQT8
240	CCT1	P12613
241	HIP	C4NYP8
242	eIF2Bepsilon	Q9W541
243	Cisd2	Q9VAM6
244	Vps2	Q9VBI3
245	Tctp	Q9VGS2
246	Ist1	M9PEC1
247	CG6178	Q9VCC6
248	Pi4KIIIalpha	M9PDM4
249	ArgRS	Q9VXN4
250	BEST:GH19547	A1ZAU4
251	BEST:GH10831	Q6NMY2
252	IleRS	Q8MSW0
253	nwk	M9NE66
254	tacc	A0A0B4JCV4
255	Pkc53E	P05130
256	Syt7	H9XVN2
257	eIF2beta	P41375
258	msn	Q9W002
259	Sgs7	P02841
260	ens	M9PE93
261	Chro	Q8T9D1
262	Prp31	Q9VUM1
263	fit	Q9VD66
264	CG3756	Q9VMX3
265	OstDelta	Q7K110
266	msps	A0A0B4K664
267	ND-13B	Q9VTB4
268	CG7300	Q9VKR7
269	sle	Q8INM3
270	stnB	Q24212
271	CG33523-RD	I0DHK9
272	cg12493	M9PHF9
273	Q4QPU9	Q4QPU9
274	MRG15	Q9Y0I1
275	HnRNP-K	A1ZBW0
276	BicC	Q24009
277	peng	O61345
278	mago	P49028
279	Sf3a1	Q9VEP9
280	Bx42	P39736
281	CG12128	A1Z830
282	Nnp-1	Q9VJZ7
283	CG8915	Q9VX63
284	Nopp140	M9PFZ1
285	mRpL12	Q2XYH0
286	CRIF	Q9VP13
287	Rfc37	Q9VX15
288	Muc12Ea	Q8IR52

Supplementary Table 1: Global Dicer-2 interactome network - list of 288 candidates

III. Extended discussion

In addition to the matters discussed in the draft paper, which were mostly focused on the potential roles of the different candidates, some technical aspects of this project should also be taken into consideration.

One of those aspects is the route of infection, as we injected DCV directly in the haemolymph of the flies because *D. melanogaster* possesses an open circulatory system. It is important to keep in mind that by doing so, we may bypass important host defense mechanism, as highlighted by the fact that whereas DCV is very toxic when injected, it results in very few symptoms when flies are infected orally (Roxström-Lindquist et al., 2004; Sparks et al., 2008). The gut for example, plays an important role in antiviral immunity but, contrary to oral infection, the virus does not have to go through it before infecting other tissues (Erttmann et al., 2022; Stefan et al., 2020). For DCV this could be especially important considering the tropism of this virus for the crop, an expanded portion of the alimentary tract used to store food before digestion (Chtarbanova et al., 2014). However, it is a lot more difficult to control oral viral infections, as we cannot control how much the flies feed, and thus when and at what Multiplicity of Infection (MOI) the flies will be infected. In our case, as the statistical analysis subsequent to mass spectrometry experiments relies heavily on the reproducibility between samples, performing oral infection would have introduced too much variability and it would have been difficult to identify candidates. Still, it is important to keep in mind that we may miss some candidates, especially since in some organisms like mosquitoes the RNAi response in the gut can vary from the rest of the organism (Olmo et al., 2018).

For this kind of experiments, the conditions of the immunoprecipitation also have to be considered carefully. For a protein that is located exclusively in one cell compartment, a whole cell lysis might not be the most adequate choice, as it may induce interactions that would not be physiologically relevant as they would not naturally occur in the cell. On the contrary, by performing cell fractionation, we may lose candidates. Here, we were determining the interactome of Dicer-2, a protein that although mostly expressed in the cell, has also been described to possess some roles in the nucleus (Harrington et al., 2017). This allowed us to identify both candidates located in the nucleus (e.g. Rump) and candidates located in the

cytoplasm (e.g. Rin). Moreover, the stringency of the immunoprecipitation, determined by the salt and detergent concentrations, is a factor of the utmost importance. If an IP is performed in high stringency conditions, it will limit the number of false positives, but also inhibit the formation of weak interactions. As we wanted to have a very global view of the protein network of Dicer-2, including proteins that interact with Dicer-2 indirectly, as part of a complex for example, we chose to perform the IP with a low stringency. In order to limit the number of false positives, the statistical analysis was therefore very important.

Different statistical analyses were performed to analyze the mass spectrometry data. First, a global analysis was performed using the Significance Analysis of INTeractome (SAINT) express method developed by the laboratory of Prof. Gingras (Teo et al., 2014). SAINT is a statistical method for probabilistically scoring protein-protein interaction data, mainly used for AP-MS experiments (Choi et al., 2011). This method uses a semi-supervised mixture model that estimates the spectral count distribution for false interactions directly from the negative controls. We chose to use this method for the global analysis of the MS data because it allows the fitting of one integrated model for all baits (i.e. GFP::Dicer-2 lines) instead of analyzing each bait separately. Another advantage of this method is that the data is normalized not only by the total number of spectra for each purification, but also by the protein length of the preys (i.e. proteins identified). Indeed, there is a known bias in label-free MS identification depending on peptide length.

In order to be able to categorize the different proteins identified depending on their interaction with the different baits and its modulation by the infection, I then performed several separate analyses using the msmsTests Bioconductor package in R, which was specifically designed to analyze label-free LC-MS/MS data (Gregori et al., 2013). Using this package, I was able to use a negative binomial test (edgeR package), to identify differentially expressed proteins between two biological conditions. As this test can only compare two conditions at a time but we had three different baits to compare to the controls, each in mock-infected and DCV-infected conditions, we had to decide on a strategy. As we did not want to lose information by grouping all GFP::Dicer-2 lines together to compare them to the controls, we decided to compare each Dicer-2 line (mock-infection + DCV infection) separately and then classify the candidates depending on what bait they interacted with. In a second time we then

compared, for each line, the mock-infected samples to the DCV-infected samples. This way, we were able to compare multiple conditions together with a test that only allowed comparison between two conditions, without having to group everything together. However, by opposition to the SAINT method, this method does not use the same model for each bait, meaning that depending on the overall protein identification for each bait, the significance of the candidates could be impacted. For example, during the second MS experiment (with or without RNase III treatment), I noticed that fewer proteins were identified globally in the DCV-infected conditions compared to the mock-infected conditions and that after the analysis, there were fewer significant candidates compared to the mock-infected conditions. This may have influenced the resulting statistics. Moreover, if the homogeneity between samples of a triplicate were not as reproducible as for other baits, we might also identify less significant candidate. This is why we wanted to have a general method like SAINT in addition to our separate analyses.

After statistical analysis of the different MS experiments, we decided to perform two functional screen, *ex vivo* and *in vivo*, to test the effect of the highlighted candidates on DCV infection. *Ex vivo* RNAi screens are a very efficient way to highlight interesting candidates to study further. Indeed, a well-prepared RNAi screen in S2 cells can be performed in a few weeks if the dsRNAs do not have to be produced, and can allow the testing of a large number of candidates. For example, we ordered the dsRNAs used in this project from DRSC Harvard, from a database containing dsRNAs that had already been used in other screens, meaning that we could select the dsRNAs depending on whether or not they caused off-target effects etc. (https://fgr.hms.harvard.edu/). In insect cells in particular, as dsRNAs can directly be used to KD gene expression without the need to synthetize siRNAs, and are absorbed quite easily in the cells, this is a very powerful tool. By comparison, *in vivo* screens like the one that I performed for the Dicer-2 interactome can take several months and be delayed several times if flies from one condition do not hatch properly. As Gal4-Gal80^{TS} crosses take three weeks to hatch, this can quickly become a problem. Moreover, variations in size, fertility, or developmental speed are not factors that can influence cell culture experiments. However, as for all experiments, *ex vivo* screens also have their limitations. For example, by performing the screen in S2 cells, we are limiting ourselves to only one cell type, but some pathways are cell-

type specific (e.g. the piRNA pathway in reproductive tissues), and we might overlook some candidates by doing this. Moreover, systemic mechanisms cannot be studied, and candidates that might play a role in this will show no effect.

For both *in vivo* and *ex vivo* screens, the large-scale handling of cells, flies and plates can induce bias in the final data. We have implemented a correction for this during the statistical analysis, and factors like the row in which the candidate was located inside the plate, the column, and the replicate were computed and taken into account by the mixed effect model used to analyze the *ex vivo* screen. Similarly, the replicate was computed as a random factor in the mixed effect model used to analyze the *in vivo* screen. However, it is still possible that we obtained some false positive or false negative results because of this. Therefore, it is very important to confirm the results outside of the context of a screen. It might also be a good idea to confirm the results of the main candidates by another method like CRISPR-Cas9, or to check if the impact that we observed in S2 cells is biologically relevant at the scale of the whole organism by performing an *in vivo* KD.

We have also been able to confirm the interaction of some of the candidates with Dicer-2 by immunoprecipitation and western blot (**Figures 8F, 10C & 10D**). However, we still need to obtain a more complete figure in order to be able to publish this. Indeed, for **Figure 8F and 10C**, the aliquot of Rump antibody was too old and we did not manage to obtain a results, even though we confirmed this interaction several times before. Moreover, for **Figure 10D** we would prefer to have the Ctrl-GFP fly line as a control instead of the Ctrl-CS fly line, as it would allow us to show immunoprecipitation of the GFP in the control. However, although the IPs have to be performed again to obtain the final figures, we can already clearly see an interaction between the candidates and Dicer-2 in the preliminary IPs.

In conclusion, this work has allowed us to highlight several interesting candidates, including proteins interacting with Dicer-2 and proteins with antiviral effects. The next step would now be to study them individually to try and understand their role in RNAi and/or antiviral immunity. For example, now that we now that some of the candidates have an impact on viral infection, we could try to determine which step of the viral replication cycle they impact, if this effect is virus specific or part of a more global mechanism, and by what mode of action

they impact the virus. Moreover, as some candidates have been shown to interact with Dicer-2, it would now be interesting to understand in which of the many Dicer-2 functions the candidates are involved. We could test the impact of the candidates on the role of Dicer-2 in polyadenylation or endo-siRNA production for example.

Chapter II: Role of Fandango in the antiviral immunity of *Drosophila melanogaster*

I. Preamble

During my thesis, my main project focused on Dicer-2, the main nucleic acid sensor in *Drosophila melanogaster*. However, as described in the review in section II of the Introduction, nucleic acid sensing is a widely used strategy to distinguish between self and non-self during viral infection across species, and many nucleic acid sensors play an important role in antiviral immunity besides Dicer-2. When I started my PhD, other projects on this research theme were ongoing in my host lab, and I was given the opportunity to study a potential viral dsRNA sensor, called Fandango (Fand).

In particular, the project of a former PhD student of my host lab, Dr. Assel Mussabekova, was performed as part of a collaborative work with the team of Prof. Andreas Pichlmair from the German Center for Infection Research in Munich. My host laboratory used a cross-species affinity purification followed by mass spectrometry (AP-MS) analysis to identify evolutionary conserved viral nucleic acid sensors (Pennemann et al., 2021). After affinity purification of 17 different nucleic acid baits (11 baits and 6 controls) in human, mouse and fly, they compared the orthologues of the proteins identified and studied their impact on the viral infection in the different species. This led to the identification of different nucleic acid interactors that conserved their antiviral properties throughout evolution, amongst which Fandango and its human orthologue XAB2.

In parallel, another PhD student from my host laboratory, Dr. Loïc Talide, was investigating how dmDicer-2 is able to sense viral dsRNA with protected termini *in vivo*. This is especially puzzling in the case of DCV infection, where the 5' end of the viral RNA is protected by a viral protein (VPg) covalently linked to the viral RNA. Moreover, high throughput small RNA sequencing at early time points of the infection revealed an accumulation of vsiRNAs inside the highly structured 5'UTR of the DCV called the cloverleaf suggesting that this region could be the entry point of dmDicer-2. The interaction between the cloverleaf, VPg and the RdRp is

important to initiate the protein-primed picornavirus RNA synthesis (Rieder et al., 2000; Lyons et al., 2001). To allow the entry of dmDicer-2, it has been hypothesized that an endoribonuclease could help dmDicer-2 recognize the dsRNA intermediate of DCV replication. In order to identify this potential nuclease, he used a literature-based approach to select 111 candidates *in silico*, and performed an RNAi screen in S2 cells to highlight candidates with an antiviral effect on DCV infection. A large number of potentially antiviral candidates were thus identified. He then wanted to check whether or not the impact of the highlighted candidates on viral infection were DCV-specific, and therefore needed to perform a new RNAi screen using other viruses. At that time I had just performed the Dicer-2 mass spectrometry myself (see Chapter I), and I had also identified some candidates that, although no statistical analysis had been performed yet, seemed interesting because of their described role in the literature. As the two other PhD students were both at the end of their PhD theses, we decided that I should add their candidates to my own and perform a new RNAi screen in S2 cells with candidates from our different projects. This RNAi screen highlighted different proteins that I then studied as side-projects during my thesis. I focused on one of those candidates in particular, Fandango (Fand), for which I will describe the results that I obtained in the following chapter.

Fandango is a subunit of the Prp19 complex, or NineTeen Complex (NTC), which has been shown to be involved in several functions such as splicing, genome maintenance, recruitment of ubiquitylated proteins to the proteasome and transcription elongation (Kuraoka et al., 2008; Chanarat and Sträßer, 2013). However, the best characterized function of this complex is splicing. This process is carried out by the spliceosome, a complex constituted of the five snRNPs (small nuclear ribonucleoproteins) U1, U2, U4, U5 & U6 that each contain snRNAs (small nuclear RNAs). In addition, associated proteins called Sm- and LSm-proteins (Sm-like proteins), as well as other non-snRNP factors such as the Prp19 complex play critical roles in the splicing process. Prp19/NTC has been shown to be necessary for the activation of the spliceosome by allowing the stabilisation of U5 and U6 on the pre-mRNA, and for the structural rearrangements within the spliceosome that are necessary throughout the splicing process (Kastner et al., 2019). The splicing mechanism and the implication of the Prp19/NTC are illustrated on **Figure 13**.

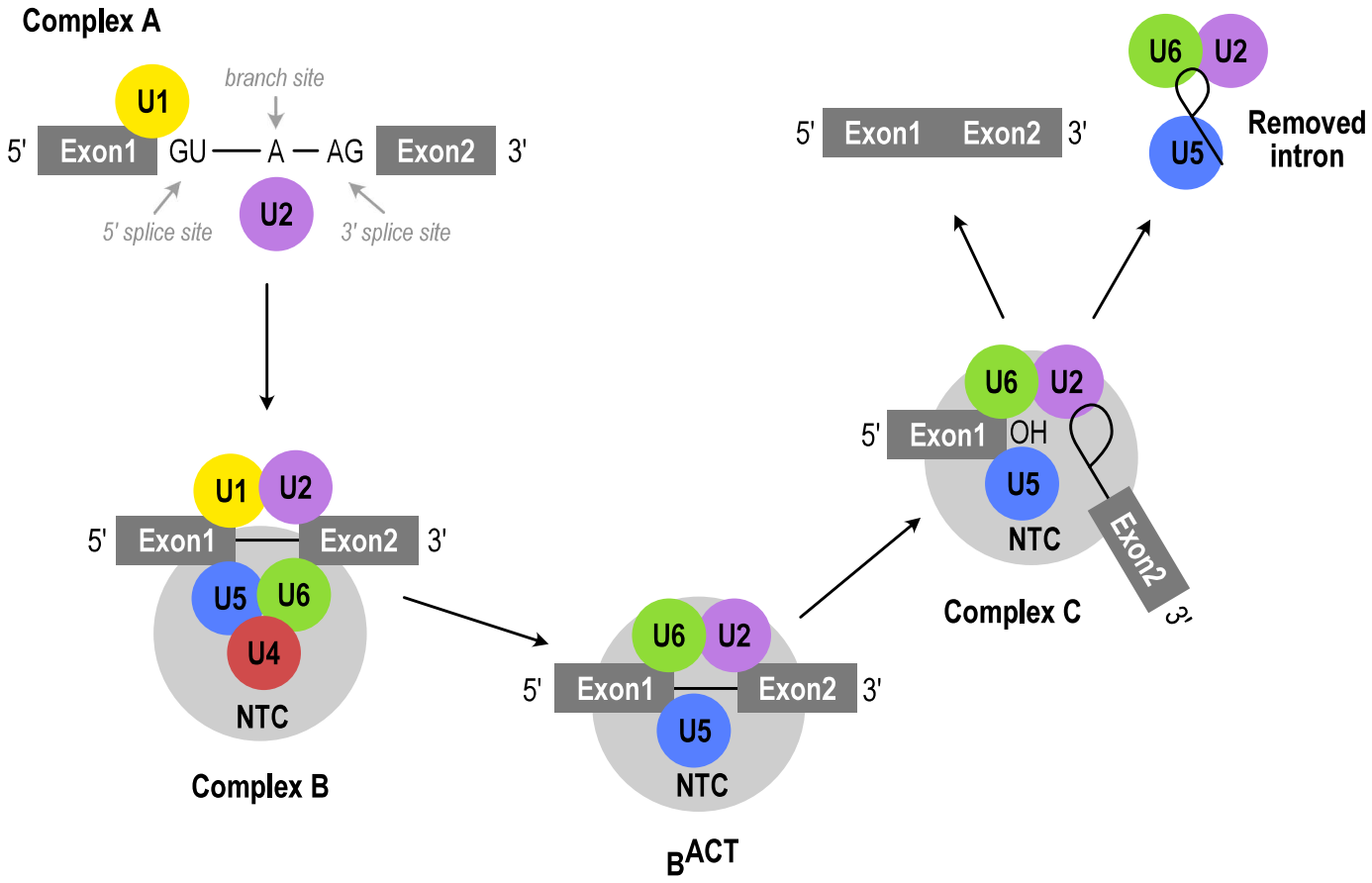

Figure 13 - Splicing and the Prp19 complex (NTC) - adapted from Hogg et al., 2010. Splicing begins with the base-pairing of U1 and U2 snRNAs to the pre-mRNA, forming the A complex. The addition of the U4/U5/U6 tri-snRNP leads to the formation of the B complex. The B complex is then activated following unwinding of U4 from U6, which in turn allows the association of U6 to U2, the removal of U1 and U4 and the activation of the complex to form B^{ACT}. A hydroxyl group (OH) on a carbon atom of the adenine at the branch point then attacks the bond of guanine at the 5' splice site, in a reaction called transesterification, leaving an OH group on the exon. Several rearrangement occurs resulting in complex C, and this OH group is then responsible for a second transesterification reaction, by attacking the phosphodiester bond at the 3' splice site. The two exons are covalently bound and the intron is released.The Prp19/NTC complex and Prp19-associated proteins play critical roles in the splicing process, as they associate with the spliceosome and facilitate conformational changes within it that are necessary for both transesterification reactions.

During the nucleic acid sensor project of my host lab, Fandango was shown to bind poly(I:C), which is a synthetic analogue of viral dsRNA, suggesting that it could be a dsRNA sensor. In this experiment, Fandango was identified in both drosophila S2 cells and adult flies, and its orthologue, XAB2, displayed the same affinity for poly(I:C) in human and mouse (Pennemann et al., 2021). Moreover, Fandango had an antiviral effect on all viruses tested in an *in vivo* screen using knock-downs of target genes in adult flies, also performed by my host lab. With this in mind, we decided to investigate the role of Fandango during viral infection, and to determine if its impact is linked with either the Prp19 complex and/or the splicing process. After discussion with my thesis advisors committee in spring 2021, we agreed that I should pause the Fandango project to concentrate on concluding the validation of the Dicer-2 partners *ex vivo* and *in vivo*. At the end of my thesis, I had the opportunity to supervise my first intern, who helped me complete some experiments on the Fandango project from March 2022 to Mid-June 2022.

II. Results

A. RNAi screen – Impact of the candidates on DCV infection in S2 cells

As mentioned above, the selection of the candidates for RNAi screening in S2 cells was based on three different projects (**Table 14A**). In addition to the 17 candidates selected after the Dicer-2 mass spectrometry experiment, 4 candidates from the AP-MS nucleic acid sensors project were added, along with 14 potential nucleases selected by literature search and already highlighted by a first screen with DCV infection only. To these 35 candidates, control dsRNAs were added: "Scramble" dsRNA, dsThread, dsAgo2 & dsRACK1. The scramble dsRNA non-targeting control was used as a negative control, as it does not have a target gene in S2 cells. The dsThread control was used to confirm that the soaking experiment worked: the target gene, also known as Death-Associated Inhibitor of Apoptosis 1 (DIAP1), is an anti-apoptotic protein that induces a high percentage of cell death when inhibited and this was checked after each soaking under the microscope. The dsAgo2 control was used as an antiviral control, as the role of Ago2 in the antiviral RNAi machinery should result in an increased viral load. However, our RNAi approach requires Ago2 activity, and therefore KD of Ago2 never leads to a strong phenotype. Finally, the dsRACK1 control was used as a dicistrovirus-specific proviral control, as it was previously described to be necessary for dicistrovirus IRES-dependent translation and as such should result in a decreased viral load in dicistroviruses when inhibited (Majzoub et al., 2014). In total, the knock-down of 39 genes was performed, using two different dsRNAs for each gene whenever possible (66 dsRNAs total), to detect potential off-target effects.

The 66 dsRNAs were transcribed *in vitro* using a homemade T7 polymerase produced at IBMC (Franck Martin UPR9002) after optimization of the protocol, and using DNA templates provided by the Drosophila RNAi Screening Center at the Harvard Medical School. Cells were soaked for 3 days with the different dsRNAs mapping candidate genes and subsequently infected with DCV MOI=0.001 for 20h (**Figure 14B**). As this experiment did not require every cell to be infected at the same time, a low MOI was chosen, to avoid cytotoxicity and to allow for multiple cycles of infection. This also reduces the risk of the same cell being infected by both functional viral particles and defective particles, which could competitively inhibit the

A

	AP-MS nucleic acid sensors	Nucleases screen	Dicer-2 interactome	Controls
Names of the different candidates	Larp4B	Hel25E	Nnp-1	Scramble
	CG5641	Clp	FASN2	Rack1
	fand	CG9272	homer	Thread
	Tao	CG13690	Hsc70-4	Ago2
		Rpp20	norpA	
		RpS3	Ns1	
		Rrp6	Pabp2	
		ZC3H3	lost	
		Xrcc2	Syp	
		Dis3	alt	
		Snm1	bt	
		CG14057	Scsalpha1	
		Rad51D	CG9684	
		pcm	CG7920	
		Pop2	CG5214	
			R2D2	
# of candidates per category	4	15	16	4
Total # of candidates	39			

B

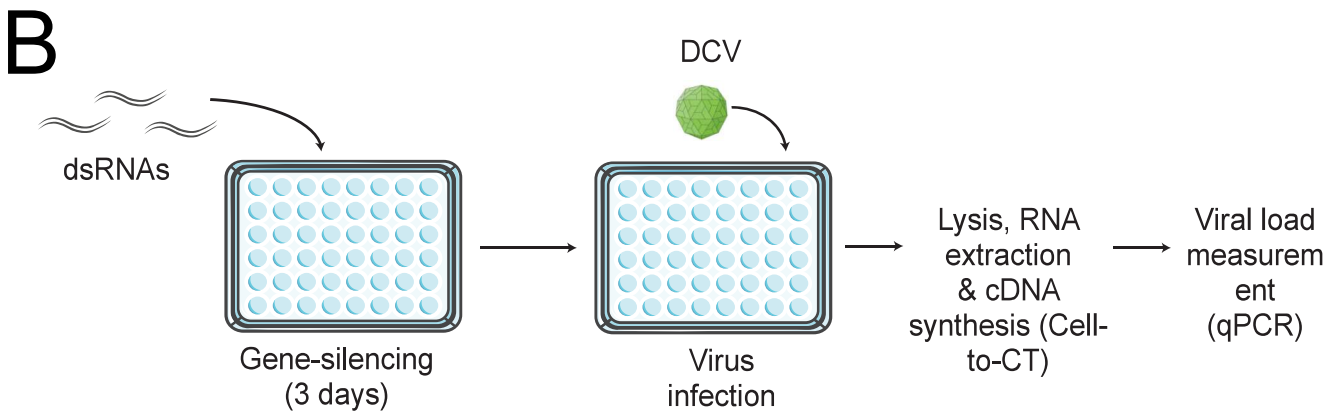

Figure 14 - Experimental strategy for the RNAi screen. A) List of the candidates used in this screen. For each project, a number of candidates were selected, and the corresponding dsRNAs were transcribed *in vitro*. B) The dsRNAs were then used to inhibit gene expression of the candidate genes, and infected by DCV before measuring the viral RNA load by RT-qPCR.

functional particles (Rezelj et al., 2018). The viral load was then determined by RT-qPCR, and the results of this experiments were analyzed using a mixed linear model that took into account the row, column, and plate effects that could impact the data (see Materials & Methods). The candidates with a significant difference (adjP < 0.05) in viral RNA load were plotted on **Figure 15A** and represent N=3 independent experiments.

As expected, we can observe that the proviral control RACK1 shows a significant decrease in viral RNA load compared to the Scramble dsRNA control, highlighting its importance for the DCV replication. However, dsAgo2 did not show the expected increased viral RNA load phenotype. This can be explained by the fact that in this case, we are using RNAi to silence a gene of the RNAi machinery. This might result in an inefficient silencing of the target *ago-2* mRNA, and therefore a near normal amount of the resulting protein at the time of the infection. Alternatively, the dsRNA chosen might just have a very low efficacy, and we should confirm the KD.

Globally, almost half of the candidates tested had a significant impact on DCV infection. This was not surprising, as we pre-selected candidates from the Dicer-2 mass spectrometry experiment and the first nuclease screen, which were performed using DCV. This means that this screen was heavily skewed towards proteins with an impact on DCV, and it was therefore likely that a number of candidates would have an antiviral effect against this virus. In total, we observed a significant impact on DCV RNA load for 27 out of the 66 dsRNAs tested, corresponding to 20 genes (19 antiviral and 1 proviral), excluding the controls (**Figure 15A**). Among the 20 candidates highlighted by this screen, 3 of them were potential nucleic acid sensors (Fand, Larp4B & Tao), 8 were nucleases potentially involved with the cleavage of viral dsRNA (Hel25E, Clp, CG13690, ZC3H3, RpS3, Dis3, Pcm & Snm1), and 9 were potential Dicer-2 interactants (Hsc70-4, CG5214, Syp, Ns1, Nnp1, Lost, CG9684, Pabp2, R2D2). Among the highlighted proteins we observed the Tao kinase, which was identified as a dsRNA-interacting antiviral protein required for type-I interferon induction in mammals, and conserved in flies (Pennemann et al., 2021). This screen also highlighted Hel25E (UAP56), confirming unpublished results from my host lab that identified it as a dicistrovirus specific antiviral protein, and consistent with its role in the piRNA pathway (Zhang et al., 2012). Another interesting protein highlighted here is Hsc70-4, which is part of the chaperone machinery

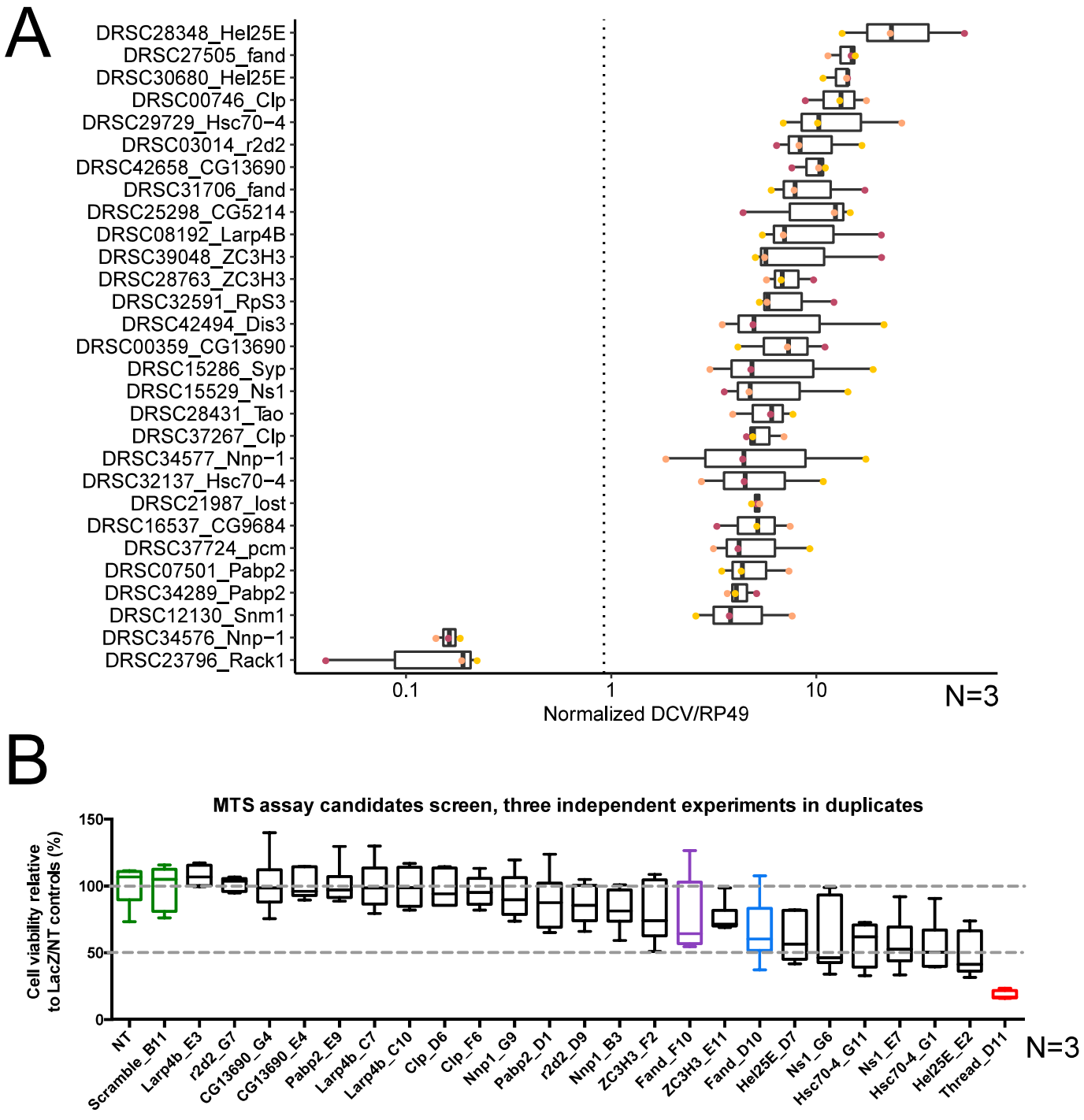

Figure 15 - Results of the DCV RNAi screen. A) DCV RNA loads after KD of the different candidate genes (N=3). For clarity, only candidates with a significant impact on DCV infection are represented here. B) Cell toxicity of each dsRNA was tested by measuring the mitochondrial activity 3 days after soaking with each dsRNA, and represented as a percentage of survival compared to the control on this box and whiskers plot (N=3).

Hsc70/Hsp90 chaperone machinery, shown to be important for RISC-loading (Iwasaki et al., 2010). Taken together, these results confirm the validity of our approach and allowed the identification of potential antiviral proteins.

Of note, the viral RNA load after Nnp-1 KD seems to be significantly higher for one dsRNA but lower for the other dsRNA targeting the same gene. This could be due a potential toxicity of the Nnp-1 depletion, which would make the viral load very inconsistent, as a strong impact on cell metabolism could randomly favor or inhibit viral replication. This issue could also give rise to the presence of false positives, which is why I then checked the cell toxicity of the dsRNA treatment against target genes. To this aim, I checked the mitochondrial activity of dsRNA-treated cells three days after soaking by measuring the reduction of a tetrazolium component into an insoluble formazan product by the mitochondria of viable cells, which is directly proportional to the number of living cells in culture (**Figure 15B**). Again, Scramble dsRNA was used as a negative control and the activity measured for these cells was taken as a baseline for 100% mitochondrial activity. The dsThread control was used as a positive control inducing cell death, and showed a mitochondrial activity close to 0%. This assay shows that some of the candidates actually have an important toxicity for the cells, including some dsRNAs that induce a decrease in mitochondrial activity of approx. 50% (e.g. Hsc70-4, Hel25E & Ns1). Of note, the two dsRNAs against Fandando also induce a decrease in mitochondrial activity.

B. RNAi screen – Specificity of the candidates' impacts

Proteins that impact viral infections, both in a proviral or antiviral manner, can have different levels of specificity. For example, they could have a virus-specific effect, an effect on a specific type or family of viruses, or they can have a global antiviral effect. In order to study the specificity of the antiviral effect of the highlighted candidates, I used the same RNAi approach in S2 cells, using three other viruses: *Cricket Paralysis Virus* (CrPV), *Flock House Virus* (FHV) and *Vesicular Stomatitis Virus* (VSV) (**Figure 16A**).

CrPV belongs to the same family of viruses as DCV, *Dicistroviridae*. Like DCV, it is a ssRNA(+) virus encoding two ORFs and two IRESs, and its genome is protected by a VPg protein covalently bound to its 5'end and a polyA tail at its 3'end. As viruses from the same family are

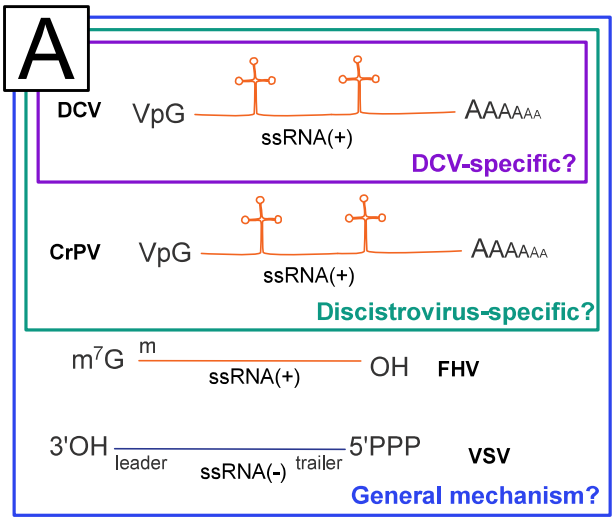

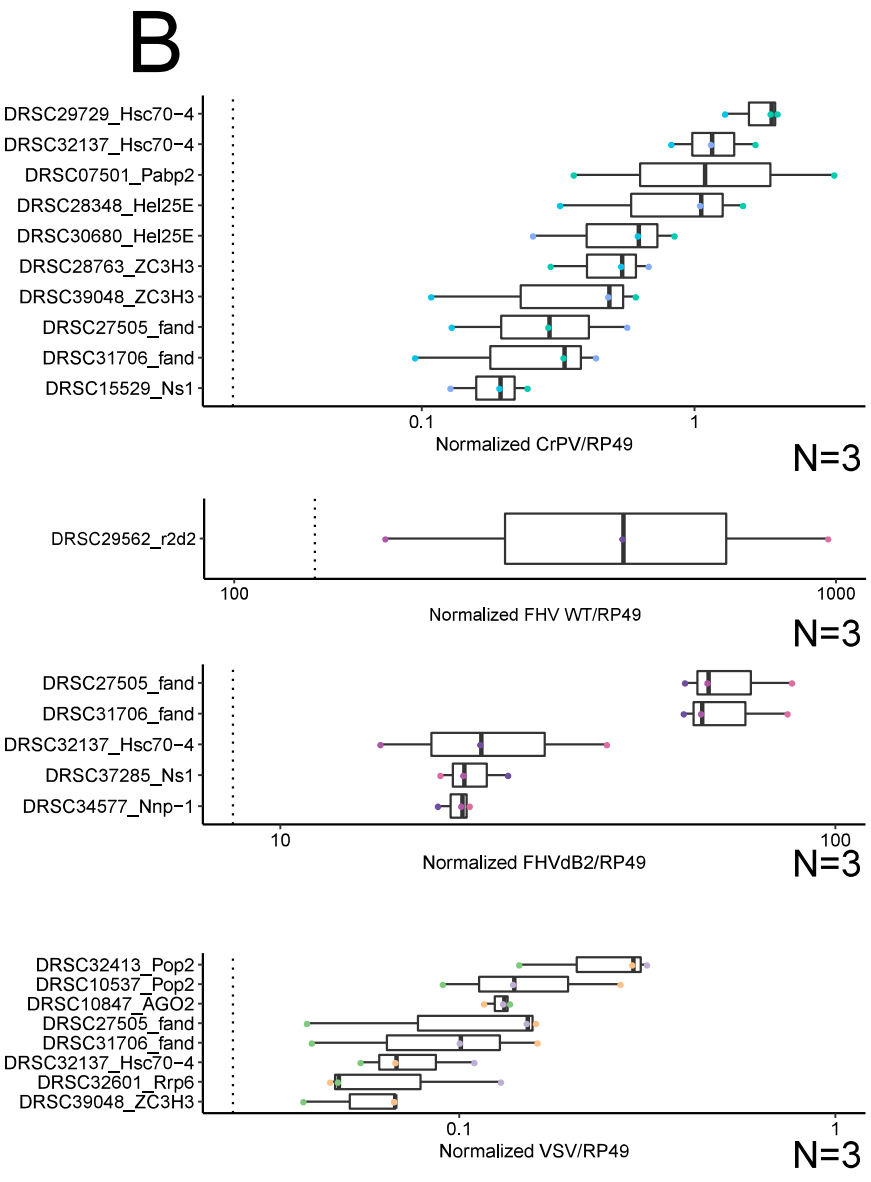

C

	DCV	CrPV	FHVdB2	VSV
Fand	2/2	2/2	2/2	2/2
Larp4B	1/2			
Tao	1/2			
Hel25E	2/2	2/2		
Clp	2/2			
CG13690	2/2			
ZC3H3	2/2	2/2		1/2
RpS3	1/2			
Dis3	1/1			
Pcm	1/2			
Snm1	1/1			
Rrp6				1/2
Pop2				2/2
Hsc70-4	2/2	2/2	1/2	1/2
CG5214	1/1			
Syp	1/2			
Ns1	1/2	1/2	1/2	
Nnp1	2/2		1/2	
Lost	1/2			
CG9684	1/1			
Pabp2	2/2	1/2		
R2D2	1/2			

Figure 16 - Specificity of the candidates' impacts on viral infection. A) Representation of the genomes of the different viruses used during this RNAi screen. If a candidate has an impact on DCV only, this effect is called DCV-specific. If it has an impact on DCV and CrPV only, it is dicistrovirus specific. If the virus has an impact on all viruses tested, it might be involved in a more general mechanism. B) Viral RNA loads after KD of the different candidate genes. For clarity, only candidates with a significant impact on DCV infection are represented here (N=3). C) Summary of the results for all viruses tested except FHV WT, as it did not highlight any candidate. Candidate genes were silenced using two different dsRNAs whenever possible. The numbers in the cells represent the number of dsRNA that had an impact on DCV infection.

very similar, it is not uncommon to find proteins that impact their replication cycle in the same manner, but have no impact on other viruses. For example, the RACK1 protein was shown to have a proviral impact on viruses from the *Dicistroviridae* family, as it is necessary for their IRES-dependent translation mechanism (Majzoub et al., 2014). If the KD of a candidate has the same impact on DCV and CrPV infection but has no effect on other viruses, it might therefore mean that its impact is dicistrovirus-specific. However, if it has an impact only on DCV but not the very similar CrPV, this might mean that its impact is DCV-specific.

The third virus used, FHV, belongs to another family of viruses, *Nodaviridae*. This family of viruses also produces non-enveloped virions and they also are ssRNA(+) viruses, but their genome is bipartite. The FHV RNA possesses a 5'cap and a 3'OH structure. FHV RNA1 encodes the RdRp and contains a frame-shifted sub-genomic RNA 3 (369 nt) that encodes the VSR B2, a dsRNA binding protein (Han et al., 2011; Lu et al., 2005; Petrillo et al., 2013). The activity of the VSR B2 might therefore hide to some extent the impact of candidates with a role in RNAi. As we were particularly interested in studying candidates that has a role in antiviral RNAi, we decided to use two versions of this virus: the WT version (FHV WT) and a version that lacks the B2 VSR (FHVΔB2) (Petrillo et al., 2013).

The last virus used, VSV, belongs to the *Rhabdoviridae* family, which are enveloped ssRNA(-) viruses, and therefore very different from DCV. The extremities of the VSV genome are constituted of a 5'-triphosphate and 3'OH, and contain a 3' trailer and a 5' leader RNA segments. These RNA segments of approx. 50 nucleotides contain important *cis*-acting sequences that serve as promoters for transcription and replication (Rose, 1975; Banerjee et al., 1977; Lyles et al., 2013). Genes are transcribed sequentially in their 3' to 5' order, to yield separate mRNAs that are then polyadenylated, capped and methylated much as cellular mRNAs. The neosynthesized genomic RNA that are formed after transcription are immediately sheltered by the nucleoprotein N, which should in theory prevent the formation of dsRNAs (Conzelmann, 1998). However, VSV dsRNAs and VSV-derived siRNAs can be detected, showing that dsRNA does indeed accumulate during VSV infection (Mueller et al., 2010; Kemp et al., 2013). As it is so different from the other viruses, it is likely that the list of candidates with an impact on this virus might differ from the other viruses. However, if a candidate has an impact on all the viruses used in this experiment, including VSV, is it possible that it is involved in a

general antiviral mechanism. Furthermore, as all viruses used in this experiment have been shown to trigger antiviral RNAi, it is possible that a candidate that has a role in this mechanism could display an antiviral impact on all the viruses tested.

After performing the RNAi screen with these different viruses at a MOI adapted for each virus, the viral RNA load was measured in the same manner as for DCV. For these viruses, we observed fewer candidates with an impact on viral infection compared to DCV, which was expected as the candidate list was skewed towards proteins with an impact on DCV. However, we also noticed that the proviral and antiviral controls did not behave as expected. Indeed, as for DCV, the KD of Ago2 had no impact on viral RNA load for CrPV, FHV and FHVΔB2, which as explained above could be due to the efficacy of the dsRNA used, or to the fact that we are using the RNAi machinery against itself. Moreover, KD of RACK1 did not lead to the expected decreased CrPV load phenotype, even though it was shown to be a dicistrovirus-specific proviral protein. However, although not significantly different from the control, dsRACK1-treated cells were still among the cells with the lowest viral RNA loads.

Although these control conditions did not behave as expected, we still managed to identify some candidates with a significantly increased viral RNA load compared to Scramble dsRNA. Those candidates were represented on **Figure 16B**, and the results for all viruses were summarized on **Table 16C**. In total, 6 candidates had an impact on CrPV RNA load (Fand, Hel25E, ZC3H3, Hsc70-4, Ns1 & Pabp2), 4 on FHVΔB2 (Fand, Hsc70-4, Ns1 & Nnp1) and 5 on VSV (Fand, ZC3H3, Rrp6, Pop2 & Hsc70-4). Except for dsR2D2, no dsRNA had any impact on the FHV WT infection at the time point and MOI chosen, which was not surprising due to the presence of the very potent VSR B2. What was more surprising however, was the increased FHV RNA load after R2D2 KD, as this protein is involved in RNAi. This could indicate that even with this VSR, the RNAi mechanism is still active enough in control cells that we can see an impact of the R2D2 KD.

Out of the 20 candidates that had an impact on DCV RNA load, 6 also had an impact on CrPV RNA load, and in particular Pabp2 and Hel25E (UAP56) did not have any effect on the other viruses, meaning that they might have a dicistrovirus-specific impact on viral infection. In addition, among the candidates with an increased DCV RNA load, 4 also induced an increased

FHVΔB2 RNA load and 3 induced an increased VSV RNA load. In particular, the KD of two candidates, Hsc70-4 and Fandango, induced an increased viral RNA load in all viruses tested except for FHV WT. There is therefore a possibility that these proteins play a role in a general antiviral mechanism. Of note, the only candidates that had a virus-specific impact on a virus other than DCV were Rrp6 and Pop2, which seem to have an antiviral impact on VSV. Pop2 is a major catalytic subunit of the CCR-NOT deadenylation complex (Temme et al., 2010). Rrp6 is an exosome-associated ribonuclease that has been shown to have an antiviral effect on Rift Valley Fever Virus (RVFV), in a screen together with Dis3 (Molleston et al., 2016). This paper suggests that components of the exosome can be repurposed to serve as an antiviral surveillance system. As RVFV is a negative-strand virus like VSV, Rrp6 could be involved in the detection of RNA(-) viruses. Of the two candidates that showed a potential global impact on viral infection, only Hsc70-4 has already been described as involved in antiviral immunity (Iwasaki et al., 2010). As its role was already well characterized, we therefore decided to focus on the second candidate, Fandango.

C. Impact of KD of Fandango on the viral infection

Our first step in studying Fandango was to confirm the results of the DCV screen in a separate experiment, using the same protocol (**Figure 17A**). In addition to the two dsRNAs targeting Fand used in the RNAi screen, a third dsRNA was tested and the efficiencies of the KD for each dsRNA was calculated using two different pairs of Fand qPCR primers. As shown on **Figure 17B**, all three dsRNAs seem to efficiently inhibit Fand expression, with respective KD efficiencies of 81.57% (dsFand1), 85.16% (dsFand2) and 84.61% (dsFand3). These values are preliminary as they represent a single experiment, and the results need to be replicated in triplicate to have a more precise estimation of the KD efficiency. It is worth noting that the expression of *Fand* seems to be quite low compared to the expression of the housekeeping gene *RP49* used to normalize the data. S2 cells are derived from a primary culture of late stage (20–24 hours old) *D. melanogaster* embryos, which express, according to the Flybase database (http://flybase.org/reports/FBgn0033859), a lower amount of *Fand* than other stages of the fruit fly life cycle. This can be an advantage as it will be easy to inhibit *Fand*, however it might mean using an antibody against endogenous Fand may be complicated in S2 cells as low expression proteins can be difficult to visualize on a western blot (WB).

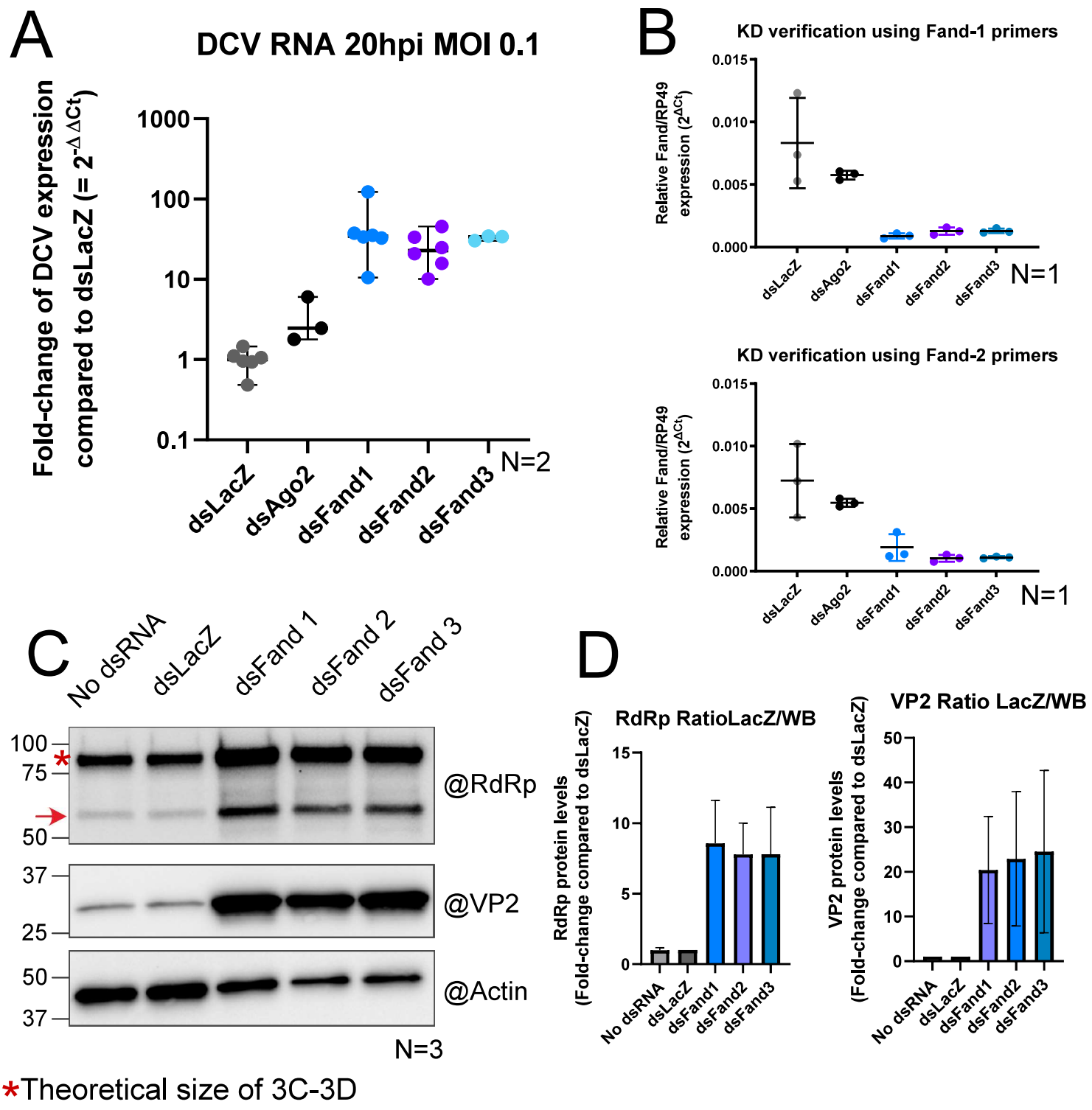

Figure 17 - Impact of the knock-down of Fandango on viral RNA load and proteins. A) Fold-change of DCV RNA load for each condition compared to the dsLacZ control. Viral RNA load were measured by qPCR after soaking using different dsRNAs and DCV infection at a MOI = 0.1 (N=2). The median and range are represented for each condition. B) Using the same samples, verification of Fand KD was performed using two different qPCR primers (N=1). The median and range are represented for each condition. The data was not normalized with the control condition to show the expression levels of Fand compared to the housekeeping gene RP49. C) Representative immunoblot showing the impact of Fand KD on viral protein loads. The experiment was performed three times and results were similar each time. The asterisk shows the theoretical size of the uncleaved 3C-3D polyprotein before cleavage by the DCV protease, and the arrow shows the size of DCV RdRp. D) The intensity of the bands on immunoblots from C) were measured using the ImageJ software (N=3). The values were normalized for each gel with the value of the housekeeping protein actin. Fold-change compared to the control condition dsLacZ were then represented here. The error bar represents standard deviation.

Next, we wanted to check if this increase in DCV load was reflected at the protein level. To this aim, I checked the expression of two DCV proteins, the capsid protein VP2 and the viral RdRp, by western blot after KD of *Fand* and subsequent DCV infection (**Figure 17C**). In both cases, the amount of viral proteins expressed is higher after KD of *Fand*, even though the housekeeping protein Actin stays stably expressed. This experiment was performed three times and each time the results were similar. The increase in DCV proteins was then quantified for the three different gels and was consistent with visual observation **Figure 17D**.

Taken together, these results indicate that *Fand* KD correlates with an increase in viral RNA and protein loads compared to the control. Moreover, this increase seems to be global as it can be observed for both the VP2 and RdRp proteins, which are expressed from two different DCV ORFs. We can even observe this tendency in the 3C-3D polyprotein, which is the precursor of the RdRp and Protease of DCV before they are cleaved (**Figure 17C**). This is consistent with the results obtained in the *ex vivo* RNAi screen (**Figure 15A**) as well as the *in vivo* screen performed by my host laboratory, and hint to a potential antiviral role of Fandango during DCV infection.

D. Impact of Fandango on the viral cycle

The viral replication cycle is composed of four core steps: (1) Attachment to the host cell and entry, followed by uncoating, i.e. degradation of the viral capsid to release the nucleic acid; (2) Genome replication and translation; (3) Assembly, which is the production of virions; and (4) Egress, which is the release of the newly produced virions outside of the cell. After observing the impact of Fand on both viral RNA and viral protein amounts (**Figure 17**), we wanted to understand the underlying mechanism involved in this impact. Therefore, a good starting point would be to know which of the viral replication steps were impacted by Fandango. To answer this question, I performed a synchronized DCV infection in S2 cells, which I collected at different time points during the replication cycle.

To make sure that the infection was indeed synchronized, the infection was performed on ice, thus inhibiting cell entry while still allowing the virus to bind to the cell. After the adsorption phase, all unbound particles were washed off and the cells were put at 25°C, inducing the

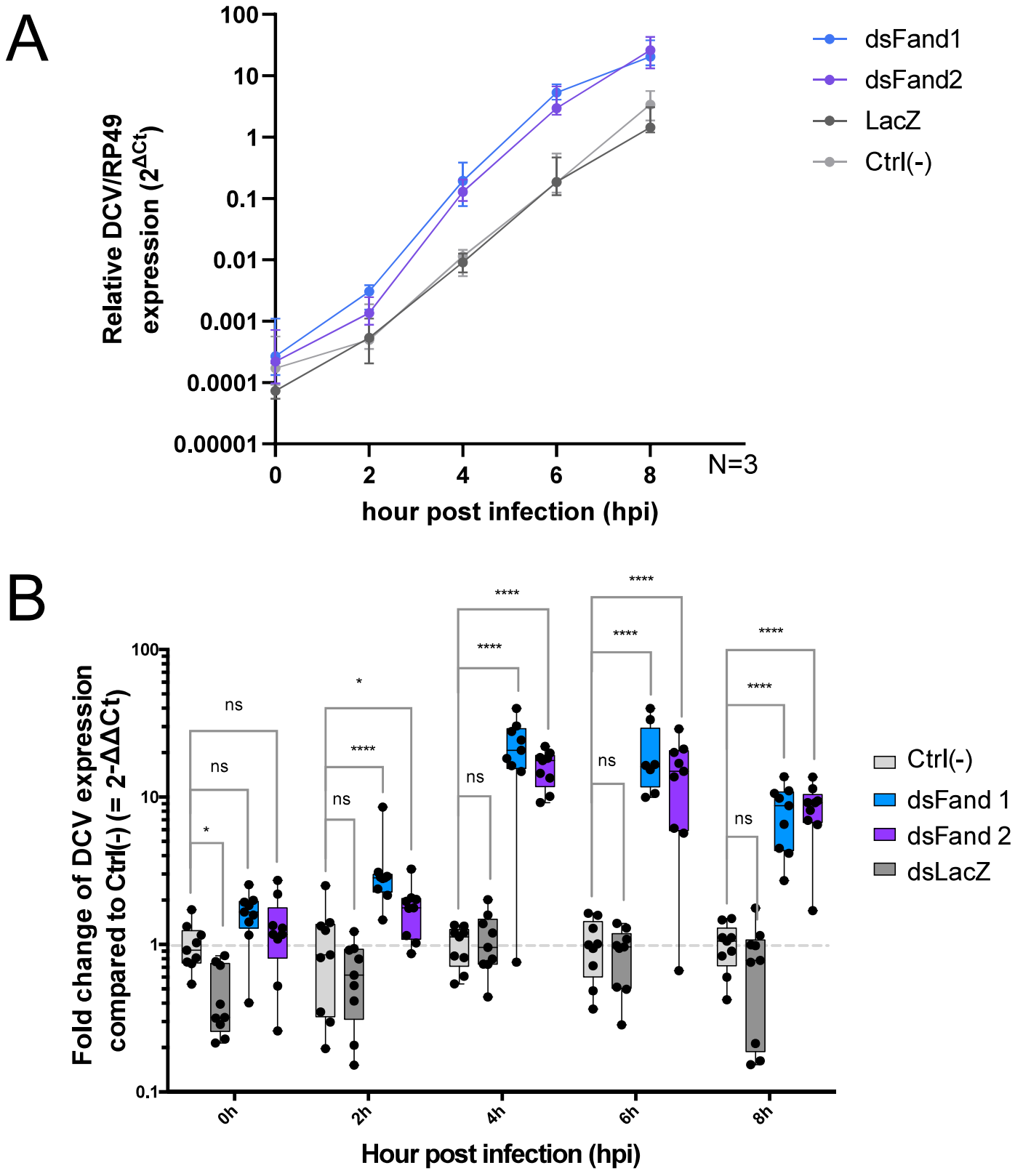

Figure 18 - Impact of Fandango knock-down on DCV replication cycle in S2 cells. After dsRNA bathing with either dsFand, dsLacZ or no dsRNA, a synchronized infection was performed on S2 cells with DCV at a very high Multiplicity Of Infection (MOI of 10) for 8 hours. Cells were collected at different timepoint during the infection cycle, and viral RNA load was measured by RT-qPCR (N=3). For each time point, the DCV/RP49 ratio was normalized using the control condition with no dsRNA. A) Kinetics of the viral RNA load from 0 to 8 hpi. The data is represented as the relative DCV RNA load compared to the housekeeping gene RP49. Error bars represent standard deviation. B) Fold-change of DCV RNA viral load compared to the control. DCV/RP49 relative expressions were used to compute the $2^{-(\Delta\Delta Ct)}$, or fold-change of expression, and represented on this box and whiskers plot. Statistics were obtained using a Repeated mesures two-way ANOVA (mixed model ANOVA).

synchronized cell entry of all bound viral particles. Moreover, the Multiplicity of Infection (MOI) chosen was very high (MOI = 10), to be certain that all cells would be infected by at least one viral particle. The cells were collected at 0, 2, 4, 6 & 8 hours post infection (hpi). This timeframe should include the whole replication cycle of DCV, which is highly pathogenic (Lamiable et al., 2016). Indeed, a RT-qPCR on strand-specific DCV RNA experiment performed by a previous PhD student of my host lab, with the same infection conditions (and supported by non-published observation in my host lab), showed that the amount of antigenomic strand does not increase between 6 and 12 hpi (cf. "Sensing of viral RNAs by Dicer-2 in drosophila" L. Talide 2019). This suggests that DCV replication inside the primary infected cells has already finished during at this time, but that the newly produced viral particles have not yet started replication in other cells. Moreover, the amount of antigenomic strand already increases at the first time point chosen, 3 hpi, meaning that replication of the DCV genome starts before 3 hpi.

Three independent experiments were performed, with technical triplicates for each experiment. Two different non-overlapping dsRNAs against Fandango were used to reduce the possibility of an off-target effect. After measuring the viral RNA load at each time point by RT-qPCR, the data was represented in two different manners: 1) Relative DCV expression compared to the housekeeping gene *RP49*, which corresponds to a DCV/RP49 ratio (**Figure 18A**); and 2) Fold-change of DCV/RP49 compared to the control with no dsRNA treatment (**Figure 18B**). The first method allows the representation of the DCV RNA increase during the viral replication cycle, while the second method allows the visualization of the fold-change of DCV RNA load compared to the control. As shown by **Figure 18A**, the virus starts to replicate and/or transcribe its genome quite early in its replication cycle, as we can already observe an increase in viral RNA load between 0 and 2 hpi. However, as this qPCR is not strand-specific, we cannot differentiate genome replication from transcription. After 2 hpi, we then see a constant increase in viral RNA load until the end of the experiment. This is consistent with the very fast replication cycle of DCV previously observed.

At the start of the experiment (0 hpi), the viral RNA load is similar to that of the control condition (**Figure 18B**). However, we can notice that it become significantly different from 2 hpi onwards (3.2x and 1.7x higher than the control on average for dsFand1 and dsFand2,

respectively). This difference then seems to increase and the impact of the *Fand* KD is at its highest between 4 and 6 hpi (22.3x higher at 4hpi and 17.7x higher at 6hpi for dsFand1; 15.9x higher at 4hpi and 14.2x higher at 6hpi for dsFand2), and then to decrease slightly at 8 hpi (7.6x higher for dsFand1 and 8.4x higher for dsFand2). These results indicate that Fand impacts DCV infection quite early during the viral replication cycle. The antiviral impact of Fandango could therefore be linked to genome replication and/or transcription, as this process starts around the same time. However, we can rule out an impact on attachment of the virus to the cell, as in this case we would already observe a difference at 0 hpi. An impact on translation of DCV proteins also seems unlikely, as we can observe an impact on viral RNA load and not only protein load. Finally, although several steps of the viral replication cycle could be affected by the same protein, this experiment points to an impact of Fand at the early stages of the viral replication cycle, rather than the end of the cycle like particle assembly or egress.

In conclusion, Fandango has an impact on DCV infection at the early stages of the viral replication cycle. In order to know more precisely which step of the viral replication is affected by Fand, it would be interesting to perform a strand-specific RT-qPCR at very early time points (i.e. between 0 and 3 hpi). By doing this, we could see if the DCV RNA fold-change increase between *Fand* KD cells and control cells correlates with the start of antigenomic strand synthesis, and therefore genome replication.In order to study the very early steps of DCV replication in S2 cells, a transmission electron microscopy approach could help visualize the interaction between the virus and the host cell. Unfortunately, at the time of this experiment we decided to focus on my main project (the Dicer-2 interactome) in order to be able to publish it, and I was not able to dig further into that aspect of the Fandango project.

E. Impact of overexpression of Fand on the viral infection

In the previous sections of this Chapter, we saw that *Fandango* KD leads to an increase in both DCV RNA and protein loads. By opposition, depending on the underlying mechanism that induces this phenotype, Fand overexpression (OE) might therefore lead to the opposite phenotype, i.e. a decrease in DCV load. However overexpression of a gene does not always amplify its role, as illustrated by the fact that Dicer-2, but neither R2D2 nor Ago2 overexpression, can lead to an enhancement of the RNAi pathway in some tissues in flies, like

neurons (Dietzl et al., 2007). This might be explained by the fact that the limiting protein here is Dicer-2, as R2D2 depends on the presence of Dicer-2 to play its role in RNAi. We therefore decided to check whether or not Fand overexpression is able to restrict DCV infection. To this aim, I constructed plasmids expressing Fand, tagged with HA at either the N-terminal (Nter) or C-terminal (Cter) end of the protein, by Gateway cloning. I also constructed a control plasmid expressing GST and tagged at the Nter end, which should not have any impact on viral infection. However, the overexpression of either Fand plasmids in S2 cells for 24h & 48h had no impact on DCV protein loads (**Figure 19A**). Of note, although the Cter-tagged Fand-HA plasmid seems to be well expressed in S2 cells, the Nter-tagged version, HA-Fand, is barely visible on the immunoblot. This may be due to either a slightly different environment surrounding the start codon, or the folding of the protein which could partially hide the HA tag from the antibodies. Moreover, in some instances the addition of a HA-tag can lead to an increased instability of the protein (Saiz-Baggetto et al., 2017).

Although Fand OE may truly have no impact on DCV infection, we wanted to be sure that those negative results were not due to the poor efficiency of transfection that we had observed in S2 cells in the lab. Indeed, we noticed that on average, only 20-30% of the cells expressed transfected constructs, which is commonly observed in drosophila S2 cells. After an immunofluorescence staining of S2 cells transfected with the Fand-HA plasmid, which is the one that is the most expressed according to the results from the WB, we observed that indeed only a small number of cells seemed to express the construct (**Figure 19B**). Moreover, the expression of the construct was uneven in the different cells, which makes it harder to differentiate between background fluorescence and true expression of the plasmid. As we also wanted to have the possibility of performing other immunofluorescence experiments with this construct, for example to study the localization of Fand upon infection, this was not ideal. In order to obtain a high percentage of cells expressing the construct and a more even expression between cells, we thus decided to establish stable cell lines expressing the different constructs.

There are two types of stable cell lines for overexpression of a construct: clonal population (i.e. cells that all derive from the same original cell expressing the gene of interest) or bulk population (i.e. a diverse population of cells expressing the gene of interest). As the first type

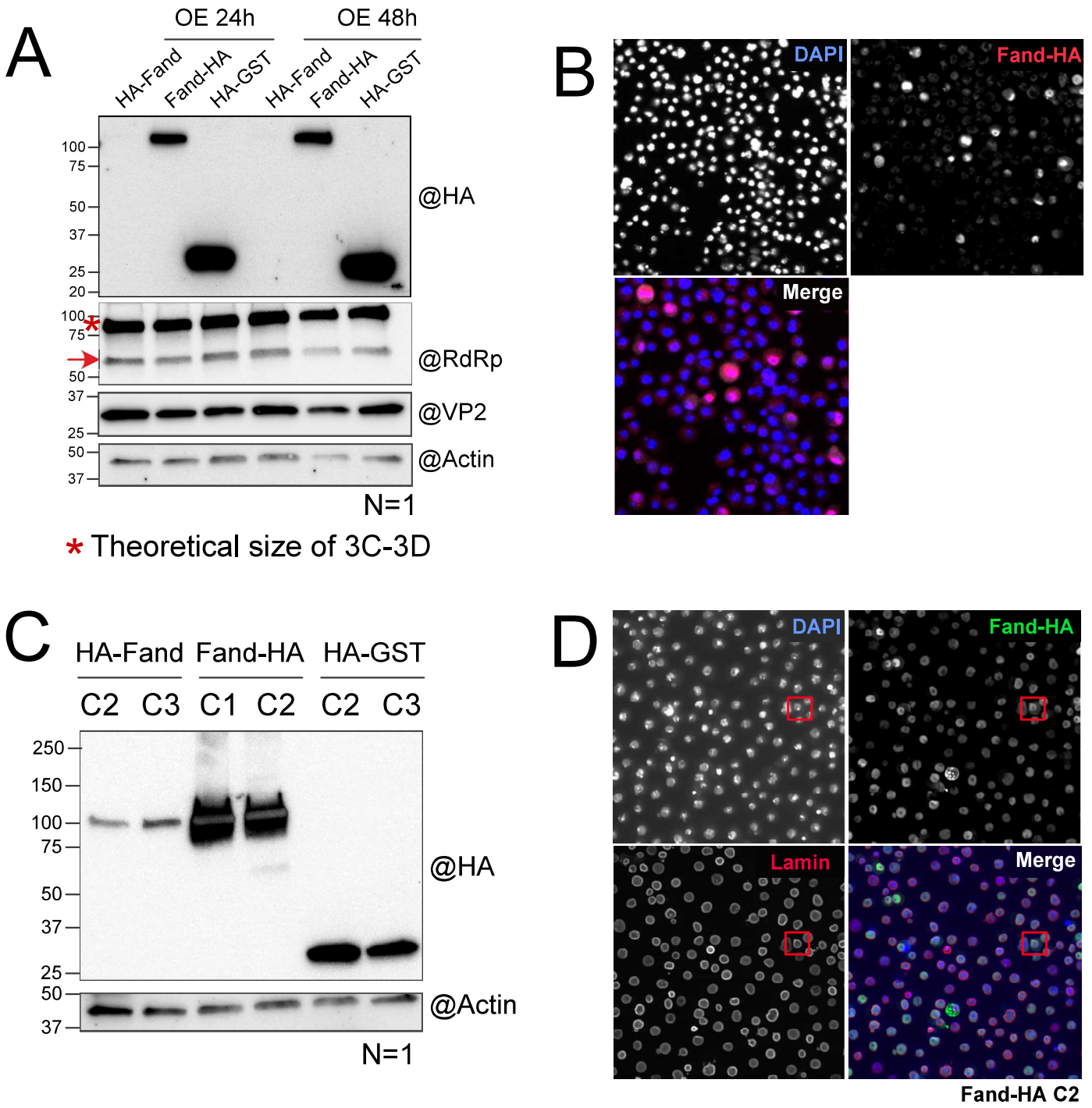

Figure 19 - Impact of the overexpression (OE) of Fandango on DCV proteins loads. A) Transient overexpression of Fand has no impact on DCV protein loads. S2 cells were transfected with plasmids containing either Fand or GST, tagged with HA. The asterisk shows the theoretical size of the uncleaved 3C-3D polyprotein before cleavage by the DCV protease, and the arrow shows the size of DCV RdRp. B) Confocal microscopy (magnification X40) after immunofluorescence experiment in S2 cells transfected with the Fand-HA plasmid. Fand-HA was stained with Alexa Fluor 546 labeled antibodies (red) and the nucleus was stained with DAPI. C) Immunoblot showing expression of HA-Fand, Fand-HA or HA-GST in the stable cell lines extablished. Two clonal populations are shown for each plasmid. D) Confocal microscopy (magnification X40) after immunofluorescence experiment in stable cells expressing Fand-HA. Fand-HA was stained with Alexa Fluor 488 labeled antibodies (green), lamin was stained with Alexa Fluor 546 labeled antibodies to mark the outline of the nucleus, and the nucleus was stained with DAPI. The red square indicates a example of a cell exhibiting slight green fluorescence in the cytoplasm, which could indicate the presence of Fand-HA outside de nucleus.

of cells are derived from the same cell, expression of the gene of interest is homogeneous and this will lead to a clear effect. However, this can mean that intrinsic differences between cells might influence the results of future experiments, and thus it is necessary to produce several different clonal lines. This allows us to make sure that the results of subsequent experiments are due to the expression of the gene of interest and not just a difference in behavior between two clones. The second type of stable cells, the bulk population, derives from a pool of cells and therefore is more heterogeneous. This induces less variability between populations, but it means that there is a higher variability inside the population, meaning that there can be varying degrees of expression of the gene of interest, and that the impact of the gene can be dampened. Moreover, this type of population is at risk of losing expression of the gene of interest if it causes a loss of fitness.

With this in mind, we decided to produce a clonal population of stable cells, using Puromycin as a selection marker, to make sure that the cells retained the plasmid. After generating the different stable cell lines, I then validated by western blot the expression of the different plasmids (**Figure 19C**). Although the Cter-tagged version of the Fand plasmid (Fand-HA) was once again visualized more easily than the Nter-tagged version on the immunoblot, the generation of the stable cell lines still allowed us to detect the Nter-tagged version better than after transient transfection. Moreover, after performing an immunofluorescence experiment using the Fand-HA stable cell line and confocal microscopy, we could observe expression of the plasmid in almost all cells, and at more homogeneous levels (**Figure 19D**).

In conclusion, although transient transfection of Fandango did not allow us to determine if overexpression of Fand lead to a decreased viral load because of a poor transfection efficiency, we now have the tools necessary to answer this question. Moreover, the stable cell lines can also be used to answer other questions on Fand, like its localization during infection. Indeed, Fandango is mainly expressed in the nucleus, although we did observe some cells in which it was slightly expressed in the cytoplasm as well (**Figure 19D**, red square). However, as DCV replication occurs in the cytoplasm, in the future we would also like to check if Fand changes localization upon infection. To this aim, new experiments should be conducted to follow the localization of Fandango at different time points of infection, using confocal microscopy.

F. Is the effect of Fand linked to the Prp19 complex?

As mentioned before, Fandango is a subunit of the Prp19 complex. Moreover, another protein of the Prp19 complex, CG9667, was identified as a potential nucleic acid sensor binding poly(I:C) along Fand during the AP-MS project that was performed in collaboration with the lab of Prof. Pichlmair. However, CG9667 did not have any antiviral impact against the viruses tested *in vivo* as opposed to Fand (Pennemann et al., 2021). We therefore wondered if the antiviral impact of Fand that we observed was dependent or not on this complex. For this part of the project and the next, I was helped by an intern, and part of the results were obtained by her under my supervision (Sophie Appleyard – Imperial College, London).

The Prp19 complex has been shown to be involved in splicing, but also in other biological mechanisms such as splicing, genome maintenance, recruitment of ubiquitylated proteins to the proteasome and transcription elongation (Kuraoka et al., 2008; Chanarat and Sträßer, 2013). In yeast, this complex is composed of 8 core subunits and several other associated proteins (Fabrizio et al., 2009), while in humans there are three complexes associated with PRP19: the PRP19/CDC5L complex, the PRP19-associated complex and the XAB2 complex, with XAB2 located in the latter two (Chanarat and Sträßer, 2013). The majority of spliceosomal proteins found in humans are also found in the *D. melanogaster*, and the Prp19 complex and its function in splicing is highly conserved between these two species and across metazoans, according to affinity purification analysis of the B and C splicing complexes (Herold et al., 2009). Because of this high conservation with humans, and the fact that a clear composition of the different complexes in the fruit fly is lacking, we based our experiments on the composition of the complexes in humans (**Figure 20A & 20B**).

In order to find out to which extent the complexes in which Fand belongs are involved in its antiviral impact on viral infection, we decided to KD the expression of genes from the different complexes by dsRNA soaking in S2 cells and check if this impacted the DCV RNA load after infection. To do this, we selected Prp19 and ISY1 (CG9667 in flies), which are both part of the XAB2 and PRP19-associated complexes in humans along with XAB2, the human orthologue of Fand. In addition, we added PRP8, which is not a part of these complexes, and was not highlighted during the nucleic acid sensor AP-MS. If the role of Fand is independent from both

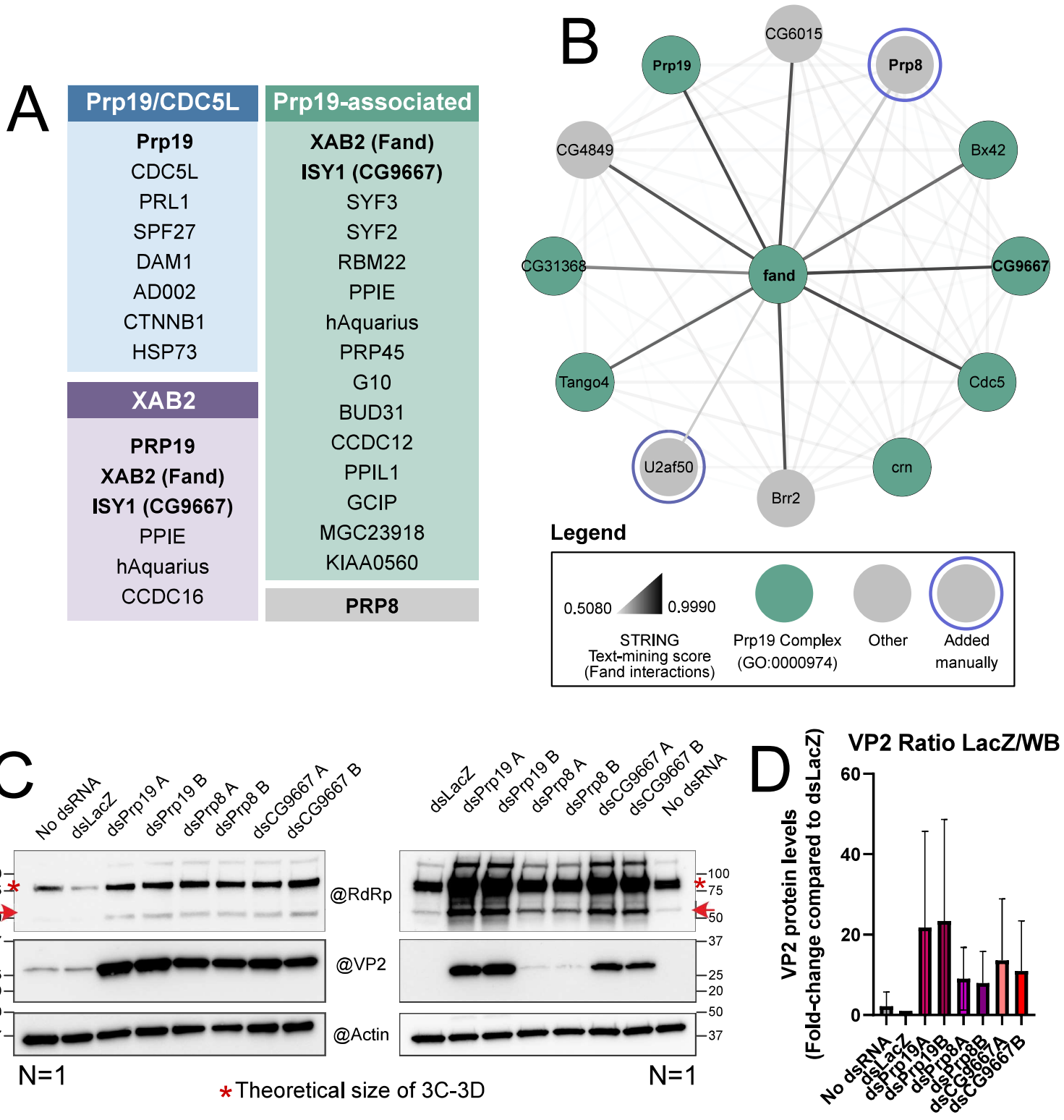

Figure 20 - Is the antiviral impact of Fand linked with the Prp19 complexes? A)Composition of the complexes associated with PRP19 in humans. The *D. melanogaster* orthologue of the human proteins tested are written inside parentheses. A protein that does not belong to any of those complexes but has a role in splicing, PRP8, was added to the experiment to see if the antiviral impact of Fand is linked with Prp19 and/or the spliceosome. B) Interaction network of Fand in *D. melanogaster*. This network was constructed using STRING and modified on Cytoscape to include U2af50 and Prp8 (cercled in blue). Interaction strength with Fand is represented by the color gradient of the edges (lines between nodes). Proteins belonging to the Prp19 complex are represented in green. C) Immunoblots showing the inconsistent impact of the different proteins on viral protein loads. The experiment was performed four times but results were not constant, they are therefore considered as four N=1. The asterisk shows the theoretical size of the uncleaved 3C-3D polyprotein before cleavage by the DCV protease, and the arrow shows the size of DCV RdRp. D) The intensity of the bands on immunoblots from C) were measured using the ImageJ software. The values were normalized for each gel with the value of the housekeeping protein actin. Fold-change compared to the control condition dsLacZ were then represented here. The error bar represents standard deviation.

the Prp19 complex and splicing, we should see no impact of these genes on DCV infection. However, if it is dependent on Prp19 but not splicing we should see an impact of Prp19 and CG9667 but not Prp8. Finally, if it is dependent on splicing, we should see an impact for all three silenced genes.

With this in mind, we checked the impact of dsRNAs targeting the different genes selected on the DCV proteins VP2 and RdRp, using the same protocol as before. However, after performing the experiment four times, we did not obtain consistent results, as some of the genes selected had varying impacts on DCV protein load depending on the experiment (**Figure 20C & 20D**). This was not the case for Fand, which has always had a reproducible impact on both DCV RNA and proteins. Indeed, although soaking with dsPrp19 induced an increase in both VP2 and RdRp compared to the controls each time, soaking with either dsPrp8 or CG9667 lead to varying results, as shown for dsPrp8 on **Figure 20C**, and as illustrated by the large range between replicates on **Figure 20D**. Moreover, these results do not correlate with the results obtained by the former PhD student in charge of the nucleic acid sensors project, who found no antiviral impact on any of the viruses tested for CG9667 *in vivo*.

Taken together, these results do not allow us to clearly determine if the Prp19 complex and/or the spliceosome are involved in the antiviral impact observed for Fand. Although this variation might of course be due to experimental error, it may also indicate an impact on cell viability, as in the case earlier with Nnp-1 and Ns1, and therefore that the effects observed on DCV are indirect. In the future, it would be very interesting to check the toxicity of the different dsRNAs using the same protocol as for the candidates of the screen. Unfortunately, because of this we cannot conclude anything from this experiment for now, other that the need to check toxicity of the dsRNAs.

G. Is the antiviral effect of Fand dependent on splicing?

As mentioned above, Fandango has been shown to be important for splicing. Moreover, although the results were inconsistent, we also observed an impact of another component of the spliceosome on DCV protein expression, suggesting a possible link with the splicing function of Fand. Unfortunately the results were not clear. To determine whether the antiviral

effect of Fand was dependent on splicing or not, we decided to inhibit splicing altogether and see if *Fand* KD still had an impact on DCV infection. To this aim, we used a splicing inhibitor called Isoginkgetin. This molecule is a biflavonoid found in the leaves of *Ginkgo biloba*. It has been shown to be a potent inhibitor of pre-mRNA splicing in human HEK293 cells and blocks the spliceosome in the A complex, preventing the A to B complex transition (O'Brien et al., 2008).

To be able to confirm the correct inhibition of splicing, we designed a construct to measure the splicing activity of the cell, based on the work of Nasim et al. in mammalian cells (Nasim et al., 2002). This seemed especially important as, to our knowledge, Isoginkgetin was never tested in S2 cells. The splicing reporter construct that we designed encodes the 5'end of the *Tubulin 84B* (*Tub84B*) mRNA sequence, including its 5'UTR, the first intron of the gene and the beginning of the first exon, in frame with the complete sequence of the Firefly Luciferase (FLuc) (**Figure 21A**). As the *Tub84B* intron contains multiple in-frame stop codons, this should lead to two scenarios, depending on the splicing activity of the cell. If splicing is ineffective, the presence of premature stop codons on the resulting mRNA could lead to its degradation through Non-Sense Mediated Decay (NMD), or the translation of an aborted protein that would then be degraded. However, if splicing is effective, the stop codons inside the intron would be removed and lead to the production of a Tub84B-FLuc fusion protein. By measuring the activity of FLuc, we should hypothetically be able to determine if splicing is active or not.

The reporter construct was obtained by Gateway cloning by an engineer in my host lab, and its expression was tested by transfection in S2 cells and Dual Luciferase Reporter (DLR) assay (**Figure 21B**). The term "dual reporter" refers to the fact that two individual reporter enzymes, FLuc and the Renilla Luciferase (RLuc) are simultaneously expressed and measured. After transfection of two different constructs together expressing either RLuc or the FLuc splicing reporter plasmid, most transfected cells will therefore express both plasmids. Normalizing the activity of the experimental reporter (FLuc) with an internal reporter (Rluc) minimizes experimental variability caused by transfection efficiency. Using the same cell viability assay as before, we tested the impact of Isoginkgetin on mitochondrial activity to check if the toxicity of the inhibitor and if it could be used in our experiment (**Figure 21C**). As it did not have any impact on mitochondrial activity at the time point chosen for the experiment, a

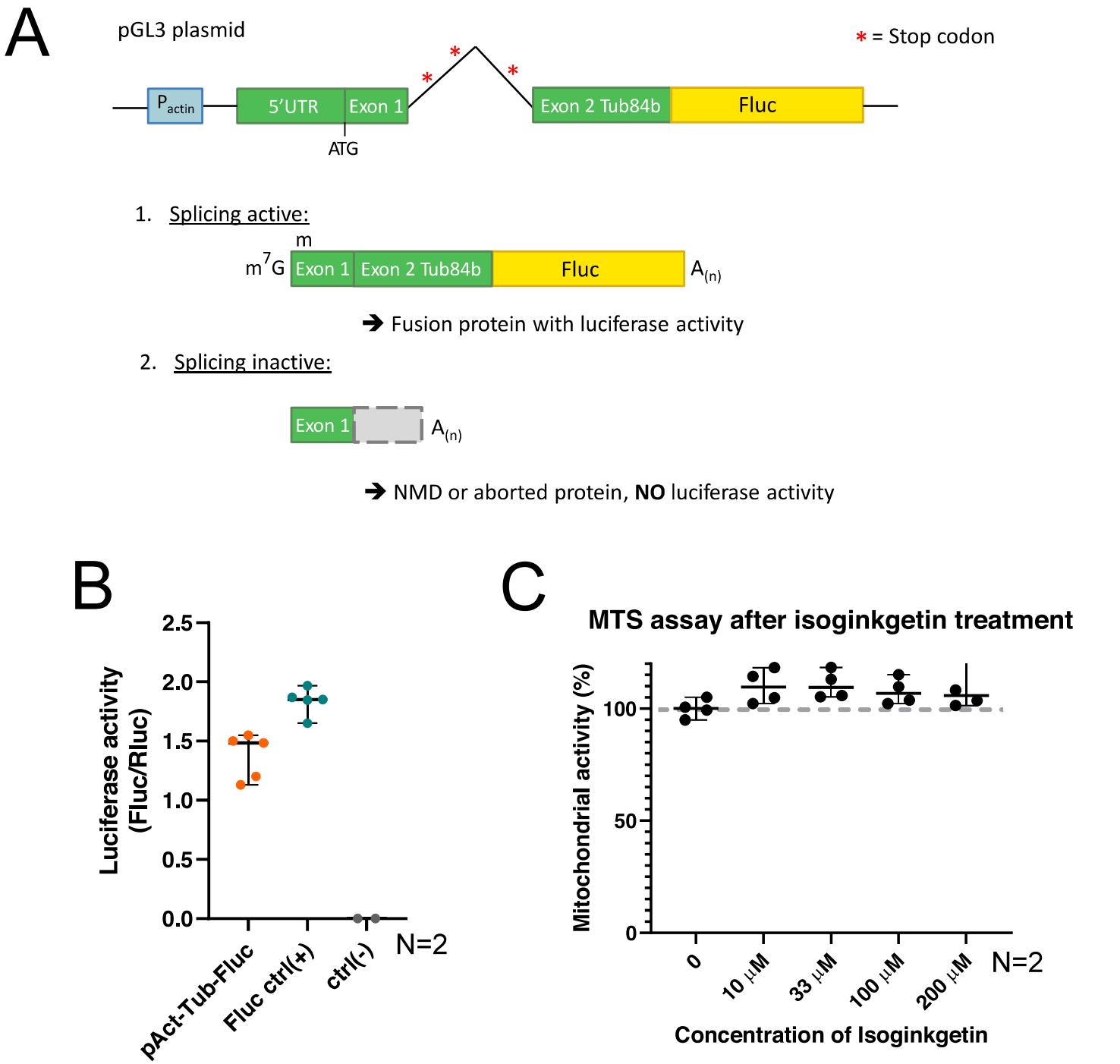

Figure 21 - Is the antiviral impact of Fand dependent on splicing? A) In order to investigate the role of splicing in the antiviral impact of Fand, a splicing reporter was designed. This construct encodes the 5'end of Tubulin 84B (Tub84B), including the 5'UTR, the first intron and the beginning of the first exon. It also encodes the complete sequence of the firefly luciferase (Fluc), in frame with Tub84B. As the Tub84B intron contrains several in frame stop codons, inactive splicing in the cell should lead to either the degradation of the resulting mRNA by non-sense mediated decay, or the production of an aborted protein that would then be degraded, and in both cases no luciferase activity. On the contrary, if splicing is active in the cell, the expression of the splicing reporter should lead to the production of a fusion protein with a luciferase activity. B) Luciferase activity after transfection of the splicing reporter, a positive control plasmid expressing the firefly luciferase, or a negative control plasmid with no luciferase in S2 cells. The luciferase activity in the cells were normalized using the activity of Renilla luciferase (Rluc), co-transfected with each plasmid. C) Cell toxicity of isoginkgetin was tested by measuring the mitochondrial activity 6 hours after treatment with different doses of isoginkgetin, and represented as a percentage of survival compared to the non-treated control. The graph represent two independent experiments (N=2).

potential impact on expression of the splicing reporter expression can be attributed to splicing inhibition and not cell death.

The ability of the splicing reporter to correctly show splicing activity now needs to be assessed using the Isoginkgetin splicing inhibitor. Unfortunately, preliminary results did not allow us to observe any decreased luciferase activity for the moment (results not shown). This could mean that either the splicing reporter construct does not work, or we need to adapt the dose and/or time point chosen compared to the conditions that were used in mammals in the paper from O'Brien et al. (O'Brien et al., 2008). Another possibility is that Isoginkgetin does not inhibit splicing at the time points and concentrations used in S2 cells. Before being able to determine if splicing is involved in the impact of Fand on viral infection, we therefore need to optimize our splicing reporter strategy. Once this is fixed, we will have the tools necessary to study the role of the splicing process on the antiviral impact observed with Fand.

III. Discussion

A. Did this RNAi screen highlight new actors of antiviral immunity?

The *ex vivo* RNAi screen presented in this Chapter highlighted candidates from three different projects: the first aimed to identify new nucleic acid sensors, the second aimed to identify nucleases that would cleave viral RNA to allow recognition of protected termini, and the third aimed to identify new Dicer-2 partners.

Nucleic acid sensor project

The first project used an AP-MS approach, wherein biotinylated nucleic acid baits were coupled to streptavidin beads and incubated with cell lysate, which were then analyzed by LC-MS/MS. The top candidates were used to perform an *in vivo* screen using Gal4-Gal80 flies allowing developmental control, through temperature shift, of inducible Gal4 knock-down for candidate genes (Brand and Perrimon, 1993). In our approach, we choose to induce KD in adult flies to avoid the impact of KD during development for the target genes. The *ex vivo* RNAi screen presented in this Chapter allowed to confirm these results for three out of four candidates from the nucleic acid sensor project (Larp4B and Tao for DCV, Fand for all viruses tested). Thousand and one (Tao) proteins are evolutionary conserved kinases, present in both mammals, which encode three Tao kinases, and flies, which encode only one. During the AP-MS project, they were found to bind poly(I:C) in both flies and human cells, and to have an antiviral impact in both species (Pennemann et al., 2021). In addition, depletion of Tao kinases in mammals induces a decreased induction of interferon stimulated genes. The La-related protein 4B (Larp4B) is an RNA-binding protein. In humans, this RBP interacts with mRNAs to regulate their stability and translation (Küspert et al., 2015). Fandango, the candidate from this project that showed a global effect on viral infection, binds poly(I:C), which is a mimic of viral dsRNA. These three proteins are good candidates as potential antiviral proteins involved in nucleic acid sensing. However, there were some differences in the results compared to the *in vivo* screen performed previously by my host laboratory in *D. melanogaster*. First, in the *ex vivo* screen described in this Chapter, CG5641, one of the four candidates from the nucleic acid sensors project, had no significant impact on viral RNA load whereas it previously was shown to have an impact *in vivo* by my lab. Second, Larp4B had an impact on DCV, CrPV and

VSV in the *in vivo* screen but in the *ex vivo* screen, with the conditions used here, they only impacted DCV. These differences could arise from the time points chosen, and we could have tested multiple time points to see if we see an impact on viral infection at other moments during the replication cycle of DCV. However, the timecourse experiment used for Fand would have been difficult to perform in the context of a screen due to the number of samples. Other approaches could have been tested, such as monitoring the viral infection in real-time using a virus replicon fused to a fluorescent marker in a temperature- and CO2-controlled fluorescence plate-reader (Garcia-Moreno et al., 2019).

Nucleases project

The second project was based on a literature-based approach that led to the selection of a large number of candidates, which were tested in a first *ex vivo* screen using DCV. The most interesting candidates were then subjected to the screen described in this Chapter, in order to determine the specificity of their impact on viral infection. By doing so, we first confirmed the impact of 8 nucleases out of 15 with DCV. After performing the screen using the different viruses, we then determined a potential DCV-specific impact for six of them (Clp, CG13690, Rps3, Dis3, pcm & Snm1), a dicistrovirus-specific impact for one of them (Hel25E), and a potential general impact for ZC3H3, although it did not have a significant impact on FHVΔB2 RNA load. Moreover, we observed a VSV-specific impact of Rrp6 and Pop2. According to these results ZC3H3, which had the impact on the most viruses, is a candidate of choice as the hypothetic nuclease helping Dicer-2 sense the protected viral RNAs. In mammals, another zinc finger protein, ZCCHC3, was actually shown to bind RNA and facilitate viral RNA sensing by associating with RIG-I and MDA5 and promoting their activation (Lian et al., 2018a). In addition to this, it was also shown to be a co-sensor of cGAS for dsDNA recognition, highlighting its major role in viral nucleic acid recognition (Lian et al., 2018b). Moreover, ZC3H3 was recently shown to suppress replication of the H9N2 influenza virus in the chicken (Chen et al., 2022). We could therefore imagine a similar role for ZC3H3 in *D. melanogaster*.

As the different viruses possess very different genomes, it is also possible that different nucleases are responsible for the cleavage of the different viruses, and that several of these nucleases could help sense viral RNA. Now that this screen has allowed use to break down the original list of candidates to a more manageable one, the highlighted nucleases should be

studied further to see if their impact on viral infection is due to an interaction with viral dsRNA. For example, it could now be interesting to study the localization of the different nucleases in relation to the viral RNA. To do this, tagged constructs expressing the candidate genes could be transfected into S2 cells, and confocal microscopy after immunostaining could allow us to see if the candidates co-localize with dsRNA (that can be stained using the anti-dsRNA J2 antibody) after viral infection. Moreover, cleavage assays of viral RNA could be performed using fly extracts expressing or not the different nucleases. Finally, we could determine if the KD of the different nucleases impacts vsiRNA production, by performing high-throughput small RNA sequencing and checking virus-mapping reads distribution. This could help us identify nucleases that may help Dicer-2 sense the viral dsRNA.

Dicer-2 interactant project

The last project was based on my *in vivo* IP-MS experiment, before the statistical analysis was performed. As described in Chapter I, after immunoprecipitation of Dicer-2 in different fly lines, its interactants were analysed by mass spectrometry. We then selected candidates identified in Dicer-2 samples but not at all in control samples, and that therefore had a high probability of interacting with Dicer-2. If we compare the two lists of candidates, before and after statistical analysis, we can observe that some of the candidates selected before the analysis were then confirmed by it. This is the case for FASN2, homer, lost, Syp, alt, SCS-α, CG9684, CG5214/alpha-KGDH and R2D2, which were highlighted by the global Dicer-2 analysis using SAINT. In particular, we were able to confirm the interaction of Dicer-2 and Syp by immunoprecipitation and western blot *in vivo*. Surprisingly, we did not obtain the same results in the two *ex vivo* screens in drosophila S2 cells. As we changed the batch of DCV used between the two experiments, we had to adjust the MOI used because we noticed that the new batch induced a DCV RNA load considerably higher, potentially because of an increased virulence in this batch. Therefore, it is possible that the difference between the two screens is due to differences in the MOI, and it would be interesting to perform an infection using both DCV batches after KD of the candidates and compare the viral RNA load.

As RNA interference is a general antiviral mechanism, we would expect that Dicer-2 interactants involved in RNAi have an impact on most viruses, except if they help the sensing of specific types of viruses that produce sub-optimal substrates for Dicer-2. This was the case

for Hsc70-4, and should have been the case for Ago2 and R2D2 if the KD had worked properly. Another possibility is that the candidates tested here, as they do not impact all viruses, could be involved in other mechanisms of Dicer-2. For example, they could be involved in the non-RNAi related mechanisms of Dicer-2, or in its function in the endo-siRNA pathway. A possible experiment to check the impact of the different candidates on the endo-siRNA pathway could be to KD the candidates and then check the expression of a common endo-siRNA in *D. melanogaster* like *esi1* or *esi2*, which are endo-siRNAs that arise from the annotated transcript *CG47744* and *CR18854*, respectively (Harrington et al., 2017). As a positive control, we could use dsRNAs targeting Loqs-PD.

Bridging the different projects

Although the candidates for this screen came from three different projects, they were all selected as part of the same general objective, namely trying to understand antiviral immunity in *D. melanogaster*. Moreover, for the three projects we were always particularly interested in the sensing of viral nucleic acids, either by Dicer-2, nucleases, or other potential nucleic acid sensors. This is probably why we can find some connections between these different projects. Indeed, after representing the network of the candidates from the different projects with an impact on the replication of at least one virus using STRING, we can observe a number of interactions between the different proteins (**Figure 22**). A number of nucleases seem to interact with Pabp2, and it would be interesting to see if this interaction is mRNA-dependent.

Moreover, the different projects have led to the identification of common candidates. For example, some proteins identified after AP-MS some NA baits were also identified after Dicer-2 IP-MS. As most Dicer-2 partners like R2D2 which was also identified in the AP-MS experiment, are RNA-binding proteins, this is not very surprising. For example, Lost, Syp, CG9684, Larp4B and CG5641 were identified in both projects. In addition, the nuclease Pacman (Pcm) was shown to bind ssRNA-PPP in the AP-MS experiment. Pcm is an exoribonuclease that degrades decapped RNA. In mammals and yeast, the pcm orthologue XRN1 seem to have an antiviral effect against some viruses, including VSV that can also infect mammals (Ng et al., 2020; Rowley et al., 2016), but a proviral effect against others like Influenza A or SINV (Garcia-Moreno et al., 2019; Liu et al., 2021). As it seems to recognize viral

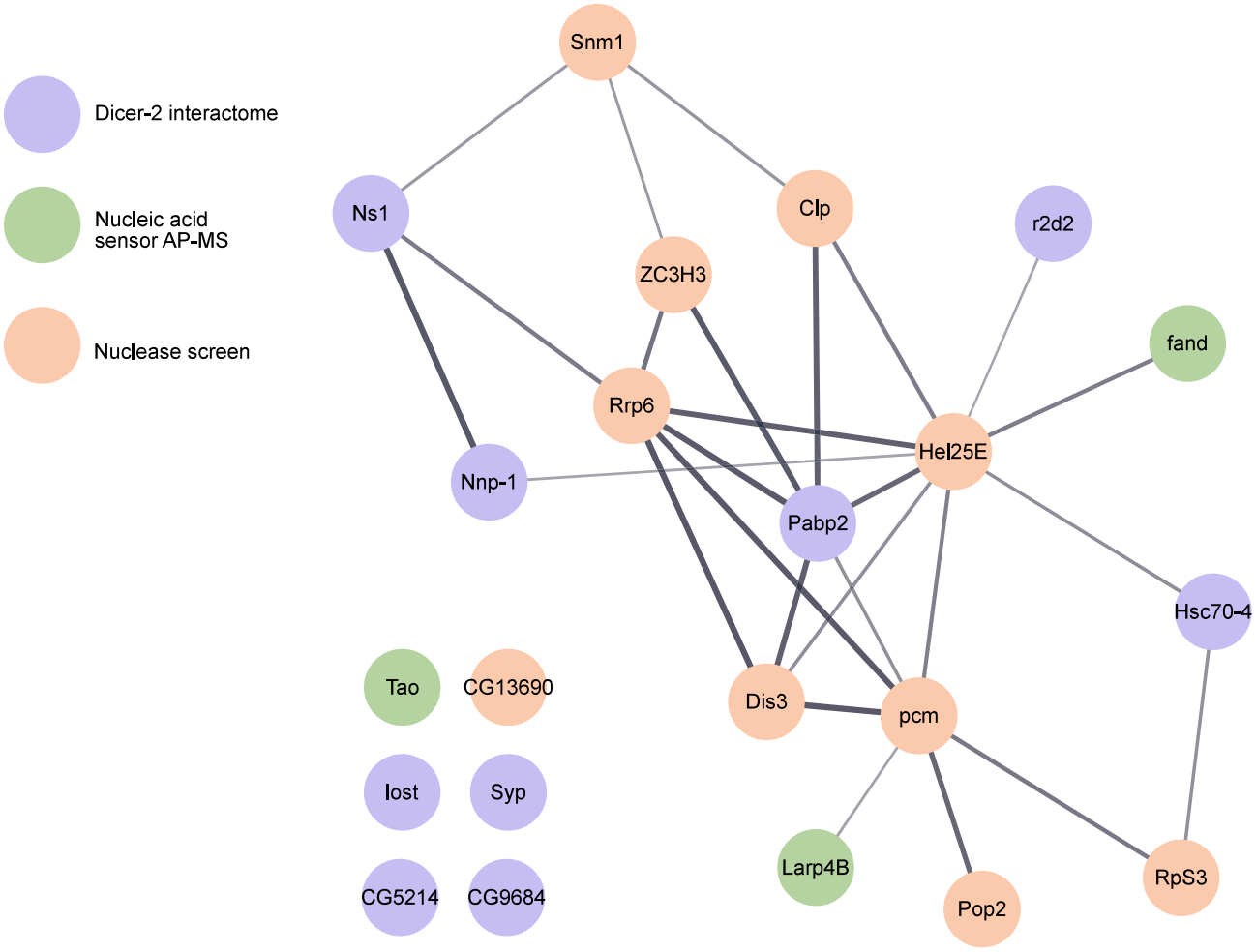

Figure 22 - Interconnection between the different projects. Representation of the interactions between the candidates that had an impact on viral RNA load for at least one virus. This network was established using STRING/Cytoscape. Thickness of the lines indicate the confidence measure for the interaction.

RNA, Pcm might be an interesting candidate as the hypothetical nuclease helping Dicer-2 sense viral RNA with a protected termini.

Technical comments on the ex vivo RNAi screen

By using RNAi to KD the different genes, we run the risk of missing some candidates that have such an important role in RNAi that their KD cannot be complete and so have no impact on the read-out. Unfortunately, for large screens it would be impossible to verify the KD efficiency of each candidate and by performing this experiment we have to accept this risk. This may also have been the reason why some of the controls for this experiment did not behave as expected. Although it would be possible to perform a screen using the CRISPR-Cas9 technique, this is a method that takes a lot more time and can lead to significant off-target effects. However the main issue with using CRISPR-Cas9 in S2 cells is that these cells are aneuploid for more than 43 Mb of the genome, meaning that all genes do not have the same number of copies (they range from one to five copies) (Zhang et al., 2010). In diploid cells, the use of CRISPR-Cas9 can give rise to either heterozygous or homozygous knock-out cells, and therefore in the aneuploid S2 cells this would be even more unreliable. Moreover, as a KD does not completely shut off gene expression, it may dampen the impact on cell survival for some candidates compared to CRISPR-Cas9. In retrospect however, the choice of controls may not have been ideal. However, very few proteins have been shown to have an impact on S2 cells outside of RNAi. For example, the paper showing an antiviral impact of Vago has been performed exclusively *in vivo* (Deddouche et al., 2008). As RACK1 is a dicistrovirus-specific proviral protein, it should have been a good control for DCV and CrPV, however it is true that a proviral control for FHV and VSV may have been useful. A possibility would be to use dsRNAs directly targeting some viral mRNAs, which could be used as a "proviral" control inducing a decreased viral RNA load after KD.

B. Interplay between splicing and antiviral immunity

In this Chapter, we wondered if splicing and/or the Prp19 complex could have an impact on antiviral immunity. Although we showed that KD of Fand leads to an increased viral load after infection with several viruses, a change in viral load is not sufficient to classify a protein as a component of antiviral immunity. Indeed, we now have to ask ourselves if the antiviral

phenotype that we observed is indeed the result of an action of Fand on the virus, and if it is biologically relevant or just an indirect effect of a weaker cell being less able to defend itself against viral infection. An important part of this project was therefore to understand to what extent splicing and the Prp19 complex are responsible for the impact of Fand on viral infection. In addition to the obvious impact that an impaired spicing of antiviral factors could have on the ability of the cell to fight against viral infection, some observations made us consider this possibility.

Indeed, I noticed in the Dicer-2 interactome established in Chapter I a large number of proteins labelled with the GO term "Spliceosomal complex". A similar observation was made by another PhD student in my institute, who is working on constructing the interactome of another RNAi protein, Loqs2, in *Aedes aegypti* mosquito (Barbarit et al., personal communication). This GO term is not limited to proteins from the different snRNPs of the core spliceosome, but is also used to label proteins associates with splicing in STRING, like proteins from the Prp19 complex. Two of those proteins, Syp and Rump, were then shown to interact with Dicer-2, as shown in Chapter I. Moreover, some but not all of the proteins of the Prp19 complex have also been identified as binding to poly(I:C) in the AP-MS experiment (e.g. Fand, CG9667). An interplay between the splicing and RNAi machineries has already been suggested by the fact that several splicing factors were shown to have an influence on the production and efficiency of miRNAs and siRNAs in a genome-wide screen in *D.* melanogaster (Zhou et al., 2008). Together, these results raise the question of a potential link between some splicing-associated proteins and antiviral immunity, or even RNA interference.

The work of Xiong and colleagues suggests that there might indeed be a certain amount of cross-talk between the spliceosome and the RNAi machinery (Xiong et al., 2013). The authors show that one of the Sm-proteins of the spliceosome, the small nuclear ribonucleoprotein SmD1, not only interacted with dsRNAs but also with the RNAi machinery. They showed an interaction (which could be direct or indirect) between SmD1 and Dicer-2, R2D2 and Ago2, suggesting that SmD1 associates with the complexes of the RNAi machinery. Moreover, they showed that KD of SmD1 leads to an increased viral load, indicating that SmD1 affects the vsiRNA pathway. Finally, they showed that KD of SmD1 and another Sm protein, SmE, impacts endo-siRNA production, and that this impact can be dissociated from the effect of impaired

splicing as the KD of a third Sm protein, SmF, which induces the same splicing defects, had no impact on endo-siRNA production. This suggests that select slicing factors, but not the splicing mechanism as a whole, affect the RNAi pathway. This is reinforced by the fact that in the AP-MS experiment performed by my host lab, Fand was found to bind poly(I:C), which is a mimic of dsRNA. The fact that Fand binds poly(I:C) specifically suggests that this protein could possess another role, separated from its splicing activity, as this type of nucleic acid does not resemble the pre-mRNA that is processed during splicing.

If Fandango, and possibly other splicing factors, have a role in antiviral immunity, the question of how they impact viral infection remains unanswered. Splicing factors are usually located in the nucleus, whereas viral replication of the viruses tested in this Chapter occur in the cytoplasm. If Fand interacts with the virus, it would therefore have to travel to the cytoplasm. This is why it would be very interesting to study the localization of Fand upon infection. In the IF experiments that I performed to check the stable cell lines, we can observe the localization of Fand in the cytoplasm of some cells (**Figure 19D**), suggesting that it could sometimes be located there although we have to remember that overexpression of proteins can induce localization artefacts.

Of note, spectras matching both SmD1 and Fand were detected in the Dicer-2 IP-MS experiment from Chapter I but were not significantly enriched. I performed an IP of Fand using anti-HA beads, however I chose not to present the data here, as this experiment still needs to be optimized. Indeed, although I managed to observe co-immunoprecipitation of Dicer-2 after Fand IP once, the results could not be replicated.

The splicing reporter developed in this Chapter, if its ability to assess splicing activity is validated, could be a useful tool to study the interplay between splicing and antiviral immunity. Unfortunately, in preliminary experiments we were not able to detect a change in Fluc activity after addition of Isoginkgetin in S2 cells. However, as we never tested Isoginkgetin in S2 cells, this may be due to either an improper inhibition of splicing, or an inefficient reporter activity. To determine which of those two possibilities is true, we could try to inhibit splicing by other means, for example by performing the KD of a major spliceosome component, or by trying another splicing inhibitor like pladienolide B. The efficiency of splicing

inhibition can also be checked by other means, for example by performing RT-PCR with primers surrounding introns.

C. Conclusion

In conclusion, although the *ex vivo* screen performed as a side project was based on three different projects, we could find a number of parallels between them. By studying Fandango, we have raised some questions about the interplay between the spliceosome and the RNAi machinery, and we have developed a few tools (plasmids, stable cell lines, and splicing reporter) to allow us to study this further.

IV. Materials & methods

A. Cell and virus stocks

Schneider 2 (S2) cells were grown in Schneider medium (Biowest) complemented with 10% heat inactivated fetal bovine serum, 2mM glutamax, 100U/mL penicillin and 100µg/mL streptomycin (Life technologies). The cells were kept at 25°C and passaged twice a week at a 1:5 dilution. The cells were kept for 20 passages maximum before being replaced by a fresh batch. DCV virus stock was produced as described (Kemp et al., 2013).

B. *Ex vivo* RNAi mini-screen and timecourse experiment

dsRNA synthesis

DNA templates for dsRNAs were provided by the Drosophila RNAi Screening Center at the Harvard Medical School. The DNA templates were added to a transcription mix containing 10 µL of 50 mM ATP, GTP, CTP & UTP, RNasin (Promega), homemade T7 polymerase produced at IBMC (Franck Martin UPR9002), and TMSDT buffer (280 mM Tris-HCl pH8.1, 154 mM $MgCl_2$, 7 mM spermidine, 35 mM DTE & 0.01% Triton X-100). After a 1h incubation at 37°C, 2 µL of pyrophosphatase (Roche) was added to the reaction, which was incubated again at 37°C for 30 min. 2 µL of DNase I (NEB) was added and the mix was incubated for 1h at 37°C again. Excess free nucleotides were removed by passing the samples through a home-made column containing G25 beads (Sigma-Aldrich). The dsRNA were then purified using 150 µL of phenol/chloroform (1:1) with 15 µL of Ammonium acetate (5M). The aqueous phase was precipitated in isopropanol 100% (v/v) and washed in EtOH 70%. Finally, the pellet was air dried, resuspended in nuclease-free H_2O, and dsRNAs were annealed by incubation at 65°C for 30 min and slow cooling to RT.

dsRNA soaking

$4.5x10^4$ cells/well were seeded in a 96-well plate with U-shaped bottoms, and resuspended in 40 µL of a solution contain 2 µg of dsRNA diluted in serum-free S2 medium. After a 4h incubation time at 25°C, 160 µL of complemented medium was added to each well. Wells located at the periphery of the plate were filled with 200 µl of PBS to prevent evaporation

over the course of the experiment. Cells were then placed at 25°C again for three days before viral infection.

Synchronized DCV infection of S2 cells

Cell concentration was measured using extra wells identically seeded for this purpose, and cell plates were put on ice for 30 min. The cell medium was replaced by 50 µL cold infective solution, containing the virus diluted in cell medium, to infect cells at the appropriate MOI. The chosen MOI were: MOI 0.001 (DCV), MOI 0.001 (CrPV), MOI 0.1 (VSV), MOI 0.1 (FHV/FHVΔB2). Cells were then incubated on ice for 1h with gentle shaking every 10 min and then washed with cold PBS to remove the infective solution before addition of 200 µL of normal S2 media. Cells were then incubated for 20h at 25°C before collection.

RNA extraction and RT-qPCR

Cell lysis and reverse transcription were performed using the Cell-To-Ct kit (Ambion), following the manufacturer's instructions, with the exception that the RT mix was diluted twice after optimization by a member of our team. The cDNA thus obtained was used to perform quantitative PCR (qPCR) using the iQ™ Custom SYBR Green Supermix Kit (BioRad) following the manufacturer's instructions, on a QuantStudio™ 5 system (ThermoScientific).

Analysis of the data

The analysis of the data was then performed by either calculating relative expression using the housekeeping gene RP49, or calculating the fold change expression compared to a control (after normalization with RP49), using the following formulas:

$$\text{Relative expression: } 2^{\Delta Ct}$$

$$\textbf{Fold change of expression: } 2^{-(\Delta\Delta Ct)}$$

For the RNAi screen, statistical analysis was performed in R. We statistically searched for bias in the data after qPCR, as this was a large-scale experiment involving a large number of samples. To this aim, we implemented a mixed effect linear model taking into account variations in plates, rows and columns using the lmer function in R. The effect of those different variables was assess by ANOVA, and as they proved to have a significant effect they

were used as random factors in the model. The corrected ratios (estimates) were extracted from the mixed effect model and statistical significance was calculated by comparing the estimates of each dsRNA to that of the Scramble dsRNA control using the emmeans function.

MTS assay

Cells were seeded and underwent dsRNA soaking using the same protocol as for the RNAi mini-screen, with the exception that the 96-well plates used had flat bottoms instead of U-shaped bottoms to allow for the correct reading of absorbance. After three days of incubation with the dsRNAs, their toxicity was determined by quantifying the mitochondrial activity of treated cells in comparison with untreated cells using an MTS assay kit (Promega CellTiter 96) following the manufacturer's instructions. Absorbance was read on a Varioskan LUX (ThermoScientific).

C. Impact of Fand and the spliceosome on DCV protein expression

Gateway cloning of expression plasmids for Fand or GST

Target sequence was amplified with attB overhangs using cDNA obtained from CS flies (Fand) or a plasmid containing GST, and subcloned into a pJet vector using the CloneJET PCR cloning kit (ThermoScientific) and following the manufacturer's instructions. For the BP reaction, 75 ng of pDONR221 donor vector, 25 fmol of PCR product and 1 µL of 5x BP clonase were incubated at RT O.N. After treatment with 10 µg proteinase K (Invitrogen) for 10 min at 37°C, the BP reaction was used to transform chemically competent *E. coli* DH5α cells on Kanamycin (50 µg/mL) plates. Clones were selected by sequencing using M13 primers and 25 ng of the selected plasmids were used along with 50 ng of destination vector (pAHW or pAWH) and 1 µL 5x LR clonase to perform the LR reaction. After another proteinase K treatment, DH5α were transformed with the LR reaction and grown on Ampicilin plates (100 µg/mL). Resulting expression vectors were sequenced using Actin5C and SV40 primers, and their expression in S2 cells was assessed by transfection and immunoblot.

Transient transfection of S2 cells & lysis

$5x10^5$ S2 cells/well were seeded in a 24-well plate, in 300 µL of normal S2 media. Using the Effecten Reagent transfection kit (Qiagen), cells were then transfected with 200 ng of plasmid

containing the gene of interest, following the manufacturer's instructions and incubated at 25°C. After 3 days, cells were then infected with DCV as described above, collected and washed with PBS before being lysed in NP40 lysis buffer (HEPES 30 mM, NaCl 150 mM, MgAc 2 mM, NP40 1%, protease inhibitor cocktail 2X) for 30 min at 4°C, using 100 µL lysis buffer per million cells.

Protein analysis by western blot

After dsRNA soaking or transient transfection, and infection using DCV at a MOI of 0.1 for 20h, protein extracts were separated on a Biorad gel and transferred to a nitrocellulose membrane. Membranes were then blocked in TBST containing 5% milk powder for 1h at RT and incubated overnight at 4°C with the different primary antibodies listed below. After washing, the corresponding secondary antibodies fused to horseradish peroxidase (HRP) were added to the membrane for 1h 2h at RT. Membranes were then washed and visualized with enhanced chemiluminescence reagent (GE Healthcare) in a ChemiDoc (Bio-Rad) apparatus. The intensity of the bands was then quantified using the ImageJ software. For each condition, the VP2/actin and RdRp/actin ratios were calculated. Then, this ratio was normalized using that of the dsLacZ control condition for each gel.

Antibodies used for western blot.

Target	Reference	Animal	Dilution
DCV VP2	3593 (IGBMC)	Rabbit	1:1,000
DCV RdRp	homemade	Guinea pig	1:2,000
Actin	MAB1501R (Millipore)	Mouse	1:2,000
HA-HRP	H9658 (Sigma-Aldrich)	Mouse	1:2,000
Mouse IgG	M365FK (Rockland)	Goat	1:10,000
Rabbit IgG	NA934 (Amersham)	Goat	1:10,000

Generation of stable cell lines

Each stable cell line was generated using two plasmids: one containing the gene of interest and another containing a selection plasmid conferring resistance to the antibiotic Puromycin. On Day 1, $1.5x10^6$ S2 cells/well were seeded in normal S2 media in a 6-well plate and both plasmids were transfected using Effecten (Qiagen) following the manufacturer's instructions, at a 1:10 ratio (50 ng selection plasmid, 500 ng plasmid of interest). High gene of interest plasmid to selection plasmid ratio helps to ensure that cells transfected with the selection

marker are also transfected with the gene of interest. After 48h, three dilutions of each transfected cell line were prepared in selection media containing Puromycin (5µg/mL): 10^5 cells/mL, 2×10^5 cells/mL and 3×10^5 cells/mL, and were seeded in one full 96-well plate each (100 µL/well). At Day 5, fresh selection media was added, and cells were then passed once a week by removing media and adding 100 µL of fresh selection media. Wells were single clones appeared were marked and once they reached confluence they were transferred to 14-well plates, then F25 Flasks (5 mL/flask). For each stable cell line, three clones expressing the plasmid at a good level were selected and amplified for further experiments. A back-up for each clonal line was made right away by freezing the cells.

Immunostaining and confocal microscopy

For transient transfection experiments, S2 cells were first transfected using the transient transfection protocol described above, and then distributed on microscope slides with chambered coverslips. Stable cells were directly distributed on the slides. The microscope slides were first pre-coated with Concanavalin A (100 µg/mL, diluted in PBS) to ensure that the cells adhere to the slides, as S2 cells are only semi-adherent, before being air dried under the cell culture hood. Then, $3x10^5$ S2 cells/chamber were distributed on the glass slides, left 10 min to attach and fixed with 1:1 volume PFA for 15 min at RT. PFA was then replaced by blocking solution containing 1% BSA in PBT (0.1% Triton in PBS) and incubated for an hour at RT on a shaker. The slides were then incubated with primary antibody O.N. at 4°C in a humid container, washed 3 x 5 min with PBT the next day, and incubated with secondary antibody for an hour at RT in a dark container. Antibodies are listed below. After 2 x 5 min washes with PBT, washing solution and slide chambers were removed, and slides were mounted using VectaShield + DAPI and sealed with nail polish.

Antibodies used for immunofluorescence.

Target	Reference	Animal	Dilution IF	Fluorescence
HA	H9658 (Sigma)	Mouse	1:200	-
HA	ab9110 (Abcam)	Rabbit	1:200	-
GFP	A11122 (Invitrogen)	Rabbit	1:200	-
Lamin	ADL67.10-5 (DSHB)	Mouse	1:100	-
Rabbit IgG	A11008 (Invitrogen)	Goat	1:500	Alexa Fluor 488 (Green)
Mouse IgG	A10036 (Invitrogen)	Donkey	1:500	Alexa Fluor 546 (Red)
Mouse IgG	A21203 (Invitrogen)	Donkey	1:500	Alexa Fluor 594 (Red)

D. Splicing reporter experiments

Splicing reporter construct

The 5' fragment of Tub84b was amplified by PCR from genomic fly DNA, with the HindIII (forward primer) and NcoI (reverse primer) restriction sites. The PCR product and destination plasmid, pGL3-Basic (Promega), were digested with HindIII/NcoI and the digestion products were purified using the QIAquick PCR purification kit (QIAGEN), following the manufacturer's instructions. Digestion products were then used for ligation using the ligase (QIAGEN) and the resulting pGL3-Tub84b plasmid was used for transformation in DH5α cells, sequenced and purified using the Plasmid Midi Kit (QIAGEN). As pGL3 does not contain a promoter, the actin promoter from the pPac-pI plasmid was amplified with KpnI (forward primer) and XhoI (reverse primers) restriction sites. After KpnI/XhoI digestion of the PCR product and pGL3-Tub84b plasmid, ligation was performed again to obtain the final splicing reporter plasmid. The plasmid was used to transform DH5α cells, sequenced and purified using by MIDIprep again. The expression of the plasmid was then tested by DLR to measure luciferase activity.

Isoginkgetin treatment

Isoginkgetin (Sigma-Aldrich) was resuspended in DMSO. $5x10^5$ S2 cells were seeded in 24-well plates in isoginkgetin-containing S2 normal media at concentrations of 10 µM, 33 µM, 100 µM and 200 µM or DMSO only. The plate was incubated for 4h at 25°C before MTS assay.

Dual luciferase assay

S2 cells were transfected in 24-well plates using Effecten (Qiagen) with 75 ng of a Fluc-containing plasmid (splicing reporter or positive control) or the negative control plasmid pUC19, and 25 ng of the Rluc plasmid, according to the manufacturer's instructions. Cells were incubated for two days at 25°C then collected and washed with PBS. Lysis and dual luciferase reporter assay (DLR) were then performed using the Dual-Luciferase® Reporter Assay System (Promega) following the manufacturer's instructions. Plates were then read using a Varioskan (Thermofisher Scientific).

List of primers used (5’ – 3’ orientation)

Primers for qPCR

Fand pair#1	CCACATGTGCGTTAAGTTTG	Forward
	GGATCACAAACCTGTGAGC	Reverse
Fand pair#2	GAGATCAATTTCGAAGTGGAGG	Forward
	CCTTCGCTTTGTGATCAATG	Reverse
RP49	GCCGCTTCAAGGGACAGTATCT	Forward
	AAACGCGGTTCTGCATGAG	Reverse
DCV	TCATCGGTATGCACATTGCT	Forward
	CGCATAACCATGCTCTTCTG	Reverse

Primers for cloning

HA-Fand	GGGGACAAGTTTGTACAAAAAAGCAGGCTTCGTGACAAAAACGATAAAATCTC	Forward
HA-Fand	GGGGACCACTTTGTACAAGAAAGCTGGGTATTACTCTCCATCAGAGTCGC	Reverse
Fand-HA	GGGGACAAGTTTGTACAAAAAAGCAGGCTTCATGGTGACAAAAACGATAAAA	Forward
Fand-HA	GGGGACCACTTTGTACAAGAAAGCTGGGTACTCTCCATCAGAGTCGCC	Reverse
HA-GST	GGGGACAAGTTTGTACAAAAAAGCAGGCTTCTCCCCTATACTAGGTTATTGG	Forward
HA-GST	GGGGACCACTTTGTACAAGAAAGCTGGGTGCTACCGATTTTGGAGGATGGTC	Reverse
Tub84b-HindIII	GGGGAAGCTTTCATATTCGTTTTACGTTTG	Forward
Tub84b-NcoI	CCCCCCATGGGCGTTTCCAATCTGGACAC	Reverse
Actin-KpnI	gggggtaccCATGAATGGCATCAACTCTG	Forward
Actin-XhoI	ccccctcgagGTCTCTGGATTAGACGACTG	Reverse

Primers for dsRNA production

LacZ	taatacgactcactatagggCTGGCGTAATAGCGAAGAGG	Forward	-
	taatacgactcactatagggCATTAAAGCGAGTGGCAACA	Reverse	-
fand_1	taatacgactcactatagggAGTGGCCCAATGTCTACGAC	Forward	DRSC31706
	taatacgactcactatagggGTACGTGGCAGGCCATAGAT	Reverse	DRSC31706
fand_2	taatacgactcactatagggACTACGGTGCCTTCATGACC	Forward	DRSC27505
	taatacgactcactatagggCGGTGGTCACAGTTTGAATG	Reverse	DRSC27505
Fand_3	taatacgactcactatagggGCAGGATTTGGCCACTGTAT	Forward	DRSC39027
	taatacgactcactatagggCGGTGGTCACAGTTTGAATG	Reverse	DRSC39027
Prp19_1	taatacgactcactatagggAGCCAGATAGGTTCCGCTTT	Forward	BKN21386
	taatacgactcactatagggACAAACACTGGGCATTCTCC	Reverse	BKN21386
Prp19_2	taatacgactcactatagggAGCCAGATAGGTTCCGCTTT	Forward	DRSC34547
	taatacgactcactatagggTAATCGATACCGCCGAAGTC	Reverse	DRSC34547
Prp8_1	taatacgactcactatagggCATCGTGCTTCATTAAACGC	Forward	DRSC07293

	taatacgactcactatagggTTTGAAAAGCTGTACGAGAAAA	Reverse	DRSC07293
Prp8_2	taatacgactcactatagggCCCACACAGAGGTGTGAATG	Forward	DRSC38440
	taatacgactcactatagggGGCCAAGTTCCTCGATTACA	Reverse	DRSC38440
CG9667_1	taatacgactcactatagggTCTTCGTCATCGATTATGCG	Forward	BKN29247
	taatacgactcactatagggGACGCTATGGTCCCAAGATG	Reverse	BKN29247
CG9667_2	taatacgactcactatagggCGGAGGATCCTGTTCAAAGA	Forward	DRSC30993
	taatacgactcactatagggGTTATTGCGTGAGAAACGGC	Reverse	DRSC30993

DNA templates ordered from DRSC Harvard

Gene	Amplicon	Size		Gene	Amplicon	Size
LacZ	Control			fand	DRSC27505	522
Thread	Control			alt	DRSC28347	342
FASN2	DRSC00610	511		Hel25E	DRSC28348	448
homer	DRSC03547	428		Tao	DRSC28431	348
Scsalpha1	DRSC08698	433		ZC3H3	DRSC28763	388
Pop2	DRSC10537	502		homer	DRSC29162	348
AGO2	DRSC10847	514		Larp4B	DRSC29411	300
Snm1	DRSC12130	513		Xrcc2	DRSC29513	400
CG5641	DRSC15852	515		r2d2	DRSC29562	319
Syp	DRSC15286	304		Hsc70-4	DRSC29729	311
Dis3	DRSC16034	517		ZC3H3	DRSC39048	426
CG7920	DRSC16346	566		Tao	DRSC19573	351
norpA	DRSC18806	163		CG13690	DRSC42658	341
CG13690	DRSC00359	493		CG5641	DRSC37486	343
pcm	DRSC20361	493		Hel25E	DRSC30680	367
Clp	DRSC00746	513		fand	DRSC31706	303
r2d2	DRSC03014	503		Hsc70-4	DRSC32137	238
CG9272	DRSC03183	412		Pop2	DRSC32413	221
Pabp2	DRSC07501	385		RpS3	DRSC32591	232
Rad51D	DRSC06840	438		Rrp6	DRSC32600	228
Larp4B	DRSC08192	511		Rrp6	DRSC32601	258
CG14057	DRSC10074	216		alt	DRSC32685	207
CG9684	DRSC16537	500		Larp4B	DRSC32812	151
Ns1	DRSC15529	512		lost	DRSC34034	266
RpS3	DRSC16838	508		Pabp2	DRSC34289	190
Xrcc2	DRSC19984	517		bt	DRSC34355	223
Rpp20	DRSC19467	536		Nnp-1	DRSC34576	551
bt	DRSC36657	534		Nnp-1	DRSC34577	234
CG7920	DRSC21594	576		Syp	DRSC34987	267
lost	DRSC21987	510		Clp	DRSC37267	300
CG5214	DRSC25298	363		Ns1	DRSC37285	512
Rack1	DRSC23796	512		pcm	DRSC37724	498
Scsalpha1	DRSC26856	313		Dis3	DRSC42494	350

Concluding remarks

This thesis manuscript summarizes the results obtained for two different projects, which were: (1) the study of modulation of the Dicer-2 interaction network upon infection and (2) the study of the role of Fandango and the spliceosome in antiviral immunity.

The study of the Dicer-2 interactome has highlighted the proteins Me31b, eIF4E1, Rump and Syp as interacting with Dicer-2, and this interaction could new be characterized further, for example by identifying which protein domains are required. Moreover, the candidate Rin has displayed a strong antiviral phenotype, and it would be interesting to test its interaction with Dicer-2. The impact of all the proteins highlighted in this project on endo-siRNA production or on the other non-RNAi-related functions of Dicer-2 could also be explored.

The *ex vivo* screen from Chapter II has highlighted several candidates from three different projects, that could be nucleases helping Dicer-2 sense viral dsRNA by freeing the termini of the viral dsRNA, nucleic acid sensors or Dicer-2 interactants. In particular, we decided to focus on the protein Fandango, which showed a strong antiviral phenotype against all viruses hitherto tested. The involvement of this protein in the splicing process made us wonder about the interconnection between the spliceosome and antiviral immunity. We have therefore designed some tools to study the impact of the spliceosome on antiviral immunity in S2 cells, and this is still ongoing.

Both projects were designed to further our understanding of antiviral immunity, and in particular the sensing of the virus by host cell proteins. Overall, this thesis illustrates the usefulness of *D. melanogaster* as an animal model to handle large amounts of samples, which led to the identification of several interesting candidates that may have a role in antiviral immunity. The study of the different candidates individually could now lead to the creation of several new projects, focused on unraveling the molecular mechanisms involved in the effect observed for the different candidates on viruses, and DCV in particular.

Bibliography

Adams, M.D., Celniker, S.E., Holt, R.A., Evans, C.A., Gocayne, J.D., Amanatides, P.G., Scherer, S.E., Li, P.W., Hoskins, R.A., Galle, R.F., et al. (2000). The genome sequence of Drosophila melanogaster. Science *287*, 2185–2195. https://doi.org/10.1126/science.287.5461.2185.

Aguado, L.C., and tenOever, B.R. (2018). RNase III Nucleases and the Evolution of Antiviral Systems. BioEssays *40*, 1700173. https://doi.org/10.1002/bies.201700173.

Aguiar, E.R.G.R., Olmo, R.P., and Marques, J.T. (2016). Virus-derived small RNAs: molecular footprints of host-pathogen interactions. Wiley Interdiscip Rev RNA *7*, 824–837. https://doi.org/10.1002/wrna.1361.

Ashe, A., Bélicard, T., Le Pen, J., Sarkies, P., Frézal, L., Lehrbach, N.J., Félix, M.-A., and Miska, E.A. (2013). A deletion polymorphism in the Caenorhabditis elegans RIG-I homolog disables viral RNA dicing and antiviral immunity. Elife *2*, e00994. https://doi.org/10.7554/eLife.00994.

Banerjee, A.D., Abraham, G., and Colonno, R.J. (1977). Vesicular stomatitis virus: mode of transcription. J Gen Virol *34*, 1–8. https://doi.org/10.1099/0022-1317-34-1-1.

Beckingham, K.M., Armstrong, J.D., Texada, M.J., Munjaal, R., and Baker, D.A. (2005). Drosophila melanogaster--the model organism of choice for the complex biology of multi-cellular organisms. Gravit Space Biol Bull *18*, 17–29. .

Bellare, P., and Ganem, D. (2009). Regulation of KSHV lytic switch protein expression by a virus-encoded microRNA: an evolutionary adaptation that fine-tunes lytic reactivation. Cell Host Microbe *6*, 570–575. https://doi.org/10.1016/j.chom.2009.11.008.

Bernstein, E., Caudy, A.A., Hammond, S.M., and Hannon, G.J. (2001). Role for a bidentate ribonuclease in the initiation step of RNA interference. Nature *409*, 363–366. https://doi.org/10.1038/35053110.

Blaszczyk, J., Tropea, J.E., Bubunenko, M., Routzahn, K.M., Waugh, D.S., Court, D.L., and Ji, X. (2001). Crystallographic and Modeling Studies of RNase III Suggest a Mechanism for Double-Stranded RNA Cleavage. Structure *9*, 1225–1236. https://doi.org/10.1016/S0969-2126(01)00685-2.

Bonning, B.C., and Miller, W.A. (2010). Dicistroviruses. Annual Review of Entomology *55*, 129–150. https://doi.org/10.1146/annurev-ento-112408-085457.

Brand, A.H., and Perrimon, N. (1993). Targeted gene expression as a means of altering cell fates and generating dominant phenotypes. Development *118*, 401–415. .

Brennecke, J., Aravin, A.A., Stark, A., Dus, M., Kellis, M., Sachidanandam, R., and Hannon, G.J. (2007). Discrete small RNA-generating loci as master regulators of transposon activity in Drosophila. Cell *128*, 1089–1103. https://doi.org/10.1016/j.cell.2007.01.043.

Bronkhorst, A.W., van Cleef, K.W.R., Vodovar, N., Ince, I.A., Blanc, H., Vlak, J.M., Saleh, M.-C., and van Rij, R.P. (2012). The DNA virus Invertebrate iridescent virus 6 is a target of the Drosophila RNAi machinery. Proc. Natl. Acad. Sci. U.S.A. *109*, E3604-3613. https://doi.org/10.1073/pnas.1207213109.

Buchon, N., Silverman, N., and Cherry, S. (2014). Immunity in Drosophila melanogaster--from microbial recognition to whole-organism physiology. Nature Reviews. Immunology *14*, 796–810. https://doi.org/10.1038/nri3763.

Carmena, A. (2009). Approaching Drosophila development through proteomic tools and databases: At the hub of the post-genomic era. Mech Dev *126*, 761–770. https://doi.org/10.1016/j.mod.2009.08.001.

Carter, M., and Shieh, J.C. (2010). Chapter 13 - Cell Culture Techniques. In Guide to Research Techniques in Neuroscience, M. Carter, and J.C. Shieh, eds. (New York: Academic Press), pp. 281–296.

Cenik, E.S., Fukunaga, R., Lu, G., Dutcher, R., Wang, Y., Tanaka Hall, T.M., and Zamore, P.D. (2011). Phosphate and R2D2 Restrict the Substrate Specificity of Dicer-2, an ATP-Driven Ribonuclease. Molecular Cell *42*, 172–184. https://doi.org/10.1016/J.MOLCEL.2011.03.002.

Chanarat, S., and Sträßer, K. (2013). Splicing and beyond: The many faces of the Prp19 complex. Biochimica et Biophysica Acta (BBA) - Molecular Cell Research *1833*, 2126–2134. https://doi.org/10.1016/j.bbamcr.2013.05.023.

Chen, X., Li, Z., Wang, S., Tong, G., Chen, K., and Zhao, Y. (2022). Proteomic analysis reveals zinc-finger CCHC-type containing protein 3 as a factor inhibiting virus infection by promoting innate signaling. Virus Research *319*, 198876. https://doi.org/10.1016/j.virusres.2022.198876.

Cherry, S., and Perrimon, N. (2004). Entry is a rate-limiting step for viral infection in a Drosophila melanogaster model of pathogenesis. Nature Immunology *5*, 81–87. https://doi.org/10.1038/ni1019.

Cherry, S., Doukas, T., Armknecht, S., Whelan, S., Wang, H., Sarnow, P., and Perrimon, N. (2005). Genome-wide RNAi screen reveals a specific sensitivity of IRES-containing RNA viruses to host translation inhibition. Genes Dev *19*, 445–452. https://doi.org/10.1101/gad.1267905.

Cherry, S., Kunte, A., Wang, H., Coyne, C., Rawson, R.B., and Perrimon, N. (2006). COPI activity coupled with fatty acid biosynthesis is required for viral replication. PLoS Pathog. *2*, e102. https://doi.org/10.1371/journal.ppat.0020102.

Choi, H., Larsen, B., Lin, Z.-Y., Breitkreutz, A., Mellacheruvu, D., Fermin, D., Qin, Z.S., Tyers, M., Gingras, A.-C., and Nesvizhskii, A.I. (2011). SAINT: probabilistic scoring of affinity purification–mass spectrometry data. Nat Methods *8*, 70–73. https://doi.org/10.1038/nmeth.1541.

Chotkowski, H.L., Ciota, A.T., Jia, Y., Puig-Basagoiti, F., Kramer, L.D., Shi, P.-Y., and Glaser, R.L. (2008). West Nile virus infection of Drosophila melanogaster induces a protective RNAi response. Virology *377*, 197–206. https://doi.org/10.1016/j.virol.2008.04.021.

Chtarbanova, S., Lamiable, O., Lee, K.-Z., Galiana, D., Troxler, L., Meignin, C., Hetru, C., Hoffmann, J.A., Daeffler, L., and Imler, J.-L. (2014). Drosophila C virus systemic infection leads to intestinal obstruction. J. Virol. *88*, 14057–14069. https://doi.org/10.1128/JVI.02320-14.

Ciechanowska, K., Pokornowska, M., and Kurzyńska-Kokorniak, A. (2021). Genetic Insight into the Domain Structure and Functions of Dicer-Type Ribonucleases. Int J Mol Sci *22*, E616. https://doi.org/10.3390/ijms22020616.

Clem, R.J. (2015). Viral IAPs, then and now. Seminars in Cell & Developmental Biology *39*, 72–79. https://doi.org/10.1016/j.semcdb.2015.01.011.

Coll, O., Guitart, T., Villalba, A., Papin, C., Simonelig, M., and Gebauer, F. (2018). Dicer-2 promotes mRNA activation through cytoplasmic polyadenylation. RNA *24*, 529–539. https://doi.org/10.1261/rna.065417.117.

Colmenares, S.U., Buker, S.M., Buhler, M., Dlakić, M., and Moazed, D. (2007). Coupling of Double-Stranded RNA Synthesis and siRNA Generation in Fission Yeast RNAi. Molecular Cell *27*, 449–461. https://doi.org/10.1016/j.molcel.2007.07.007.

Conzelmann, K.K. (1998). Nonsegmented negative-strand RNA viruses: genetics and manipulation of viral genomes. Annu Rev Genet *32*, 123–162. https://doi.org/10.1146/annurev.genet.32.1.123.

Costa, A., Jan, E., Sarnow, P., and Schneider, D. (2009). The Imd pathway is involved in antiviral immune responses in Drosophila. PLoS ONE *4*, e7436. https://doi.org/10.1371/journal.pone.0007436.

Crick, F.H. (1958). On protein synthesis. Symp Soc Exp Biol *12*, 138–163. .

Crook, N.E., Clem, R.J., and Miller, L.K. (1993). An apoptosis-inhibiting baculovirus gene with a zinc finger-like motif. Journal of Virology *67*, 2168–2174. https://doi.org/10.1128/jvi.67.4.2168-2174.1993.

Czech, B., Zhou, R., Erlich, Y., Brennecke, J., Binari, R., Villalta, C., Gordon, A., Perrimon, N., and Hannon, G.J. (2009). Hierarchical rules for Argonaute loading in Drosophila. Mol. Cell *36*, 445–456. https://doi.org/10.1016/j.molcel.2009.09.028.

Czech, B., Munafò, M., Ciabrelli, F., Eastwood, E.L., Fabry, M.H., Kneuss, E., and Hannon, G.J. (2018). piRNA-Guided Genome Defense: From Biogenesis to Silencing. Annu. Rev. Genet. *52*, 131–157. https://doi.org/10.1146/annurev-genet-120417-031441.

Deddouche, S., Matt, N., Budd, A., Mueller, S., Kemp, C., Galiana-Arnoux, D., Dostert, C., Antoniewski, C., Hoffmann, J.A., and Imler, J.-L. (2008). The DExD/H-box helicase Dicer-2

mediates the induction of antiviral activity in drosophila. Nat. Immunol. *9*, 1425–1432. https://doi.org/10.1038/ni.1664.

Denli, A.M., Tops, B.B.J., Plasterk, R.H.A., Ketting, R.F., and Hannon, G.J. (2004). Processing of primary microRNAs by the Microprocessor complex. Nature *432*, 231–235. https://doi.org/10.1038/nature03049.

Desset, S., Meignin, C., Dastugue, B., and Vaury, C. (2003). COM, a heterochromatic locus governing the control of independent endogenous retroviruses from Drosophila melanogaster. Genetics *164*, 501–509. .

DeVeale, B., Swindlehurst-Chan, J., and Blelloch, R. (2021). The roles of microRNAs in mouse development. Nat Rev Genet *22*, 307–323. https://doi.org/10.1038/s41576-020-00309-5.

Dietrich, I., Jansen, S., Fall, G., Lorenzen, S., Rudolf, M., Huber, K., Heitmann, A., Schicht, S., Ndiaye, E.H., Watson, M., et al. (2017). RNA Interference Restricts Rift Valley Fever Virus in Multiple Insect Systems. MSphere *2*, e00090-17. https://doi.org/10.1128/mSphere.00090-17.

Dietzl, G., Chen, D., Schnorrer, F., Su, K.-C., Barinova, Y., Fellner, M., Gasser, B., Kinsey, K., Oppel, S., Scheiblauer, S., et al. (2007). A genome-wide transgenic RNAi library for conditional gene inactivation in Drosophila. Nature *448*, 151–156. https://doi.org/10.1038/nature05954.

Dogini, D.B., Pascoal, V.D.B., Avansini, S.H., Vieira, A.S., Pereira, T.C., and Lopes-Cendes, I. (2014). The new world of RNAs. Genet Mol Biol *37*, 285–293. .

Donelick, H.M., Talide, L., Bellet, M., Aruscavage, P.J., Lauret, E., Aguiar, E.R.G.R., Marques, J.T., Meignin, C., and Bass, B.L. (2020). In vitro studies provide insight into effects of Dicer-2 helicase mutations in Drosophila melanogaster. RNA *26*, 1847–1861. https://doi.org/10.1261/rna.077289.120.

Dostert, C., Jouanguy, E., Irving, P., Troxler, L., Galiana-Arnoux, D., Hetru, C., Hoffmann, J.A., and Imler, J.-L. (2005). The Jak-STAT signaling pathway is required but not sufficient for the antiviral response of drosophila. Nat. Immunol. *6*, 946–953. https://doi.org/10.1038/ni1237.

Elbashir, S.M., Harborth, J., Lendeckel, W., Yalcin, A., Weber, K., and Tuschl, T. (2001). Duplexes of 21-nucleotide RNAs mediate RNA interference in cultured mammalian cells. Nature *411*, 494–498. https://doi.org/10.1038/35078107.

Erttmann, S.F., Swacha, P., Aung, K.M., Brindefalk, B., Jiang, H., Härtlova, A., Uhlin, B.E., Wai, S.N., and Gekara, N.O. (2022). The gut microbiota prime systemic antiviral immunity via the cGAS-STING-IFN-I axis. Immunity *55*, 847-861.e10. https://doi.org/10.1016/j.immuni.2022.04.006.

Ewart, G.D., and Howells, A.J. (1998). [15] ABC transporters involved in transport of eye pigment precursors in Drosophila melanogaster. In Methods in Enzymology, (Elsevier), pp. 213–224.

Fabrizio, P., Dannenberg, J., Dube, P., Kastner, B., Stark, H., Urlaub, H., and Lührmann, R. (2009). The evolutionarily conserved core design of the catalytic activation step of the yeast spliceosome. Mol Cell *36*, 593–608. https://doi.org/10.1016/j.molcel.2009.09.040.

de Faria, I.J.S., Aguiar, E.R.G.R., Olmo, R.P., Alves da Silva, J., Daeffler, L., Carthew, R.W., Imler, J.-L., and Marques, J.T. (2022). Invading viral DNA triggers dsRNA synthesis by RNA polymerase II to activate antiviral RNA interference in Drosophila. Cell Rep *39*, 110976. https://doi.org/10.1016/j.celrep.2022.110976.

Ferrandon, D., Imler, J.-L., Hetru, C., and Hoffmann, J.A. (2007). The Drosophila systemic immune response: sensing and signalling during bacterial and fungal infections. Nat. Rev. Immunol. *7*, 862–874. https://doi.org/10.1038/nri2194.

Ferreira, Á.G., Naylor, H., Esteves, S.S., Pais, I.S., Martins, N.E., and Teixeira, L. (2014). The Toll-dorsal pathway is required for resistance to viral oral infection in Drosophila. PLoS Pathog. *10*, e1004507. https://doi.org/10.1371/journal.ppat.1004507.

Ferreira, F.V., Aguiar, E.R.G.R., Olmo, R.P., de Oliveira, K.P.V., Silva, E.G., Sant'Anna, M.R.V., Gontijo, N. de F., Kroon, E.G., Imler, J.L., and Marques, J.T. (2018). The small non-coding RNA response to virus infection in the Leishmania vector Lutzomyia longipalpis. PLoS Negl Trop Dis *12*, e0006569. https://doi.org/10.1371/journal.pntd.0006569.

Filone, C.M., Hanna, S.L., Caino, M.C., Bambina, S., Doms, R.W., and Cherry, S. (2010). Rift valley fever virus infection of human cells and insect hosts is promoted by protein kinase C epsilon. PLoS One *5*, e15483. https://doi.org/10.1371/journal.pone.0015483.

Fire, A., Xu, S., Montgomery, M.K., Kostas, S.A., Driver, S.E., and Mello, C.C. (1998). Potent and specific genetic interference by double-stranded RNA in Caenorhabditis elegans. Nature *391*, 806–811. https://doi.org/10.1038/35888.

Förstemann, K., Tomari, Y., Du, T., Vagin, V.V., Denli, A.M., Bratu, D.P., Klattenhoff, C., Theurkauf, W.E., and Zamore, P.D. (2005). Normal microRNA maturation and germ-line stem cell maintenance requires Loquacious, a double-stranded RNA-binding domain protein. PLoS Biol. *3*, e236. https://doi.org/10.1371/journal.pbio.0030236.

Fukunaga, R., Han, B.W., Hung, J.-H., Xu, J., Weng, Z., and Zamore, P.D. (2012). Dicer Partner Proteins Tune the Length of Mature miRNAs in Flies and Mammals. Cell *151*, 533–546. https://doi.org/10.1016/j.cell.2012.09.027.

Galiana-Arnoux, D., Dostert, C., Schneemann, A., Hoffmann, J.A., and Imler, J.-L. (2006). Essential function in vivo for Dicer-2 in host defense against RNA viruses in drosophila. Nat. Immunol. *7*, 590–597. https://doi.org/10.1038/ni1335.

Ganetzky, B., and Hawley, R.S. (2016). The Centenary of GENETICS: Bridges to the Future. Genetics *202*, 15–23. https://doi.org/10.1534/genetics.115.180182.

Garcia-Moreno, M., Noerenberg, M., Ni, S., Järvelin, A.I., González-Almela, E., Lenz, C.E., Bach-Pages, M., Cox, V., Avolio, R., Davis, T., et al. (2019). System-wide Profiling of RNA-Binding

Proteins Uncovers Key Regulators of Virus Infection. Molecular Cell *74*, 196-211.e11. https://doi.org/10.1016/j.molcel.2019.01.017.

Gebert, L.F.R., and MacRae, I.J. (2019). Regulation of microRNA function in animals. Nat Rev Mol Cell Biol *20*, 21–37. https://doi.org/10.1038/s41580-018-0045-7.

Ghildiyal, M., Xu, J., Seitz, H., Weng, Z., and Zamore, P.D. (2010). Sorting of Drosophila small silencing RNAs partitions microRNA* strands into the RNA interference pathway. RNA *16*, 43–56. https://doi.org/10.1261/rna.1972910.

Girardi, E., Lefèvre, M., Chane-Woon-Ming, B., Paro, S., Claydon, B., Imler, J.-L., Meignin, C., and Pfeffer, S. (2015). Cross-species comparative analysis of Dicer proteins during Sindbis virus infection. Sci Rep *5*, 10693. https://doi.org/10.1038/srep10693.

Gomariz-Zilber, E., Poras, M., and Thomas-Orillard, M. (1995). Drosophila C virus: experimental study of infectious yields and underlying pathology in Drosophila melanogaster laboratory populations. J Invertebr Pathol *65*, 243–247. https://doi.org/10.1006/jipa.1995.1037.

Goto, A., Okado, K., Martins, N., Cai, H., Barbier, V., Lamiable, O., Troxler, L., Santiago, E., Kuhn, L., Paik, D., et al. (2018). The Kinase IKKβ Regulates a STING- and NF-κB-Dependent Antiviral Response Pathway in Drosophila. Immunity *49*, 225-234.e4. https://doi.org/10.1016/j.immuni.2018.07.013.

Gregori, J., Sanchez, A., and Villanueva, J. (2013). msmsTests package LC-MS/MS post test filters to improve reproducibility.

Gregory, R.I., Yan, K., Amuthan, G., Chendrimada, T., Doratotaj, B., Cooch, N., and Shiekhattar, R. (2004). The Microprocessor complex mediates the genesis of microRNAs. Nature *432*, 235–240. https://doi.org/10.1038/nature03120.

Gunawardane, L.S., Saito, K., Nishida, K.M., Miyoshi, K., Kawamura, Y., Nagami, T., Siomi, H., and Siomi, M.C. (2007). A slicer-mediated mechanism for repeat-associated siRNA 5′ end formation in Drosophila. Science *315*, 1587–1590. https://doi.org/10.1126/science.1140494.

Gupta, V., Stewart, C.O., Rund, S.S.C., Monteith, K., and Vale, P.F. (2017). Costs and benefits of sublethal Drosophila C virus infection. J Evol Biol *30*, 1325–1335. https://doi.org/10.1111/jeb.13096.

Hamilton, A.J., and Baulcombe, D.C. (1999). A species of small antisense RNA in posttranscriptional gene silencing in plants. Science *286*, 950–952. .

Hammond, S.M., Bernstein, E., Beach, D., and Hannon, G.J. (2000). An RNA-directed nuclease mediates post-transcriptional gene silencing in Drosophila cells. Nature *404*, 293–296. https://doi.org/10.1038/35005107.

Hammond, S.M., Boettcher, S., Caudy, A.A., Kobayashi, R., and Hannon, G.J. (2001). Argonaute2, a Link Between Genetic and Biochemical Analyses of RNAi. Science *293*, 1146–1150. https://doi.org/10.1126/science.1064023.

Han, Y.-H., Luo, Y.-J., Wu, Q., Jovel, J., Wang, X.-H., Aliyari, R., Han, C., Li, W.-X., and Ding, S.-W. (2011). RNA-Based Immunity Terminates Viral Infection in Adult Drosophila in the Absence of Viral Suppression of RNA Interference: Characterization of Viral Small Interfering RNA Populations in Wild-Type and Mutant Flies. Journal of Virology *85*, 13153–13163. https://doi.org/10.1128/JVI.05518-11.

Harrington, A.W., McKain, M.R., Michalski, D., Bauer, K.M., Daugherty, J.M., and Steiniger, M. (2017). Drosophila melanogaster retrotransposon and inverted repeat-derived endogenous siRNAs are differentially processed in distinct cellular locations. BMC Genomics *18*, 304. https://doi.org/10.1186/s12864-017-3692-8.

Hartig, J.V., and Förstemann, K. (2011). Loqs-PD and R2D2 define independent pathways for RISC generation in Drosophila. Nucleic Acids Research *39*, 3836–3851. https://doi.org/10.1093/nar/gkq1324.

Herold, N., Will, C.L., Wolf, E., Kastner, B., Urlaub, H., and Lührmann, R. (2009). Conservation of the protein composition and electron microscopy structure of Drosophila melanogaster and human spliceosomal complexes. Mol Cell Biol *29*, 281–301. https://doi.org/10.1128/MCB.01415-08.

Hertz, M.I., and Thompson, S.R. (2011). Mechanism of translation initiation by Dicistroviridae IGR IRESs. Virology *411*, 355–361. https://doi.org/10.1016/j.virol.2011.01.005.

Horwich, M.D., Li, C., Matranga, C., Vagin, V., Farley, G., Wang, P., and Zamore, P.D. (2007). The Drosophila RNA methyltransferase, DmHen1, modifies germline piRNAs and single-stranded siRNAs in RISC. Curr. Biol. *17*, 1265–1272. https://doi.org/10.1016/j.cub.2007.06.030.

Huntzinger, E., and Izaurralde, E. (2011). Gene silencing by microRNAs: contributions of translational repression and mRNA decay. Nat Rev Genet *12*, 99–110. https://doi.org/10.1038/nrg2936.

Hussain, M., and Asgari, S. (2014). MicroRNA-like viral small RNA from Dengue virus 2 autoregulates its replication in mosquito cells. Proc Natl Acad Sci U S A *111*, 2746–2751. https://doi.org/10.1073/pnas.1320123111.

Hussain, M., Torres, S., Schnettler, E., Funk, A., Grundhoff, A., Pijlman, G.P., Khromykh, A.A., and Asgari, S. (2012). West Nile virus encodes a microRNA-like small RNA in the 3' untranslated region which up-regulates GATA4 mRNA and facilitates virus replication in mosquito cells. Nucleic Acids Res *40*, 2210–2223. https://doi.org/10.1093/nar/gkr848.

Hutvágner, G., McLachlan, J., Pasquinelli, A.E., Bálint, É., Tuschl, T., and Zamore, P.D. (2001). A Cellular Function for the RNA-Interference Enzyme Dicer in the Maturation of the let-7 Small Temporal RNA. Science *293*, 834–838. https://doi.org/10.1126/science.1062961.

Ingle, H., Kumar, S., Raut, A.A., Mishra, A., Kulkarni, D.D., Kameyama, T., Takaoka, A., Akira, S., and Kumar, H. (2015). The microRNA miR-485 targets host and influenza virus transcripts to regulate antiviral immunity and restrict viral replication. Sci Signal *8*, ra126. https://doi.org/10.1126/scisignal.aab3183.

Ipsaro, J.J., Haase, A.D., Knott, S.R., Joshua-Tor, L., and Hannon, G.J. (2012). The structural biochemistry of Zucchini implicates it as a nuclease in piRNA biogenesis. Nature *491*, 279–283. https://doi.org/10.1038/nature11502.

Ishikawa, H., and Barber, G.N. (2008). STING is an endoplasmic reticulum adaptor that facilitates innate immune signalling. Nature *455*, 674–678. https://doi.org/10.1038/nature07317.

Iwasaki, S., Kobayashi, M., Yoda, M., Sakaguchi, Y., Katsuma, S., Suzuki, T., and Tomari, Y. (2010). Hsc70/Hsp90 chaperone machinery mediates ATP-dependent RISC loading of small RNA duplexes. Mol. Cell *39*, 292–299. https://doi.org/10.1016/j.molcel.2010.05.015.

Jia, H., Kolaczkowski, O., Rolland, J., and Kolaczkowski, B. (2017). Increased Affinity for RNA Targets Evolved Early in Animal and Plant Dicer Lineages through Different Structural Mechanisms. Mol Biol Evol *34*, 3047–3063. https://doi.org/10.1093/molbev/msx187.

Jiang, F., Ye, X., Liu, X., Fincher, L., McKearin, D., and Liu, Q. (2005). Dicer-1 and R3D1-L catalyze microRNA maturation in Drosophila. Genes Dev. *19*, 1674–1679. https://doi.org/10.1101/gad.1334005.

Johnson, K.N., and Christian, P.D. (1998). The novel genome organization of the insect picorna-like virus Drosophila C virus suggests this virus belongs to a previously undescribed virus family. J Gen Virol *79 (Pt 1)*, 191–203. https://doi.org/10.1099/0022-1317-79-1-191.

Jopling, C.L., Yi, M., Lancaster, A.M., Lemon, S.M., and Sarnow, P. (2005). Modulation of hepatitis C virus RNA abundance by a liver-specific MicroRNA. Science *309*, 1577–1581. https://doi.org/10.1126/science.1113329.

Jousset, F.X., Plus, N., Croizier, G., and Thomas, M. (1972). [Existence in Drosophila of 2 groups of picornavirus with different biological and serological properties]. C.R. Hebd. Seances Acad. Sci., Ser. D, Sci. Nat. *275*, 3043–3046. .

Jousset, F.X., Bergoin, M., and Revet, B. (1977). Characterization of the Drosophila C virus. J. Gen. Virol. *34*, 269–283. https://doi.org/10.1099/0022-1317-34-2-269.

Kandasamy, S.K., and Fukunaga, R. (2016). Phosphate-binding pocket in Dicer-2 PAZ domain for high-fidelity siRNA production. Proceedings of the National Academy of Sciences 201612393. https://doi.org/10.1073/pnas.1612393113.

Karlikow, M., Goic, B., Mongelli, V., Salles, A., Schmitt, C., Bonne, I., Zurzolo, C., and Saleh, M.-C. (2016). Drosophila cells use nanotube-like structures to transfer dsRNA and RNAi machinery between cells. Sci Rep *6*, 27085. https://doi.org/10.1038/srep27085.

Kastner, B., Will, C.L., Stark, H., and Lührmann, R. (2019). Structural Insights into Nuclear pre-mRNA Splicing in Higher Eukaryotes. Cold Spring Harb Perspect Biol *11*, a032417. https://doi.org/10.1101/cshperspect.a032417.

Kawamata, T., Seitz, H., and Tomari, Y. (2009). Structural determinants of miRNAs for RISC loading and slicer-independent unwinding. Nat Struct Mol Biol *16*, 953–960. https://doi.org/10.1038/nsmb.1630.

Kemp, C., Mueller, S., Goto, A., Barbier, V., Paro, S., Bonnay, F., Dostert, C., Troxler, L., Hetru, C., Meignin, C., et al. (2013). Broad RNA Interference–Mediated Antiviral Immunity and Virus-Specific Inducible Responses in Drosophila. The Journal of Immunology *190*, 650–658. https://doi.org/10.4049/jimmunol.1102486.

Kincaid, R.P., Chen, Y., Cox, J.E., Rethwilm, A., and Sullivan, C.S. (2014). Noncanonical MicroRNA (miRNA) Biogenesis Gives Rise to Retroviral Mimics of Lymphoproliferative and Immunosuppressive Host miRNAs. MBio *5*, e00074-14. https://doi.org/10.1128/mBio.00074-14.

Koonin, E.V., Dolja, V.V., and Krupovic, M. (2015). Origins and evolution of viruses of eukaryotes: The ultimate modularity. Virology *479*, 2–25. https://doi.org/10.1016/j.virol.2015.02.039.

Kopek, B.G., Perkins, G., Miller, D.J., Ellisman, M.H., and Ahlquist, P. (2007). Three-dimensional analysis of a viral RNA replication complex reveals a virus-induced mini-organelle. PLoS Biol *5*, e220. https://doi.org/10.1371/journal.pbio.0050220.

Kuraoka, I., Ito, S., Wada, T., Hayashida, M., Lee, L., Saijo, M., Nakatsu, Y., Matsumoto, M., Matsunaga, T., Handa, H., et al. (2008). Isolation of XAB2 complex involved in pre-mRNA splicing, transcription, and transcription-coupled repair. J Biol Chem *283*, 940–950. https://doi.org/10.1074/jbc.M706647200.

Küspert, M., Murakawa, Y., Schäffler, K., Vanselow, J.T., Wolf, E., Juranek, S., Schlosser, A., Landthaler, M., and Fischer, U. (2015). LARP4B is an AU-rich sequence associated factor that promotes mRNA accumulation and translation. RNA *21*, 1294–1305. https://doi.org/10.1261/rna.051441.115.

Lamiable, O., Arnold, J., de Faria, I.J. da S., Olmo, R.P., Bergami, F., Meignin, C., Hoffmann, J.A., Marques, J.T., and Imler, J.-L. (2016). Analysis of the Contribution of Hemocytes and Autophagy to Drosophila Antiviral Immunity. J. Virol. *90*, 5415–5426. https://doi.org/10.1128/JVI.00238-16.

Lau, P.-W., Potter, C.S., Carragher, B., and MacRae, I.J. (2009). Structure of the human Dicer-TRBP complex by electron microscopy. Structure *17*, 1326–1332. https://doi.org/10.1016/j.str.2009.08.013.

Lee, Y.S., Nakahara, K., Pham, J.W., Kim, K., He, Z., Sontheimer, E.J., and Carthew, R.W. (2004). Distinct Roles for Drosophila Dicer-1 and Dicer-2 in the siRNA/miRNA Silencing Pathways. Cell *117*, 69–81. https://doi.org/10.1016/S0092-8674(04)00261-2.

Lemaitre, B., Nicolas, E., Michaut, L., Reichhart, J.M., and Hoffmann, J.A. (1996). The dorsoventral regulatory gene cassette spätzle/Toll/cactus controls the potent antifungal response in Drosophila adults. Cell *86*, 973–983. https://doi.org/10.1016/s0092-8674(00)80172-5.

Lewis, B.P., Shih, I. -hung, Jones-Rhoades, M.W., Bartel, D.P., and Burge, C.B. (2003). Prediction of mammalian microRNA targets. Cell *115*, 787–798. https://doi.org/10.1016/s0092-8674(03)01018-3.

Lewis, S.H., Quarles, K.A., Yang, Y., Tanguy, M., Frézal, L., Smith, S.A., Sharma, P.P., Cordaux, R., Gilbert, C., Giraud, I., et al. (2018). Pan-arthropod analysis reveals somatic piRNAs as an ancestral defence against transposable elements. Nat Ecol Evol *2*, 174–181. https://doi.org/10.1038/s41559-017-0403-4.

L'heritier, P. (1958). The hereditary virus of Drosophila. Adv Virus Res *5*, 195–245. .

Li, Q., Lowey, B., Sodroski, C., Krishnamurthy, S., Alao, H., Cha, H., Chiu, S., El-Diwany, R., Ghany, M.G., and Liang, T.J. (2017). Cellular microRNA networks regulate host dependency of hepatitis C virus infection. Nat Commun *8*, 1789. https://doi.org/10.1038/s41467-017-01954-x.

Lian, H., Zang, R., Wei, J., Ye, W., Hu, M.-M., Chen, Y.-D., Zhang, X.-N., Guo, Y., Lei, C.-Q., Yang, Q., et al. (2018a). The Zinc-Finger Protein ZCCHC3 Binds RNA and Facilitates Viral RNA Sensing and Activation of the RIG-I-like Receptors. Immunity *49*, 438-448.e5. https://doi.org/10.1016/j.immuni.2018.08.014.

Lian, H., Wei, J., Zang, R., Ye, W., Yang, Q., Zhang, X.-N., Chen, Y.-D., Fu, Y.-Z., Hu, M.-M., Lei, C.-Q., et al. (2018b). ZCCHC3 is a co-sensor of cGAS for dsDNA recognition in innate immune response. Nat Commun *9*, 3349. https://doi.org/10.1038/s41467-018-05559-w.

Liang, C., Wang, Y., Murota, Y., Liu, X., Smith, D., Siomi, M.C., and Liu, Q. (2015). TAF11 Assembles the RISC Loading Complex to Enhance RNAi Efficiency. Mol. Cell *59*, 807–818. https://doi.org/10.1016/j.molcel.2015.07.006.

Liu, Q., Rand, T.A., Kalidas, S., Du, F., Kim, H.-E., Smith, D.P., and Wang, X. (2003). R2D2, a bridge between the initiation and effector steps of the Drosophila RNAi pathway. Science *301*, 1921–1925. https://doi.org/10.1126/science.1088710.

Liu, Y., Ye, X., Jiang, F., Liang, C., Chen, D., Peng, J., Kinch, L.N., Grishin, N.V., and Liu, Q. (2009). C3PO, an endoribonuclease that promotes RNAi by facilitating RISC activation. Science *325*, 750–753. https://doi.org/10.1126/science.1176325.

Liu, Y., Gordesky-Gold, B., Leney-Greene, M., Weinbren, N.L., Tudor, M., and Cherry, S. (2018). Inflammation-Induced, STING-Dependent Autophagy Restricts Zika Virus Infection in the Drosophila Brain. Cell Host & Microbe *24*, 57-68.e3. https://doi.org/10.1016/j.chom.2018.05.022.

Liu, Y.-C., Mok, B.W.-Y., Wang, P., Kuo, R.-L., Chen, H., and Shih, S.-R. (2021). Cellular 5′-3′ mRNA Exoribonuclease XRN1 Inhibits Interferon Beta Activation and Facilitates Influenza A Virus Replication. MBio *12*, e00945-21. https://doi.org/10.1128/mBio.00945-21.

Longdon, B., Murray, G.G.R., Palmer, W.J., Day, J.P., Parker, D.J., Welch, J.J., Obbard, D.J., and Jiggins, F.M. (2015). The evolution, diversity, and host associations of rhabdoviruses. Virus Evolution *1*. https://doi.org/10.1093/ve/vev014.

Lu, R., Maduro, M., Li, F., Li, H.W., Broitman-Maduro, G., Li, W.X., and Ding, S.W. (2005). Animal virus replication and RNAi-mediated antiviral silencing in Caenorhabditis elegans. Nature *436*, 1040–1043. https://doi.org/10.1038/nature03870.

Lu, R., Yigit, E., Li, W.-X., and Ding, S.-W. (2009). An RIG-I-Like RNA helicase mediates antiviral RNAi downstream of viral siRNA biogenesis in Caenorhabditis elegans. PLoS Pathog *5*, e1000286. https://doi.org/10.1371/journal.ppat.1000286.

Lyles, D., Kuzmin, I., and Rupprecht, C. (2013). Rhabdoviridae. In Fields Virology, p.

Lyons, T., Murray, K.E., Roberts, A.W., and Barton, D.J. (2001). Poliovirus 5′-Terminal Cloverleaf RNA Is Required in cis for VPg Uridylylation and the Initiation of Negative-Strand RNA Synthesis. Journal of Virology *75*, 10696–10708. https://doi.org/10.1128/JVI.75.22.10696-10708.2001.

Ma, E., MacRae, I.J., Kirsch, J.F., and Doudna, J.A. (2008). Autoinhibition of human dicer by its internal helicase domain. J. Mol. Biol. *380*, 237–243. https://doi.org/10.1016/j.jmb.2008.05.005.

Macrae, I.J., Zhou, K., Li, F., Repic, A., Brooks, A.N., Cande, W.Z., Adams, P.D., and Doudna, J.A. (2006). Structural basis for double-stranded RNA processing by Dicer. Science *311*, 195–198. https://doi.org/10.1126/science.1121638.

Maillard, P.V., Van der Veen, A.G., Deddouche-Grass, S., Rogers, N.C., Merits, A., and Reis e Sousa, C. (2016). Inactivation of the type I interferon pathway reveals long double-stranded RNA-mediated RNA interference in mammalian cells. EMBO J. *35*, 2505–2518. https://doi.org/10.15252/embj.201695086.

Mailliot, J., and Martin, F. (2018). Viral internal ribosomal entry sites: four classes for one goal. Wiley Interdiscip Rev RNA *9*. https://doi.org/10.1002/wrna.1458.

Majzoub, K., Hafirassou, M.L., Meignin, C., Goto, A., Marzi, S., Fedorova, A., Verdier, Y., Vinh, J., Hoffmann, J.A., Martin, F., et al. (2014). RACK1 controls IRES-mediated translation of viruses. Cell *159*, 1086–1095. https://doi.org/10.1016/j.cell.2014.10.041.

Marques, J.T., Kim, K., Wu, P.-H., Alleyne, T.M., Jafari, N., and Carthew, R.W. (2010). Loqs and R2D2 act sequentially in the siRNA pathway in Drosophila. Nat. Struct. Mol. Biol. *17*, 24–30. https://doi.org/10.1038/nsmb.1735.

Marques, J.T., Wang, J.-P., Wang, X., de Oliveira, K.P.V., Gao, C., Aguiar, E.R.G.R., Jafari, N., and Carthew, R.W. (2013). Functional Specialization of the Small Interfering RNA Pathway in Response to Virus Infection. PLoS Pathogens *9*, e1003579. https://doi.org/10.1371/journal.ppat.1003579.

Mason, J.M., Frydrychova, R.C., and Biessmann, H. (2008). Drosophila telomeres: an exception providing new insights. Bioessays *30*, 25–37. https://doi.org/10.1002/bies.20688.

Medd, N.C., Fellous, S., Waldron, F.M., Xuéreb, A., Nakai, M., Cross, J.V., and Obbard, D.J. (2018). The virome of Drosophila suzukii, an invasive pest of soft fruit. Virus Evolution *4*, vey009. https://doi.org/10.1093/ve/vey009.

Merkling, S.H., Bronkhorst, A.W., Kramer, J.M., Overheul, G.J., Schenck, A., and Van Rij, R.P. (2015). The Epigenetic Regulator G9a Mediates Tolerance to RNA Virus Infection in Drosophila. PLoS Pathog *11*, e1004692. https://doi.org/10.1371/journal.ppat.1004692.

Miesen, P., Girardi, E., and van Rij, R.P. (2015). Distinct sets of PIWI proteins produce arbovirus and transposon-derived piRNAs in Aedes aegypti mosquito cells. Nucleic Acids Res. *43*, 6545–6556. https://doi.org/10.1093/nar/gkv590.

Ming, M., Obata, F., Kuranaga, E., and Miura, M. (2014). Persephone/Spätzle pathogen sensors mediate the activation of Toll receptor signaling in response to endogenous danger signals in apoptosis-deficient Drosophila. J. Biol. Chem. *289*, 7558–7568. https://doi.org/10.1074/jbc.M113.543884.

Mogensen, T.H. (2009). Pathogen Recognition and Inflammatory Signaling in Innate Immune Defenses. Clin Microbiol Rev *22*, 240–273. https://doi.org/10.1128/CMR.00046-08.

Mohr, S., Bakal, C., and Perrimon, N. (2010). Genomic screening with RNAi: results and challenges. Annu Rev Biochem *79*, 37–64. https://doi.org/10.1146/annurev-biochem-060408-092949.

Mohr, S.E., Hu, Y., Kim, K., Housden, B.E., and Perrimon, N. (2014). Resources for functional genomics studies in Drosophila melanogaster. Genetics *197*, 1–18. https://doi.org/10.1534/genetics.113.154344.

Molleston, J.M., Sabin, L.R., Moy, R.H., Menghani, S.V., Rausch, K., Gordesky-Gold, B., Hopkins, K.C., Zhou, R., Jensen, T.H., Wilusz, J.E., et al. (2016). A conserved virus-induced cytoplasmic TRAMP-like complex recruits the exosome to target viral RNA for degradation. Genes Dev. *30*, 1658–1670. https://doi.org/10.1101/gad.284604.116.

Monsanto-Hearne, V., Asad, S., Asgari, S., and Johnson, K.N. (2017a). Drosophila microRNA modulates viral replication by targeting a homologue of mammalian cJun. J. Gen. Virol. *98*, 1904–1912. https://doi.org/10.1099/jgv.0.000831.

Monsanto-Hearne, V., Tham, A.L.Y., Wong, Z.S., Asgari, S., and Johnson, K.N. (2017b). Drosophila miR-956 suppression modulates Ectoderm-expressed 4 and inhibits viral replication. Virology *502*, 20–27. https://doi.org/10.1016/j.virol.2016.12.009.

Montavon, T.C., Baldaccini, M., Lefèvre, M., Girardi, E., Chane-Woon-Ming, B., Messmer, M., Hammann, P., Chicher, J., and Pfeffer, S. (2021). Human DICER helicase domain recruits PKR and modulates its antiviral activity. PLoS Pathog *17*, e1009549. https://doi.org/10.1371/journal.ppat.1009549.

Morazzani, E.M., Wiley, M.R., Murreddu, M.G., Adelman, Z.N., and Myles, K.M. (2012). Production of Virus-Derived Ping-Pong-Dependent piRNA-like Small RNAs in the Mosquito Soma. PLOS Pathogens *8*, e1002470. https://doi.org/10.1371/journal.ppat.1002470.

Mueller, S., Gausson, V., Vodovar, N., Deddouche, S., Troxler, L., Perot, J., Pfeffer, S., Hoffmann, J.A., Saleh, M.-C., and Imler, J.-L. (2010). RNAi-mediated immunity provides strong protection against the negative-strand RNA vesicular stomatitis virus in Drosophila. Proc. Natl. Acad. Sci. U.S.A. *107*, 19390–19395. https://doi.org/10.1073/pnas.1014378107.

Mukherjee, K., Campos, H., and Kolaczkowski, B. (2013). Evolution of Animal and Plant Dicers: Early Parallel Duplications and Recurrent Adaptation of Antiviral RNA Binding in Plants. Mol Biol Evol *30*, 627–641. https://doi.org/10.1093/molbev/mss263.

Myers, E.W., Sutton, G.G., Delcher, A.L., Dew, I.M., Fasulo, D.P., Flanigan, M.J., Kravitz, S.A., Mobarry, C.M., Reinert, K.H., Remington, K.A., et al. (2000). A whole-genome assembly of Drosophila. Science *287*, 2196–2204. https://doi.org/10.1126/science.287.5461.2196.

Nasim, M.T., Chowdhury, H.M., and Eperon, I.C. (2002). A double reporter assay for detecting changes in the ratio of spliced and unspliced mRNA in mammalian cells. Nucleic Acids Res *30*, e109. https://doi.org/10.1093/nar/gnf108.

Ng, C.S., Kasumba, D.M., Fujita, T., and Luo, H. (2020). Spatio-temporal characterization of the antiviral activity of the XRN1-DCP1/2 aggregation against cytoplasmic RNA viruses to prevent cell death. Cell Death Differ *27*, 2363–2382. https://doi.org/10.1038/s41418-020-0509-0.

Nishimasu, H., Ishizu, H., Saito, K., Fukuhara, S., Kamatani, M.K., Bonnefond, L., Matsumoto, N., Nishizawa, T., Nakanaga, K., Aoki, J., et al. (2012). Structure and function of Zucchini endoribonuclease in piRNA biogenesis. Nature *491*, 284–287. https://doi.org/10.1038/nature11509.

Nüsslein-Volhard, C., and Wieschaus, E. (1980). Mutations affecting segment number and polarity in Drosophila. Nature *287*, 795–801. https://doi.org/10.1038/287795a0.

Obbard, D.J., Welch, J.J., Kim, K.-W., and Jiggins, F.M. (2009). Quantifying Adaptive Evolution in the Drosophila Immune System. PLOS Genetics *5*, e1000698. https://doi.org/10.1371/journal.pgen.1000698.

O'Brien, K., Matlin, A.J., Lowell, A.M., and Moore, M.J. (2008). The biflavonoid isoginkgetin is a general inhibitor of Pre-mRNA splicing. J Biol Chem *283*, 33147–33154. https://doi.org/10.1074/jbc.M805556200.

Olmo, R.P., Ferreira, A.G.A., Izidoro-Toledo, T.C., Aguiar, E.R.G.R., de Faria, I.J.S., de Souza, K.P.R., Osório, K.P., Kuhn, L., Hammann, P., de Andrade, E.G., et al. (2018). Control of dengue

virus in the midgut of Aedes aegypti by ectopic expression of the dsRNA-binding protein Loqs2. Nat Microbiol *3*, 1385–1393. https://doi.org/10.1038/s41564-018-0268-6.

Paingankar, M.S., Gokhale, M.D., Deobagkar, D.D., and Deobagkar, D.N. (2020). Drosophila melanogaster as a model host to study arbovirus–vector interaction. 2020.09.03.282350. https://doi.org/10.1101/2020.09.03.282350.

Palmer, W.H., Hadfield, J.D., and Obbard, D.J. (2018). RNA-Interference Pathways Display High Rates of Adaptive Protein Evolution in Multiple Invertebrates. Genetics *208*, 1585–1599. https://doi.org/10.1534/genetics.117.300567.

Palmer, W.H., Dittmar, M., Gordesky-Gold, B., Hofmann, J., and Cherry, S. (2020). Drosophila melanogaster as a model for arbovirus infection of adult salivary glands. Virology *543*, 1–6. https://doi.org/10.1016/j.virol.2020.01.010.

Peck, K.M., and Lauring, A.S. (2018). Complexities of Viral Mutation Rates. J Virol *92*, e01031-17. https://doi.org/10.1128/JVI.01031-17.

Pennemann, F.L., Mussabekova, A., Urban, C., Stukalov, A., Andersen, L.L., Grass, V., Lavacca, T.M., Holze, C., Oubraham, L., Benamrouche, Y., et al. (2021). Cross-species analysis of viral nucleic acid interacting proteins identifies TAOKs as innate immune regulators. Nat Commun *12*, 7009. https://doi.org/10.1038/s41467-021-27192-w.

Petit, M., Mongelli, V., Frangeul, L., Blanc, H., Jiggins, F., and Saleh, M.-C. (2016). piRNA pathway is not required for antiviral defense in Drosophila melanogaster. Proc. Natl. Acad. Sci. U.S.A. *113*, E4218-4227. https://doi.org/10.1073/pnas.1607952113.

Petrillo, J.E., Venter, P.A., Short, J.R., Gopal, R., Deddouche, S., Lamiable, O., Imler, J.-L., and Schneemann, A. (2013). Cytoplasmic granule formation and translational inhibition of nodaviral RNAs in the absence of the double-stranded RNA binding protein B2. J. Virol. *87*, 13409–13421. https://doi.org/10.1128/JVI.02362-13.

Pfeffer, S., Zavolan, M., Grässer, F.A., Chien, M., Russo, J.J., Ju, J., John, B., Enright, A.J., Marks, D., Sander, C., et al. (2004). Identification of virus-encoded microRNAs. Science *304*, 734–736. https://doi.org/10.1126/science.1096781.

Plus, N., Croizier, G., Duthoit, J.L., David, J., Anxolabéhère, D., and Périquet, G. (1975). [The discovery, in Drosophila, of viruses belonging to three new groups]. C R Acad Hebd Seances Acad Sci D *280*, 1501–1504. .

Poltorak, A., He, X., Smirnova, I., Liu, M.Y., Van Huffel, C., Du, X., Birdwell, D., Alejos, E., Silva, M., Galanos, C., et al. (1998). Defective LPS signaling in C3H/HeJ and C57BL/10ScCr mice: mutations in Tlr4 gene. Science *282*, 2085–2088. https://doi.org/10.1126/science.282.5396.2085.

Prud'homme, N., Gans, M., Masson, M., Terzian, C., and Bucheton, A. (1995). Flamenco, a Gene Controlling the Gypsy Retrovirus of Drosophila Melanogaster. Genetics *139*, 697–711. .

Reavy, B., and Moore, N.F. (1983). Cell-free translation of Drosophila C virus RNA: identification of a virus protease activity involved in capsid protein synthesis and further studies on in vitro processing of cricket paralysis virus specified proteins. Arch Virol *76*, 101–115. https://doi.org/10.1007/BF01311694.

Rezelj, V.V., Levi, L.I., and Vignuzzi, M. (2018). The defective component of viral populations. Current Opinion in Virology *33*, 74–80. https://doi.org/10.1016/j.coviro.2018.07.014.

Rieder, E., Paul, A.V., Kim, D.W., van Boom, J.H., and Wimmer, E. (2000). Genetic and biochemical studies of poliovirus cis-acting replication element cre in relation to VPg uridylylation. J. Virol. *74*, 10371–10380. https://doi.org/10.1128/jvi.74.22.10371-10380.2000.

van Rij, R.P., Saleh, M.-C., Berry, B., Foo, C., Houk, A., Antoniewski, C., and Andino, R. (2006). The RNA silencing endonuclease Argonaute 2 mediates specific antiviral immunity in Drosophila melanogaster. Genes & Development *20*, 2985–2995. https://doi.org/10.1101/gad.1482006.

Roignant, J.-Y., Carré, C., Mugat, B., Szymczak, D., Lepesant, J.-A., and Antoniewski, C. (2003). Absence of transitive and systemic pathways allows cell-specific and isoform-specific RNAi in Drosophila. RNA *9*, 299–308. .

Rose, J. (1975). Heterogneeous 5'-terminal structures occur on vesicular stomatitis virus mRNAs. Journal of Biological Chemistry *250*, 8098–8104. https://doi.org/10.1016/S0021-9258(19)40821-1.

Rosenberger, C.M., Podyminogin, R.L., Diercks, A.H., Treuting, P.M., Peschon, J.J., Rodriguez, D., Gundapuneni, M., Weiss, M.J., and Aderem, A. (2017). miR-144 attenuates the host response to influenza virus by targeting the TRAF6-IRF7 signaling axis. PLoS Pathog *13*, e1006305. https://doi.org/10.1371/journal.ppat.1006305.

Rousseau, C., and Meignin, C. (2020). Viral sensing by RNA helicases. Virologie *24*, 36–52. https://doi.org/10.1684/vir.2020.0872.

Rowley, P.A., Ho, B., Bushong, S., Johnson, A., and Sawyer, S.L. (2016). XRN1 Is a Species-Specific Virus Restriction Factor in Yeasts. PLOS Pathogens *12*, e1005890. https://doi.org/10.1371/journal.ppat.1005890.

Roxström-Lindquist, K., Terenius, O., and Faye, I. (2004). Parasite-specific immune response in adult Drosophila melanogaster: a genomic study. EMBO Rep *5*, 207–212. https://doi.org/10.1038/sj.embor.7400073.

Saito, K., Ishizuka, A., Siomi, H., and Siomi, M.C. (2005). Processing of pre-microRNAs by the Dicer-1-Loquacious complex in Drosophila cells. PLoS Biol. *3*, e235. https://doi.org/10.1371/journal.pbio.0030235.

Saiz-Baggetto, S., Méndez, E., Quilis, I., Igual, J.C., and Bañó, M.C. (2017). Chimeric proteins tagged with specific 3xHA cassettes may present instability and functional problems. PLOS ONE *12*, e0183067. https://doi.org/10.1371/journal.pone.0183067.

Saleh, M.-C., Tassetto, M., van Rij, R.P., Goic, B., Gausson, V., Berry, B., Jacquier, C., Antoniewski, C., and Andino, R. (2009). Antiviral immunity in Drosophila requires systemic RNA interference spread. Nature *458*, 346–350. https://doi.org/10.1038/nature07712.

Schneider, J., and Imler, J.-L. (2020). Sensing and signalling viral infection in drosophila. Dev Comp Immunol *117*, 103985. https://doi.org/10.1016/j.dci.2020.103985.

Shcherbata, H.R., Ward, E.J., Fischer, K.A., Yu, J.-Y., Reynolds, S.H., Chen, C.-H., Xu, P., Hay, B.A., and Ruohola-Baker, H. (2007). Stage-Specific Differences in the Requirements for Germline Stem Cell Maintenance in the Drosophila Ovary. Cell Stem Cell *1*, 698–709. https://doi.org/10.1016/j.stem.2007.11.007.

Singh, C.P., Singh, J., and Nagaraju, J. (2012). A baculovirus-encoded MicroRNA (miRNA) suppresses its host miRNA biogenesis by regulating the exportin-5 cofactor Ran. J Virol *86*, 7867–7879. https://doi.org/10.1128/JVI.00064-12.

Singh, M., Chazal, M., Quarato, P., Bourdon, L., Malabat, C., Vallet, T., Vignuzzi, M., van der Werf, S., Behilil, S., Donati, F., et al. (2022). A virus-derived microRNA targets immune response genes during SARS-CoV-2 infection. EMBO Reports *23*, e54341. https://doi.org/10.15252/embr.202154341.

Singh, R.K., Jonely, M., Leslie, E., Rejali, N.A., Noriega, R., and Bass, B.L. (2021). Transient kinetic studies of the antiviral Drosophila Dicer-2 reveal roles of ATP in self–nonself discrimination. ELife *10*, e65810. https://doi.org/10.7554/eLife.65810.

Sinha, N.K., Trettin, K.D., Aruscavage, P.J., and Bass, B.L. (2015). Drosophila Dicer-2 Cleavage Is Mediated by Helicase- and dsRNA Termini-Dependent States that Are Modulated by Loquacious-PD. Molecular Cell *58*, 406–417. https://doi.org/10.1016/j.molcel.2015.03.012.

Sinha, N.K., Iwasa, J., Shen, P.S., and Bass, B.L. (2018). Dicer uses distinct modules for recognizing dsRNA termini. Science *359*, 329–334. https://doi.org/10.1126/science.aaq0921.

Skalsky, R.L., and Cullen, B.R. (2010). Viruses, microRNAs, and Host Interactions. Annu Rev Microbiol *64*, 123–141. https://doi.org/10.1146/annurev.micro.112408.134243.

Sparks, W.O., Bartholomay, L.C., and Bonning, B.C. (2008). 9 - INSECT IMMUNITY TO VIRUSES. In Insect Immunology, N.E. Beckage, ed. (San Diego: Academic Press), pp. 209–242.

Stefan, K.L., Kim, M.V., Iwasaki, A., and Kasper, D.L. (2020). Commensal Microbiota Modulation of Natural Resistance to Virus Infection. Cell *183*, 1312-1324.e10. https://doi.org/10.1016/j.cell.2020.10.047.

Su, S., Wang, J., Deng, T., Yuan, X., He, J., Liu, N., Li, X., Huang, Y., Wang, H.-W., and Ma, J. (2022). Structural insights into dsRNA processing by Drosophila Dicer-2–Loqs-PD. Nature *607*, 399–406. https://doi.org/10.1038/s41586-022-04911-x.

Sullivan, C.S., Grundhoff, A.T., Tevethia, S., Pipas, J.M., and Ganem, D. (2005). SV40-encoded microRNAs regulate viral gene expression and reduce susceptibility to cytotoxic T cells. Nature *435*, 682–686. https://doi.org/10.1038/nature03576.

Tabara, H., Yigit, E., Siomi, H., and Mello, C.C. (2002). The dsRNA Binding Protein RDE-4 Interacts with RDE-1, DCR-1, and a DExH-Box Helicase to Direct RNAi in C. elegans. Cell *109*, 861–871. https://doi.org/10.1016/S0092-8674(02)00793-6.

Takeuchi, O., and Akira, S. (2010). Pattern Recognition Receptors and Inflammation. Cell *140*, 805–820. https://doi.org/10.1016/j.cell.2010.01.022.

Talide, L., Imler, J.-L., and Meignin, C. (2020). Sensing Viral Infections in Insects: A Dearth of Pathway Receptors. Curr Issues Mol Biol *34*, 31–60. https://doi.org/10.21775/cimb.034.031.

Taylor, D.W., Ma, E., Shigematsu, H., Cianfrocco, M.A., Noland, C.L., Nagayama, K., Nogales, E., Doudna, J.A., and Wang, H.-W. (2013). Substrate-specific structural rearrangements of human Dicer. Nat Struct Mol Biol *20*, 662–670. https://doi.org/10.1038/nsmb.2564.

Temme, C., Zhang, L., Kremmer, E., Ihling, C., Chartier, A., Sinz, A., Simonelig, M., and Wahle, E. (2010). Subunits of the Drosophila CCR4-NOT complex and their roles in mRNA deadenylation. RNA *16*, 1356–1370. https://doi.org/10.1261/rna.2145110.

Teo, G., Liu, G., Zhang, J., Nesvizhskii, A.I., Gingras, A.-C., and Choi, H. (2014). SAINTexpress: improvements and additional features in Significance Analysis of Interactome software. J Proteomics *100*, 37–43. https://doi.org/10.1016/j.jprot.2013.10.023.

Thomas-Orillard, M. (1988). Interaction between a picornavirus and a wild population ofDrosophila melanogaster. Oecologia *75*, 516–520. https://doi.org/10.1007/BF00776414.

Tomari, Y., Matranga, C., Haley, B., Martinez, N., and Zamore, P.D. (2004). A Protein Sensor for siRNA Asymmetry. Science *306*, 1377–1380. https://doi.org/10.1126/science.1102755.

Umbach, J.L., Kramer, M.F., Jurak, I., Karnowski, H.W., Coen, D.M., and Cullen, B.R. (2008). MicroRNAs expressed by herpes simplex virus 1 during latent infection regulate viral mRNAs. Nature *454*, 780–783. https://doi.org/10.1038/nature07103.

Varjak, M., Gestuveo, R.J., Burchmore, R., Schnettler, E., and Kohl, A. (2020). aBravo Is a Novel Aedes aegypti Antiviral Protein That Interacts with, but Acts Independently of, the Exogenous siRNA Pathway Effector Dicer 2. Viruses *12*, 748. https://doi.org/10.3390/v12070748.

Venken, K.J.T., and Bellen, H.J. (2014). Chemical mutagens, transposons, and transgenes to interrogate gene function in Drosophila melanogaster. Methods *68*, 15–28. https://doi.org/10.1016/j.ymeth.2014.02.025.

Vodovar, N., Bronkhorst, A.W., van Cleef, K.W.R., Miesen, P., Blanc, H., van Rij, R.P., and Saleh, M.-C. (2012). Arbovirus-derived piRNAs exhibit a ping-pong signature in mosquito cells. PLoS ONE *7*, e30861. https://doi.org/10.1371/journal.pone.0030861.

Wallace, M.A., Coffman, K.A., Gilbert, C., Ravindran, S., Albery, G.F., Abbott, J., Argyridou, E., Bellosta, P., Betancourt, A.J., Colinet, H., et al. (2021). The discovery, distribution, and diversity of DNA viruses associated with Drosophila melanogaster in Europe. Virus Evolution *7*, veab031. https://doi.org/10.1093/ve/veab031.

Wang, H.-W., Noland, C., Siridechadilok, B., Taylor, D.W., Ma, E., Felderer, K., Doudna, J.A., and Nogales, E. (2009). Structural insights into RNA processing by the human RISC-loading complex. Nat Struct Mol Biol *16*, 1148–1153. https://doi.org/10.1038/nsmb.1673.

Wang, Y., Luo, J., Zhang, H., and Lu, J. (2016). microRNAs in the Same Clusters Evolve to Coordinately Regulate Functionally Related Genes. Mol Biol Evol *33*, 2232–2247. https://doi.org/10.1093/molbev/msw089.

Weber, F., Wagner, V., Rasmussen, S.B., Hartmann, R., and Paludan, S.R. (2006). Double-Stranded RNA Is Produced by Positive-Strand RNA Viruses and DNA Viruses but Not in Detectable Amounts by Negative-Strand RNA Viruses. J Virol *80*, 5059–5064. https://doi.org/10.1128/JVI.80.10.5059-5064.2006.

Webster, C.L., Waldron, F.M., Robertson, S., Crowson, D., Ferrari, G., Quintana, J.F., Brouqui, J.-M., Bayne, E.H., Longdon, B., Buck, A.H., et al. (2015). The Discovery, Distribution, and Evolution of Viruses Associated with Drosophila melanogaster. PLOS Biology *13*, e1002210. https://doi.org/10.1371/journal.pbio.1002210.

Webster, C.L., Longdon, B., Lewis, S.H., and Obbard, D.J. (2016). Twenty-Five New Viruses Associated with the Drosophilidae (Diptera). Evol Bioinform Online *12s2*, EBO.S39454. https://doi.org/10.4137/EBO.S39454.

Welker, N.C., Maity, T.S., Ye, X., Aruscavage, P.J., Krauchuk, A.A., Liu, Q., and Bass, B.L. (2011). Dicer's Helicase Domain Discriminates dsRNA Termini to Promote an Altered Reaction Mode. Molecular Cell *41*, 589–599. https://doi.org/10.1016/j.molcel.2011.02.005.

Weng, Y., Xiao, H., Zhang, J., Liang, X.-J., and Huang, Y. (2019). RNAi therapeutic and its innovative biotechnological evolution. Biotechnol Adv *37*, 801–825. https://doi.org/10.1016/j.biotechadv.2019.04.012.

White, E., Schlackow, M., Kamieniarz-Gdula, K., Proudfoot, N.J., and Gullerova, M. (2014). Human nuclear Dicer restricts the deleterious accumulation of endogenous double-stranded RNA. Nat Struct Mol Biol *21*, 552–559. https://doi.org/10.1038/nsmb.2827.

Wieschaus, E., and Nüsslein-Volhard, C. (2016). The Heidelberg Screen for Pattern Mutants of Drosophila: A Personal Account. Annu. Rev. Cell Dev. Biol. *32*, 1–46. https://doi.org/10.1146/annurev-cellbio-113015-023138.

Wu, Q., Luo, Y., Lu, R., Lau, N., Lai, E.C., Li, W.-X., and Ding, S.-W. (2010). Virus discovery by deep sequencing and assembly of virus-derived small silencing RNAs. Proceedings of the National Academy of Sciences *107*, 1606–1611. https://doi.org/10.1073/pnas.0911353107.

Xiong, X.-P., Kurthkoti, K., Chang, K.-Y., Lichinchi, G., De, N., Schneemann, A., MacRae, I.J., Rana, T.M., Perrimon, N., and Zhou, R. (2013). Core small nuclear ribonucleoprotein particle splicing factor SmD1 modulates RNA interference in Drosophila. Proc Natl Acad Sci U S A *110*, 16520–16525. https://doi.org/10.1073/pnas.1315803110.

Yamaguchi, S., Naganuma, M., Nishizawa, T., Kusakizako, T., Tomari, Y., Nishimasu, H., and Nureki, O. (2022). Structure of the Dicer-2-R2D2 heterodimer bound to a small RNA duplex. Nature *607*, 393–398. https://doi.org/10.1038/s41586-022-04790-2.

Yi, R., Qin, Y., Macara, I.G., and Cullen, B.R. (2003). Exportin-5 mediates the nuclear export of pre-microRNAs and short hairpin RNAs. Genes Dev *17*, 3011–3016. https://doi.org/10.1101/gad.1158803.

Yoon, J.-S., Kim, K., and Palli, S.R. (2020). Double-stranded RNA in exosomes: Potential systemic RNA interference pathway in the Colorado potato beetle, Leptinotarsa decemlineata. Journal of Asia-Pacific Entomology *23*, 1160–1164. https://doi.org/10.1016/j.aspen.2020.09.012.

Zambon, R.A., Nandakumar, M., Vakharia, V.N., and Wu, L.P. (2005). The Toll pathway is important for an antiviral response in Drosophila. Proceedings of the National Academy of Sciences *102*, 7257–7262. https://doi.org/10.1073/pnas.0409181102.

Zamore, P.D., Tuschl, T., Sharp, P.A., and Bartel, D.P. (2000). RNAi: Double-Stranded RNA Directs the ATP-Dependent Cleavage of mRNA at 21 to 23 Nucleotide Intervals. Cell *101*, 25–33. https://doi.org/10.1016/S0092-8674(00)80620-0.

Zhang, F., Wang, J., Xu, J., Zhang, Z., Koppetsch, B.S., Schultz, N., Vreven, T., Meignin, C., Davis, I., Zamore, P.D., et al. (2012). UAP56 Couples piRNA Clusters to the Perinuclear Transposon Silencing Machinery. Cell *151*, 871–884. .

Zhang, H., Kolb, F.A., Jaskiewicz, L., Westhof, E., and Filipowicz, W. (2004). Single processing center models for human Dicer and bacterial RNase III. Cell *118*, 57–68. https://doi.org/10.1016/j.cell.2004.06.017.

Zhang, L., Xu, W., Gao, X., Li, W., Qi, S., Guo, D., Ajayi, O.E., Ding, S.-W., and Wu, Q. (2020). lncRNA Sensing of a Viral Suppressor of RNAi Activates Non-canonical Innate Immune Signaling in Drosophila. Cell Host Microbe *27*, 115-128.e8. https://doi.org/10.1016/j.chom.2019.12.006.

Zhang, Y., Malone, J.H., Powell, S.K., Periwal, V., Spana, E., MacAlpine, D.M., and Oliver, B. (2010). Expression in Aneuploid Drosophila S2 Cells. PLoS Biol *8*, e1000320. https://doi.org/10.1371/journal.pbio.1000320.

Zhou, R., Hotta, I., Denli, A.M., Hong, P., Perrimon, N., and Hannon, G.J. (2008). Comparative Analysis of Argonaute-dependent Small RNA Pathways in Drosophila. Mol Cell *32*, 592–599. https://doi.org/10.1016/j.molcel.2008.10.018.

Zhu, M., Wang, J., Deng, R., Xiong, P., Liang, H., and Wang, X. (2013). A microRNA encoded by Autographa californica nucleopolyhedrovirus regulates expression of viral gene ODV-E25. J Virol *87*, 13029–13034. https://doi.org/10.1128/JVI.02112-13.

Résumé étendu en Français

Introduction générale

La discrimination entre le « soi » et le « non-soi » est essentielle pour la lutte contre les infections virales. En effet, un aspect clé de l'immunité antivirale est la distinction des composants du virus de ceux de l'hôte. Cette discrimination repose principalement sur la détection d'acides nucléiques, car la plupart des agents pathogènes exposent leurs acides nucléiques à un moment donné de leur cycle viral (Hornung, 2014a, 2014b). La détection d'acides nucléiques en particulier, l'ARN double brin (ARNdb), permet de détecter un éventail particulièrement large de virus. Cependant, si un large panel de récepteurs nucléiques a été identifiés et étudiés chez les mammifères, le tableau semble néanmoins moins clair chez les insectes.

Chez *Drosophila melanogaster*, le récepteur cytosolique d'ARNdb le plus étudié est Dicer-2 (Dcr-2), qui joue un rôle majeur dans l'immunité antivirale, puisqu'il est un composant clé de la voie de l'ARN interférence (ARNi). Dicer-2 est capable de reconnaître les extrémités des ARNdb et de synthétiser des duplexes de siARN. Dicer-2 peut effectuer cette synthèse soit par découpage distributif (Dicer-2 doit se détacher de l'ARNdb puis se rattacher à un autre ARNdb entre chaque clivage), soit par découpage processif (Dicer-2 se déplace le long de la molécule d'ARNdb et synthétise plusieurs duplexes de siARN avant de se détacher de l'ARNdb) (Cenik et al., 2011 ; Sinha et al., 2015, 2018). Les siARN de 21 nucléotides produits seront ensuite chargés sur le *RNA-induced Silencing Complex* (RISC) afin d'induire le clivage puis la dégradation des ARN viraux complémentaires.

Il a cependant été montré *in vitro* que Dicer-2 reconnaît les extrémités des ARNdb, mais les ARNdb viraux produits ont souvent des extrémités protégées. Par exemple, le *Drosophila C Virus* (DCV) est protégé à la fois par une protéine liée de manière covalente à son extrémité 5', appelée VpG, et par une queue polyA à son extrémité 3'. Dans ce cas, comment Dicer-2 peut-il reconnaître ces ARNdb viraux en contexte infectieux ? Cela a été le focus principal de ma thèse. En effet, des données non publiées du laboratoire nous ont amenés à penser que d'autres cofacteurs pourraient aider Dicer-2 à cette étape du mécanisme de l'ARNi. Afin de définir le réseau de protéines associées à Dicer-2 lors de l'infection virale, j'ai donc utilisé une approche de spectrométrie de masse qui m'a permis d'identifier plusieurs candidats.

De plus, étant donné la grande diversité des virus capables d'infecter *Drosophila melanogaster*, nous nous sommes demandé si d'autres récepteurs et effecteurs pourraient être responsables du contrôle de l'infection virale chez la drosophile. C'est pourquoi l'objectif d'un ancien doctorant de notre laboratoire a été d'identifier de nouveaux récepteurs d'acides nucléiques viraux chez *Drosophila melanogaster*. En utilisant une approche d'affinité-purification et de spectrométrie de masse (AP-MS), elle a ainsi identifié des candidats se liant préférentiellement à un certain nombre de ligands acides nucléiques (Pennemann *et al.*, 2021). Cela lui a permis d'identifier un nouveau senseur d'ARNdb potentiel appelé Fandango (Fand). L'objectif secondaire de ma thèse a donc été d'étudier ce candidat, ainsi que son rôle dans l'immunité antivirale.

Partie 1 : Identification de nouveaux partenaires protéiques de Dicer-2 pendant l'infection virale *in vivo*

I) Résultats

Afin de définir le réseau de protéines associées à Dicer-2 lors de l'infection virale, j'ai utilisé une approche de spectrométrie de masse (MS) afin d'identifier les partenaires protéiques de Dicer-2 lors d'une infection virale *in vivo* par le virus DCV. Pour cela, trois lignées de drosophiles ont été infectées ou non et expriment différentes versions d'une protéine de fusion GFP::Dicer-2 dans un fond génétique nul mutant pour le gène *dicer-2* avec DCV ou une solution TRIS comme contrôle. La première lignée exprime la version sauvage (WT) de Dicer-2, fusionnée à la GFP (GFP::Dicer-2^{WT}), qui permet de complémenter *dicer-*$2^{-/-}$ et de retrouver un phénotype sauvage. La deuxième lignée exprime un mutant ATPase de Dicer-2, incapable d'hydrolyser l'ATP et donc d'effectuer uniquement le mécanisme de découpage distributif (GFP::Dicer-$2^{ATPase\text{-}mut}$). Enfin, la troisième lignée exprime un mutant RNAseIII, toujours capable de se fixer aux ARNdb mais incapable de les cliver (GFP::Dicer-$2^{RNAseIII\text{-}mut}$). De plus, deux lignées contrôles ont été utilisées : une lignée WT (exprimant le gène endogène *dicer-2* du fond génétique CantonS (CS)), et une lignée exprimant la GFP seule, sous le contrôle d'un promoteur d'ubiquitine (Ctrl-GFP). Des immunoprécipitations (IP) ont ensuite été réalisées avec des billes anti-GFP sur des drosophiles adultes injectées avec DCV ou TRIS, à deux jours post-injection. L'intégralité de cette expérience a été réalisée en triplicata.

Les outils d'analyse et de visualisation de données de protéomique, SAINT-express et Prohits-viz, m'ont permis de visualiser les résultats et de déterminer une liste de candidats enrichis dans les différents échantillons par rapport aux contrôles (Figure 1A). J'ai ainsi été en mesure d'établir un réseau global de protéines interagissant avec Dicer-2, contenant un enrichissement en protéine de type DEAD-box hélicases, ainsi que de protéines impliquées dans l'épissage des ARN, l'ovogenèse ou la biogenèse des P-bodies (Figure 1B). De plus, les différentes conditions utilisées dans cette expérience m'ont permis d'étudier à la fois l'impact des mutations ponctuelles de Dicer-2 et l'impact de l'infection par DCV sur l'interactome de Dicer-2 (Figure 1C). Pour cela, j'ai analysé l'enrichissement des différentes protéines identifiées par MS pour chaque lignée en comparant : (1) échantillons GFP::Dicer-2 *versus* contrôles ; (2) échantillons non infectés *versus* échantillons infectés par DCV. En regroupant ces données, j'ai pu déterminer comment l'interactome de Dicer-2 varie selon les mutants et conditions utilisés.

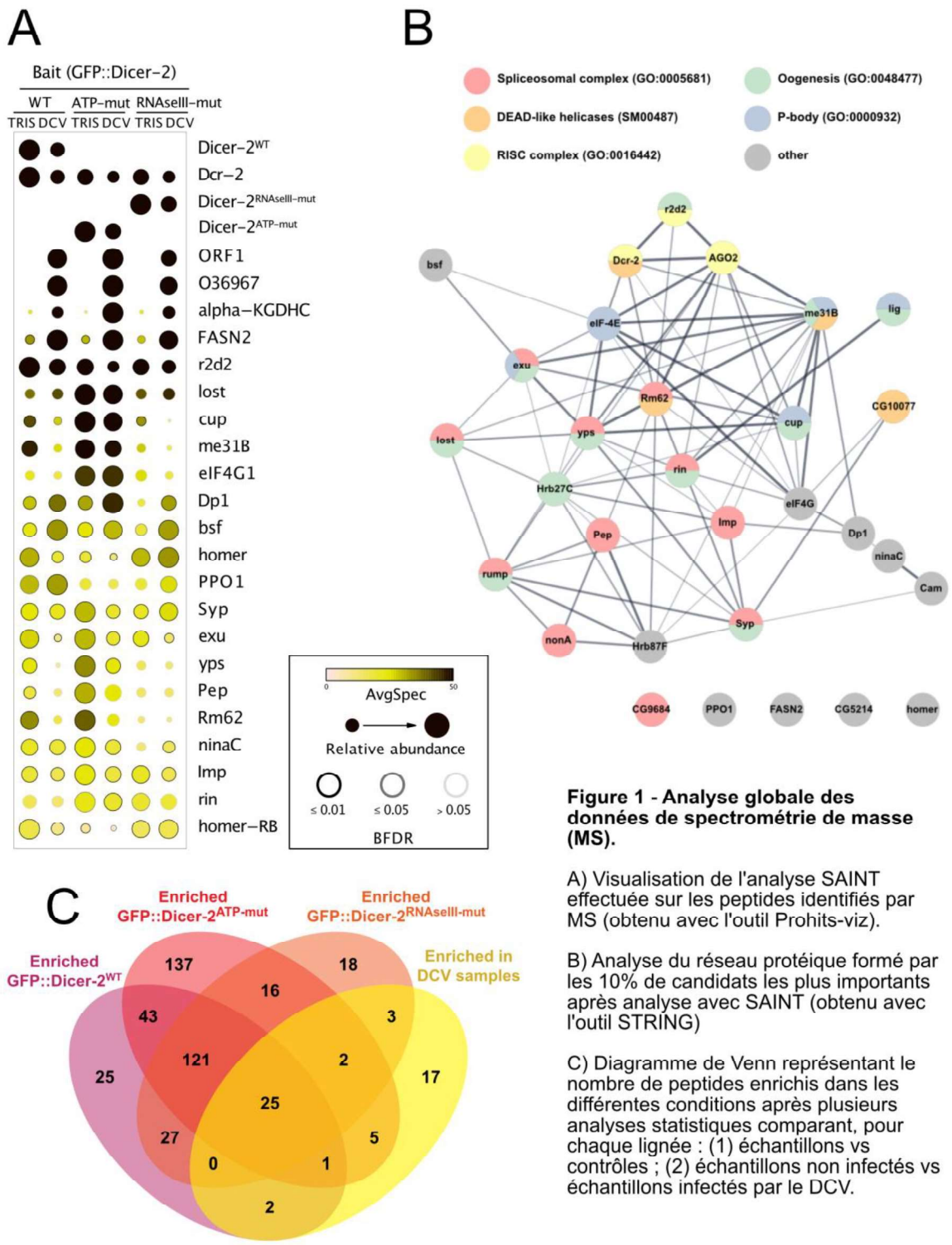

Figure 1 - Analyse globale des données de spectrométrie de masse (MS).

A) Visualisation de l'analyse SAINT effectuée sur les peptides identifiés par MS (obtenu avec l'outil Prohits-viz).

B) Analyse du réseau protéique formé par les 10% de candidats les plus importants après analyse avec SAINT (obtenu avec l'outil STRING)

C) Diagramme de Venn représentant le nombre de peptides enrichis dans les différentes conditions après plusieurs analyses statistiques comparant, pour chaque lignée : (1) échantillons vs contrôles ; (2) échantillons non infectés vs échantillons infectés par le DCV.

Ces différentes analyses m'ayant permis d'établir une liste d'interactants potentiels de Dicer-2, j'ai commencé par confirmer l'interaction avec Dicer-2 par IP et western blot des différentes protéines candidates pour lesquelles un anticorps est disponible. Nous avons pu confirmer ces interactions dans la lignée mutante GFP::Dicer-2$^{ATPase-mut}$, qui est la lignée pour laquelle ces protéines étaient le plus enrichi par rapport aux lignées contrôles lors de l'expérience de LC-MS/MS (Figure 2A). Ces résultats suggèrent que Dicer-2$^{ATPase-mut}$, qui fixe les molécules d'ARNdb et les clive uniquement de manière distributive, a des interactions plus stables que la version sauvage.

J'ai ensuite voulu tester l'impact de ces candidats sur l'infection virale en réalisant deux cribles ARNi : un crible en cellules S2 de drosophile et un crible *in vivo* par invalidation au stage adulte des gènes candidats (Figure 2B&C). Ces deux cribles ont permis de mettre en avant différents candidats, dont Rasputin (Rin), une *RNA-binding protein* (RBP) qui semble

avoir une activité antivirale à la fois *ex vivo* et *in vivo*. Il est intéressant de noter que cette protéine a précédemment été montrée comme ayant un impact proviral sur le virus du Chikungunya (CHIVK) (Fros et al., 2018).

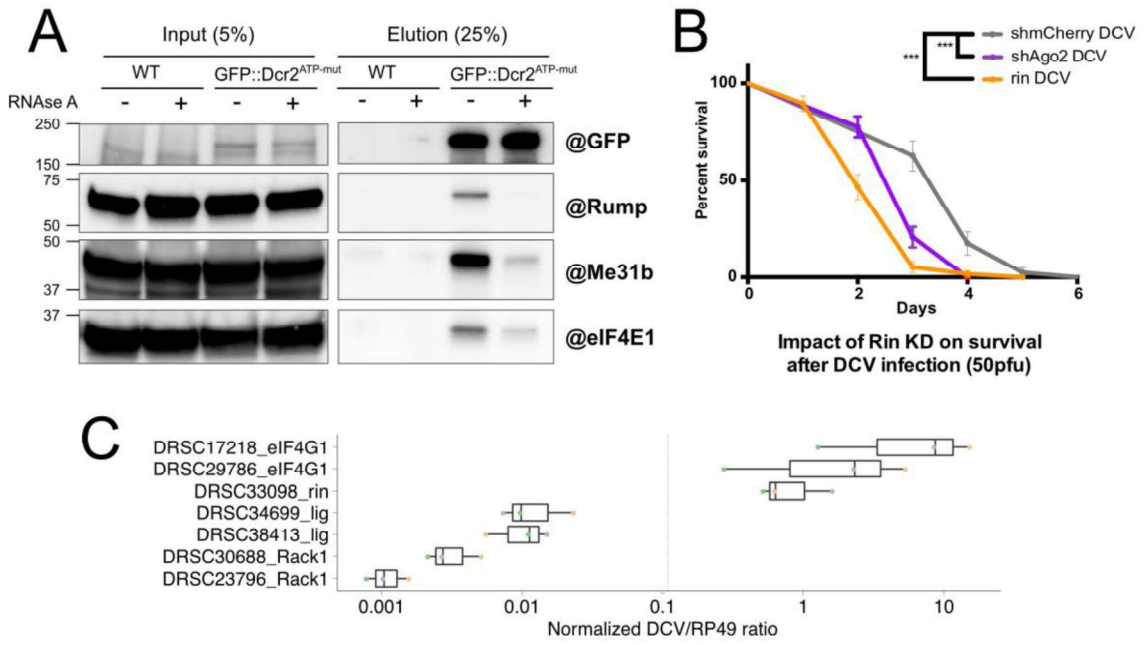

Figure 2 - Confirmation des interactions et impact sur l'immunité antivirale des candidats.

A) Les interactions entre Dicer-2 et différents candidats mis en valeur par l'analyse MS ont pu être confirmées par western blot après immunoprécipitation avec des billes @GFP sur des extraits protéiques de mouches entières.

B) Screen *in vivo* effectué sur des mouches Gal4Gal80 thermosensibles, dans lesquelles l'expression des candidats est inhibée. La survie des drosophiles après infection par DCV a été mesurée, et voici un example de résultats.

C) Candidats montrant un effet anti- ou pro-viral significatif après un screen *in vitro*. Les candidats mis en valeur par l'analyse MS ont été inhibés par dsRNA en cellules S2, puis infectées 20h par DCV. La charge d'ARN viral de DCV a ensuite été mesurée par RT-qPCR.

II) Conclusions et perspectives

Cette étude nous a fourni une quantité importante de données, et la visualisation du réseau protéique dans lequel Dicer-2 évolue peut nous aider à mieux comprendre différents aspects de l'ARNi antivirale et des protéines impliquées dans ce mécanisme. Nous avons par exemple pu observer au sein des candidats principaux des protéines d'épissage ainsi que des protéines localisées dans les P-bodies. Il pourrait être intéressant d'étudier le lien entre ces différents mécanismes/composants. De plus, ce réseau de protéines est modulé par différents facteurs, et les interactants de Dicer-2 changent selon : les mutations des domaines hélicase et RNAseIII, l'infection virale et le traitement à la RNAse. Nous avons pu valider les interactions entre Dicer-2 et certains candidats identifiés par LC-MS/MS dans la lignée GFP::Dicer-2$^{ATPase\text{-}mut}$, elles doivent maintenant être confirmées dans tous les génotypes et après infection. Enfin, nous avons pu observer un effet pro- ou antiviral pour certains candidats mis en valeur par les cribles *ex vivo* et *in vivo*. Je prévois quelques expériences complémentaires avec les candidats validés pour définir leur localisation par rapport à Dicer-2 lors de l'infection.

Partie 2 : Etude de Fandango, une protéine de liaison au poly(I:C) et facteur antiviral potentiel

I) Résultats

En collaboration avec le laboratoire du Pr. A. Pichlmair, Dr. Assel Mussabekova, au cours de sa thèse, a étudié des senseurs potentiels d'acides nucléiques chez la drosophile, en utilisant à la fois des drosophiles entières et des cellules d'insectes. Ces deux conditions ont mis en évidence Fandango, un membre du complexe PRP19/NTC, en tant que protéine de liaison au poly(I:C). Dr. Assel Mussabekova a également observé un effet antiviral de Fandango *in vivo* contre DCV, CrPV (*Cricket Paralysis Virus*) et le VSV (*Vesicular Stomatitis Virus*) (Pennemann *et al.*, 2021).

De mon côté, j'ai réalisé un crible ARNi en cellules S2 de drosophile en ciblant différents candidats de mon propre projet, dans lequel nous avons inclus Fandango ainsi que d'autres RNP et nucléases qui étaient suspectées de jouer un rôle antiviral potentiel. Les ARNdb correspondants du DRSC (Harvard) pour les différents candidats ont été utilisés pour réaliser ce crible ARNi sur des cellules S2 après infection par DCV (20h, MOI 0,01). Après incorporation des ARNdb dans les cellules S2 et infection par DCV, la charge en ARN viral a été mesurée par RT-qPCR. Dans ce crible, Fandango s'est avéré avoir un effet antiviral contre DCV, CrPV, FHVΔB2(1-74) (*Flock House Virus*, délétion d'une partie de la protéine B2) et VSV. Les résultats du crible ont été confirmés au niveau de l'ARN (Figure 3A) et des protéines (Figure 3B), par l'invalidation de Fand en utilisant trois ARNdb différents et, respectivement, RT-qPCR ou WB contre deux protéines DCV différentes (VP2 et RdRp). Pour les trois ARNdb de *Fand*, la quantité d'ARN viral ainsi que la quantité de protéines VP2 et RdRp du DCV sont plus élevés que dans la condition contrôle.

Ensuite, afin de comprendre le mécanisme moléculaire par lequel Fand entrave l'infection par le DCV, j'ai cherché quelle étape du cycle viral est impactée par l'invalidation de *Fand*. Par conséquent, j'ai étudié la cinétique de l'infection par DCV à une MOI de 10 après invalidation de Fand dans les cellules S2 (Figure 3C). Les niveaux d'ARN du DCV ont été vérifiés à différents temps post-infections, de 0 à 8 heures post-infection (hpi). Les résultats indiquent que l'impact de Fand sur l'infection par DCV est significatif de 2-4 hpi jusqu'à la fin du cycle viral (8hpi). Ceci suggère que Fand pourrait être lié à l'étape de réplication de l'ARN du cycle viral, mais n'influence probablement pas les étapes antérieures comme la liaison ou l'entrée dans la cellule.

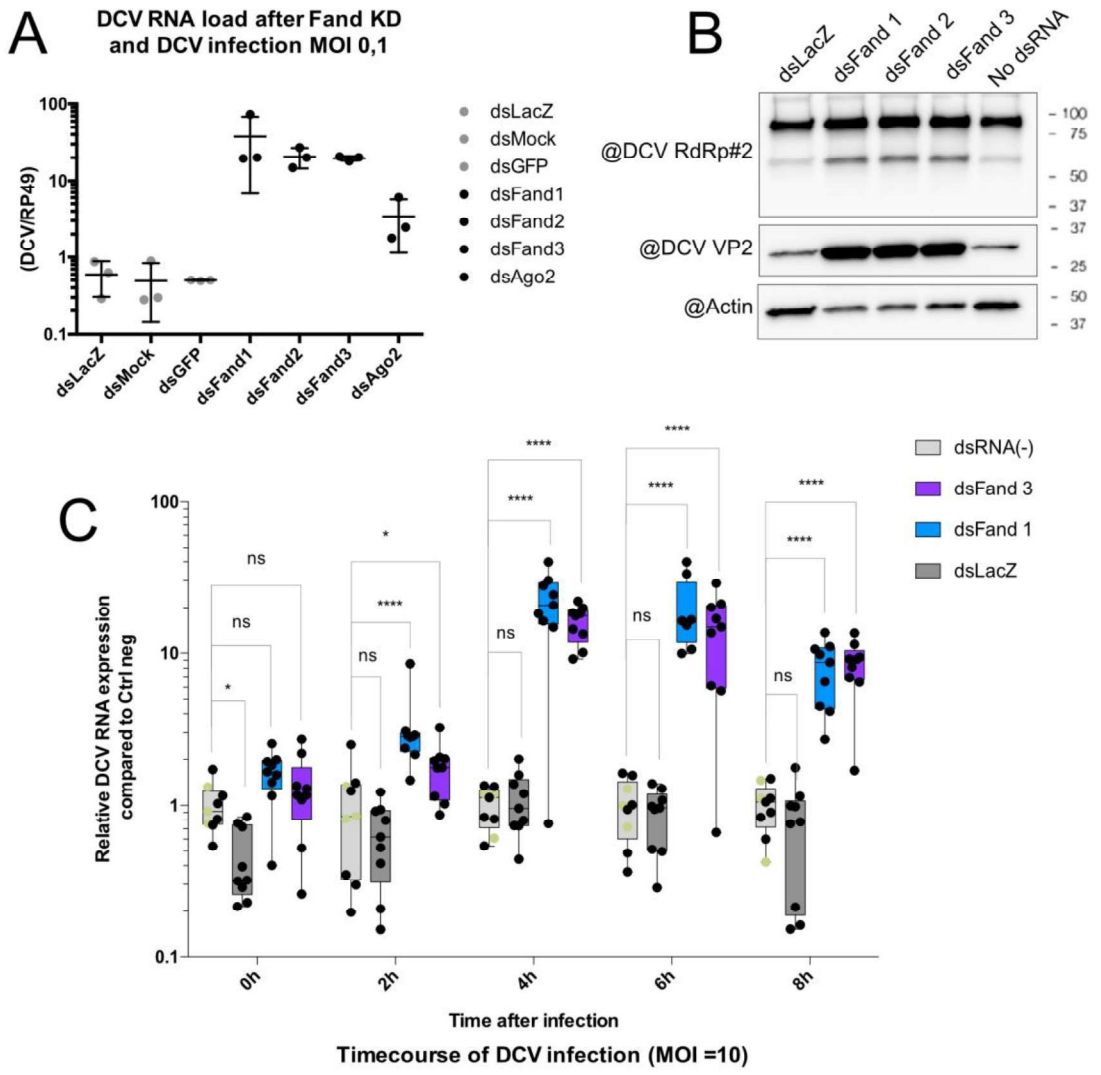

Figure 3 - Rôle de Fandango dans l'immunité innée.

A) Impact du KD de Fandango sur la charge en ARN viral après infection par DCV de cellules S2. La charge en ARN viral a été mesurée par RT-qPCR après KD de Fand par plusieurs ARNdb et infection par DCV à une MOI de 0,1 à 20h post-infection.

B) Impact du KD de Fandango sur la charge en protéines virales après infection par DCV de cellules S2. La charge en protéines virales à été visualisée par western blot contre deux protéines de DCV, VP2 et RdRp, après KD de Fand par plusieurs ARNdb et infection par DCV à une MOI de 0,1 à 20h post-infection.

C) Cinétique de l'impact de Fandango sur le cycle viral de DCV. La charge en ARN viral a été mesurée par RT-qPCR après KD de Fand par plusieurs ARNdb et infection par DCV à une MOI de 10 aux temps 0, 2, 4, 6 et 8h post-infection.

Comme Fand est un membre du complexe Prp19/NTC, il a déjà été identifié comme étant impliqué dans différentes fonctions cellulaires comme l'épissage. Nous sommes donc demandés si l'impact antiviral de Fand est lié à ses autres fonctions connues. Afin de confirmer que l'impact de Fand n'est pas juste un effet indirect lié à l'épissage, nous utilisons l'Isoginkgetin, un inhibiteur général de l'épissage, dans des cellules S2 tout en effectuant une invalidation de Fand, afin de vérifier si l'impact sur l'infection par le DCV est toujours présent lorsque l'épissage est altéré. L'inhibition correcte de l'épissage après le traitement à l'Isoginkgetin sera confirmée à l'aide d'un rapporteur d'épissage à la luciférase que nous avons conçu et sommes actuellement en train de tester. L'ensemble de ces résultats sont actuellement répétés et complétés afin de terminer ce projet avec une étudiante Erasmus (Imperial College) jusqu'en Juin 2022.

II) Conclusions et perspectives

En conclusion, nous avons accumulé un certain nombre de résultats suggérant que Fand pourrait avoir une fonction antivirale, mais certaines expériences sont encore nécessaires, en particulier pour déterminer le mécanisme moléculaire impliqué et pour exclure un effet indésirable de l'altération de l'épissage. De plus, nous aimerions vérifier si l'effet de Fand est conservé chez son orthologue chez les mammifères, Xab2. En effet, lors de notre collaboration avec le laboratoire de A. Pichlmair, ils ont trouvé un impact de Xab2 sur le virus de l'Influenza A (IAV). Nous pouvons inhiber son expression dans les cellules Hek293T en utilisant des siARN avant d'infecter les cellules avec VSV ou SINV. Enfin, nous prévoyons également d'examiner les différents domaines putatifs de Fand pour savoir s'ils sont impliqués dans sa fonction antivirale.

Bibliographie

Ashley, J., Cordy, B., Lucia, D., Fradkin, L.G., Budnik, V., and Thomson, T. (2018). Retrovirus-like Gag Protein Arc1 Binds RNA and Traffics across Synaptic Boutons. Cell *172*, 262-274.e11.

Cenik, E.S., Fukunaga, R., Lu, G., Dutcher, R., Wang, Y., Tanaka Hall, T.M., and Zamore, P.D. (2011). Phosphate and R2D2 Restrict the Substrate Specificity of Dicer-2, an ATP-Driven Ribonuclease. Mol. Cell *42*, 172–184.

Fros, J., Geertsema, C., Zouache, K., Baggen, J., Domeradzka, N., Leeuwen, D. van, Flipse, J., Vlak, J., Failloux, A.-B., and Pijlman, G. (2015). Mosquito Rasputin interacts with chikungunya virus nsP3 and determines the infection rate in Aedes albopictus. Parasites and Vectors *8*, 464. https://doi.org/10.1186/s13071-015-1070-4.

Goic, B., Vodovar, N., Mondotte, J.A., Monot, C., Frangeul, L., Blanc, H., Gausson, V., Vera-Otarola, J., Cristofari, G., and Saleh, M.-C. (2013). RNA-mediated interference and reverse transcription control the persistence of RNA viruses in the insect model Drosophila. Nat. Immunol. *14*, 396–403.

Hornung, V. (2014a). SnapShot: nucleic acid immune sensors, part 1. Immunity *41*, 868, 868.e1.

Hornung, V. (2014b). SnapShot: Nucleic acid immune sensors, part 2. Immunity *41*, 1066-1066.e1.

Liu, X., Fu, R., Pan, Y., Meza-Sosa, K.F., Zhang, Z., and Lieberman, J. (2018). PNPT1 Release from Mitochondria during Apoptosis Triggers Decay of Poly(A) RNAs. Cell *174*, 187-201.e12.

Sinha, N.K., Trettin, K.D., Aruscavage, P.J., and Bass, B.L. (2015). Drosophila Dicer-2 Cleavage Is Mediated by Helicase- and dsRNA Termini-Dependent States that Are Modulated by Loquacious-PD. Mol. Cell *58*, 406–417.

Sinha, N.K., Iwasa, J., Shen, P.S., and Bass, B.L. (2018). Dicer uses distinct modules for recognizing dsRNA termini. Science *359*, 329–334.

Claire ROUSSEAU

Caractérisation de l'interactome du récepteur d'ARNdb cytosolique Dicer-2 *in vivo* au cours de l'infection virale chez *Drosophila melanogaster*

Résumé

Le sujet de cette thèse porte sur l'immunité antivirale chez la drosophile. Mon projet principal est axé sur une protéine majeure de l'immunité antivirale chez les insectes, Dicer-2. Cette protéine est un senseur d'acides nucléiques pour la voie de l'ARN interférence (ARNi) antivirale. Dicer-2 s'associe avec et est régulé par différents partenaires, et mon but a été de comprendre comment ce réseau protéique est modulé lors de l'infection par le *Drosophila C Virus* (DCV). Ceci a permis l'identification de différents candidats dont j'ai pu, par la suite, confirmer l'interaction avec Dicer-2. En réalisant deux cribles ARNi, *in vivo* et *ex vivo*, j'ai pu identifier plusieurs autres candidats comme ayant un impact sur l'infection par DCV.

En parallèle, j'ai travaillé sur une protéine liée à l'épissage, Fandango, qui a été identifiée comme interactant du poly(I:C) par mon laboratoire d'accueil. L'effet antiviral global de cette protéine a été mis en évidence lors d'un crible ARNi utilisant plusieurs virus. Après avoir étudié l'impact de Fandango sur l'infection par DCV, nous avons étudié son lien avec le spliceosome.

Globalement, ce travail a fourni une ressource composée de différents candidats qui peuvent maintenant être étudiés plus en détails afin d'obtenir une meilleure compréhension de l'immunité antivirale chez la drosophile.

Résumé en anglais

The topic of this thesis is centered on antiviral immunity in *D. melanogaster*. My main project was focused on a major protein of insect antiviral immunity, Dicer-2. This protein is a nucleic acid sensor for the antiviral RNA interference (RNAi) pathway. Dicer-2 associates with and is regulated by several partners, and my aim has been to understand how this network is modulated by *Drosophila C Virus* (DCV) infection. Amongst the identified candidates, some were subsequently confirmed to interact with Dicer-2. By performing two RNAi screens, *in vivo* and *ex vivo*, I have highlighted several other proteins as having an impact on DCV infection.

In parallel, I worked on a protein linked with splicing, Fandango, that was identified as a poly(I:C) interactant by my host laboratory. The global antiviral effect of this protein was shown in an *ex vivo* screen using different viruses. After studying the impact of Fandango on DCV infection, we attempted to determine if this impact was linked to the spliceosome.

Overall, this work has provided a pool of candidates that can now be investigated further to gain a better understanding of antiviral immunity in drosophila.